

SUPPLEMENTO
AL VOLUME IX, SERIE X
DEL
NUOVO CIMENTO

A CURA DELLA SOCIETÀ ITALIANA DI FISICA

1958

3° Trimestre

PRINTED IN ITALY

NICOLA ZANICHELLI EDITORE
BOLOGNA

Alfredo Lucio

SUPPLEMENTO
AL VOLUME IX, SERIE X, DEL
NUOVO CIMENTO
A CURA DELLA SOCIETÀ ITALIANA DI FISICA

1958

3° Trimestre

N. 1

CONVEGNO INTERNAZIONALE
SUGLI STATI CONDENSATI DI SISTEMI SEMPLICI
ORGANIZZATO DALLA SOCIETÀ ITALIANA DI FISICA
SOTTO GLI AUSPICI E COL CONCORSO
DELL'UNIONE INTERNAZIONALE DI FISICA PURA ED APPLICATA
E DEL CONSIGLIO NAZIONALE DELLE RICERCHE

VILLA MONASTERO
VARENNA SUL LAGO DI COMO

11-15 SETTEMBRE 1957

RENDICONTI

INDICE

INTRODUZIONE

G. POLVANI - Discorso inaugurale.	pag. 5
G. CARERI - Opening address	» 8

PARTE PRIMA - Simple solids and melting.

C. DOMB - Some theoretical aspects of melting	pag. 9
J. S. DUGDALE - The equation of state of solid helium	» 27
E. R. DOBBS, B. F. FIGGINS and G. O. JONES - Properties of solid argon	» 32
G. BORELIUS - Thermal expansion and melting of simple metals.	» 36
M. TODA - On the quantum effect on melting	» 39

PARTE SECONDA - Experimental methods.

B. N. BROCKHOUSE - Structural dynamics of water by neutron spectrometry.	pag. 45
G. CARERI - Atom movements in simple liquids by tracer technique	» 72
E. J. ALLIN, N. P. GUSH, W. F. HARE and H. L. WELSCH - The infrared spectrum of liquid and solid hydrogen	» 77
J. WILKS - The thermal conductivity of condensed helium	» 84
H. C. TORREY - Effects of translational diffusion on nuclear spin relaxation in simple condensed systems	» 95
L. GIULOTTO - Nuclear magnetic resonance and molecular association in liquids	» 101
C. P. SLICHTER - Magnetic resonance studies of self-diffusion in simple solids	» 104

PARTE TERZA - Dense gases.

J. G. KIRKWOOD and S. A. RICE - The statistical mechanical basis of the Enskog theory of transport in dense gases	pag. 112
H. C. LONGUET-HIGGINS - The transport properties of dense assemblies of rigid spheres	» 115

T. WAINWRIGHT and B. J. ALDER - Molecular dynamics computations for the hard sphere system	pag. 116
W. W. WOOD, F. R. PARKER and J. D. JACOBSON - Recent Monte Carlo calculations of the equation of state of Lenard-Jones and hard sphere molecules	» 133
J. YVON - Note sur un calcul de perturbation en mécanique statistique	» 144
A. MICHELS - Some remarks on experiments in the dense state	» 152
H. N. V. TEMPERLEY - The equation of state of an imperfect gas of elastic spheres	» 163

PARTE QUARTA - Theory of liquids.

S. ONO - Equation of state and surface tension of liquids	pag. 166
I. OPPENHEIM - Quantum mechanical effects on the surface tension of simple liquids	» 180
A. BELLEMANS - The properties of isotopic liquids	» 181
L. SAROLEA - Integral equation method in the theory of liquids	» 189
A. PIEKARA - Saturation diélectrique et forces intermoléculaires dans les liquides	» 192

PARTE QUINTA - Review papers on helium 4.

J. DE BOER - Liquid helium as a quantum liquid	pag. 199
K. MENDELSSOHN - Recent experiments on superfluidity	» 228

PARTE SESTA - Statistical mechanics of quantum systems.

J. E. MAYER - The equilibrium phase transition in liquid helium	pag. 2 4
E. W. MONTROLL and J. C. WARD - Quantum statistics of interacting particles	» 235
J. YVON - Note sur les corrélations dans un fluide quantique en équilibre	» 237
P. G. DE GENNES - Note sur les corrélations dans les gaz comprimés	» 240

PARTE SETTIMA - Helium 4.

A. THELLUNG - Quantum hydrodynamics and the theory of helium II	pag. 243
O. PENROSE - Bose-Einstein condensation in liquid helium	» 256
R. EISENSCHITZ and A. CROWE - Contribution to the phonon theory of fluids	» 262
O. K. RICE - Energy fluctuations in liquid helium and its flow properties	» 267
S. FRANCHETTI - On the structure of liquid ⁴ He	» 286
A. VAN ITTERBEEK - Velocity of sound in liquid helium	» 291

PARTE OTTAVA - Helium 3.

W. M. FAIRBANK and G. K. WALTERS - Nuclear alignment in liquid and solid ^3He	pag. 297
M. J. BUCKINGHAM - Some comments on the theory of liquid ^3He	» 306
B. WEINSTOCK, B. M. ABRAHAM and D. W. OSBORNE - Some properties of liquid ^3He	» 310
K. W. TACONIS and D. H. N. WANSINK - Some experiments with ^3He - ^4He mixtures	» 320
H. A. FAIRBANK - Second Sound in ^3He - ^4He mixtures	» 325
J. G. DASH and R. D. TAYLOR - Influence of ^3He on some flow properties of He II	» 334
E. W. GUPTILL, A. C. HOLLIS and C. C. LIM - Velocity of sound in a ^3He - ^4He mixture	» 341

PARTE NONA - Mixtures.

I. PRIGOGINE and A. BELLEMANS - Isotopic mixtures	pag. 342
H. C. LONGUET-HIGGINS - The statistical thermodynamics of a one-dimensional multicomponent assembly	» 345
A. ENGLERT-CHVOLES and I. PRIGOGINE - On the statistical theory of the surface tension of binary mixtures	» 347
V. MATHOT - Thermodynamic properties of the system argon methane liquid	» 356
A. MICHELS - An experiment on the interaction of dissimilar molecules	» 358
R. HEASTIE and G. O. JONES - Solid solutions of argon and krypton	» 365

*La Direzione del Nuovo Cimento ringrazia vivamente il
prof. GIORGIO CARERI, il prof. ROBERTO FIESCHI e il
dott. VITTORIO NARDI per il prezioso aiuto dato nella
compilazione di questo fascicolo.*

INTRODUZIONE

Discorso inaugurale.

G. POLVANI

Presidente della Società Italiana di Fisica

È questa la terza volta quest'anno che fisici di tutto il mondo si adunano a Varenna, qui nella Villa Monastero, per parlare dei loro studi, scambiarsi idee, pareri, critiche.

La prima volta fu nel Giugno passato per il Convegno, organizzato con la collaborazione della nostra Società, dall'Unione Internazionale di Fisica pura ed applicata, relativo ai raggi cosmici, anzi più propriamente alla loro origine, o se si vuole, direi meglio, a questioni astrofisiche studiate attraverso le radiazioni cosmiche di più alta energia.

La seconda volta fu questo Luglio-Agosto per il V Corso della Scuola Internazionale di Fisica della nostra Società: si parlò allora molto di solidi, della loro costituzione, di problemi cristallini e di perfezione dei cristalli, lasciando ex professo da parte le questioni magnetiche che già l'anno precedente erano state trattate nel IV Corso.

Quest'ultima volta è un Convegno anch'esso internazionale, organizzato dalla nostra Società, relativamente alla Fisica degli Stati condensati dei Sistemi semplici.

Ormai abituati come siamo a sentire, in quasi tutte le occasioni in cui si parli di Fisica degli ultimi sessant'anni, usare parole un po' roboanti come elettroni, protoni, nucleoni, neutroni, mesoni, sincrotroni, ciclotroni, ecc, ecc., quelle così semplici e quasi dimesse che costituiscono il titolo del Convegno attuale — Stati condensati di Sistemi semplici — potrebbero far pensare a cose vecchie e desuete e quindi di poco momento e di scarso interesse. Ma così non è. Sotto quelle parole si nasconde una Fisica raffinata, ultramoderna, rara, ricca di sorprese e di singolari comportamenti. È in gran parte la Fisica delle basse temperature, la Fisica dell'Elio liquido,

dell'Elio solido, delle discriminazioni delle varie statistiche, delle tecniche tra le più ingegnose e particolari...: coronamento di più di tre secoli di studi se si vuole rimontare attraverso i tempi e fissare in un qualche modo un'origine ad essi nelle vecchie e pur tanto significative esperienze di BOYLE sulle miscele frigorifere. Ma chi diede il colpo d'ala decisivo e aperse a questo capitolo della Fisica gli orizzonti su cui oggi spazia, fu l'indimenticabile KAMERLING ONNES, il grande maestro della Fisica delle basse temperature e il primo grande esploratore di quel mondo totalmente sconosciuto cinquant'anni fa.

* * *

Ma è del tutto superfluo che io ricordi queste date e questi episodi a Voi fisici che dell'argomento siete così esimi cultori.

Piuttosto permettetemi che io porga a Voi tutti partecipanti al Convegno, convenuti da ben quindici nazioni diverse, il saluto più cordiale e il ringraziamento più vivo per avere accolto il nostro invito.

Alcuni di Voi io già conobbi or sono otto anni a Firenze in occasione del Convegno internazionale che fu là tenuto nel 1949 sulla Meccanica statistica. E loro rivedendo non posso non ripensare al lungo cammino che da allora ha fatto la nostra scienza in Italia. Nè posso non ricordare anche la figura eletta del prof. KRAMERS, Presidente allora dell'Unione Internazionale di Fisica, col quale ebbi la sorte di stringere quei primi legami di collaborazione e di simpatia che poi tanto hanno giovato, tra l'Unione e la nostra Società, tra i fisici stranieri e quelli italiani.

Là, a Firenze, frequentava il Convegno un ragazzino, un po' spaurito, che si appassionava a quegli stessi problemi che qui ora ci occupano. Oggi egli siede in cattedra a Padova e ha organizzato questo Convegno con perizia e passione ammirevoli. Ed io voglio a lui, che è il prof. GIORGIO CARERI, porgere a nome mio, della Società e di tutti quanti qui sono riuniti — certo d'interpretarne i sentimenti — le congratulazioni, gli auguri e i ringraziamenti più cordiali e affettuosi.

E poichè siamo in tema di ringraziamenti, desidero anche esprimerne dei più vivi al Ministro della Pubblica Istruzione e particolarmente al Direttore Generale dott. MARIO DI DOMIZIO, al Consiglio Nazionale delle Ricerche e al suo Presidente, prof. FRANCESCO GIORDANI, e all'Ente Provinciale per il Turismo di Como e al suo Presidente, Comm. GIUSEPPE RUSSO, per il contributo finanziario da loro porto a vantaggio del nostro Convegno. Ma soprattutto desidero ringraziare l'avv. EMILIO SANCASSANI, Presidente dell'Unione Industriali di Como, e Socio benemerito della nostra Società, il quale in un momento particolarmente difficile, quando cioè questo Convegno minacciava di crollare per insufficienza di mezzi, volle, appena sollecitato da me, chiamare — dirò così — a soccorso i colleghi della Lombardia, ossia i Presidenti delle singole Associazioni Industriali di Lombardia, — di Bergamo, Brescia, Busto

Arsizio, Legnano, Monza, Pavia, Voghera, — e la stessa Associazione Industriale Lombarda di Milano, perchè insieme con quella di Como, procurassero quei fondi che ancora mancavano per la vita di questo Convegno. Veramente grazie dunque a lui e ai suoi colleghi e grazie anche al Direttore della stessa Unione comasca, dott. ACHILLE BAGLIONI. E infine, e ancora un grazie particolare all'ottimo Presidente dell'Ente Villa Monastero, avv. GIBERTO BOSISIO, così sempre tanto premurosamente amico a tutte le attività che si svolgono in questa Villa.

* * *

Ma non voglio col mio discorrere, far ritardare troppo l'inizio delle conversazioni scientifiche: molto avete da dire e da discutere: vedo infatti un programma estremamente nutrito ed interessante.

Ho quindi l'onore di dichiarare aperto questo Convegno Internazionale sugli Stati condensati di Sistemi semplici e augurare ad esso il migliore e il più proficuo dei successi.

Opening Address.

G. CARERI

Istituto di Fisica dell'Università di Padova - Padova

I think I have to add only a few words now, to thank Professor POLVANI for his enthusiastic support for this meeting, and to welcome the scientists who have joined us here to discuss arguments of common interest.

The real topic of our meeting concerns the nature of the simple liquids, where the word «simple» means «not associated», or such as not to need any chemistry. This topic has been so far considered an application of Statistical Mechanics, and therefore this meeting is sponsored by the International Union of Pure and Applied Physics Committee on Statistical Mechanics and Thermodynamics. However, we have realized lately that we are still far from having a «theory» of the liquid state, and that a picture is still wanted. Therefore a meeting in which we would go into both the theoretical and experimental aspects, and also into the neighbouring fields of the dense gases and of the melting of simple crystals, seems to us to be worth holding. Such a meeting can be successful if we have an open-minded approach and the desire to reach that ultimate picture underlying these different aspects.

PARTE PRIMA

Simple Solids and Melting.

Some Theoretical Aspects of Melting.

C. DOMB

King's College - London

1. - Introduction.

At the Paris Conference on Phase Transitions in 1952 Sir FRANCIS SIMON drew attention to a number of points of importance for an understanding of the melting transition. It is my purpose to consider some of these points in detail and to discuss progress which has been made towards clarifying their significance.

The first point which I wish to raise is the position of the melting transition. The Lindemann melting formula

$$(1) \quad T_m = Cm\Theta^2v_m^{\frac{1}{3}},$$

where T_m is the melting point, m the molecular weight, V_m the melting volume, Θ the Debye temperature of the substance, and C a constant, is well satisfied by the experimental melting data of simple substances. The formula (1) was applied originally to melting at atmospheric pressure; for melting at high pressures the experimental data on the melting volume and Θ values were not available, and the formula (1) could not be tested. Instead of (1), however, the Simon melting formula

$$(2) \quad \frac{p_m}{a} = \left(\frac{T_m}{T_0}\right)^c - 1$$

provides a correlation between melting temperature and melting pressure. Here p_m is the melting pressure, a the internal pressure, T_0 the normal melting temperature at atmospheric pressure, and c a constant for each particular substance. The formula (2) is in satisfactory agreement with experimental data. SALTER [2] has shown that if assumptions of the Grüneisen type are

made regarding the dependence of Θ on volume, the formula (2) is a consequence of (1), the constant c being related to Grüneisen's γ . SALTER's work has been extended and generalized by GILVARRY [3] particularly in relation to the melting of metals. It thus appears that formula (1) has an extremely wide range of validity.

A more direct check on the applicability of (1) at high pressures can be made for simple solids of the inert gas type if the intermolecular potentials between pairs of atoms are reasonably well known. Thus Θ can be calculated

simply and with good accuracy as a function of volume by lattice dynamics [4], and hence the pressure can be determined in the solid phase [5]. Combining this with the melting temperature given by (1) an estimate can be obtained for the melting curve, and this can be compared with experimental data available. This procedure has been followed by I. J. ZUCKER at King's College for Argon and the result is shown in Fig. 1. Since the melting curve at high pressures is quite sensitive to the form of the intermolecular potential, and this potential is only well established near equilibrium the resulting agreement can be regarded as reasonably satisfactory.

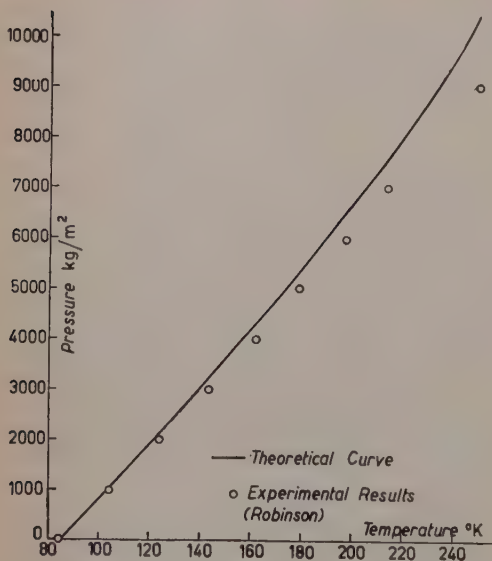


Fig. 1.

The original argument used by LINDEMANN to derive (1) was semiempirical in nature, and was concerned with the amplitude of thermal vibrations of molecules in the lattice. LINDEMANN assumed that when the ratio of the amplitude of these vibrations to the lattice spacing of neighbouring atoms reached a certain critical value the crystal became unstable and broke up into a liquid. In the language of Professor FRANK, the picture behind this derivation was that of a solid shaking itself to pieces at the melting point. This idea was supported by the absence of evidence of superheating of the solid phase. However there are indications that this absence of superheating can be attributed to surface effects. Thus many puzzling properties of liquid metals have found an explanation on this basis [6]; and the only direct experiment on superheating in the absence of surface effects also confirms this assumption [7]. Hence the classical description of two continuous phases meeting

at the melting point seems to provide a more valid description of the facts. In this case an adequate understanding of a melting formula such as (1) must be based on the properties of the liquid as well as the solid phase.

The experiments of DUGDALE and SIMON [8] on solid helium showed clearly that it is not vibration amplitudes themselves which have any significance for melting [9], vibrations arising from zero point energy can have large amplitude, and yet make little contribution towards melting.

It is sometimes loosely contended that the Lindemann formula is a « dimensional formula » and is therefore uniquely specified. This is quite untrue since many other dimensional formulae are possible; for example if anyone side of the above equation (1) is multiplied by any function of T_m/Θ a different dimensional formula results. The formula may correctly be described as one aspect of a « law of corresponding states ». The limits of validity of such a law, and the modifications required when quantum effects become important, will be considered in the following sections.

2. - The Lindemann formula. Law of corresponding states.

We shall find it convenient to deal with the process of melting at constant volume. As the temperature of the substance is increased two critical points will be encountered, the first, T_m , corresponding to the onset of melting of the solid phase, and the second, T'_m , to the final disappearance of the solid phase. Below T_m the substance is purely solid, between T_m and T'_m solid and fluid co-exist in equilibrium, and above T'_m the substance is purely fluid. From a knowledge of T_m , T'_m and the free energy F for all specific volumes of the substance, all the thermodynamic melting data can be determined.

The partition function (and hence the free energy) is completely determined in principle when the molecular mass and intermolecular force law are specified, but its practical calculation for the fluid phase is a problem of great difficulty. Confining our attention to the range in which classical theory provides a valid approximation, the kinetic energy terms can be separated, and only the intermolecular energy function plays any significant part in the description of melting. If this intermolecular energy depends only on two parameters, and can be put in the form $\varepsilon_0 f(r/r_0)$ the characteristic energy ε_0 and the characteristic length r_0 varying from one substance to another, then an exact law of corresponding states exists. Measuring temperatures in terms of ε_0/k as unit, and lengths in terms of r_0 , the thermodynamic functions are the same for all substances. DE BOER [10] has shown that this assumption is well satisfied by the heavy inert gases; for the lighter inert gases deviations occur as a result of quantum effects, and these will be discussed in further detail in Sect. 4.

If we now consider anyone reduced specific volume the melting temperature will be given by

$$(3) \quad kT_m = \alpha \varepsilon_0 ,$$

where α depends on the universal function $f(u)$ and is thus a function of reduced volume. Similarly the Debye temperature is given by

$$(4) \quad k\Theta = h\nu_D = h\sqrt{\beta\varepsilon_0/mr_0^3} ,$$

where β depends on the first and second derivations of $f(u)$ (the term $1/r_0^3$ arising since two differentiations are involved) and is determined by lattice dynamics. Again β will vary with reduced volume.

Combining (3) and (4) we obtain

$$(5) \quad \frac{T_m}{m v^{\frac{1}{3}} \Theta^2} = C(u) \quad (u = v/v_0),$$

which is of the same form as (1) except that the constant C is a function of reduced volume. Thus we have an exact derivation of (1) as an expression of the law of corresponding states, but its region of validity would be narrow since C would vary with volume, and the formula could apply only to substances such as the inert gas solids for which the assumptions regarding the form of the law of force were reasonable. We shall endeavour to show why to a fair approximation the variation of C with reduced volume can be neglected, and at the same time our considerations may throw light on the applicability of the formula to other substances.

3. - More general interpretation.

It is quite easy to formulate rigorously the combinatorial problem, which corresponds to the melting of a solid [11]. As before we shall assume classical theory, interactions between molecules being given by central forces of limited range. The partition function for an assembly of classical particles reduces to a product of two factors, a kinetic energy factor $(2\pi mkT)^{\frac{3}{2}}/h^3$ per particle, and a configurational factor arising from the potential energy terms. To specify the configurational factor, let us take an arbitrary lattice structure whose

spacing is small compared with the intermolecular distance in the solid state. Suppose that molecules are restricted to occupy positions in the centre of a lattice cell. The lowest energy state will correspond to a regular arrangement (as illustrated in Fig. 2) and the intermolecular forces can be ignored outside a certain radius (which can to a reasonable approximation correspond only to nearest neighbours in the solid state). Between any two molecules in different lattice cells there is an interaction energy ε_i , and for any finite lattice spacing the ε_i form a finite set t . The configurational partition function for the assembly depends only on the ε_i , and hence likewise all transition temperatures and melting properties depend on the ε_i . We may therefore write instead of (3)

$$(6) \quad kT_m = \chi(\varepsilon_1, \dots, \varepsilon_t),$$

where χ is a function determined by the combinatorial factors involved.

In fact it is not the absolute value of the ε_i which is significant, and we may deduct from the ε_i a term corresponding to the lattice energy at absolute zero ε^0 which does not affect the thermodynamic properties of the assembly at constant volume. We are then concerned with the deviations of the energies of interaction from their equilibrium static values because of interstitial displacements.

We now make two assumptions which lead to a more generalized Lindemann melting formula.

1) To a good approximation only values of ε_i near to the equilibrium static value have any significance up to the melting point.

2) Values of ε_i near to this equilibrium static value are determined by a knowledge of the characteristic Debye temperature for the lattice at the given volume.

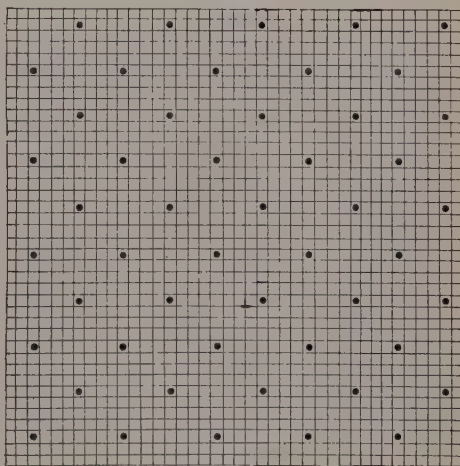


Fig. 2.

The first assumption is an expression of the experimental fact that vibration amplitudes are small right up to the melting point and displacements far from equilibrium are comparatively rare, and can be ignored to a reasonable approximation. The energies ε_i may therefore be obtained by a Taylor expansion of the lattice potential energy in powers of the displacements from

equilibrium in the form

$$(7) \quad \varepsilon(u_\alpha, u_\beta) = \varepsilon^0 + \sum_{\alpha=1}^3 A_\alpha u_\alpha + \sum_{\beta=1}^3 A_\beta u_\beta + \\ + \frac{1}{2} \sum_{\alpha\beta=1}^6 (A_{\alpha\alpha} u_\alpha^2 + 2A_{\alpha\beta} u_\alpha u_\beta + A_{\beta\beta} u_\beta^2) + \dots,$$

where u_α and u_β are the co-ordinates of the displacements of two neighbouring atoms from their equilibrium values. The coefficients of the powers of u are the same as arise in standard lattice dynamics theory [12]; the linear term is zero for static equilibrium, and the second order terms determine the frequency spectrum of lattice vibrations. Our first assumption enables us to stop the expansion in (7) with the second order terms; and our second assumption is equivalent to the statement that the second order coefficients $A_{\alpha\beta}$ depend on one parameter only. This is not rigorously true even for central forces for different specific volumes since if $\varphi(r)$ is the intermolecular potential both $\varphi'(r)$ and $\varphi''(r)$ enter into $A_{\alpha\beta}$; but it seems a reasonable approximation rather of the same type as the Debye approximation to the properties of a solid.

We have already observed that the properties of the liquid phase must be taken into account in a discussion of melting and we are therefore also assuming that in the liquid phase in the neighbourhood of the melting point the local order is not very different from that of the solid, and the spacing of neighbouring atoms does not usually differ markedly from the equilibrium static value.

If we now replace r_0 of Sect. 2 by r' , the mean distance between nearest neighbour atoms in static equilibrium, and measure displacements in terms of r' we will obtain a law of corresponding states; ε_0' is now given by $r'^2 f''(r')$ and instead of (3) and (4) we have,

$$(7) \quad \begin{cases} kT_m = \alpha' r'^2 f''(r') \\ \Theta^2 = (\beta'/m) f''(r') \end{cases}$$

leading to the Lindemann formula (1). The constants α' , β' will depend on the crystal structure of the solid, and our argument indicates why a law such as (1) is a reasonable approximation for a simple solid of the inert gas type along the melting curve.

However it is known that the formula (1) applies more widely, and the constant C does not vary widely for metals and for different types of crystal structure. In a rough way our argument can still apply; the constants α' and β' depend on the crystal structure but are apparently not very sensitive.

For metals non-central forces are involved but an expansion such as (7) is still possible, and the coefficients $A_{\nu\beta}$ are approximately determined by the Debye Θ value.

4. — Quantum effects.

The argument of the previous section has shown that if we measure distances in terms of r' as unit, and energies in terms of ε'_0 , the thermodynamic functions of all simple substances up to the melting point in the region where a classical approximation is valid can be reduced to equivalent form.

Let us define a reduced temperature τ equal to $T/mv^{\frac{2}{3}}\Theta^2$. Then if as in Sect. 2 we heat our solid at constant volume from the absolute zero, we reach a temperature τ_m at which the solid first begins to melt, and then a higher temperature τ'_m at which the solid phase disappears; τ_m and τ'_m are both constants.

In the region of validity of our classical approximation energy and entropy changes depend on τ only; for example the entropy change between the first appearance of the liquid phase and the final disappearance of the solid phase is $S(\tau'_m) - S(\tau_m)$, and is the same for all specific volumes. However at sufficiently low temperatures quantum effects become important, and hence for example the absolute values of the entropy at the melting point change as the volume is varied. We shall now see that this effect can approximately be taken into account quite simply by additive constants depending on the volume.

For the energy at any temperature the constant to be added is the static lattice energy at absolute zero E_0 , and we have

$$(8) \quad E = E_0 + \varepsilon'_0 \mathcal{E}_0(\tau).$$

If we define change in E from its static value by means of the integral of specific heat, $\int c_v dT$, the difference between classical and quantum values for the integral is exactly balanced by the zero point energy. This can be readily confirmed for the Debye model.

The entropy can be defined by

$$(9) \quad S(T) = \int_0^T \frac{c_v}{T} dT = \int_0^K \frac{c_v}{T} dT + \int_K^T \frac{c_v}{T} dT,$$

where K is a temperature above which the specific heat may be regarded as classical. Replacing c_v by its classical value in the second integral, we find that

$$(10) \quad S(T) = S_0 + S(\tau),$$

where S_0 depends on K , and would therefore be determined by the Debye Θ . In fact in the region in which c_v differs from its classical value we may regard

the Debye approximation as reasonable for the properties of the solid and we may use it to determine S_0 . For a Debye model at high temperatures the entropy is given by,

$$(11) \quad \left\{ \begin{aligned} S_D &= 3nk \ln (T/\Theta) + 3nk \\ &= 3nk \ln \tau + 3nk \ln (mv^{\frac{3}{2}}/\Theta) + 3nk \\ &= S_0 + S_D(\tau) \end{aligned} \right.$$

and hence S_0 in (10) is equal to $3nk \cdot \ln (mv^{\frac{3}{2}}/\Theta)$. We shall make further use of formula (10) in the next section.

We shall now consider the modifications necessary when the solid is still

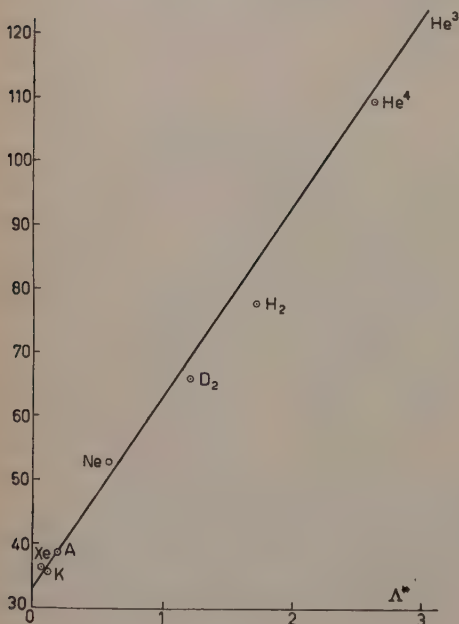


Fig. 3.

in a degenerate state at the melting point, so that classical theory is not a valid approximation. When the intermolecular potentials are as in Sect. 2, so that an exact law of corresponding states is valid on the classical theory, we may follow DE BOER [10] in introducing a parameter A^* ($= \hbar/r_0 \sqrt{(m\epsilon_0)}$) when quantum effects are present. We should then replace $C(u)$ in (5) by $C(u, A^*)$, and if we confine our attention to melting at atmospheric pressure we can obtain a function $K(A^*)$ which represents the values of $C(u, A^*)$ at volumes u which correspond to melting at atmospheric pressure (u will thus also depend on A^*) Table I represents the melting data for the inert gases, and from this values of $K(A^*)$ can be plotted as a function of A^* [13] (Fig. 3). It will be seen that the values lie reasonably well on a smooth curve (effectively linear); the values corresponding to H_2 and D_2 are somewhat displaced but this is not surprising. For 4He there is no melting point at atmospheric pressure, but we have assumed that the value of $K(A^*)$ is not very critical to changes of pressure, and have used a low temperature value at which the fluid phase is still $He I$, so that peculiarities due to quantum statistics do not enter. We can also estimate from the curve that for 3He ($A^* = 3.05$) the value of K would be about 122.

When we come to examine the variation of $C(u, A^*)$ with u for 4He (which

TABLE I.

Sub- stance	Molecular mass	De Boer para- meter Λ^*	Specific volume on melting cm^3/mole	Melting temp. T_m ($^\circ\text{K}$)	Debye θ value ($^\circ\text{K}$)	T_m/Θ	Lindeman constant $T_m/m\Theta^2v^{\frac{1}{3}}$ ($\cdot 10^{-6}$)
^4He	4.00	2.64	18.3	3.1	32	0.097	109
			14.4	7.9	55	0.144	110
			13.1	11.3	72	0.157	98
			11.6	17.3	92	0.188	100
			10.6	23.3	110	0.212	100
H_2	2.02	1.73	23.31	13.96	105	0.133	76.6
D_2	4.03	1.22	20.48	18.72	97	0.193	65.4
Ne	20.18	0.591	13.98	24.57	63	0.390	52.8
A	39.94	0.187	24.61	83.85	80	1.05	38.8
Kr	83.7	0.102	29.65	115.95	64	1.81	35.3
Xe	131.3	0.064	37.09	161.3	55	2.93	36.5

Data for Helium have been taken from J. S. DUGDALE and F. E. SIMON: *Proc. Roy. Soc.*, A 218, 291 (1953); for the remainder from the experimental results of CLUSIUS and his co-laborators.

is the only substance for which data are available) the surprising feature previously noted by SIMON [1] is the insensitivity of $C(u, \Lambda^*)$ to changes in u . Thus C changes by only 10% even though T_m/Θ and u change by a factor of 2. At sufficiently high temperatures and pressures we should expect C to attain its classical value, but it seems to be approaching this value extremely slowly.

It has been pointed out previously by the writer that the amplitudes of vibration of helium atoms vary along the melting curve, and are far in excess of their classical values. This was also interpreted as indicating that zero-point vibrations had little influence on melting since their frequency distribution did not include a sufficient contribution from long waves. However for a given value of T_m/Θ the partition between zero point energy and thermal energy is completely specified, and one might have expected the amplitude of vibration at the melting point to be likewise determined. It is thus surprising in comparing hydrogen at its melting point, and helium under pressure to find that for the same T_m/Θ the amplitudes of vibration (proportional to $T_m/m\Theta^2v^{\frac{1}{3}}$) are different at the melting point. This point would seem worthy of further investigation.

5. - Further consequences of a law of corresponding states.

If an exact law of corresponding states is valid, then for melting at the triple point we should expect $\Delta v/v$ and ΔS to be constant in the transition from the solid to the liquid phase. For the heavier inert gases this is well satisfied (see Table II). We shall now examine the consequences of our wider assumption of Sect. 3, which will enable us to say something of the behaviour of $\Delta v/v$ and ΔS along the melting curve.

As in Sect. 4 our reduced temperatures τ are defined in units of $mv_s^{\frac{2}{3}}\Theta^2$, and we identify two critical values τ_m, τ'_m corresponding to the initiation of melting, and the disappearance of the solid phase respectively. To transform to standard melting at constant temperature and pressure with change of volume we must choose a volume of the liquid v_l so that $T_m = T'_m$. Thus we have

$$(12) \quad \begin{cases} T_m = m\Theta^2 v_s^{\frac{2}{3}} \tau_m, \\ T'_m = m\Theta'^2 v_l^{\frac{2}{3}} \tau'_m \end{cases}$$

and hence the solid and liquid volumes are determined by the relation

$$(13) \quad \frac{\tau_m}{\tau'_m} = \frac{\Theta'^2 v_l^{\frac{2}{3}}}{\Theta^2 v_s^{\frac{2}{3}}}.$$

For a given intermolecular potential equation (13) enables v_l to be uniquely determined from v_s along the melting curve. But to determine the general behaviour to be expected from (13) we shall make the Grüneisen assumption $\Theta \propto v^{-\gamma}$ and we shall also assume that $\Delta v/v$ is small so that a Taylor expansion can be used. We then find that

$$(14) \quad \frac{\Delta v}{v} = \frac{\tau'_m - \tau_m}{\tau_m} \frac{1}{(2\gamma - \frac{2}{3})},$$

which would indicate that $\Delta v/v$ decreases as γ increases. At high pressures γ is determined by the repulsive part of the intermolecular potential, and is determined by the «hardness» of the substance. The relation (14) is only strictly valid if γ is constant, but we are using it to obtain a rough idea of the behaviour of $\Delta v/v$.

The change in entropy can be determined by using the results of Sect. 4, equations (10) and (11). We then have

$$(15) \quad \begin{cases} S_{\text{solid}} = S(\tau_m) + 3nk \ln (mv_s^{\frac{2}{3}}\Theta) \\ S_{\text{liquid}} = S(\tau'_m) + 3nk \ln (mv_l^{\frac{2}{3}}\Theta') \end{cases}$$

and hence

$$(16) \quad \Delta S = [\mathcal{S}(\tau'_m) - \mathcal{S}(\tau_m)] + 3nk \ln \left(\frac{v_e^{\frac{2}{3}} \Theta}{v_s^{\frac{2}{3}} \Theta'} \right).$$

The first term in (16) $[\mathcal{S}(\tau'_m) - \mathcal{S}(\tau_m)]$ is constant; the second term which is negative represents a decrease in entropy arising from the transition from τ to T variables, and depends on the value of γ . Making, as before, the assumption that $\Delta v/v$ is small and using (14), we find that

$$(17) \quad \Delta S = [\mathcal{S}(\tau'_m) - \mathcal{S}(\tau_m)] - \frac{\tau'_m - \tau_m}{\tau_m} \frac{\gamma - \frac{2}{3}}{2\gamma - \frac{2}{3}}.$$

Again (17) is only strictly valid if γ is constant, but it would seem to indicate that the entropy change on melting is not very sensitive to changes in pressure.

When quantum effects are present we shall consider only an exact law of corresponding states, and introduce the parameter Λ^* as before for melting at atmospheric pressure. ΔS and $\Delta v/v$ will now be functions of Λ^* and their values are given in Table II, and plotted graphically in Fig. 4.

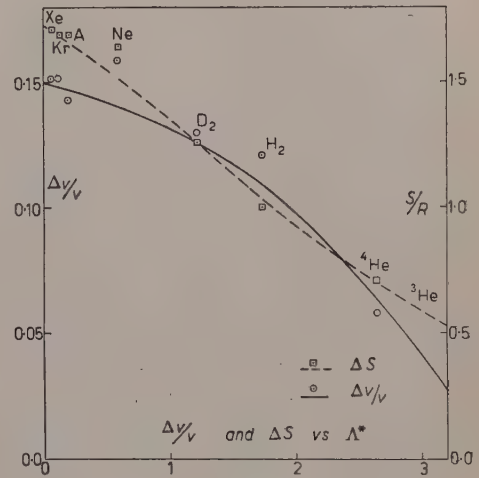


Fig. 4.

TABLE II. — *Melting data.*

Substance	De Boer parameter Λ^*	$\Delta v/v$	$\Delta S/R$
^4He (at 4 °K)	2.64	.058	0.715
H_2	1.73	.121	1.01
D_2	1.22	.130	1.26
Ne	0.591	.157 (*)	1.64
A	0.187	.143	1.69
Kr	0.102	.151	1.69
Xe	0.064	.151	1.71

(*) The data for Neon are taken from an early paper, and the volume changes would seem to require revision.

6. - Possibility of a critical point.

The two main sources of experimental data on $\Delta v/v$ for the melting of the solidified inert gases are those of BRIDGMAN [14] on Argon and Nitrogen, and recently GRILLY and MILLS [15] on Nitrogen. The variation of $\Delta v/v$ is quite substantial over the pressure range covered; thus even though the change in volume of the solid is only about 20%, $\Delta v/v$ changes by a factor of 2.5. If the relation (14) is valid this would imply a considerable variation of γ with pressure. The Lennard-Jones form of intermolecular potential does not lead to any such large variation of γ , but the potential may not be reliable for higher pressures and smaller specific volumes. It is also likely that the theory of corresponding states is less reliable for sensitive features of the melting transition such as $\Delta v/v$ and ΔS than for the position of the melting point. Further evidence regarding the variation of γ with volume at high pressures would be useful in this connection.

Many years ago the question was raised whether the solid-fluid transition ended in a critical point analogous to the liquid-vapour critical point. The matter has been discussed at considerable length in the literature, and in 1951 the present writer [11] suggested that there was sufficient theoretical information to rule out the existence of a critical point. The fundamental difference between a solid and a fluid was the presence or absence of long range order, and the point at which long range order disappeared could be identified with the melting point and would correspond to a singularity in the thermodynamic functions. The Lennard-Jones and Devonshire crude model of melting, and the above criterion for the melting point, led to a formula of the correct type (the Simon formula) for melting under pressure.

However, the above argument can say nothing about the nature of the melting transition, but merely that a singularity exists and that there is no continuity of state. It is still possible that at some point melting might cease to be a first-order transition, and this suggestion has recently been taken up by EBERT [16] and GRILLY and MILLS [15]. It seems to the writer that this possibility can now also be ruled out on theoretical grounds. EBERT and GRILLY and MILLS base their suggestion on an extrapolation formula for Δv , but it should be emphasized that such an extrapolation formula with no theoretical foundation can be quite unreliable. The earlier predictions of TAMMAN were of this type and led to erroneous conclusions [17].

The Lennard-Jones and Devonshire model replaces the many interstitial positions in Fig. 2 by a single interstitial position. This is a crude approximation, but may be sufficient to give some idea of the behaviour of a melting solid. The mathematical problem to be solved is the three dimensional Ising model

in the absence of a magnetic field. For the two dimensional Ising model an exact solution is available, and the specific heat is logarithmically infinite at the Curie point [18]. Although an exact solution is not available for the three-dimensional model, 9 terms of a series expansion for the specific heat at high temperatures have been derived for the f.c.c. lattice and these can be compared with the corresponding expansions for the two dimensional triangular lattice [19]. There seems little doubt after this comparison that the specific heat is also infinite for the three dimensional model.

Recently O. K. RICE [20] has pointed out that an infinite specific heat in an incompressible lattice would give rise to curves of Van der Waals type for a compressible lattice, and hence to a first order transition. This result can be applied to the Lennard-Jones and Devonshire model of melting [21], and shows that as long as the lattice is compressible the transition will always be first order. It is interesting to note that equation (14) leads to exactly the same conclusion; $\Delta v/v$ can only become zero if γ is infinite or if the lattice ceases to be compressible. This will be the case, for example, for a fluid of hard spheres, and the properties of such a fluid cannot therefore be used as a guide to the nature of the melting transition. Our tentative conclusion is that with the possible exception of such a fluid the melting transition will always be first order.

It is also interesting to note that for sufficiently high pressures, for which the attractive terms in the Lennard-Jones potential can be neglected, the repulsive term can be put in the form $Ar'^{-n}(r'/r)^n = \epsilon'f(r'/r)$, so that an *exact* law of corresponding states is valid for all volumes. From this we can deduce exactly that in the range covered by this form of potential $\Delta v/v$ and ΔS are constant for all volumes. (This is consistent with (14) and (17) since γ is constant for such a purely repulsive potential).

A transition point is to be expected along the melting curve of a solidified inert gas when the atoms begin to ionize so that the substance becomes metallic. Recent calculations by TEN SELDAM [22] for helium indicate that such a transition would not be expected below a pressure of about 10^8 atmospheres. In any case we should not expect such a transition point to be a critical point, but rather more analogous to a polymorphic transition point.

7. — Hard spheres.

A good deal of theoretical work has been devoted to attempting to determine the nature of the transition associated with a fluid of hard spheres. This problem has great intrinsic interest, although the considerations of the previous section show that we must be careful in drawing conclusions from it

regarding the nature of the melting transition. We may however be able to use it to throw some light on the problem raised in Sect. 1, i.e. the possibility of superheating of the solid phase. The Lennard-Jones and Devonshire model in conjunction with the observation of Rice lead to the conclusion that superheating should be possible.

The hard sphere problem has been reviewed recently by TEMPERLEY [23], who points out that any conclusions based on approximations of the superposition type cannot be regarded as reliable; also recent calculations of ZWANZIG [24] on hard squares and cubes seem to indicate that the higher virial coefficients will change sign. The basic difficulty at the moment is the lack of a sufficient number of virial coefficients to warrant any detailed calculations.

In the opinion of the present writer an insight into the nature of the melting transition can be obtained from a study of the Ising model of an antiferromagnetic in the presence of a magnetic field. The Ising model of a ferromagnetic has proved of great assistance in elucidating the properties of liquid-vapour

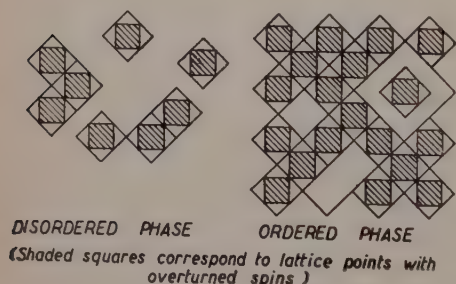


Fig. 5.

equilibrium and phenomena associated with the critical point [25]. For the breakdown of an ordered phase, and for the properties of order-disorder transitions with unequal ratios of constituents, the model of an antiferromagnetic should be capable of fulfilling a similar role. In particular at very low temperatures a critical field exists below which the ordered phase is stable, and above which the disordered phase is stable [26]. Decreasing the field corresponds to increasing the density, and for the two dimensional quadratic lattice, for example, the model bears close similarity to the condensation of hard squares. The zero order term in the expansion arises from spins no two of which are adjacent, and this corresponds to the condition of non-overlap of hard squares (Fig. 5). The major difference between the Ising model and the condensation problem is that the squares cannot take up continuous positions, but are restricted to discrete positions because of the lattice structure. However one would not expect this to have a serious influence on the nature of the transition. For the simple cubic lattice the model corresponds to hard cubes.

Although an exact solution is not available for the Ising model several terms of series expansions have been derived, and these can be transformed into the form of virial expansions. This approach is being followed by my research student D. M. BURLEY at King's College who finds that for the hard

squares problem,

$$(18) \quad \frac{P}{nkT\rho} = 1 + 2.5\rho + 4.333\rho^2 + 4.25\rho^3 - 3.8\rho^4 - 29.166\rho^5 - 71.857\rho^6 - 86.875\rho^7$$

and for hard cubes,

$$(19) \quad \frac{P}{nkT\rho} = 1 + 3.5\rho + 6.333\rho^2 + 1.75\rho^3 - 29.80\rho^4 - 138.833\rho^5 - 509.857\rho^6 - 1819.125\rho^7; \quad (\rho = \text{density}).$$

It will thus be seen that the virial coefficients change sign as suggested by TEMPERLEY [23]. The form of pressure-density relationship implied by (19) is shown in Fig. 6 for 6, 7 and 8 terms of the virial expansion. The maximum in the curve represents the limit of stability of the phase, and it seems that above a certain density the disordered phase ceases to be stable.

The breakdown of the ordered phase can also be considered similarly although the detailed treatment is more difficult. If the free energy is plotted as a function of density for the two phases some idea can be obtained of the singularity corresponding to their intersection. The result of the best approximations so far dealt with is shown in Fig. 7.

It seems that a closer investigation is necessary before any definite conclusions can be drawn regarding the nature of the transition. However it is worth noting that there is no evidence of a singularity at the transition point on either ordered or disordered phase; the classical description of melting as the meeting point of two continuous phases seems to be valid.

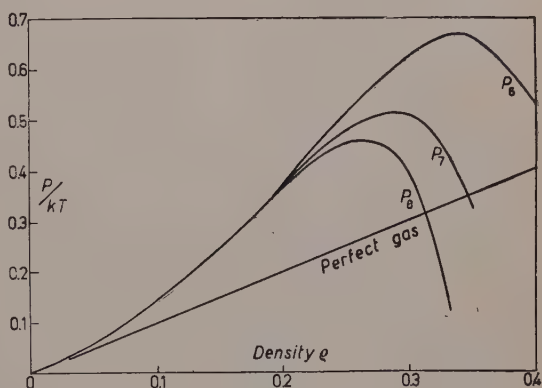


Fig. 6.

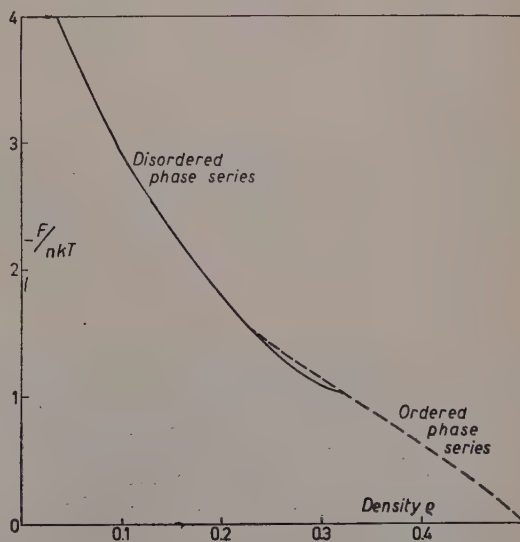


Fig. 7.

REFERENCES

- [1] F. E. SIMON: *Changements de Phases* (Paris, 1952), p. 329.
- [2] L. SALTER: *Phil. Mag.*, **45**, 369 (1954).
- [3] J. J. GILVARRY: *Phys. Rev.*, **102**, 308, 317, 325, 331 (1956).
- [4] C. DOMB and L. S. SALTER: *Phil. Mag.*, **43**, 1083 (1952).
- [5] I. J. ZUCKER: *Journ. Chem. Phys.*, **25**, 915 (1956).
- [6] F. C. FRANK: *Proc. Roy. Soc., A* **215**, 43 (1952); D. TURNBULL and J. C. FISHER: *Journ. Chem. Phys.*, **17**, 71 (1949); D. TURNBULL: *Journ. Metals*, **188**, 1144 (1950); D. TURNBULL and R. E. CECH: *Journ. Appl. Phys.*, **21**, 804 (1950); D. TURNBULL: *Journ. Chem. Phys.*, **18**, 198 (1950), **20**, 411 (1952).
- [7] P. W. BRIDGMAN: *The Physics of High Pressures* (New York, 1949) p. 210.
- [8] J. S. DUGDALE and F. E. SIMON: *Proc. Roy. Soc., A* **218**, 291 (1953).
- [9] C. DOMB: *Changements de Phases* (Paris, 1952), p. 338; C. DOMB and J. S. DUGDALE: in *Progress in Low Temperature Physics*, vol. II (Amsterdam 1957), p. 338.
- [10] J. DE BOER: *Physica*, **14**, 139 (1948).
- [11] C. DOMB: *Phil. Mag.*, **42**, 1316 (1951).
- [12] M. BORN and K. HUANG: *Dynamical Theory of Crystal Lattices* (Oxford, 1954).
- [13] This variation of K was noted by J. S. DUGDALE and F. E. SIMON: *Proc. Roy. Soc.*, **218**, 291 (1953).
- [14] P. W. BRIDGMAN: *Phys. Rev.*, **46**, 930 (1934); *Proc. Am. Acad. Arts Sci.*, **70**, 1 (1935).
- [15] E. R. GRILLY and R. L. MILLS: *Phys. Rev.*, **105**, 1140 (1957).
- [16] L. EBERT: *Oesterr. Chem. Ztg.*, No. 1/2, 1 (1954).
- [17] F. E. SIMON: *L. Farkas: Memorial Volume* (Jerusalem, 1952), p. 37.
- [18] L. ONSAGER: *Phys. Rev.*, **65**, 117 (1944); G. F. NEWELL and E. W. MONTROLL: *Rev. Mod. Phys.*, **25**, 353 (1953).
- [19] C. DOMB and M. F. SYKES: *Phys. Rev.* **108**, 1415 (1957).
- [20] O. K. RICE: *Journ. Chem. Phys.*, **22**, 1935 (1954).
- [21] C. DOMB: *Journ. Chem. Phys.*, **25**, 783 (1956).
- [22] C. A. TEN SELDAM: *Proc. Phys. Soc., A* **70**, 97 (1957).
- [23] H. N. V. TEMPERLEY: *Proc. Phys. Soc., B* **70**, 536 (1957).
- [24] R. W. ZWANZIG: *Journ. Chem. Phys.*, **24**, 855 (1956).
- [25] C. N. YANG and T. D. LEE: *Phys. Rev.*, **87**, 404, 410 (1952).
- [26] J. E. BROOKS and C. DOMB: *Proc. Roy. Soc., A* **207**, 343 (1951).

INTERVENTI E DISCUSSIONI

— J. S. DUGDALE:

I should like to point out that the values of the Lindeman constant usually derived for the inert gas solids (other than helium) make use of the volume V of the solid at the melting temperature, T_m . On the other hand the θ -value is taken from low temperature measurements corresponding to an appreciable different volume. For theo-

retical comparison it would be more satisfactory to take the θ corresponding to the volume V at the melting temperature. Unfortunately the data for this are not yet available but the limitation of the present figures should be born in mind: the true values would be markedly different.

— R. A. UBBELOHDE:

According to the speaker's theory, all the changes in various parameters on melting are attributed to changes in the content of vibrational energy. It seems worth considering, however, whether quite large positional defects such as the formation of holes in the melt may also contribute to $\Delta v/v$ and ΔS .

— C. DOMB:

There are many types of hole corresponding to different displacements of molecules from their static equilibrium values. The approximation I propose assumes that holes arising from displacements far from equilibrium are not significant up to the melting point. If they were they would in fact make a contribution to the specific heat of the solid near the melting point (pre-melting). I believe this contribution is very small for simple solids, although it may be significant for solids consisting of more complicated molecules investigated by Prof. UBBELOHDE.

— J. E. MAYER:

I believe that Mr. DOMB uses «law of corresponding states» to any two equations of state which can be superimposed by changing the kT and volume scale.

— E. A. GUGGENHEIM:

It is unfortunate that DOMB should mention the principle of corresponding states and then dismiss it in such an off-hand manner. If he will study the literature, in particular CLUSIUS (*Zeits. Phys. Chem.*, B, **31**, 459 (1936)), he will find a much simpler and more convincing treatment of the properties of the inert elements at their melting-points.

— C. DOMB:

The method which I suggested does not consider vibrations, but attempts to formulate the configurational partition function. The approximation will be valid for the liquid phase if the spacing between atoms which are nearest neighbours does not usually deviate very considerably from the mean static value in the solid phase at the same volume. This is only assumed for liquids just above the melting point.

— J. E. MAYER:

May I add to the reply of Mr. DOMB, merely by way of possible clarification for a classical system, if the potential energy can be expressed as the value at some equilibrium configuration plus terms proportional to the square of the displacements, then all the thermodynamic properties would be given exactly by the equations for a crystal with some fixed Debye Θ_0 . If there are important terms which are cubic or quartic in the displacements but which are random in sign, one may expect this to have little effect on the thermodynamic functions. However, the mechanical properties would be strongly altered by these terms, and the system would no longer be capable of oscillating with any single pure frequency.

— J. WILKS:

The specific heat at liquid ^4He below 0.6°K has a value very similar to that which is given by Debye's theory for a continuum which can only support longitudinal waves. This would seem good evidence for atomic motion of a vibrational type in at least one liquid.

— R. EISENSCHITZ:

The mean distance of atoms in a liquid is such that on the average a molecule moves on a flat maximum of potential rather than about a minimum.

— M. TODA:

If we take Lennard-Jones-Devonshire model, the vibration of atom in liquid is far from harmonic. But I think that in liquid state structures with nearly the same free energy come into play at the same time.

Expansion of liquid introduces large anharmonicity if we use Lennard-Jones model. But actually it seems to me that expansion of liquid is not directly connected to increase of anharmonicity and introduction of other structures (like body-centered cubic) than closed packed one is responsible for the expansion, and the motion of atoms in liquid state will be nearly harmonic than would seem first from crude model. We can improve the model taking many structures into account. And this will be responsible for the entropy of melting (the entropy of structural change).

The Equation of State of solid Helium.

J. S. DUGDALE

Division of Pure Physics, National Research Council - Ottawa

1. - Introduction.

Solid helium (*) has recently been used as a pressure-transmitting medium in experiments to find out how the electrical resistance of metals at low temperatures changes under pressure [1,2]. The method employed was to apply the pressure at such a temperature that the helium was fluid and then to cool the bomb, containing the specimen and the helium, under conditions of constant volume to the desired low temperature. By knowing the equation of state of solid helium the final pressure could be deduced (+). For the pressures so far used (up to 3000 atmospheres) the equation of state of the solid as determined experimentally by DUGDALE and SIMON [3] is sufficient, but if the pressure range is to be extended, more information on the equation of state is needed. The recent measurements of STEWART [4] provide the basis for obtaining this information. The method used to derive the equation of state and the results obtained will now be briefly described.

2. - The method and assumptions.

The steps in the calculation are as follows:

a) The first step is to use the isotherm measured at 4.2 °K to deduce U_0 , the internal energy at absolute zero, as a function of the volume, V .

(*) Unless otherwise stated, the helium referred to is ^4He .

(+) It should be possible to invert this procedure and investigate the equation of state of solid ^3He by using the electrical resistance of a suitable substance to determine the pressure in the solid as a function of temperature and volume.

(For this purpose 4.2 °K is effectively the absolute zero [3]). The change in internal energy, ΔU_0 , in altering the volume from V_1 to V_2 at 0 °K is given by:

$$\Delta U_0 = - \int_{V_1}^{V_2} p \, dV.$$

b) The second step is then to derive from the $U_0 - V$ curve so obtained the relationship between the Debye temperature of the solid, θ_D^2 , and the volume V . (Experiments [3] have shown that a Debye approximation is quite good for solid helium). To do this, it is assumed that $\theta_D^2 \propto d^2 U_0 / dr^2$, where r is the interatomic distance [5]. To evaluate the constant of proportionality, one value of θ_D was taken from specific heat measurements [3].

c) Thirdly the Lindemann melting formula relating θ , V , and the melting temperature, T_m , is used to find T_m as a function of V . A value for the Lindemann constant for helium was taken from the work of DUGDALE and SIMON [3], which had already shown that the Lindemann melting formula was valid for solid helium throughout the range of their experiments (up to 3 000 atmospheres).

d) The last step is to use a Debye-Grüneisen model (*) of the solid to calculate the pressure corresponding to the volume, V , at the melting temperature. This gives the melting curve.

e) As a further check on the calculations, one can calculate the zero point energy $((9/8)R\theta_D)$ and subtract it from the internal energy. This gives the lattice energy, which may then be compared with that calculated from a suitable interatomic potential.

3. - The results.

The results are represented in Fig. 1 and 2. Fig. 1 shows the isochores (lines of constant volume) of solid helium calculated in the manner outlined above. It also shows the melting curve so derived: for comparison a melting curve based on experiment is also plotted. MILLS and GRILLY [6] have measured

(*) By this is meant a solid in which (a) the specific heat at constant volume, for example, is a function of θ/T , where θ depends only on volume, and (b) the temperature dependence of C_V is given by the Debye function. The calorimetric experiments of Dugdale and Simon showed that this was approximately true of solid helium.

the melting curve of helium up the 3500 atmospheres; they gave their results in the form of the following equation:

$$P + 17.80 = 17.315 T^{1.5554},$$

where P is the melting pressure in kg/cm^2 corresponding to the temperature T in $^{\circ}\text{K}$. Points of this curve have been plotted up to 20 000 atmospheres in Fig. 1. Other experimenters [7] have made measurements up to higher pressures (up to 9 000 atmospheres) but their results are less accurate. In any case, all measurements so far are consi-

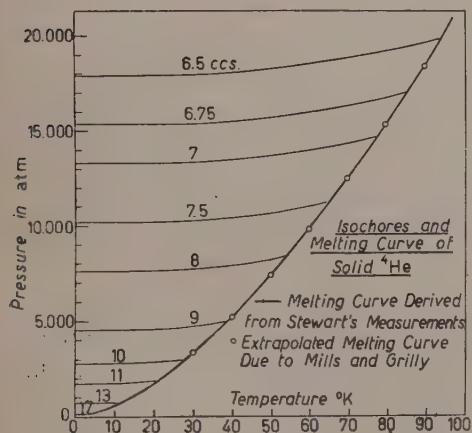


Fig. 1.

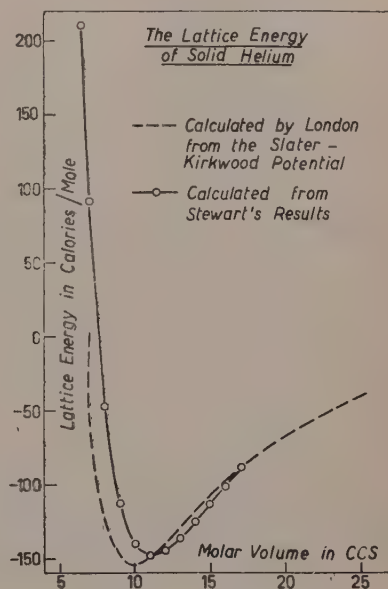


Fig. 2.

istent with the equation given by MILLS and GRILLY. It is seen that the agreement between the extrapolated experimental curve and the melting curve deduced, as described above, from Stewart's experiments is very close indeed.

Fig. 2 shows the lattice energy of solid helium calculated as described together with London's calculation of the lattice energy assuming a Slater-Kirkwood potential [8]. The agreement for large molar volumes is satisfactory: at the minimum of energy and at molar volumes smaller than this the agreement is not good. It is of course known that the Slater-Kirkwood potential does not predict altogether correctly the properties of the gas phase [9]; moreover, the values of θ_D which have been taken were chosen to represent the low temperature specific heats [3] reasonably well and they may differ signi-

ficantly from the values of θ_∞ , which strictly are needed for calculating the zero point energy [10]. For completeness, the Debye temperature, the Grüneisen parameter γ ($\gamma = -d \log \theta / d \log V$), and the melting temperature as calculated for various values of the volume are listed in Table I.

TABLE I. - *The Debye temperature, the Grüneisen γ and melting temperature of solid helium calculated for various values of volume.*

V (cm ³)	θ_D (°K)	γ	T_m (°K)
16	44	2.71	4.9
15	52	2.49	6.6
14	62	2.31	8.8
13	73	2.17	11.7
12	86	2.06	15.5
11	102	1.96	20.8
10	123	1.87	28.0
9	149	1.8	38.5
8	184	1.74	53.9
7	230	1.68	77.7
6.5	261	1.65	94.5

4. - Conclusions.

From the remarkably close agreement between the extrapolated experimental melting curve and that calculated by the methods outlined in this paper, one may draw the following conclusions:

a) that the calculated melting curve and isochores of the solid can be accepted with considerable confidence;

b) that in spite of the large zero point motion of the atoms composing it, a relatively simple model of solid helium is sufficient to account quite well for its properties provided that the effect of the zero point energy is taken into account at the very outset of the calculations (*); and

c) that the Lindemann melting formula appears to be valid over an enormous region of the melting curve, a fact which deserves close theoretical attention.

(*) To carry out the calculation from first principles, the U_0 - V relationship should be derived from the interatomic potential. This has already been attempted with some success [11] but the difficulty is that a really satisfactory theoretical interatomic potential for helium does not yet exist.

* * *

The author is much indebted to Miss D. SOUBLIÈRE for carrying out the calculations involved in this paper and to Dr. D. K. C. MACDONALD for his helpful comments on the manuscript.

REFERENCES

- [1] J. S. DUGDALE and J. A. HULBERT: *Can. Journ. Phys.*, **35**, 720 (1957).
- [2] J. S. DUGDALE and D. GUGAN: *Proc. Roy. Soc.*, A **241**, 397 (1957).
- [3] J. S. DUGDALE and F. E. SIMON: *Proc. Roy. Soc.*, A **218**, 291 (1953).
- [4] J. W. STEWART: *Journ. Phys. Chem. Solids*, **1**, 146 (1956).
- [5] C. DOMB: *Changements de Phases* (Paris, 1952), p. 338.
- [6] R. L. MILLS and E. R. GRILLY: *Phys. Rev.*, **99**, 480 (1955).
- [7] For a summary of this work, see: C. DOMB and J. S. DUGDALE: *Progress in Low Temperature Physics*, vol. 2 (Amsterdam, 1957), p. 338.
- [8] F. LONDON: *Proc. Roy. Soc.*, A **153**, 576 (1936).
- [9] J. L. YNTEMA and W. G. SCHNEIDER: *Journ. Chem. Phys.*, **18**, 646 (1950).
- [10] C. DOMB and L. S. SALTER: *Phil. Mag.*, **43**, 1083 (1952).
- [11] J. S. DUGDALE and D. K. C. MACDONALD: *Phil. Mag.*, **45**, 811 (1954).

INTERVENTI E DISCUSSIONI

— C. DOMB:

Dr. DUGDALE's observation that the θ values used in estimating the Lindemann constant C need to be revised would mean a far smaller variation of C with A^* than indicated in my paper. It may help to account for the apparent discrepancy noted between solid hydrogen and solid helium.

Properties of Solid Argon.

E. R. DOBBS, B. F. FIGGINS and G. O. JONES

Department of Physics, Queen Mary College, University of London - London

The solidified inert gases are extremely useful subjects for fundamental studies on crystal dynamics because of their spherically symmetrical and short-range interatomic potential fields and because one can usually ignore the electronic contributions to physical properties. There have accordingly been many theoretical and experimental investigations in recent years into the properties of solid argon, the most convenient of the inert gas substances for such studies.

In our laboratory we have determined accurately the density and expansivity (α) of solid argon down to 20 °K, using X-ray diffraction techniques, and the compressibility (κ) at temperatures near 60 °K, using ultrasonic techniques. We have also re-determined the specific heat down to about 15 °K.

The measurements of density, illustrated in Fig. 1, show that the expansivity is about double the previously assumed value. This has a number of important consequences. Since C_p/C_v now appears to have the very high value 1.45 at the melting point, the anomalously high value of C_p

(8.5 cal mole⁻¹ deg⁻¹) found by CLUSIUS [1] is accounted for. C_v does not in fact rise above $3R$. The discrepancies between our values of adiabatic com-

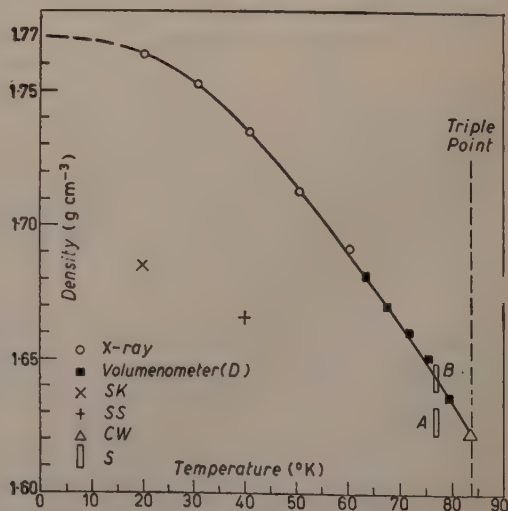


Fig. 1. — Experimental density of solid argon. *D*, DOBBS *et al.* (1956); *SK*, DE SMEDT and KEESOM (1925); *SS*, SIMON and VON SIMON (1924); *CW*, CLUSIUS and WEIGAND (1940); *S*, STEWART (1956).

compressibility and Stewart's values [2] of isothermal compressibility are also resolved.

Using the new values of C_p , together with unpublished values by R.¹W. HILL at lower temperatures and those of CLUSIUS, we can make a comparison with the theoretical Debye curve derived from Leighton's frequency spectrum for the cubic close-packed lattice [3] and this is shown in Fig. 2. It will be

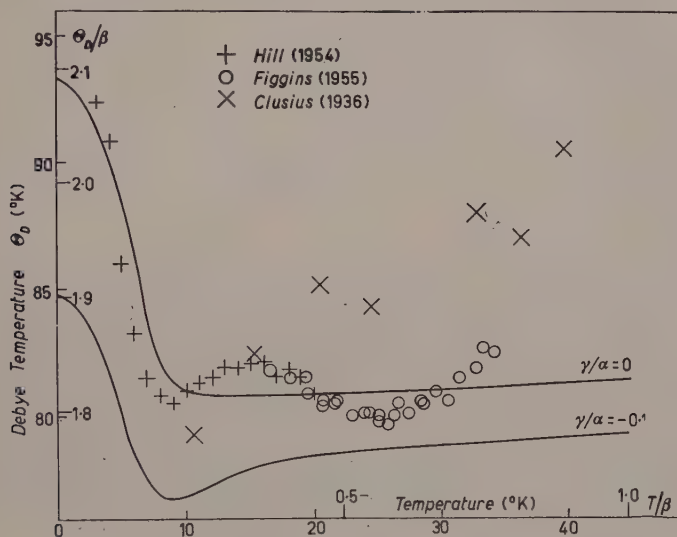


Fig. 2. - Debye plots for argon with central-force interactions ($\gamma/\alpha = 0$) and small anisotropy ($\gamma/\alpha = -0.1$). (After LEIGHTON).

seen that good agreement is obtained with the curve for central-force interactions ($\gamma/\alpha = 0$), the experimental points showing the rise predicted by LEIGHTON.

It is now possible to estimate with fair accuracy the value of Grüneisen's parameter ($\gamma = \alpha V / \kappa_s C_p$) for solid argon, and the following table gives values at four temperatures

T (°K)	20	40	60	80
γ (exp.)	2	2.8	2.8	2.4
γ (theor.)	2.9	2.8	2.8	2.8

together with the theoretical values derived by DOMB and ZUCKER [4] using a (12,6) inter-atomic potential and an anharmonic Einstein model (after HENKEL [5]) with improved constants.

The best constants in $\varphi(r) = Ar^{-12} - Br^{-6}$ are found to be

$$A = 1.63 \cdot 10^{-7} A^{12} \text{ erg}$$

$$B = 1.05 \cdot 10^{-10} A^6 \text{ erg}$$

and this function is shown in Fig. 3 to be in remarkable agreement with that of WHALLEY and SCHNEIDER [6] derived from their measurements on the second virial coefficients of argon gas. These curves however differ greatly from the curve obtained by adding the theoretical estimates of KUNIMUNE [7]

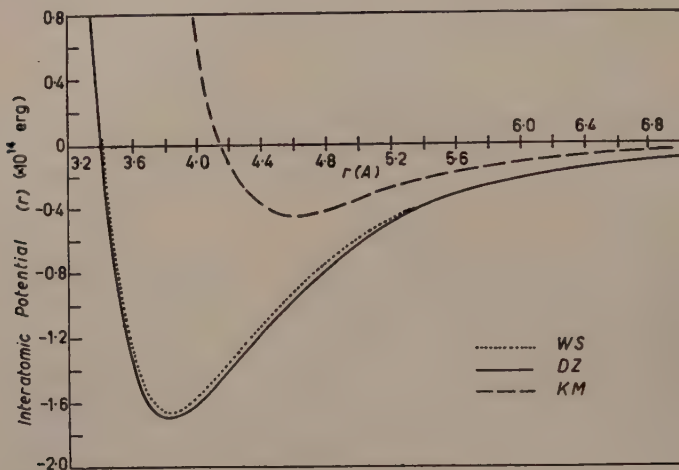


Fig. 3. — Interatomic potentials for a pair of argon atoms. WS, WHALLEY and SCHNEIDER, from gas data; DZ, DOMB and ZUCKER, from crystal data; KM, KUNIMUNE-MARGENAU, from quantum theory.

and of MARGENAU [8] for the repulsive and attractive parts of the interatomic potential.

A fuller account of the comparison between experiment and theory has recently been published by two of us [9].

REFERENCES

- [1] K. CLUSIUS: *Zeits. Phys. Chem.*, B **31**, 459 (1936).
- [2] J. W. STEWART: *Phys. Rev.*, **97**, 578 (1956).
- [3] R. B. LEIGHTON: *Rev. Mod. Phys.*, **20**, 165 (1948).
- [4] C. DOMB and I. J. ZUCKER: *Nature*, **178**, 484 (1956).
- [5] J. H. HENKEL: *Journ. Chem. Phys.*, **23**, 681 (1955).
- [6] E. WHALLEY and W. G. SCHNEIDER: *Journ. Chem. Phys.*, **23**, 1644 (1955).
- [7] M. KUNIMUNE: *Journ. Chem. Phys.*, **18**, 754 (1950).
- [8] H. MARGENAU: *Rev. Mod. Phys.*, **11**, 1 (1939).
- [9] E. R. DOBBS and G. O. JONES: *Rep. Progr. Phys.*, **20**, 516 (1957).

INTERVENTI E DISCUSSIONI

— C. DOMB:

The theoretical derivations of γ values by BARRON and ZUCKER are not inconsistent. BARRON dealt with a harmonic model and took account of the vibration spectrum; this should become correct at lower temperatures. ZUCKER dealt with anharmonic effects by an Einstein type of approximation (following HENTEEL) and this would not be correct at low temperatures. It may well be invalid at 20 °K for solid argon.

— G. O. JONES:

I agree: in making the comparison I was referring to the results for the models of Barron and Zucker as published.

— J. E. MAYER:

The remarkable agreement between the pair intermolecular potential functions obtained from the second virial coefficients and from the equation of state of the solid is most gratifying. We have always assumed that the potential energy of the crystal can, for most purposes, be regarded as the sum of the pair potentials without the introduction of terms depending on the positions of triples of atoms, or quadruples etc. However, the quantum mechanical justification of this due to uncertainties of convergence and the large number of close triples, quadruples etc., in the condensed phase, has always been shaky. It is gratifying to find experimental justification for the neglect of these higher order terms.

— B. N. BROCKHOUSE:

I would like to remark that in recent neutron diffraction work on liquid argon, HENSHAW (*Phys. Rev.*, 1957) found that the distance of closest approach of the argon atoms was too small to be consistent with existing potentials.

— G. O. JONES:

Our X-ray measurements of inter-atomic distance give a value smaller by less than 2% than the distance from $V=0$ to the potential minimum, and are accurate to better than 1 in 1000. (The difference is due to the interaction of other than nearest neighbours). Henshaw's measured distance of closest approach in the liquid is thus presumably smaller than the inter-atomic distance in the solid.

Thermal Expansion and Melting of Simple Metals.

G. BORELIUS

Department of Physics, Royal Institute of Technology, - Stockholm

The usual way of theoretical treatment of the changes of energy and entropy of simple solids is to discuss the lattice vibrations on the simplifying assumption of constant volume and to compare the results with values obtained from measurements at constant practically zero pressure after corrections to constant volume. This procedure, however, leaves aside the influence on energy, entropy and volume of the thermal structural changes in the lattice. At present, we have, however, good reasons to believe that the structural defects are of a considerable magnitude already in the solid state and that they may be related to the changes on melting and in the liquid state. It has therefore been tempting to discuss and compare with each other the changes of energy, entropy, and volume directly observed at zero pressure, and to try to divide them in parts due to the lattice vibrations and to the structural defects of the lattice.

At low temperatures where the vibrational parts are dominating, it is known that the energy and entropy can be approximately described by Debye functions and that the increase of volume is proportional to the increase of energy. If these experiences are supplemented by the simple assumption that the vibrational molar energy at high temperatures approach the classical value $3RT$ and thus is described approximately by a Debye function over the whole range of temperature covering the solid as well as the liquid states, the vibrational parts of energy, entropy, and volume can be numerically determined. The structural parts are then obtained as differences between the observed total changes and the vibrational parts. The changes of energy, entropy, and volume on melting thus are assumed to be entirely, or at least preponderantly of structural nature. The structural changes computed in this way are starting in the solid range, increasing discontinuously at the melting point, and continuing to increase with temperature in the liquid range.

In the case of the closepacked cubic metals for which usable measurements are available, that is Cu, Ag, Au, Al, and Pb, the structural changes of energy, entropy and volume are found to be simply related. The structural entropy plotted against the structural change of volume gives a diagram where for all five metals the experimental points within the limits of error fit to a common curve which also simply connects the solid and liquid states. The plots of structural energy against structural change of volume are different from metal to metal, but it is for all the closepacked cubic metals possible to connect the solid and liquid ranges by continuous curves. The structural changes, including the discontinuous changes at the melting point, thus appear as an order-disorder transformation of the first order, that is a transition where a continuous variation of the degree of order is structurally possible but where a certain range is thermodynamically unstable, causing the two-phase equilibrium at the melting point.

This simple behaviour is, however, limited to the metals with the simplest of all structures, the cubic closepacked one. In metals with bodycentered or other less simple structures there seems to be at the melting point, besides the discontinuous increase of the lattice defects, also a change of the basic structure, which probably in most cases is a transition into the closepacked cubic structure.

E detailed survey of the speaker's papers on this subject will in a near future be published elsewhere in *Solid State Physics*, vol. VI.

INTERVENTI E DISCUSSIONI

— J. A. PRINS:

Your group of critically close packed metals shows an exceptionally small melting expansion ($< 5\%$). In other substances these are much bigger ($> 10\%$). How large is the volume change you find for hexagonally close packed metals?

— G. BORELIUS:

Of the hexagonal metals we only investigated zinc and did not find it so very different from the face centered cubical group.

— A. R. UBBELOHDE:

Has the author any model for the structural changes postulated by him? For example, does the coordination number (number of nearest neighbours) change more markedly in melting the group of metals referred to, than for some of the crystal packings exhibited by other metals?

— G. BORELIUS:

I think that melting without a change of the basic structure is characteristic for the closed packed cubic metals and that the close packed cubic structure is preferred by many other metals in the liquid state. KLEPPA has found very simple dependence in concentration for the heat of solution of the binary liquid mixtures PbCd, PbSn, PbBi, CdSn and SnZn. One could scarcely expect such simple relationships if the components had different structures. It is therefore probable that liquid Cd, Sn, Bi and Zn have the same basic structure as Pb, that is the close packed cubic one.

On the Quantum Effect on Melting.

M. TODA

Department of Physics, Faculty of Science of the Tokyo University - Tokyo

1. - The present communication aims to clarify the quantum effect on melting, which will help us in testing the fundamental ideas with respect to this phenomenon.

Thermodynamically the melting temperature is the point where the free energy of the solid state becomes equal to that of the liquid state. For heavy elements (in classical limit) the melting point T_m^0 is thus given by

$$(1) \quad F_l^0(T_m^0) = F_s^0(T_m^0),$$

where F_l^0 and F_s^0 are respectively the classical free energies of the liquid and the solid states, which are considered as smooth functions of temperature beyond the melting point. As we go to lighter elements the quantum effect comes into play, which is known to lower the melting point. Let $F = F^0 + F^q$ be the free energy, in which F^q stands for the quantum correction. The melting point T_m is now given by

$$(2) \quad F_l^0(T_m) + F_l^q(T_m) = F_s^0(T_m) + F_s^q(T_m).$$

If the quantum effect is relatively small we may use the expansion

$$F^0(T_m) = F^0(T_m^0) - S^0(T_m - T_m^0) + O\{(T_m - T_m^0)^2\},$$

where $S^0 = -\partial F^0/\partial T$ denotes the entropy in classical limit and we have assumed $\dot{p}^0 = -\partial F^0/\partial V \cong 0$. We get thus

$$(3) \quad T_m - T_m^0 = -\frac{T_m^0}{L^0} \{F_s^q(T_m^0) - F_l^q(T_m^0)\},$$

in which L^0 is the heat of melting in classical limit. We must note that we have got the shift in melting point without referring to the detailed classical theory of melting.

Going over to quantum statistical mechanics we may use the expression based on Kirkwood's expansion:

$$(4) \quad F^q(T) = \frac{1}{kT} \frac{\hbar^2}{12m} \int \exp[-\beta V] \sum_j \left\{ \nabla_j^2 V - \frac{\beta}{2} (\nabla_j V)^2 \right\} dq,$$

where k is the Boltzmann constant, m the mass of an atom, V the potential energy due to mutual interaction and $\beta = 1/kT$. The above formula is written for monoatomic substances. For a harmonic oscillator we have $F^q = \hbar^2 \omega^2 / 24kT$. If we assume Debye spectrum and three degrees of freedom for each atom

$$(5) \quad T_m - T_m^0 = -\frac{3}{40} \frac{Nk}{L^0} \{1 - (\Theta_l/\Theta_s)^2\} \Theta_s^2,$$

where Θ stands for the Debye temperature, and N is Avogadro's number. As to rare gases the mutual interaction between molecules is of the form

$$(6) \quad \varphi(r) = \frac{\varepsilon}{n-6} \left\{ 6 \left(\frac{r_0}{r} \right)^n - n \left(\frac{r_0}{r} \right)^6 \right\},$$

where $n \cong 12$. It is convenient to use the de Boer's reduced units

$$(7) \quad T^* = kT/\varepsilon, \quad L^{0*} = L^0/N\varepsilon, \quad \text{etc.}$$

Eq. (5) can be written as

$$(8) \quad T_m^* = T_m^{0*} \left[1 - \frac{3}{40} \{1 - (\Theta_l/\Theta_s)^2\} \Theta_m^{*2} / L^{0*} T_m^{0*} \right]$$

To see the order of magnitude we shall assume the plausible value

$$\Theta_l/\Theta_s = 0.9$$

and use the experimental values

$$L^{0*} = 1.19, \quad T_m^{0*} = 0.70,$$

then we get

$$T_m^* = T_m^{0*} (1 - 0.017 \Theta_s^{*2}).$$

From the experimental data for ^{20}Ne and ^{22}Ne , assuming the same formula as the above, we get the coefficient 0.0196 instead of 0.017 and $T_m^{0*} = 0.73$ instead of 0.70. (Neon is not a nice example, because $\Theta_m^* = 1.77$ for ordinary neon is a value rather too large to cut off the higher terms. Nevertheless the agreement above is not so bad.) We shall not be interested in small points; but the following is worth mentioning. Due to the atomic core the exponent n of the repulsive force seems to increase with atomic number in the series of rare gases. If this were true, there is no corresponding principle covering the rare gases, say from Ne to Xe, and it is not strange that the apparent limiting value $T_1^* = 0.70$ for this series does not coincide with the limiting value for hypothetical neon with infinitely heavy nucleus. With increasing n , the melting point T_1^* seems to decrease. This fact can be understood qualitatively when one considers that strong unharmonicity in the mutual potential energy will cause the melting point to be lower, or when one uses Mayer's theory of melting. In a similar way we get the heat of melting

$$(9) \quad L_m^* = L^{0*} - \frac{3}{20} \{1 - (\Theta / \Theta_s)^2\} \Theta_s^{*2} / T_m^{0*},$$

which gives the ratio of L_m for ^{20}Ne and ^{22}Ne in good agreement with experiment.

2. — What is the structural difference between solid and liquid states? Consider a liquid behaving classically. Its difference to solid state lies therein that in liquid phase molecules behave more freely and the structure is more disordered. Actually LENNARD-JONES and DEVONSHIRE worked out a theory of melting assuming that molecules can occupy interstitial lattice points in liquid state. Though this kind of restriction on molecular arrangements is undoubtedly far from reality the entropy of disordering in this model, which is $2Nk \ln 2$, roughly accounts for the actual entropy of melting.

We may understand the disordering in another way. For a monoatomic substance face-centered cubic is the structure with the lowest energy in solid region. If we calculate the energies of f.c.c., b.c.c. and other structures as functions of volume, we find that in liquid region the energy of f.c.c. comes out to be nearly the same as that of b.c.c. (and for larger volume such structures as simple cubic or diamond have energies lower than f.c.c.). Owing to large thermal fluctuations the probability for the liquid to take b.c.c. will be nearly the same as to take f.c.c. structure. As the possibility to take more than two structures lowers the free energy, structures with smaller co-ordination number will become more favourable at higher temperature. Thus the number of nearest neighbours, 12 in solid state, will become 10 or less, in average, in liquid state.

We may further take it, in accordance with the cell-model of liquid, that each cell accommodate two or more molecules, which change their places mutually and thus give rise to the so-called communal entropy. Actually if each cell contains two molecules and if one assumes that these two molecules rotate around each other like a dumb-bell the communal entropy of the system is $(Nk/2) \ln(2\pi)$.

It seems the common conclusion of the above considerations that the entropy of liquid is higher than that of the corresponding solid state by the entropy of disordering S_d which amounts approximately to Nk . As the volume change on melting is quite large (about 10%) for molecular substances, it seems safe to say that the disordering process completes its course during the transition. Disordering is accompanied by an energy increment $U_d = U_l - U_s$ and roughly $U_d/T_m \cong S_d$. If we denote by Z the partition function of molecular vibration we get the following equation for the melting point:

$$(10) \quad \frac{U_d}{T_m} - S_d = Nk \ln \frac{Z_l}{Z_s}.$$

If the vibration is harmonic U_d is nothing but the heat of melting in classical limit:

$$U_d = L^0.$$

S_d can be estimated from the classical limit:

$$S_d/Nk = L^{0*}/T_m^{0*} - 3 \ln(\Theta_s/\Theta_l).$$

With $\Theta_s/\Theta_l = 1.1$ we get $S_d = 1.3Nk$. As we have expected S_d is of the order of Nk .

As the disordering process completes its course during the transition it is natural to assume that U_d , S_d and Θ_s/Θ_l are not influenced so much by quantum effect. Assuming the Debye model through-out one gets a relation between T_m^* and Θ_s^* . One sees that this relation reproduces roughly the real situation. One of the interesting results of this relation is that it gives the limit of quantum effect, above which there exists no melting point, this corresponds to the fact that helium does not solidify under small pressure down to the absolute zero of temperature.

3. - The thermodynamical formula (3) can be generalized. Consider two substances 1 and 2, which differ from each other slightly, for example, by an isotopic difference, like $^{12}\text{CH}_4$ and $^{13}\text{CH}_4$ or CH_4 and CD_4 . The free energy of the second substance can be written as

$$(11) \quad F_2(T) = F_1(T) + \{F_2(T) - F_1(T)\},$$

in which $F_2(T) - F_1(T)$ is a small term. Let T_{m1} and T_{m2} designate the melting point of each substance, then

$$(12) \quad T_{m2} - T_{m1} = -\frac{T_{m1}}{L_{m1}} [\{F_2(T_{m1}) - F_{i1}(T_{m1})\} - \{F_{i2}(T_{m1}) - F_{i1}(T_{m1})\}],$$

where L_{m1} denotes the heat of melting of the substance 1.

We shall not treat the problem of methane in detail, because the most interesting behavior of this substance lies in its vapor pressure which demands detailed analysis of hindered rotation. The isotopic difference in the vapor pressure is directly connected to the free energy difference and hereby to the difference in melting point.

One may easily verify the following relation. Let p_{s1} and p_{s2} be the vapor pressures of substance 1 and 2 for solid state, and p_{l1} and p_{l2} those for liquid state. Then

$$(13) \quad NkT \left\{ \ln \frac{p_{l1}}{p_{l2}} - \ln \frac{p_{s2}}{p_{s1}} \right\} = \{F_{l2}(T) - F_{l1}(T)\} - \{F_{s2}(T) - F_{s1}(T)\}.$$

Treating p and F as smooth functions of temperature beyond the melting point we get thus

$$(14) \quad T_{m2} - T_{m1} = (NkT_m^2/L_m) \{\ln(p_{l2}/p_{s2})\}_{T=T_{m1}},$$

where we have used $p_{l1} = p_{s1}$ ($T = T_{m1}$).

Empirically we have

$$\ln p_l(^{12}\text{CH}_4)/p_l(^{13}\text{CH}_4) = -0.442/T + 85.0/T^2,$$

$$\ln p_s(^{12}\text{CH}_4)/p_s(^{13}\text{CH}_4) = -0.24/T + 70.0/T^2,$$

from which we get, using eq. (14),

$$T_m(^{12}\text{CH}_4) - T_m(^{13}\text{CH}_4) = -0.03^\circ\text{K},$$

which is in fair agreement with the experimental value -0.031°K .

For CD_4 we have the empirical formulas

$$\ln p_l(\text{CD}_4)/p_l(\text{CH}_4) = 11.9/T - 970/T^2,$$

$$\ln p_s(\text{CD}_4)/p_s(\text{CH}_4) = 12.8/T - 945/T^2,$$

from which, using eq. (14) again, we get

$$T_m(\text{CD}_4) - T_m(\text{CH}_4) = -0.95^\circ\text{K}$$

in agreement with the empirical value -0.87°K .

The author and one of his co-workers are making a detailed analysis for CH_4 and CD_4 taking into account the large difference in the moment of inertia and a slight difference in hindrance potential for molecular rotation. The latter comes from the difference in polarizabilities of these substances. The result will be published elsewhere.

INTERVENTI E DISCUSSIONI

— J. DE BOER:

Would it not be advantageous to evaluate T^* as function of $A^* = h/\sigma\sqrt{m\varepsilon}$, instead of $\theta^* = k\theta_{D/\varepsilon}$. The experimental values of θ_D are influenced by the quantum effects themselves, whereas A^* is an independent parameter expressed in the molecular parameters.

— M. TODA:

Of course we may plot T_m^* against A ; is it not the same to plot it against θ^* if we use θ^* values at lowest temperatures?

θ^* is proportional to A near the classical limit, so it is the same thing to plot T_m^* against A . (Ne for instance). I hoped to get a little better results using θ^* instead of A because the theory is based on θ^* -values and not on A .

PARTE SECONDA

Experimental Methods.

Structural Dynamics of Water by Neutron Spectrometry (*).

B. N. BROCKHOUSE

General Physics Branch, Atomic Energy of Canada Limited - Chalk River, Ontario

1. - Introduction.

Considerable information about the instantaneous structure of liquids has become available through measurement of X-ray and neutron diffraction patterns of liquids [1]. The measurements yield the instantaneous pair correlation function $g(r)$, «the probability that given an atom at position zero, there is also an atom at position r at the same time». The pair correlation for near neighbours is found to be strong with appreciable correlation existing in many cases between atoms at two or even three mean atomic distances.

There is little direct information about the time dependence of the correlations, whether they are evanescent fluctuations vanishing almost as soon as they appear, or whether there exists a structure in the liquid which persists in recognizable form over appreciable periods of time. The marked resemblance of the pair correlation function of a liquid to that of the parent solid which is often observed, suggests that a structure which is only slowly time-dependent does in fact exist in liquids, and many discussions [2-4] of liquid properties have been based on consideration of a liquid as a disordered solid. The fact that the diffusion coefficient and the viscosity at constant pressure of liquids have generally the same form of temperature dependence as the corresponding quantities for a solid [3] has strengthened the belief in the solid-like model of the liquid state. The most widely accepted view of liquid structure [2, 3] has thus probably been that the liquid possesses a semi-stable

(*) This paper besides presented being at the Conference on the Condensed State of Simple Systems at Varenna, Italy, in September, 1957, was communicated also at the *Congress of the International Union of Crystallography at Montreal, Canada*, in July, 1957. Part of the work was presented at the Washington, D.C. meeting of the American Physical Society in April 1956 (*Bull. Amer. Phys. Soc.*, II, 1, 188 (1956)). A short report appeared in *Acta Cryst.*, 10, 827 (1957).

structure in which atomic oscillations occur, and that diffusion takes place at fairly wide time intervals through activation over potential barriers similar to, though several times smaller than, the potential barriers against diffusion in a crystalline solid.

There exist however several items of evidence against this model. One is the fact that the Maxwell relaxation time [5] of a liquid is about the same size as the reciprocal Debye frequency, if the modulus of rigidity and the Debye frequency for the parent solid at the melting point are used for the liquid. The significance of this fact is that any « transverse » vibrations are probably quickly damped out. Furthermore recent measurements of the diffusion coefficient of CCl_4 at constant volume [6] and of the viscosity of several liquids at constant volume [7] show an activation energy for diffusion so small that almost continuous diffusion should occur. Measurements of chemical recombination rates [8] also suggest continuous diffusion.

The powerful methods of neutron spectrometry [9] can go far towards answering these problems of the structure of liquids. By study of the energy changes of slow neutrons when they are scattered by a liquid—the neutron analogue of Raman effect—very detailed information is obtained about the atomic motions. Neutron measurements give more information than do Raman effect or infrared transmission measurements because neutron scattering is sensitive to all types of motions, regardless of their momenta.

The information to be obtained from the experiments depends on the type of scattering involved, whether coherent or incoherent. Coherent scattering involves interference of the scattering between different atoms and thus gives information about the spatial distribution, in general as a function of time. Incoherent scattering does not involve interference and gives information about the motion of an individual atom. For crystalline solids coherent scattering leads to the dispersion relation of the normal modes of the crystal [10], incoherent scattering leads to the frequency distribution of the normal modes [11-13]. The results for liquids should be of equivalent generality. It seemed best to commence with the simplest situation, incoherent scattering, which involves motion of only one atom.

Vanadium and hydrogen are the only naturally occurring elements for which the scattering is predominantly incoherent [14]. Liquid vanadium is a difficult subject for experiment, and of the compounds of hydrogen water seemed the simplest and most interesting. The scattering from light water is about 95% incoherent scattering by the protons while on the other hand the scattering from heavy water is about 80% coherent. Light and heavy water thus constitute an isotopic pair scattering in both ways and are thus suitable subjects for study. In addition to their interest from the point of view of liquid theory the results may be of value in understanding neutron moderation in reactors.

The free water molecule has its two hydrogens at 0.96 Å from the oxygen, the angle between the two O-H « bonds » being $\sim 105^\circ$. In ice OH bonds on one molecule point towards the oxygens of adjacent molecules, forming a structure in which four hydrogens are arranged nearly tetrahedrally around each oxygen, two being at 1.01 Å and two at 1.75 Å [15, 16]. There are a large number of possible arrangements of nearly equal energy, corresponding to the « molecules » orienting themselves differently within the overall « tetrahedral » structure and hence ice has a configurational entropy which turns out to be $0.4 R$ per mole [17]. From the specific heat [18] at low temperature the Debye temperature of the acoustic modes of ice is approximately $\Theta_{\text{DS}} \sim 250^\circ$.

On the prevailing view [19, 20] liquid water has a broken-down ice-like structure, with presumably still higher configurational entropy. The latent heat of melting of ice is extraordinarily high, the entropy of melting being $2.66 R$ per mole in contrast to values $\sim R$ for most simple solids. This is probably to be ascribed principally to a higher configurational entropy for water. If however the entire entropy of melting were to be ascribed to the change of acoustic frequencies by use of Mott's relation [4], the Debye temperature for water (if it exists!) would be given by

$$\Theta_{\text{DL}} = \Theta_{\text{DS}} \exp [-\Delta S_{\text{M}}/3R] \sim 100.$$

Thus if the concept of a Debye temperature has any validity at all for a liquid, Θ_{D} for water should be at least 100.

Using the rigidity modulus [18] (G) of ice at the melting point and the viscosity of water [18] (η) at the freezing point the Maxwell relaxation time of water $\tau_{\text{M}} = \eta/G = 0.2 \cdot 10^{-12}$ s. The Debye temperature of ice corresponds to a period of $0.2 \cdot 10^{-12}$ s also. Thus the Maxwell relaxation time for water is shorter than the period of any transverse vibrations.

The above considerations should hold also for heavy water.

In this paper an extensive series of measurements on light water by neutron diffraction and spectrometry and less extensive measurements on heavy water are presented. Experimental methods are discussed. The results have been analysed by comparison with calculations for crystals and gases, systems which are well understood, and by use of the methods of VAN HOVE [21] which are discussed in Sect. 2. The results are not good enough to enable a complete solution of the problem to be given, but nevertheless permit some unambiguous statements to be made about the dynamical structure of liquids in general and of water in particular.

2. - Theory.

2.1. *Correlation functions and scattering.* - A powerful method of analysis has been introduced by VAN HOVE [21]. He has defined important generalizations of the pair correlation function $g(r)$ already defined and demonstrated

their relation to neutron scattering. For monatomic *classical* systems the generalized correlation functions have simple physical interpretations. The self correlation function $G_s(\mathbf{r}, t)$ can be defined as «the probability that, given an atom at position 0 at time 0, the same atom is at position \mathbf{r} at time t ». The pair correlation function $G_p(\mathbf{r}, t)$ can be defined as «the probability that, given an atom at position 0 at time 0, any atom is at position \mathbf{r} , at time t ». $G_p(\mathbf{r}, t)$ thus contains $G_s(\mathbf{r}, t)$. For classical systems the correlation functions are real; to the extent that the system has quantum properties they are complex. VAN HOVE has given general mathematical definitions of the functions which will not be reproduced here. At zero time $G_s(\mathbf{r}, 0) = \delta(\mathbf{r})$ and $G_p(\mathbf{r}, 0) = \delta(\mathbf{r}) + g(\mathbf{r})$. At large times $G_s(\mathbf{r}, t)$ must yield the correct diffusion coefficient.

The partial differential cross-sections for incoherent and coherent scattering are [21]

$$(1) \quad \frac{d^2 \sigma_{\text{INC}}}{d\Omega d\omega} = \frac{k'}{k_0} \frac{\sigma_{\text{INC}}}{8\pi^2} \int \exp[i(\mathbf{Q} \cdot \mathbf{r} - \omega t)] G_s(\mathbf{r}, t) d\mathbf{r} dt,$$

$$(2) \quad \frac{d^2 \sigma_{\text{COH}}}{d\Omega d\omega} = \frac{k'}{k_0} \frac{\sigma_{\text{COH}}}{8\pi^2} \int \exp[i(\mathbf{Q} \cdot \mathbf{r} - \omega t)] G_p(\mathbf{r}, t) d\mathbf{r} dt,$$

where $E_0 = \hbar^2 k_0^2 / 2m_n$ and $E' = \hbar^2 k'^2 / 2m_n$ are the incoming and outgoing neutron energies, \mathbf{k}_0 and \mathbf{k}' are the incoming and outgoing neutron propagation vectors, m_n is the neutron mass, $\mathbf{Q} = \mathbf{k}_0 - \mathbf{k}'$, $\omega = \hbar^{-1}(E_0 - E')$, and Φ is the angle of scattering. If the ingoing and outgoing energies of the neutron are the same $|\mathbf{Q}| = Q_0 = 2k_0 \sin \Phi/2 = 4\pi \sin(\Phi/2)/\lambda_0$, where λ_0 is the wavelength in angstroms. The partial differential cross-sections are thus Fourier transforms over space and time of the generalized correlation functions. In principle the correlations can be obtained by Fourier transformation of the cross-section [21].

A crude picture of the situation is that, neglecting diffraction effects, the neutron experiments constitute a microscope with a field $\sim Q^{-1}$ cm in diameter. The time in which particles escape from the field of the microscope is related through the uncertainty principle to the energy changes observed.

VAN HOVE shows that the correlation functions are Hermitian in the sense that

$$G^*(\mathbf{r}, t) = G(-\mathbf{r}, -t).$$

For a system in which no flow or convection occurs a more restrictive condition can be applied

$$G(\mathbf{r}, t) = \mathcal{E}(\mathbf{r}, t) + i\mathcal{O}(\mathbf{r}, t),$$

where \mathcal{E} and \mathcal{O} are real, even in r , and even and odd in t respectively.

Equations (1), (2) can thus be rewritten as

$$(3) \quad \frac{d^2\sigma}{d\Omega d\omega} = \frac{\sigma}{8\pi^2 k_0} \int \exp[i\mathbf{Q} \cdot \mathbf{r}] d\mathbf{r} \int (\mathcal{E} \cos \omega t + \mathcal{O} \sin \omega t) dt.$$

In this form the significance of the complex nature of the correlation function is clear. The real part of the correlation function produces neutron energy gains and losses equally, that is in terms of energy levels the real part is connected with symmetry of the available energy levels about the particular level in which the system is found. The imaginary part produces asymmetry between neutron energy gains and losses, that is it represents the asymmetry of the distribution of the available energy levels about the particular level in which the system is found. Thus the correlation function is real if the system is far above its ground state (classical system) and is complex if it is near its ground state (quantum system).

2.2. *The differential cross-section.* — To obtain the measured angular distribution Eq. (1), (2) must be integrated over the outgoing energy. Thus the measured differential cross-section is

$$(4) \quad \frac{d\sigma}{d\Omega} = \int_{-\infty}^{E/h} S(\omega) \frac{d^2\sigma}{d\Omega d\omega} d\omega,$$

where $S(\omega)$ is the counter sensitivity.

If the energy changes are neglected the «static approximation» ordinarily used [1] in X-ray and neutron diffraction is obtained, i.e.

$$(5) \quad \frac{d\sigma}{d\Omega} = \frac{\sigma}{4\pi} \int d\mathbf{r} \exp[i\mathbf{Q}_0 \cdot \mathbf{r}] G(\mathbf{r}, 0).$$

By the Fourier transform method $G(\mathbf{r}, 0) = \delta(\mathbf{r}) + g(\mathbf{r})$ can be obtained from $d\sigma/d\Omega$.

A higher approximation may be obtained by expanding \mathbf{Q} as follows

$$(6) \quad \mathbf{Q} = \mathbf{Q}_0 + \frac{\hbar\omega}{2E_0} \mathbf{k}' + \dots,$$

where \mathbf{k}' is a vector of magnitude k_0 in the direction of \mathbf{k}' . For a $1/v$ counter $S \propto k_0/k'$. Inserting (1), (2) and (6) in (4), replacing the limits of integration over ω by $\pm \infty$, and inverting the order of integration, it is found that, for a classical system,

$$\frac{d\sigma}{d\Omega} = \frac{\sigma}{4\pi} \int d\mathbf{r} \exp[i\mathbf{Q}_0 \cdot \mathbf{r}] G(\mathbf{r}, t_0),$$

where $t_0 = \hbar(\mathbf{k}'_0 \cdot \mathbf{r})/2E_0$ is the time in which the neutron travels the component of the distance \mathbf{r} along the outgoing direction \mathbf{k}' , at its incident velocity. For a classical system the question of the validity of the static approximation [5] thus reduces to the question of whether anything of interest happens to the system in the time t_0 . The static approximation is therefore good at small distances, but deteriorates as the distance \mathbf{r} increases.

If, as in an experiment to be described later, the range of neutron energies accepted by the counter is limited so that ω is restricted to values between $\pm \omega_1$, then

$$\left(\frac{d\sigma}{d\Omega}\right)_1 = \frac{\sigma}{4\pi^2} \int d\mathbf{r} \exp[i\mathbf{Q}_0 \cdot \mathbf{r}] \int_{-\infty}^{\infty} dt G(\mathbf{r}, t) \frac{\sin \omega_1(t - t_0)}{(t - t_0)}.$$

The result of limitation of detection of the outgoing neutrons to those with energies in the range $E' = E_0 \pm \hbar\omega_1$ is to make the neutron pattern respond to a kind of average behaviour of the scattering system over the time range $\sim [t_0 \pm \omega_1^{-1}]$.

3. Experimental results for light water.

Several types of experiments were performed which will be discussed in turn. The specimens were thin films of water about three inches in diameter clamped between two thin aluminum sheets. The thickness of the water films ranged from about 0.01 inches (~ 0.08 M.F.P.) to 0.035 inches (~ 0.3 M.F.P.) depending on the amount of multiple scattering which could be tolerated. The films were not completely uniform.

3.1. *Angular distributions.* — Angular distributions were obtained in the conventional way using 1.12_0 \AA neutrons with two counters of different energy sensitivity. This permitted a check on the effect of energy changes on the angular distribution. The counters used had calculated sensitivities given by

$$a) \quad S = \exp[-0.02\lambda] (1 - \exp[-0.069\lambda]).$$

$$b) \quad S = \exp[-0.103\lambda] (1 - \exp[-0.867\lambda]).$$

Counter *a*) was thin for all energies and therefore had a sensitivity proportional to the wavelength, while counter *b*) had a more nearly constant sensitivity over the energy range of interest.

Using a specimen with a measured transmission of 90%, the curves of

Fig. 1 were obtained for water at room temperature. Multiple scattering was estimated roughly [22] as shown by the horizontal lines.

3.2. *Energy distribution of initially «cold» neutrons.* — An energy distribution was obtained for neutrons of initial energy 0.004 eV at an angle of scattering of 90° . The specimen was less than 0.010 in. in thickness and was used in «reflection». The monoenergetic neutrons were produced by means of a filter difference technique and the outgoing neutrons measured by time-of-flight [13]. The measured spectrum is shown in Fig. 2(a). It includes a component (A) of low energy neutrons which actually belongs to the preceding frame. Two estimates of this component A_1 and A_2 are shown. In Fig. 2(b) the e-

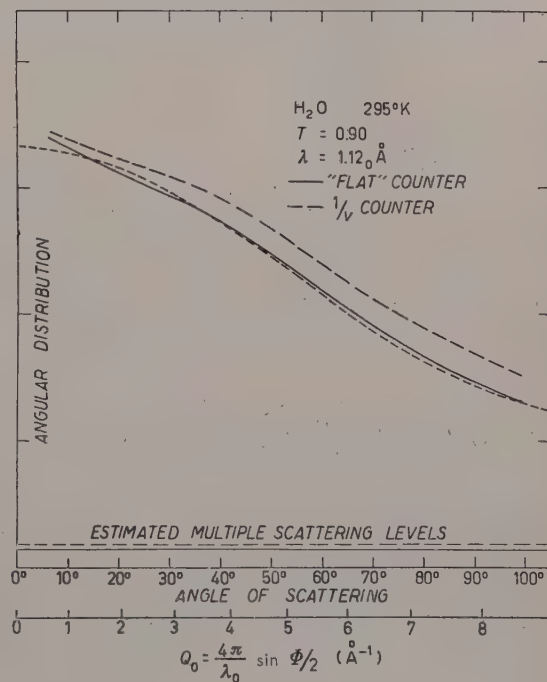


Fig. 1. — Angular distribution of 1.12 \AA neutrons scattered by a thin specimen of water into a relatively energy-insensitive counter, and into a $1/v$ counter. Estimated multiple scattering levels are as shown. The dotted curve represents the function $\exp [-(0.12 Q_0)^2]$.

nergy distribution with this component subtracted and a correction for instrument sensitivity applied [13], is shown.

3.3. *Energy distributions with crystal spectrometer method.* — A number of energy distributions were obtained using a crystal spectrometer to supply the initially monoenergetic beam and another crystal spectrometer to analyze the scattered neutrons. The apparatus is shown schematically in Fig. 3(a). Monoenergetic neutrons of the desired wavelength were selected from the NRX reactor spectrum by Bragg reflection from the 111-plane of an aluminum single crystal (X_1). These monoenergetic neutrons impinged on the thin specimen of water and neutrons which were scattered at some angle Φ were observed through the set of collimating slits C_2 . These scattered neutrons impinged on the analyzing crystal (X_2) which was oriented so that neutrons of the correct

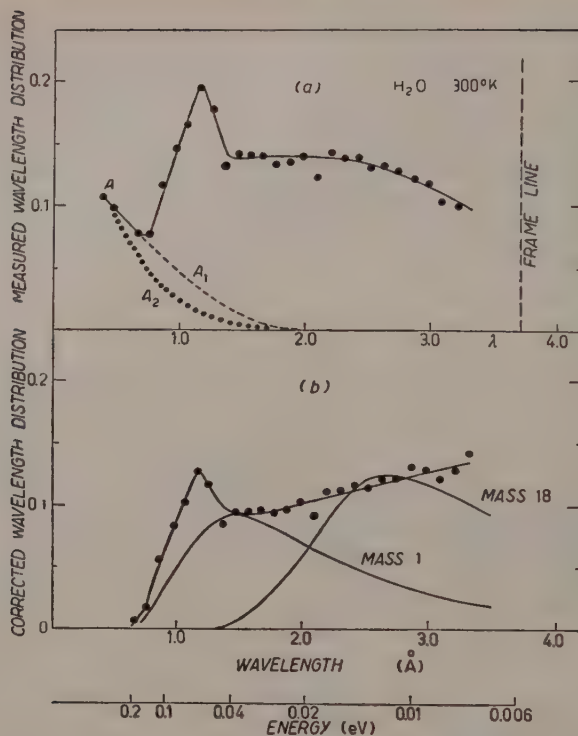


Fig. 2. — Energy distribution of 0.004 eV neutrons scattered through 90°. (a) The measured counting rate as a function of the nominal wavelength. The component *A* actually belongs to the preceding frame and is part of the «elastic» component. *A*₁ and *A*₂ are alternative estimates of this component under the extreme assumptions that the energy changes are large or small respectively. (b) The average of *A*₁ and *A*₂ was subtracted from the curve of Fig. 2(a) and the result, corrected for instrument sensitivity, is shown. Curves for a monatomic gas of mass 18 and mass 1 are shown for comparison.

wavelength were Bragg reflected by the 111-plane into the counter. A mechanical device kept the crystal aligned as the counter was rotated. In order to keep the beam size under control both crystals were cut in the Fankuchen manner, the faces being at about 6° to the 111-planes.

The counter was ordinarily moved in steps of (1/4)° and counting took place for the time necessary to accumulate a preset number of counts in a monitor counter. At each angular position counts were accumulated with analyzing crystal in the normal position for Bragg reflection (signal) and for an equal effective time with the analyzing crystal turned away from the Bragg position so that no Bragg reflection could occur (background). The background count was then subtracted directly from the signal count for the appropriate position. In Fig. 4 curves of counting rate corrected for background are shown as a function of the angle of the analyzing spectrometer for several diffe-

rent angles of scattering and two different specimen temperatures. The wave length is given by the Bragg law $\lambda' = 2d \sin \theta_A$, where d is the spacing of the 111-planes of the aluminum crystal.

The resolution function of the instrument for elastically scattered neutrons was obtained by measuring the elastic scattering from vanadium metal [12]. The resolution function was individually determined for each experiment and is shown in Fig. 4 and succeeding figures as solid curves. Measurements of the elastic scattering were also made in the second order of the analyzing crystal, and assisted in establishing the zero of the spectrometer.

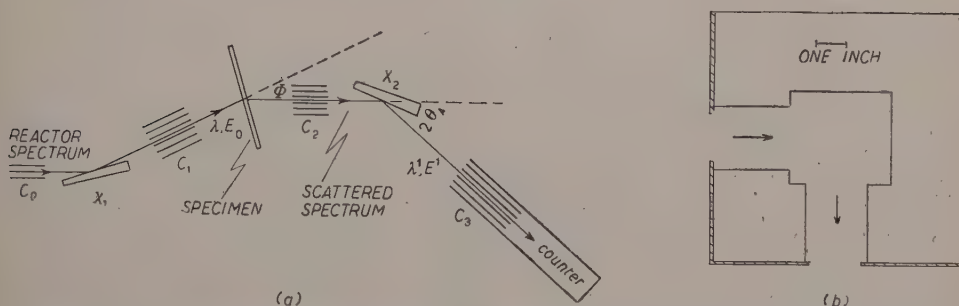


Fig. 3. -- (a) Schematic diagram of the apparatus for the crystal spectrometer energy distribution measurements. (b) Scale diagram of the paraffin moderator used to generate a Maxwellian spectrum.

The sensitivity function of the analyzing spectrometer was obtained by measuring the spectrum emitted from the interior of a large block of paraffin into which monoenergetic neutrons were incident as shown in Fig. 3(b), and assuming the emitted spectrum to be Maxwellian. The measured spectrum is shown in Fig. 5. It consists of two spectra measured in the first and second orders of the analyzing crystal. The relative sensitivities of the analyzing crystal in the first and second order were known from measurements on the elastic scattering of vanadium made at several different energies. The second order component could therefore be calculated from the measurements and is shown as the dashed line in Fig. 5. Subtracting the second order component from the measured spectrum and dividing by the assumed Maxwellian spectrum the instrument sensitivity function was obtained.

In the measurements shown in Fig. 4 (and in some of the other measurements) it was necessary to take a number of independent runs and add the results point-by-point to get the necessary statistics. Where this was done the vanadium elastic curves are also the result of point-by-point addition of several runs. Thus any broadening due to misalignment should show up also in the vanadium patterns.

The measurements of Fig. 4 were made with a beam of neutrons of nominal energy 0.0308 eV which contained about 17% of second order neutrons (energy 0.123 eV) as measured using resonant absorbers. These neutrons when scattered were observed in the first and second orders of the analyzing crystal. It was possible to calculate corrections to fair accuracy using the knowledge

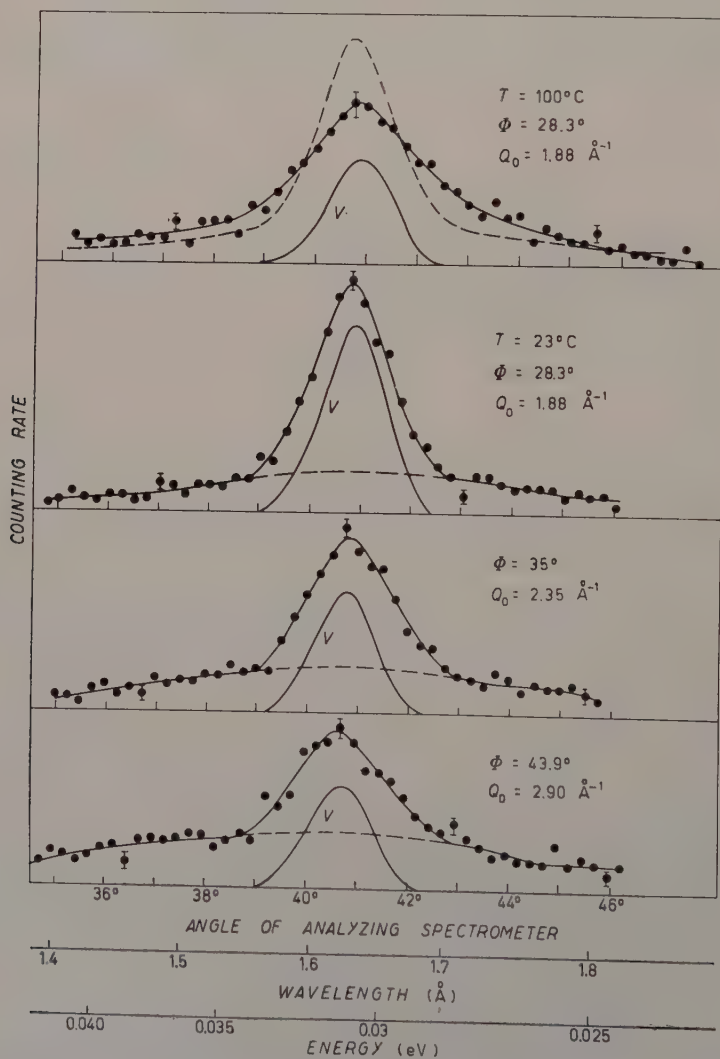


Fig. 4. - Measured energy distributions of 1.62\AA neutrons scattered by specimens of water with transmission ~ 0.8 at room temperature for angles $\Phi = 28.3^\circ, 35^\circ, 43.9^\circ$, and at 100°C for $\Phi = 28.3^\circ$, plotted as a function of the angle of the analyzing spectrometer. The resolution function as measured with vanadium is also shown. The dashed curve in the 100°C figure represents the room temperature results at the same angle.

obtained in the entire series of experiments. In other experiments the second order content was much smaller, and the corrections were unimportant.

The measured spectra also contained a component of multiply scattered neutrons. The fraction of multiply scattered neutrons was estimated from

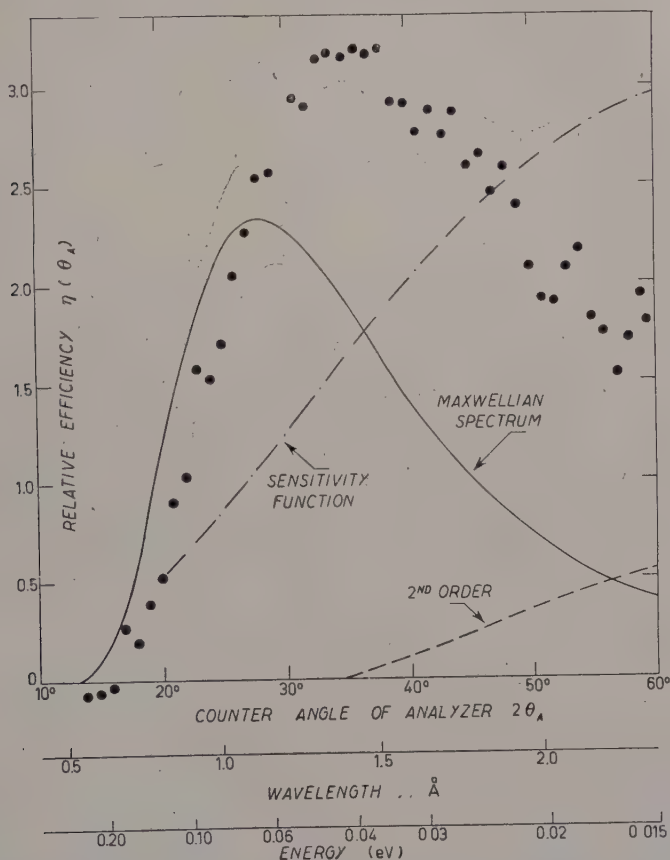


Fig. 5. - Measurement of an energy distribution of 1.5 Å neutrons diffused by the moderator of Fig. 4, plotted as a function of the angle of the analyzing spectrometer ($2\theta_A$). The estimated amount of scattering detected in the second order of the analyzing crystal is also shown. A theoretical Maxwellian spectrum and the sensitivity function deduced by comparison of this spectrum with the measurements are shown as functions of $2\theta_A$.

the measured transmissions of the specimen and the differential cross-section of Fig. 1 (assumed to be a function of Q_0). The multiply scattered neutrons were assumed to have a Maxwellian energy distribution. Since multiple scattering involves on the average folding of two distributions resembling the spectra of Fig. 8 and Fig. 9 it is thought that this assumption is fairly good.

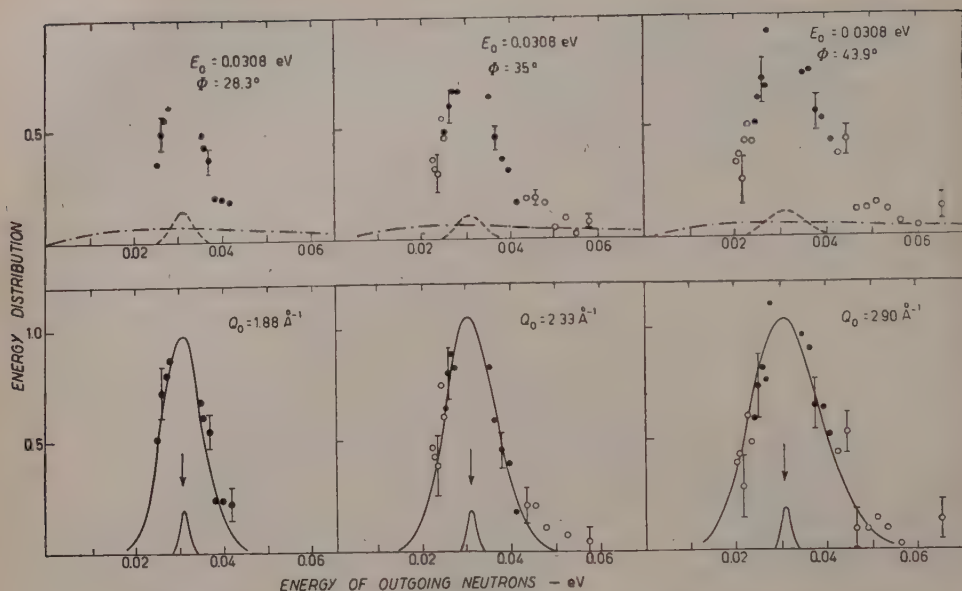
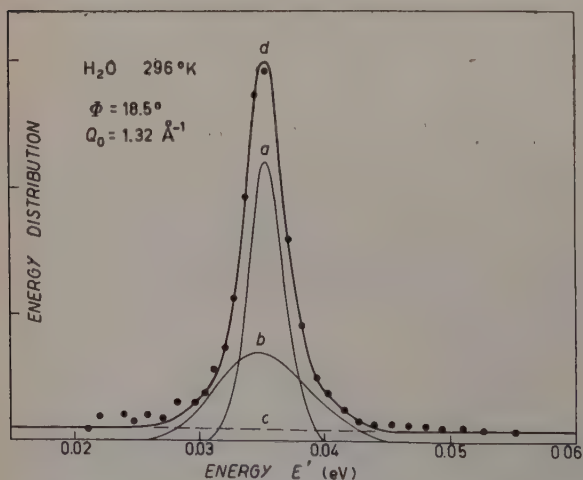


Fig. 6. — Upper figures - the inelastic components of the room temperature curves of Fig. 4 together with estimates of the second order and multiple scattering components. Lower figures - the inelastic components all corrections made, fitted to calculated spectra for a monatomic gas of mass 18. The resolution functions are also shown.

It is observed that the spectra of Fig. 4 consist of two components one being approximately for the shape the elastic resolution function and the other more widely spreading in energy.



These will be termed hereafter the «elastic» and «inelastic» components respectively. The inelastic components of the three room temperature spectra of Fig. 4

Fig. 7. — Energy distribution of 0.035 eV neutrons scattered through 18.5°. The observed spectrum has been fitted by (a) an elastic component the shape of the observed scattering by vanadium; (b) a component the shape of the scattering by

a monatomic gas of mass 18 as broadened by the known resolution, and (c) a component of multiple scattering estimated as described in the text.

have been converted to energy distributions by use of the instrument sensitivity function and plotted as a function of energy in the upper half of Fig. 6. Additional measurements not shown in Fig. 4 were obtained (under somewhat poorer resolution) and are shown as open circles. The expected contaminant scattering as previously discussed is also shown. After subtraction of this contaminant scattering (and renormalization) the points shown in the lower half of Fig. 6 are obtained.

An energy distribution was obtained for a value of Q_0 (1.32 \AA^{-1}) smaller than for the curves of Fig. 4 and is shown in Fig. 7. In this case the separation of inelastic and elastic components is not as clear as for the curves of Fig. 4, presumably because the resolution function is comparable with the width of the inelastic component. As shown, the spectrum can probably be fitted with a multiple scattering component (c) estimated both as to intensity and shape as previously discussed, plus components whose shapes are given by the resolution function (a) and by the spectrum for a gas of mass 18 as broadened by the resolution function (b).

Similar measurements were made at large equivalent Q_0 and are shown in Fig. 8 and 9 as energy distributions, corrected for scattering by the containing foils and for multiple scattering.

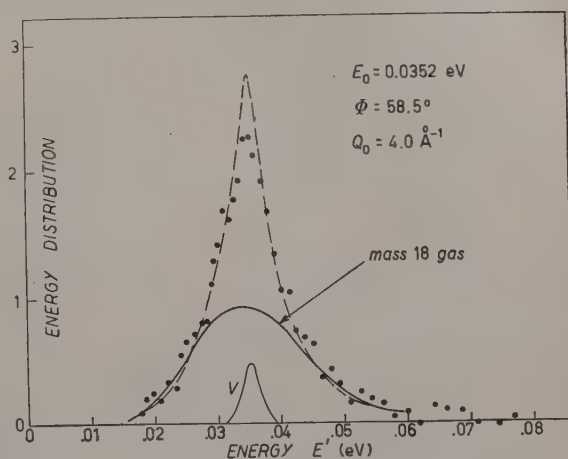


Fig. 8. — The energy distribution of 0.035 eV neutrons scattered through 58.5° , all corrections made. The spectrum corrected approximately for resolution is indicated by the dashed line. The spectrum for a gas of mass 18 and the resolution function are also shown.

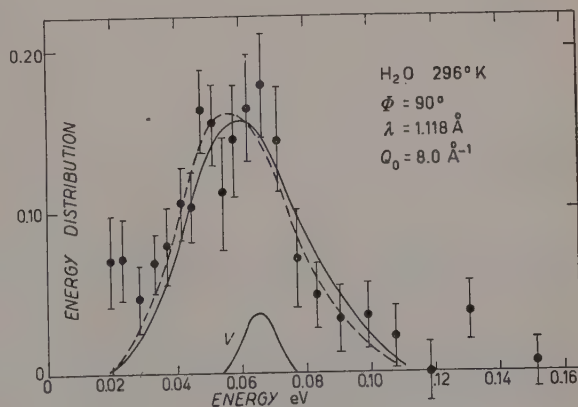


Fig. 9. — The energy distribution of 0.065 eV neutrons scattered through 90° , all corrections made. The solid line shows the distribution for a gas of mass 18, the dashed line the same distribution modified by the form factor of Fig. 1, considered as a function of Q .

The dashed line in Fig. 8 represents the measurements corrected for resolution. It will be seen that for this distribution division into «elastic» and «inelastic» components has little meaning. The statistics in Fig. 9 are particularly bad because it was necessary to use an extremely thin specimen in

order to keep the effects of multiple scattering within bounds.

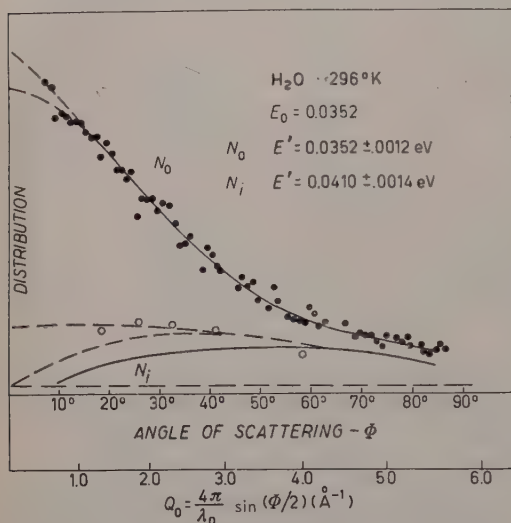


Fig. 10. — Angular distribution of neutrons of initial energy 0.0352 eV (1.52\AA) scattered by water into an energy sensitive detector (a crystal spectrometer set to Bragg reflect neutrons of a certain energy). Curve N_0 represents neutrons scattered «elastically» into a detector set at 0.0352 with a half width at half maximum of 0.0012 eV. Curve N_i represents neutrons scattered with an energy (0.0408 ± 0.0014) eV. The open circles and curves N'_i represent estimates of the inelastic component at 0.0352 eV from the energy distributions of Figs. 4, 7, 8.

and at large angles include the inelastic component in the same amount. At smaller angles the amounts of the inelastic component at the «elastic» position have been obtained from the energy distributions and are shown as open circles (N'_i). Possible extrapolations of N_0 and N'_i are shown as dashed lines. $N_0 - N'_i$ represents the amount of the «elastic» component within the resolution function.

4. — Discussion of light water results.

4.1. *Vibrations and hindered rotations.* — In water most of the scattering is incoherent scattering by the protons, the oxygens contributing only about 3%.

3.4. Elastic angular distribution.

— An experiment was performed in which the angle of the analyzing spectrometer ($2\theta_A$) was fixed at the Bragg angle of the incident neutrons and the angle of scattering (Φ) varied, thus obtaining the angular distributions of those neutrons scattered with an energy in a certain range about the incoming energy. Neutrons of energy 0.0352 eV were used and the resolution function had a half width at half maximum of 0.0012 eV. The results are shown in Fig. 10 labelled N_0 . A similar curve was taken with the analyzing spectrometer displaced from the elastic position by a little more than the full width at the base of the resolution function and is shown in Fig. 10 as curve N_i . The two curves include multiple scattering in about the same amount,

The primary interest in these experiments has been in water as a typical liquid. It is necessary therefore to ascertain to what extent the results are affected by the motions of the hydrogens with respect to the oxygens. The molecular vibrations of the water molecules are known to be of too high energy (0.20, 0.40, 0.43 eV) to affect these experiments appreciably but the water molecules are believed to undergo hindered rotations which might be of importance. Raman effect measurements of CROSS, BURNHAM and LEIGHTON [23] indicate that the hindered rotations form a band from about 0.03 to 0.11 eV. However measurements of BOLLA [24] showed a band at 0.007 eV which MAGAT [25] assigned to hindered rotations also. The measured spectrum for $Q_0 = 8$ (Fig. 9) and the inelastic components for $Q_0 = 1.8$ to 2.9 (Fig. 6) can be fitted very well by the spectrum calculated [26] for a monatomic gas of mass 18 as shown by the heavy lines. This fact argues that the hindered rotations are all of high frequency as assigned by CROSS *et al.* The cold neutron experiment, Fig. 2(b), shows strong evidence for such modes of oscillatory character over the same range of energies in which the Raman effect frequencies were observed and indicates a maximum at about 0.06 eV.

Little can be said about the cold neutron spectrum otherwise. The scattering expected for a gas of mass 18 (arbitrarily normalized) is shown, and together with the hindered rotational peak, effectively conceals any evidence for the hindered translational mode observed by CROSS *et al.* at 0.025 eV. The width of the hindered rotational peak is not readily interpretable. The peak is reduced on the high energy side by the Boltzmann factor and is considerably Doppler broadened.

The fall off with angle of the differential cross section Fig. 1 can be considered as arising from the fact that, with the center of mass of the molecules fixed, each proton is spread out as a cloud due to its vibrational and hindered rotational motions. Because of their high energy these motions are not much excited either thermally or by the neutrons and hence most of the cross section comes from scattering by the molecule as a whole. This is borne out by Fig. 9 and by the comparatively small separation between the curves shown in Fig. 1 for the two counters. This separation is however two or three times that expected for a gas of mass 18 and indicates the occurrence of some energy losses to the hindered rotations. Taking the form factor of the motion to be a Gaussian $\exp[-Q_0^2 u_H^2]$, the parameter $u_H \cong 0.12 \text{ \AA}$ as indicated by the dotted curve of Fig. 1. The amplitude of each of the vibrational modes is approximately 0.07 \AA . Correcting u_H for the contribution of the vibrations, the amplitude of the rotational motion is found to be $u_R \cong 0.13 \text{ \AA}$, corresponding to an energy of about 0.06 eV for the hindered rotations. With the oxygens fixed the hydrogen cloud is thus roughly an ellipsoid with semi-axes about 0.07, 0.13, 0.13 \AA respectively.

The evidence thus seems clear that all motions of the protons with respect

to the oxygens are of relatively high frequency, and that small energy transfers are associated with motion of the molecules as a whole.

4'3. *The inelastic component.* — As has already been observed the spectrum of Fig. 9 and the inelastic components of Fig. 4 can be satisfactorily fitted by the spectrum of a monatomic gas of mass 18. On Van Hove's picture the qualitative significance of this fact is that for small r and t the self correlation function of the liquid is like that of a gas. This is of course also true of a solid for sufficiently small r and t , but it seems fair to say that in the liquid this behaviour occurs at smaller values of Q_0 and therefore larger r than it does in solids. In a solid, for small Q , the width of the energy distribution is almost independent of Q , the intensity increasing with Q but not the width. This irreducible width is that of the spectrum of normal modes of the crystal. At larger Q the width also increase as multiple phonon processes become important.

It would be interesting to see if an irreducible width could be reached for the case of a liquid. The inelastic component of the distribution shown in Fig. 7 for $Q_0 = 1.3$ is narrower than the distributions of Fig. 6, and probably compatible with the distribution for a monatomic gas of mass 18. At the present time it cannot be said for certain whether an irreducible width exists or not. It should however be pointed out that these experiments emphasize modes of small energy transfer. In fact for solids the partial cross-sections for small energy transfer are proportional to $(E_0 - E')^{-2}$. Thus the presence of a characteristic spectrum might be disguised by the presence of an abnormally high (but still comparatively small) number of modes of small energy transfer.

4'3. *The « elastic » component.* — Fig. 4 shows the existence of the two components in the energy distributions; one has much the same shape as the scattering by a monatomic gas of mass 18, and the other is substantially elastic. The existence of the two components corresponds on Van Hove's picture to the existence of two time scales. Consider the situation in a solid. At time zero the position of the particle is known by definition and on the average it is moving with substantially the velocity it would have in a gas. Thus the Debye-Waller thermal cloud is quickly formed and thereafter changes only slightly. The formation and fluctuations of the cloud give rise to the inelastic component. The scattering from the cloud as a form factor gives rise to the elastic component, elastic because the cloud endures « forever ». The two energy components reflect the quick formation of the cloud and the long life of the cloud when formed. Analogously the two components in the liquid energy distributions refer to the formation of a thermal cloud in the liquid and to the subsequent life of the cloud. Energy broadening of the « elastic » com-

ponent implies that the cloud has a finite lifetime. The fall off with angle of the « elastic » component—its form factor—measures the spatial extent of the cloud. For the moment the form factor will be taken as a Debye-Waller factor ($\exp [-Q^2 u^2]$) in analogy to a solid. Thus the cloud is assumed to have a Gaussian distribution, as for a harmonically bound solid.

On the microscope analogy (2.1), the energy width measures the rate of escape of the particles from the microscope field of radius $\sim Q^{-1}$. If the particle moves to a distance $\gg Q^{-1}$, then for a given fractional escape rate the width will be independent of Q . On the other hand if the cloud simply expands uniformly with time, the changes in the cloud will be reflected in changes in the energy width with Q . Thus different types of diffusive motion will be exhibited as different behaviours of the width of the « elastic » component as a function of Q .

To make the discussion more definite consider two extreme models of diffusion. After the thermal cloud has been formed it may expand by continuous diffusion in which case the self-correlation function can be represented asymptotically as:

$$(7) \quad G_s(r, t) = \text{constant} \times (u^2 + \gamma |t|)^{-\frac{3}{2}} \exp [-r^2/4(u^2 + \gamma |t|)].$$

Here $\sqrt{6}u$ is the RMS radius of the self-correlation function extrapolated to $t = 0$. The factor $\sqrt{6}$ arises because of the three directions of space (u is the component of the RMS radius along Q) and the fact that the origin is not a point fixed in space as for a lattice, but is itself a point on the cloud. The quantity γ is the coefficient of continuous diffusion, that is the part of the diffusion coefficient that arises from « small » motions. Inserting Eq. (7) into Eq. (1) and making the good approximation $Q = Q_0$, the partial differential cross-section of the elastic component is found to be:

$$(8) \quad \left(\frac{d^2 \sigma_{\text{INC}}}{d\Omega d\omega} \right)_{\text{el}} = \text{constant} \times \exp [-Q_0^2 u^2] \gamma Q_0^2 / [(\gamma Q_0^2)^2 + \omega^2].$$

The energy distribution has the form of a Lorentz function of half width at half maximum $\hbar \gamma Q_0^2$, the width thus increasing with angle of scattering. When integrated over the outgoing energy E' the differential « elastic » cross-section is found to be

$$(9) \quad \left(\frac{d\sigma_{\text{INC}}}{d\Omega} \right)_{\text{el}} = \frac{\sigma_{\text{INC}}}{4\pi} \exp [-Q_0^2 u^2]$$

as expected.

The other model to be considered is the model of diffusion by activation into another « lattice » site or interstitial position—that is diffusion by « large »

motions. In this case the asymptotic self correlation function can be written approximately

$$(10) \quad G_s(r, t) = \text{Const} \times u^{-\frac{3}{2}} \exp[-r^2/4u^2] \exp[-\beta|t|] + \\ + F_1(r)(1 - \exp[-\beta|t|]) \exp[-\beta|t|] + \dots$$

The quantity β is the jump frequency. The functions $F_1(r)$ and higher have appreciable values only at distances of, say, 2 angstroms or more and hence are important only when Q^{-1} is of this order (except for diffraction effects).

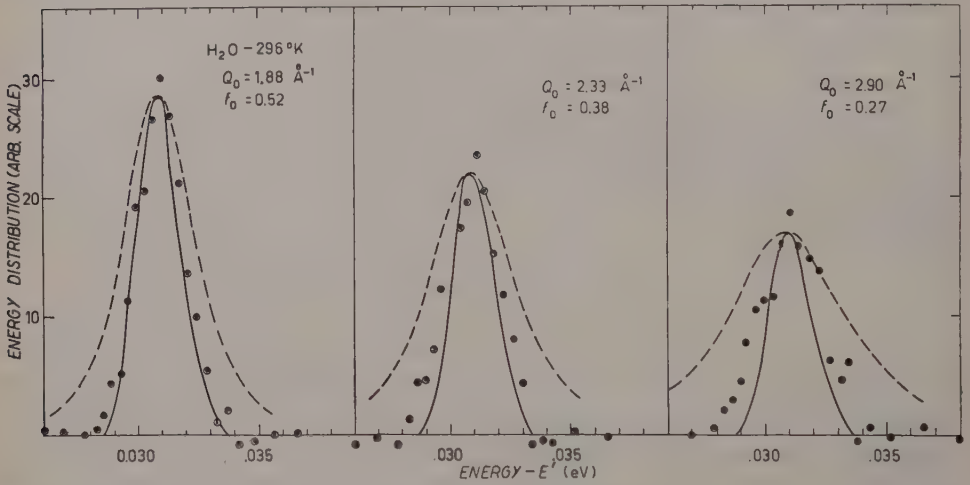


Fig. 11. — The «elastic» components of the spectra of Fig. 4 plotted as a function of energy, all corrections made. The resolution functions measured with vanadium are shown as heavy lines. The dashed lines are calculated from the diffusion coefficient assuming small motions only, as discussed in the text.

For the comparatively large Q 's involved in these experiments only the first term is important and therefore

$$(11) \quad \left(\frac{d^2 \sigma_{\text{INC}}}{d\Omega d\omega} \right)_{\text{el}} = \text{Constant} \times \exp[-Q_0^2 u^2] \beta / (\beta^2 + \omega^2).$$

For this case, therefore, the width ($\hbar\beta$) of the Lorentz distribution is independent of the angle of scattering. The differential cross-section is again given by Eq. (9).

The room temperature curves of Fig. 4 have been corrected for contaminant scattering and for instrument efficiency, and the inelastic components fitted by mass 18 gas distributions as shown in Fig. 6. These mass 18 distributions were subtracted from the corrected distributions to give the «elastic» components shown in Fig. 11. The resolution functions measured with vanadium

are shown as heavy solid lines. The width of the experimental curves is seen to increase with Q_0 suggesting a contribution from small motions.

The 100 °C curve of Fig. 4 has been corrected for contaminant scattering and for instrument efficiency and is shown in Fig. 12(a), together with a fitted mass 18 spectrum. The «elastic» component obtained by subtracting the calculated mass 18 spectrum from the measured points is shown in Fig. 12(b), together with the resolution function measured with vanadium. From Fig. 4 and Fig. 12(b) it is clear that the energy broadening of the «elastic» component is considerably greater at 100 °C than at room temperature. If real, the apparent asymmetry of the 100 °C «elastic» component would be of great significance. Until it has been confirmed it is being considered to be an experimental anomaly. The fraction of the pattern comprised in the «elastic» component is less at 100 °C than at room temperature indicating that the cloud expands with temperature. Quantitative comparison of these patterns, and of other unpublished measurements, suggests that the rate of expansion of the cloud with temperature is not much greater than for a solid (for which $u^2 \propto T$).

The diffusion coefficient of water has been measured as a function of temperature by WANG *et al.* [27] using tracer methods. Both deuterium and oxygen 18 were used as tracers with essentially the same results, indicating that diffusion of hydrogens independently of water molecules is not important. Measurements were made from 0 °C to 55 °C and a value $D = 2.8 \cdot 10^{-5} \text{ cm}^2/\text{s}$ was found at 25 °C. Extrapolation to 100 °C leads to the value $D = 10 \cdot 10^{-5} \text{ cm}^2/\text{s}$

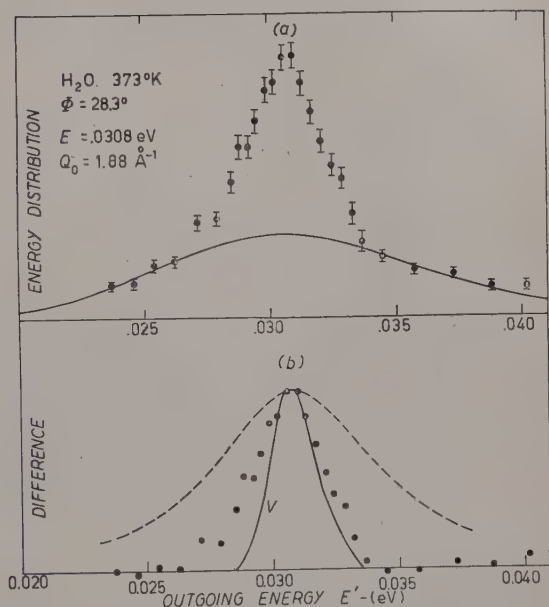


Fig. 12. — (a) The energy distribution of 0.0308 eV neutrons scattered through 28.3° by water at 100 °C, all corrections made. The shape expected for a monatomic gas of mass 18 is shown by the heavy lines. (b) The «elastic» component obtained by subtracting the fitted gas scattering pattern from the measurements. The resolution function is shown as a solid line and a calculated distribution obtained from the diffusion coefficient assuming small motions is shown by the dashed line.

for that temperature. The temperature dependence was found to obey a theoretical activation curve very well. The activation energy of 4.6 kcal/mole was essentially the same as the activation energy for reorientation of the molecules, as found by COLLIE *et al.* [28] from studies of the high frequency dielectric constant, suggesting that diffusion and reorientation occur together. At 25 °C the dielectric relaxation time τ was found to be $8.3 \cdot 10^{-12}$ s. It is not clear how τ is to be related to the actual Debye time of relaxation of the water molecules, the relationship depending on the theory of the internal field in the dielectric. Setting the jump frequency β equal to τ^{-1} leads to $\beta = 1.2 \cdot 10^{11}$ at room temperature and $\beta = 4 \cdot 10^{11}$ at 100 °C. These are of the same order as the jump frequencies expected from the random walk relation $\beta = 6D/\delta^2$ where δ , the jump distance, is of atomic dimensions, i.e. 3 Å or so. The corresponding energy broadenings $\hbar\beta$ are small compared with the resolution, and the « elastic » components for both temperatures have essentially the shape of the resolution function. In fact, however, appreciable broadening is observed. On the other hand setting γ equal to D in Eq. (8) and folding the resulting Lorentz function with the resolution function results in the dashed curves of Fig. 11 and 12, curves which are considerably broader than the measured, distributions. Thus neither of the two extreme models of diffusion can explain the results, features of both models being required.

This result, that both small and large motions contribute to diffusion, is

reasonable. For example if an atom makes a jump of several angstroms the neighbours of its old position must be expected to close in while the neighbours of its new position will move

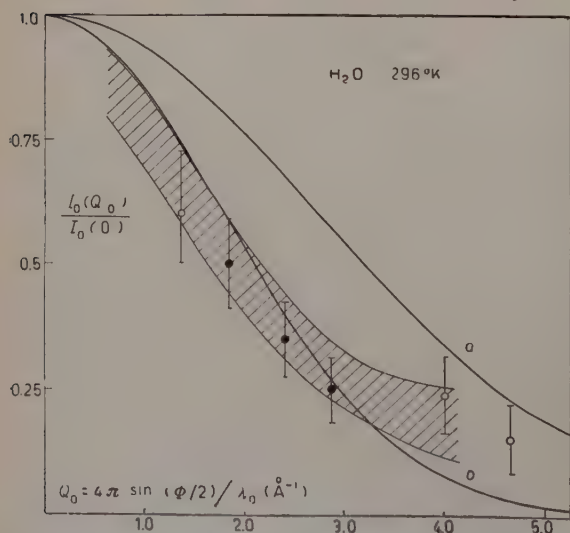


Fig. 13. — The form factor of the thermal cloud for the protons in light water at room temperature. The filled circles are obtained from the patterns of Fig. 4 for which an intuitive separation into « elastic » and inelastic components is possible. The open circles are

obtained from patterns for which the « mass 18 » hypothesis must be invoked to obtain a separation. The shaded area is the form factor obtained from Fig. 10. Curve (a) is a Debye-Waller factor with $u = 0.26$ Å, the value applicable for ice extrapolated to room temperature. Curve (b) is the « best fit » of a Debye-Waller factor to the measurements, for which $u = 0.4$ Å.

out to make room for it. Thus a large diffusive motion will always be accompanied by many small motions.

It is of interest to determine the form factor of the elastic component and thus the size and shape of the thermal cloud. The fraction of the total scattering at Q_0 comprised in the «elastic» component was calculated from the measured energy distributions by subtracting the mass 18 component fitted to the wings of the distribution as described previously. This fraction was converted to a form factor by use of Fig. 1 considered as a function of Q_0 , together with the assumption that all the scattering in the forward direction is elastic. Where the separation into two components has intuitive validity (Fig. 4) the results are plotted in Fig. 13 as solid circles, where the separation can only be accomplished by use of the mass 18 hypothesis the results are plotted as open circles. The errors are estimated. The form factor was also estimated from $N_0 - N'_i$ as given in Fig. 10, and lies within the shaded area of Fig. 13, whose limits are largely determined by the various possible extrapolations of N_0 and N'_i to $Q_0 = 0$. A correction was applied at large Q_0 for the angle-dependent energy broadening previously discussed.

The measured form factor approximates a Debye-Waller factor with $u = 0.4 \text{ \AA}$ (curve *b*) but is more spread out, indicating that the thermal cloud is more diffuse than a Gaussian. From Fig. 13 all that can be said is that the R.M.S. radius of the asymptotic self correlation function is probably greater than $\sqrt{6} u \cong 1 \text{ \AA}$.

The Debye-Waller factors for heavy ice at -50°C and -150°C have been measured by PETERSON and LEVY [16]. Extrapolating their results, the quantity u appropriate to ice at room temperature is 0.26 \AA . Comparison with the experiments in Fig. 13 demonstrates that the thermal cloud is much larger in water than it would be in ice at the same temperature.

Comparison of Fig. 11 and Fig. 8 suggests that the width of the elastic component is increasing with Q_0 more rapidly than Q_0^2 . This effect could arise if diffusion outwards takes place at a faster rate from the inner part of the non-Gaussian thermal cloud than from the outer part.

The analysis outlined in this section cannot have any more than qualitative significance. The lack of information at small Q_0 especially would make any precise treatment doubtful. However, it seems likely that the general features of the discussion are valid.

5. - Heavy water results and discussion.

Angular distributions of 1.12 \AA neutrons scattered by a specimen of heavy water about 0.1 in. thick, were obtained as discussed in Sect. 3'1. The specimen contained about 99.8% D_2O and 0.2% HDO . The results were typ-

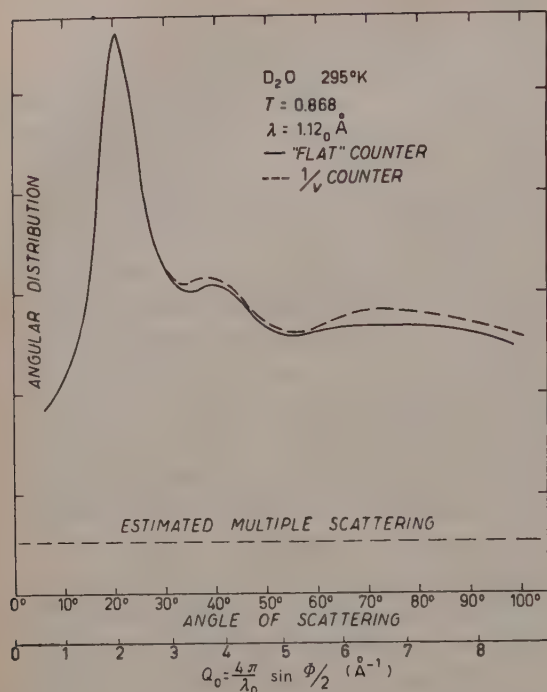
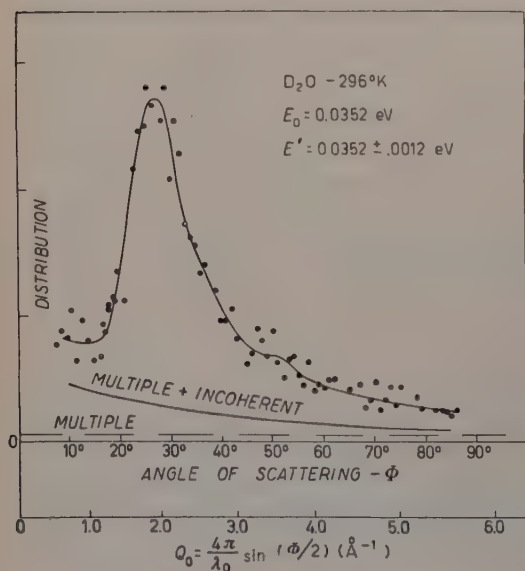


Fig. 14. — Angular distributions of 1.12 Å neutrons scattered by D_2O into a $1/v$ detector and into a relatively energy insensitive counter.



ical liquid diffraction curves as shown in Fig. 14. The transmission of the specimen was 0.868, resulting in a calculated multiple scattering component as shown. The pattern includes some incoherent scattering by the deuterons, which from the accepted cross-sections, amounts to approximately 22% of the total scattering by heavy water, but is difficult to estimate in detail.

An elastic angular distribution was obtained for heavy water as described in Sect. 3'4, and is shown in Fig. 15. It should be noted that this distribution also contains a component arising from incoherent scattering by the deuterons. The elastic angular distribution for light water is probably a fair approximation to the shape of this component (Fig. 10), estimated as shown.

Energy distributions were obtained using neutrons of nominal energy 0.0308 eV for values of $Q_0 = 1.88$ and 2.33 \AA^{-1} as shown in Fig. 16. The measured resolution function is also shown. The patterns contain roughly 15% of a component with the shape of the corresponding patterns of Fig. 4

Fig. 15. — Angular «elastic» distribution of 0.0352 eV (1.52 Å) neutrons scattered by D_2O with rough estimates of the multiple and incoherent scattering included.

because of the deuterium incoherence. This component and multiple scattering accounts for a considerable part of the larger energy changes in the pattern for $Q_0 = 1.88 \text{ \AA}^{-1}$. For this pattern, taken almost at the liquid diffraction peak, separation into elastic and inelastic components is difficult.

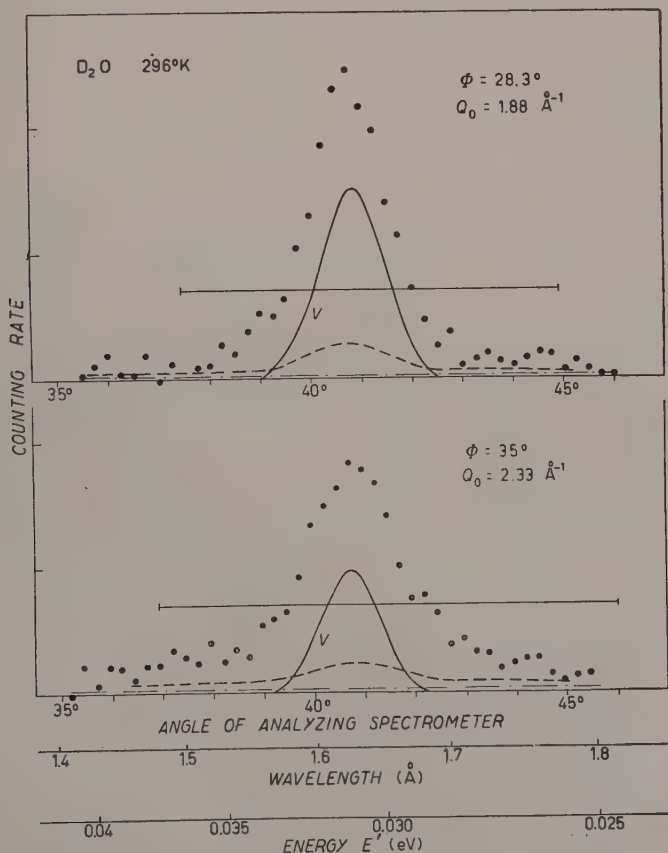


Fig. 16. - Energy distributions, as measured, for 1.62 \AA neutrons scattered by D_2O through angles of 28.3° and 35° , plotted as a function of the analyzing spectrometer angle. The dashed curves show rough estimates of the amount of incoherent and multiple scattering included. The bars indicate the full width at half maximum of the patterns for a gas of mass 20.

The inelastic component is, however, certainly much narrower than would be obtained with a gas of mass 20, the width at half maximum of which is indicated by the horizontal bar. For $Q_0 = 2.33 \text{ \AA}^{-1}$ the inelastic component is considerably broader than that for $Q_0 = 1.88 \text{ \AA}^{-1}$ but is still probably narrower than that for a gas of mass 20.

No quantitative deductions have been made from these measurements. Qualitatively the results show that strong spatial correlations still exist at times $\sim 5 \cdot 10^{-13}$ s, times corresponding to the energy resolutions. For comparison a thermal water molecule moves 2.5 Å in this time, about the distance between nearest neighbours. The behaviour of the inelastic component indicates that there are considerable correlations between the velocities of different particles.

6. - General discussion.

The results of the neutron and other experiments are consistent in general with the accepted picture of water as a structure of water molecules linked up in somewhat the same way as ice, the molecules vibrating with frequencies high compared to their translational motions. It is not yet clear to what extent the translational motions have a vibratory character but there is clearly some correlation between the motions of adjacent molecules. The neutron results can be interpreted by assuming that a thermal cloud is formed which can be approximated roughly by a Gaussian self-correlation function of RMS radius $\cong 1.0$ Å. However the thermal cloud is in fact more diffuse than a Gaussian. After formation the cloud apparently expands slowly by small motions, but this expansion does not account for the whole of the measured diffusion coefficient and large diffusion jumps must also be invoked. It seems likely that actually a variety of diffusive motions occur. The dimensions of the thermal cloud increase with increasing temperature, probably at a faster rate than for a solid. The fact that measurements of the high frequency dielectric constant can be fitted by means of a single relaxation time suggest that both the diffusive motions and the reorientation of the molecules occur simultaneously at a time of breakdown of the local structure.

The main features of the neutron scattering patterns can thus be explained by reasonable pictures of the structure of water. To make more quantitative statements more accurate information, especially high resolution data ($\sim 10^{-4}$ eV) at small Q , is required. The best way of treating such data will probably turn out to be through use of space-time Fourier transforms, as suggested by VAN HOVE. It is hoped to carry out such work in the future (*).

(*) *Note added in proof.* - Some additional measurements of the «elastic» component have been made recently using a new instrument of high resolution (*Bull. Amer. Phys. Soc.*, 11, 3, 233 (1958)). At $Q_0 = 1.95$ Å both light and heavy water showed an energy broadening which increased with temperature from 6 °C to 60 °C roughly as the diffusion coefficient. The absolute magnitudes of the energy broadening indicated that the constant $\gamma \sim \frac{1}{2}D$, in agreement with the results in this paper.

* * *

The author wishes to thank Mr. E. GLASER for technical assistance, and Drs. H. CARMICHAEL, L. G. ELLIOTT, D. G. HENSHAW and N. K. POPE for helpful criticisms.

REFERENCES

- [1] N. S. GINGRICH: *Rev. Mod. Phys.*, **15**, 90 (1943); D. G. HENSHAW, D. G. HURST and N. K. POPE: *Phys. Rev.*, **92**, 1229 (1953).
- [2] J. FRENKEL: *Kinetic Theory of Liquids* (London, 1946).
- [3] S. GLASSTONE, K. J. LAIDLER and H. EYRING: *The Theory of Rate Processes* (New York, 1941).
- [4] N. F. MOTT: *Proc. Roy. Soc. London*, **146**, 465 (1934).
- [5] See reference [2] p. 198 for a discussion of the Maxwell relaxation time of a viscous solid.
- [6] H. WATTS, B. J. ALDER and J. H. HILDEBRAND: *Journ. Chem. Phys.*, **23**, 659 (1955).
- [7] N. F. ŽDANOVA: *Žu. Èksper. Teor. Fiz.*, **31**, 14 (1956); **31**, 724 (1956); *Soviet Physics JETP* **4**, 19 (1957); **4**, 749 (1957).
- [8] R. M. NOYES: *Journ. Amer. Chem. Soc.*, **78**, 5486 (1956).
- [9] B. N. BROCKHOUSE: *Phys. Rev.*, **98**, 1171 (1955) (A).
- [10] R. WEINSTOCK: *Phys. Rev.*, **65**, 1 (1944); G. PLACZEK and L. VAN HOVE: *Phys. Rev.*, **93**, 1207 (1954); B. N. BROCKHOUSE and A. T. STEWART: *Phys. Rev.*, **100**, 756 (1955) and *Rev. Mod. Phys.* **30**, 236 (1958); R. S. CARTER, D. J. HUGHES and H. PALEVSKY: *Phys. Rev.*, **106**, 1168 (1957).
- [11] G. PLACZEK and L. VAN HOVE: ref. [10]; R. S. CARTER, D. J. HUGHES and H. PALEVSKY: *Phys. Rev.* **104**, 271 (1956); C. M. EISENHAEUER, I. PELAH, D. J. HUGHES and H. PALEVSKY: *Phys. Rev.*, **109**, 1046 (1958).
- [12] B. N. BROCKHOUSE: *Can. Journ. Phys.*, **33**, 889 (1955).
- [13] A. T. STEWART and B. N. BROCKHOUSE: *Rev. Mod. Phys.* **30**, 250 (1958).
- [14] See D. J. HUGHES and J. A. HARVEY: *Neutron Cross Sections*, BNL 325.
- [15] E. D. WOLLAN, W. L. DAVIDSON and C. G. SHULL: *Phys. Rev.*, **75**, 1348 (1949).
- [16] G. W. PETERSON and H. A. LEVY: *Acta Cryst.*, **10**, 70 (1957).
- [17] L. PAULING: *Journ. Amer. Chem. Soc.*, **57**, 2680 (1935).
- [18] See N. E. DORSEY: *Properties of Ordinary Water Substance* (New York, 1940).
- [19] J. D. BERNAL and R. H. FOWLER: *Journ. Chem. Phys.*, **1**, 515 (1933).
- [20] J. MORGAN and B. E. WARREN: *Journ. Chem. Phys.*, **6**, 666 (1938).
- [21] L. VAN HOVE: *Phys. Rev.*, **95**, 249 (1954).
- [22] B. N. BROCKHOUSE, L. M. CORLISS and J. M. HASTINGS: *Phys. Rev.*, **98**, 1721 (1955).
- [23] P. C. CROSS, J. BURNHAM and P. A. LEIGHTON: *Journ. Amer. Chem. Soc.*, **59**, 1134 (1937).
- [24] G. BOLLA: *Nuovo Cimento*, **9**, 290 (1932); **10**, 101 (1932).
- [25] M. MAGAT: *Ann. Phys.*, **6**, 108 (1936).

- [26] Calculated by averaging the laboratory - center of mass transformation over a Maxwellian velocity distribution following J. A. SPIERS unpublished report CRT-417 (NRC No. 1940) (1949). The formula used is given explicitly as equation (5) by B. N. BROCKHOUSE and D. G. HURST: *Phys. Rev.*, **88**, 542 (1952).
- [27] J. H. WANG, C. V. ROBINSON and I. S. EDELMAN: *Journ. Amer. Chem. Soc.*, **75**, 466 (1953).
- [28] C. H. COLLIE, J. B. HASTED and D. M. RITSON: *Proc. Phys. Soc. London*, **60**, 145 (1948).

INTERVENTI E DISCUSSIONI

— G. CARERI:

Can you apply your technique to other more simple liquids than water?

— B. N. BROCKHOUSE:

Using natural elements the self-correlation function can be determined only for liquid vanadium, a difficult subject for experimentation, and liquids containing hydrogen of which water is probably the simplest. Liquid hydrogen would probably not be suitable because of the existence of ortho and para hydrogen. By preparation of suitable mixtures of isotopes a few other elements could be studied, notably liquid lithium which is probably the best prospect for future work.

— J. REUSS:

Is your conclusion that self-diffusion in water exists:

- 1) in some sort of small vibration with varying equilibrium position and
- 2) jumps over larger distances?

From the ^3He - ^4He diffusion results as quoted in the paper of CARERI, we come from the opposite side to the conclusion that it is not possible to account for the measured $D \approx (3 \div 4) \cdot 10^{-5}$ only by a jump mechanism, because then the jump frequency had to be very near to the vibration frequency of a molecule in its potential deep.

— B. N. BROCKHOUSE:

Substantially yes. The direct evidence is for the existence of some small motions, which quantitatively do not seem to be able to account for the entire rate of diffusion thus implying that large jumps probably also take place.

— E. BAUER:

Je voudrais rappeler que dans le cas des liquides polaires comme l'eau, le temps de relaxation de la dispersion électrique donne une mesure directe de la durée de vie moyenne des édifices polymoléculaires, et que les énergies d'activation que l'on en déduit concordent bien avec celles qui régissent la self-diffusion.

— B. N. BROCKHOUSE:

The proportionality observed to hold between the time of relaxation and the diffusion constant at different temperatures would seem to mean that molecular reorient-

ation takes place in the same fraction of diffusive processes at all temperatures. It may give a measure of the *mean* length of a diffusive step. I would add that recent work on the self diffusion of CCl_4 at constant volume, and on the viscosities of liquid argon and liquid nitrogen at constant volume, show much smaller temperature dependence than at constant pressure. The existence of an apparent activation constant at constant pressure cannot be taken as sure evidence that diffusion over a barrier is taking place.

— A. MICHELS:

The temperature coefficient $(\partial\eta/\partial T)_s$ in the liquid density range does not differ substantially from that of the gas range. However, around the critical point there are big variations even with a change of sign. Recent measurement on CO_2 gave results of this nature.

— B. N. BROCKHOUSE:

My recollection is that the recent Russian work on the viscosity of liquid argon and nitrogen show quite low apparent activation energies at constant volume, so low that the concept of a barrier has little meaning.

Atom Movements in Simple Liquids by Tracer Technique.

G. CARERI

Istituto di Fisica dell'Università di Padova - Padova

1. - It is the purpose of this paper to show the possibilities of the tracer method in the study of some simple liquids. This work was carried out by the author and his co-workers on the following systems

- a) liquid indium, and indium-lead solutions
(by A. PAOLETTI and M. VICENTINI);
- b) liquid nitrogen-argon, and nitrogen-tritium mixtures
(by G. CINI-CASTAGNOLI, G. PIZZELLA and F. P. RICCI);
- c) liquid ^3He - ^4He mixtures, and pure liquid helium
(by F. SCARAMIZZI, J. REUSS and J. O. THOMSON).

In all the cases we started by measuring the diffusion coefficient but sooner or later, some other features were investigated, to learn more about the atomic movements in these liquid systems.

Let us start with the liquid metals. Here we developed a method to measure the diffusion coefficient in a wide range of temperature by letting two rods of active and non-active material diffuse together inside a capillary. The technique has been fully described elsewhere [1] and will be only briefly mentioned here. One uses a one ended closed capillary of about 150 mm length, and fills it at room temperature with the two rods of solid metal. Then the temperature is raised under vacuum in a well controlled way, the material is melted, and then the liquid is kept for some hours at constant temperature to allow the diffusion to take place. The sample is then quickly cooled down and the solid rod cut into many small pieces, the radioactivity of which is measured by standard methods. One can then plot the activity versus length and obtain the penetration curve, from which the diffusion coefficient is calculated.

We will not describe here the many corrections and the precautions which

are taken to avoid convection. But will only mention that we believe we have measured the true diffusion coefficient for the following reasons: 1) the reproducibility of the data with different duration of the experiment, and 2) the correct dependence of the activity versus length to satisfy the diffusion equation. Furthermore the thermal gradients, melting and freezing speeds were changed in the different runs with no effect at all. Therefore we believed to have measured the true diffusion coefficients and published our results together with an interpretation on molecular terms.

But soon after a paper appeared by LODDING [2], who measured the self diffusion in indium by a different technique and found some lower values. Because convection can spoil the data only in the sense of increasing the diffusion coefficient, we thought that the Lodding data were perhaps better than ours, although we could not understand indeed the reason of the discrepancy.

A careful and broader investigation was made by PAOLETTI and VICENTINI recently, which resulted in the conclusion that both our and Lodding's methods gave the same results if capillaries of the same diameter and of the same material were employed. But the additional most interesting feature comes out: that the capillary diameter had had some influence in the value of the diffusion coefficient! The larger the diameter the larger the diffusion coefficient, up to a diameter where a further

increase gives no appreciable rise. The situation is illustrated in Fig. 1, from which the reproducibility of the data and these results are clear. The conclusion is that the diffusivity is larger in the core than at the walls, and a direct test on rods attacked by nitric acid confirmed this.

In a forthcoming paper these experiments will be fully described but let ask now ourselves why the material diffuses less at the wall than in the core. If one tries to compute the depth of this skin effect, one finds about $50 \mu\text{m}$, a figure much too large. It must be said that also ECKERT and DRICKAMER working at Urbana (Illinois) found on indium a strange skin effect of a similar magnitude. The question is still to be understood on molecular terms, but we believe it cannot be caused by some spurious effect like convection or

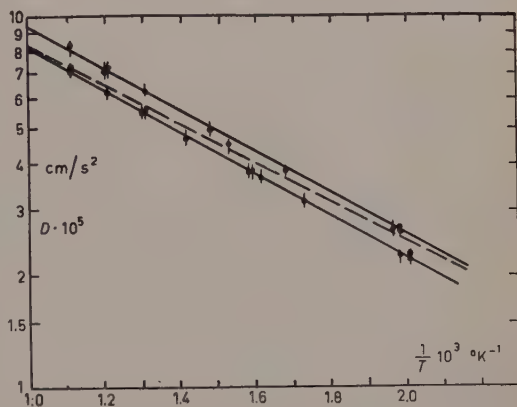


Fig. 1. — The self diffusion coefficient plotted versus the reciprocal of the absolute temperature. Solid lines: a) capillary diameter 0.8 mm; b) capillary diameter 1.6 mm. Dotted line: Lodding's results.

turbulence, of the true diffusion. A process involving micro-vortices turbulence in thermal equilibrium, would describe the above features but should be substantiated by further theoretical and experimental work.

Let us now see what happens when convection sets in; this happens, for instance, when the bottom of the capillary is kept hotter than the top during the experiment. Then, the penetration curve of the radioactive material has an erratic profile and does not anymore satisfy the diffusion equation. In this case one is well aware of the spurious processes and may disregard the run.

However, a few cases were noticed, when turbulence could set in due to the wrong thermal gradient, and the diffusion profile was still the one of the diffusion equation, yielding a value of the diffusion coefficient one order of magnitude larger than the one obtained in the good runs. This apparently strange behaviour can be explained in terms of the theoretical work by G. I. TAYLOR [4], who showed the turbulent diffusion to follow still some diffusion differential equation, when the dispersion time (which is actually nearly the duration of the experiment) is much larger than the time scale of turbulence L_T .

To our knowledge this is the first check of this theorem in a liquid system.

2. - In the above, we have seen how many more features than simply the diffusion coefficient, the tracer method can give.

We will omit here for sake of briefness our similar investigations on liquid nitrogen, and give a brief report on the liquid helium experiments. Now the only possible tracers are the ^3He atoms and the helium ions. We succeeded in measuring the diffusion coefficient of ^3He in liquid helium above the λ temperature, this being probably the first direct measurement of this quantity at low temperature. Details of the technique will be published elsewhere, but we will mention here that the changes in the concentrations due to the sample fractioning, makes accurate measurements very difficult.

We devised therefore a new technique consisting in the production of ions directly in liquid helium, to measure their mobility under well defined conditions. Now the heat input in the apparatus is negligible and one can also easily detect transient phenomena. Much work of this kind is now in progress, and we will mention here only the one intended to test the Landau-Pomerančuk picture of the motion of impurities in liquid helium. Following this theory, every impurity will interact with the normal fluid, and not with the superfluid component, regardless to the statistics of the impurity atoms themselves. Therefore in a ^3He - ^4He liquid solution, the ^3He will move from the warm side to the cold one, following the motion of the normal fluid; this effect was actually observed by DAUNT and co-workers in 1948, and called « heat flush » effect. However, it was still open to question whether the foreign particle velocity was the normal fluid velocity (easy to calculate from the rate of entropy production) or somewhat different.

We have built a kind of ionization chamber in which we could detect the drift of the ionic current along a heat current flow, which was normal to the electric field. We found a heat flush effect indeed; in all the range of temperature and voltage the displacement of the ions in the direction of the heat current was proportional to the heat current density. Furthermore, we were able, by geometrical considerations, to derive the mobility of positive and negative ions from the drift current under the assumption that the drift velocity was equal to the normal fluid velocity. These so calculated mobilities turned out to be consistent with the one directly measured in some recent experiments by WILLIAMS.

From the experimental values of the mobilities, one can deduce the diffusion coefficient of the ions by help of the Einstein relation. These latter, and our measured diffusion coefficient of the ^3He atoms above T_λ , allow the following schematic picture of the motion of impurities in liquid helium: above the λ temperature the movements are the one of a hard sphere fluid; below the λ temperature the mean free path increases, because only the collisions with the normal component are effective.

The negative ions, namely electrons, follow a similar pattern in the whole range of temperature, but the absolute value of their diffusivity is lower than the one of the positive ions. It seems that there is some kind of binding which shows their motion, but so far, we have not found an adequate explanation to this effect.

REFERENCES

- [1] G. CARERI and A. PAOLETTI: *Nuovo Cimento*, **2**, 574 (1955).
- [2] A. LODDING: *Zeits. f. Naturfor.*, **11**, 200 (1955).
- [3] R. E. ECKERT and H. G. DRICKAMER: *Journ. Chem. Phys.*, **20**, 13 (1952).
- [4] G. I. TAYLOR: *Proc. London Math. Soc.*, A **20**, 196 (1921).

INTERVENTI E DISCUSSIONI

— J. A. PRINS:

Concerning the skin effect I would suggest that the skin value for the diffusion coefficient would be the right one and that the core value would be enhanced by macroscopical movements; these may be turbulence or laminar convection, but I suppose rather that they would be due to the turning over of blocks which occur in the liquid matrix at the moment of melting.

— G. CARERI:

Then these movements would have to be present too with all other investigators as they find values of the same order of magnitude; so these movements would be inherent to the liquid and presumably just be the molecular phenomenon we call diffusion.

I do not think so. We have the evidence of the time independence of the measured diffusion coefficient, which rules out any turbulence.

— L. ONSAGER:

Within the last ten years the chemists have two methods which yield coefficients of diffusion good to about 0.1%. One method involves an optical setup which allows continuous observation of a fringe system, the other applies to preferably dilute solutions of electrolytes and depends on measurement of conductivity in silver. Where the two methods overlap they yield identical results, and the second method agrees in extrapolation with the limiting mobilities derived from conductivity measurements, all within about 0.1%. The precautions taken to avoid convection are rather elaborate. The fringe method depends in principle on the establishment of a sharp initial boundary; but in practice an extrapolation to « zero » time is needed to compensate for the initial mixing.

The Infrared Spectrum of Liquid and Solid Hydrogen.

E. J. ALLIN, H. P. GUSH, W. F. J. HARE and H. L. WELSH

McLennan Laboratory, University of Toronto - Toronto

The study of the infrared spectrum of compressed hydrogen gas has been very fruitful in delineating the characteristics of pressure-induced absorption. This type of absorption has its origin in the asymmetric distortion of the electron distributions of molecules during collisions, as a consequence of which vibrations and rotations, inactive in the free molecule for reasons of symmetry, can become active in the pressurized gas. At lower pressures the absorption is conditioned by binary collisions, but at higher pressures ternary and higher order collisions become important and have a marked influence on the spectrum. These effects in hydrogen gas have been studied over a wide range of pressures and temperatures; for example, at room temperature the experiments have been extended up to 5000 atm where the gas density is greater than that of the liquid at its normal boiling point [1,2]. It was then natural to inquire how the collision-induced spectrum changes in going to the condensed phases. The experiments on liquid and solid hydrogen have a particular interest which arises from the fact that, as a consequence of the lower thermal energies at low temperatures, the spectral lines are relatively sharp and much more detail can be observed than for the gas at room temperature.

In the following paragraphs the main results of the observations on the spectrum of liquid and solid hydrogen will be summarized. The earlier work at low resolution [3-5] has now been supplemented by recent experiments with a high resolution grating spectrometer. The spectra thus obtained show a wealth of detail which has not yet been fully interpreted.

Fig. 1(a) shows the fundamental vibrational band of solid normal hydrogen at 11°K obtained with a spectral resolution of 20 cm⁻¹. The designations used for the various components follow, where possible, the nomenclature of molecular spectroscopy. For the Q components the vibrational transition is un-

accompanied by a change of rotational quantum number ($\Delta J = 0$). For the $S(0)$ and $S(1)$ transitions the vibrational transition is accompanied by the rotational transition, $J = 0 \rightarrow J = 2$ for para molecules, and $J = 1 \rightarrow J = 3$ for ortho molecules. The selection rule $\Delta J = 2$ follows from the fact that the

distortion producing the transition is unchanged for a rotation of the molecule by the angle π . The presence of the S lines in the spectrum shows that the molecular rotation in solid hydrogen is more or less unhindered; this has been confirmed by the Raman spectrum [6].

The broad components labelled Q_R , $S_R(0)$ and $S_R(1)$ constitute a « normal » crystal spectrum. Because of the symmetry of the crystal lattice in solid hydrogen the molecular vibration is not infrared active; however, summation tones of the vibration frequency with frequencies of translational modes of the lattice are presumably active. The component Q_R thus constitutes a spectrum of certain of the lattice modes. This component can be correlated with a

similar component in the spectrum of the compressed gas and of the liquid; in these latter cases it has been ascribed to induction by the short-range overlap forces operative during close collisions [1]. The form of Q_R in the gas spectrum is similar to that for the solid, but of much greater extent; its shape in the gas spectrum has been interpreted in terms of the participation of the relative kinetic energies of the colliding molecules in the collision process. The components $S_R(0)$ and $S_R(1)$ in Fig. 1(a) are similar to Q_R ; these must be ascribed to a coupling of the molecular rotation with the vibrational motions of the molecule and of the crystal lattice.

The components Q_R , $S_R(0)$ and $S_R(1)$ in the spectrum of the solid are similar in form and extent to the corresponding components in the spectrum of the liquid. In fact, in the earlier experiments it was believed that the entire spectrum persisted unchanged from the solid phase to the liquid phase at least 1°K above the fusion point. More precise temperature control has now shown that there is an abrupt but small change in the spectrum at the fusion point. Nevertheless, the similarity in the two spectra is very striking; from this one can conclude that, since the induced spectrum is due to short-range inter-

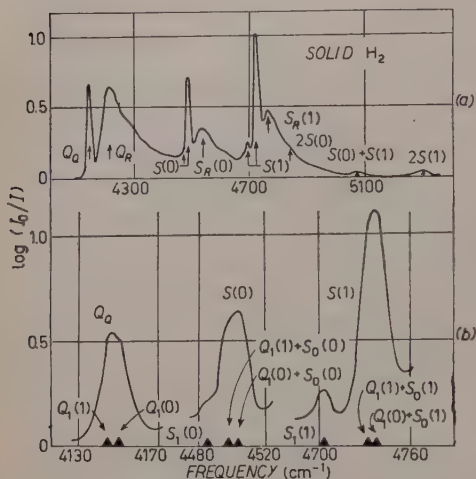


Fig. 1. — The infrared fundamental band of solid normal hydrogen at 11 °K. Path length, 0.6 cm. (a) Prism spectrometer; spectral slit width 20 cm^{-1} . (b) Grating spectrometer; spectral slit width 2 cm^{-1} .

actions, the liquid just above the fusion point possesses a short-range order very similar to the lattice arrangement of the molecules in the solid.

As shown by VAN KRANENDONK and BIRD [7,8] in their theory of pressure-induced absorption, the overlap or exchange interaction for hydrogen is almost spherically symmetrical and produces absorption mainly in the Q branch. There is also a longer range interaction, that due to the molecular quadrupole moments; this interaction is strongly orientation-dependent and accounts for most of the S branch absorption while making only a small contribution to the Q branch. The sharp S lines and the Q_0 line in Fig. 1(a) are therefore ascribed to the interaction of the molecular quadrupoles in the solid. Thus for the interpretation of the finer details of these lines we should consider the interaction of a regular array of quadrupole moments situated at the lattice points of the solid; except at very low temperatures, $\sim 1^\circ\text{K}$, the axes of rotation of the quadrupoles probably have random orientations. A theoretical approach to this problem has not yet been made.

When the sharp components of the spectrum of the solid were examined with a spectral resolution of $\sim 2\text{ cm}^{-1}$, the profiles in Fig. 1(b) were obtained. A frequency analysis of the components of the S lines showed that the very weak lines, designated $S_1(0)$ and $S_1(1)$, have frequencies which coincide with the S lines of the Raman spectrum of the solid; these lines are therefore due to transitions in single molecules. The strong S lines, on the other hand, correspond to double transitions in which one molecule performs the vibrational transition and a second molecule performs simultaneously a rotational transition in its ground vibrational state. The single and double transitions are separated in frequency because of the difference in the rotation-vibrational interaction in the upper and lower vibrational states. A double transition can take place in two ways: for example, the $S(0)$ double transition can be represented by $Q_1(1)+S_0(0)$ or $Q_1(0)+S_0(0)$, where the suffix (0 or 1) indicates the change in vibrational quantum number. The frequencies of the transitions as calculated from the Raman effect data are plotted on the frequency axis in Fig. 1(b); the agreement with the observed absorption profiles is very satisfactory.

The reason for the predominance of double transitions in the solid can be understood in principle by the theory of induced absorption in dense gases. In ternary and higher order collisions the distortion of the electron distribution is less asymmetric than in binary collisions, and the induced dipole moment which causes the absorption is, on the average, smaller. In the extreme case in which a central molecule is surrounded symmetrically by perturbing molecules there can be no induced dipole and hence no absorption. The very low intensity of the single S transitions in solid hydrogen can therefore be interpreted in terms of this «cancellation principle». On the other hand, in a recent general theoretical treatment of induced absorption VAN KRANEN-

DONK [9] has shown that the cancellation principle does not apply if transitions in two coupled molecules take place simultaneously. The high intensity of the double S transitions in solid hydrogen can therefore be understood in a qualitative way. It may be noted that certain other double transitions appear

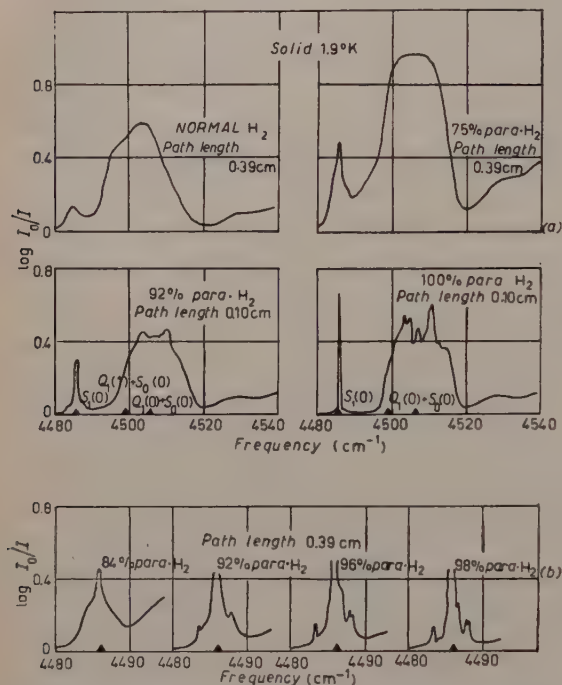


Fig. 2. — Variation of the profile of the $S(0)$ group with ortho-para ratio; spectral slit width 0.2 cm^{-1} . (a) The $S(0)$ group. (b) Detail of the single transition, $S_1(0)$.

sists however, since the upper rotational state has $J=2$. The alteration of the $S(0)$ lines with ortho-para ratio is shown in the spectra of Fig. 2, which were obtained at 1.9°K with a spectral resolution of 0.2 cm^{-1} .

As the ortho-para ratio is decreased the intensity of the double transition $S(0)$ shifts towards higher frequencies as the component $Q_1(1)+S_0(0)$ decreases and the component $Q_1(0)+S_0(0)$ increases in intensity. In pure parahydrogen the latter double transition shows a close fine structure centred about the calculated frequency of the double transition. It is suggested that this structure is due to the possibility of the rotational transition being associated with any one of the twelve nearest neighbors of the molecule making the vibrational transition. When orthohydrogen is added different absorbing para molecules will have different numbers and arrangements of ortho molecules in their shells

with low intensity; these are designated $2S(0)$, $S(0)+S(1)$ and $(2S1)$ in Fig. 1(a), and can be assigned to a rotation-vibrational transition in one molecule taking place simultaneously with a purely rotational transition in a second molecule.

When the ortho-para ratio of solid hydrogen is altered, the spectrum changes in a quite remarkable way especially in the region of high para concentrations. In pure parahydrogen the ortho line, $S(1)$, is of course absent; the Q branch also disappears, presumably because there can be no quadrupole interaction when the molecules are in the spherically symmetrical $J=0$ rotational state in both the lower and the upper vibrational state of the transition.

The $S(0)$ group of lines per-

of nearest neighbors and the pattern of splitting must differ from one molecule to another; the superposition of these different patterns thus leads to a diffuseness in the band even at quite low ortho concentrations.

In pure parahydrogen the single transition $S_1(0)$ appears as an extremely sharp line with a high peak absorption; its half-width is certainly less than the spectral slit width of 0.2 cm^{-1} . The addition of only 2% of orthohydrogen is accompanied by the appearance of several satellites near the main $S_1(0)$ peak at 4486.0 cm^{-1} , as shown in Fig. 2(b). With increasing ortho concentration the main peak diminishes and the satellites increase in intensity until, in normal hydrogen, only a single broad band with a maximum at 4484.5 cm^{-1} is observed. The reason for these changes in the $S_1(0)$ transition is not as yet understood.

The behaviour of the Q branch as the ortho-para ratio is changed is illustrated in Fig. 3. Since its intensity is comparable with that of the S double transitions (Fig. 1(b)), it seems probable that the Q branch should be associated with double transitions. That this is perhaps the case is shown by the fact that the integrated intensity of the Q branch is of the form,

$$\int \log_{10} \frac{I_0}{I} d\nu = aC_oC_p + bC_o^2,$$

where C_o and C_p are the ortho and para concentrations, respectively, and a and b are constants. The only double transition

which seems possible for the Q branch is that in which one molecule makes the vibrational transition and the second molecule makes an *orientational* transition ($\Delta M \neq 0$, $|M| = 0, \dots J$, where M is the magnetic quantum number). Since $M = 0$ for para molecules no orientational transition for these is possible; hence no term in C_p^2 appears in the expression for the integrated intensity of the Q branch and the Q branch disappears entirely in pure parahydrogen.

The Q branch components appear to fall into two groups which are near the positions of the $Q(0)$ and $Q(1)$ lines of the Raman spectrum; these latter frequencies are marked on the abscissa axis in Fig. 3. It should be noted that the $Q(0)$ line is forbidden for the quadrupole interaction in binary collisions according to the theory of van Kranendonk and Bird (?); its appearance here must therefore be the result of a double transition in which an *ortho* molecule changes its orientation. With 2% orthohydrogen the $Q(0)$ group

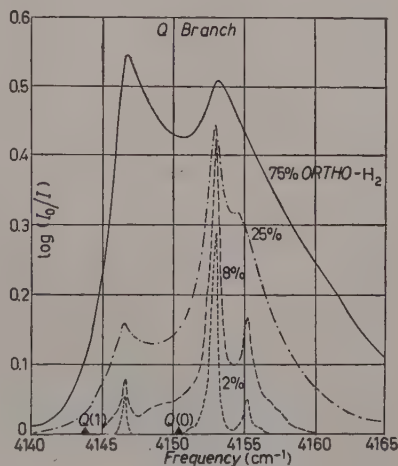


Fig. 3. — Variation of the profile of the Q branch with ortho-para ratio; spectral slit width 0.2 cm^{-1} ; path length, 0.39 cm ; temp. 1.9°K .

consists of two sharp lines; the stronger of these is probably to be associated with the case in which the shell of twelve nearest neighbors contains one ortho molecule, and the weaker with a shell containing two ortho molecules. At higher ortho concentrations further possibilities are present and the pattern quickly becomes diffuse. It is considered that ultimately, when very precise intensity measurements in the region of low ortho concentrations become available, analyses of the patterns along these lines will be possible.

It is well known that solid hydrogen at temperatures of the order of 1.5°K shows anomalies in the specific heat curve [10] and in the nuclear magnetic resonance absorption [11]; these effects are believed to be due to co-operative ordering of the orientations of the ortho molecules. It seems probable that anomalies should also exist in the infrared spectrum, but none have yet been observed, even though experiments have been performed with the absorption cell immersed in liquid helium II at 1.2°K . However, the interior of the solid may well have been at a higher temperature than the helium bath because of the absorption of infrared radiation; more refined experimental arrangements are therefore required.

The most outstanding feature of the observations outlined above on the fundamental band of liquid and solid hydrogen is the prevalence of double transitions. Other experiments have also shown this same general result. For example, the spectrum of solid hydrogen in the overtone region is a superposition of two rather complex bands, of which one can be assigned to a pure overtone, that is, to the $v=0$ to $v=2$ vibrational transition in a single molecule, the other to a double transition in which each of two molecules makes the fundamental transition. In solid hydrogen the double transition is much more intense than the single transition, whereas in gaseous hydrogen the two transitions have been shown to have approximately equal intensities [12]. The spectrum of the fundamental band of HD in dilute mixtures with H_2 and D_2 has also been studied; here the most prominent feature of the band is the double transition in which the HD molecule makes a vibrational transition and one of the surrounding H_2 (or D_2) molecules makes a rotational transition. An interesting feature of the fundamental band of pure HD is the appearance of the $J=0 \rightarrow J=1$ rotational line; the reason for the occurrence of this transition in induced absorption is apparently the fact that the electrical centre of symmetry of the HD molecule does not coincide with its centre of mass.

REFERENCES

- [1] D. A. CHISHOLM and H. L. WELSH: *Can. Journ. Phys.*, **32**, 291 (1954).
- [2] W. F. J. HARE and H. L. WELSH: *Can. Journ. Phys.*, **36**, 88 (1958).

- [3] E. J. ALLIN, W. F. J. HARE and R. E. McDONALD: *Phys. Rev.*, **98**, 554 (1955).
 - [4] W. F. J. HARE, E. J. ALLIN and H. L. WELSH: *Phys. Rev.*, **99**, 1887 (1955).
 - [5] H. P. GUSH, W. F. J. HARE, E. J. ALLIN and H. L. WELSH: *Phys. Rev.*, **106**, 1101 (1957).
 - [6] E. J. ALLIN, T. FELDMAN and H. L. WELSH: *Journ. Chem. Phys.*, **24**, 1116 (1956).
 - [7] J. VAN KRANENDONK and R. V. BIRD: *Physica*, **17**, 953, 968 (1952).
 - [8] J. VAN KRANENDONK: *Thesis* (Amsterdam, 1952).
 - [9] J. VAN KRANENDONK: *Physica*, **23**, 825 (1957).
 - [10] R. W. HILL and B. W. A. RICKETSON: *Phil. Mag.*, **45**, 277 (1954).
 - [11] F. REIF and E. M. PURCELL: *Phys. Rev.*, **91**, 631 (1953).
 - [12] H. L. WELSH, M. F. CRAWFORD, J. C. F. McDONALD and D. A. CHISHOLM: *Phys. Rev.*, **83**, 1264 (1951).
-

INTERVENTI E DISCUSSIONI

— K. MENDELSSOHN:

If the temperature of your experience was 1.9 °K, did you see any effect of the splitting of the ortho terms?

— H. L. WELSH:

No effect of splitting of the ortho terms was observed, probably because the line widths become small only when the ortho concentration is very low.

The Thermal Conductivity of Condensed Helium.

J. WILKS

Clarendon Laboratory - Oxford

1. - Introduction.

At low temperatures the thermal conductivity of a condensed phase is very sensitive to its structure, and the various phases of condensed helium exhibit an exceptionally wide range of behaviour. The two stable isotopes, ^3He and ^4He , obey different statistics, and have solid and liquid phases which are very compressible, thus permitting measurements to be made at quite different densities using only moderate pressures. Hence in many ways condensed helium is an ideal « simple substance », but it is not completely representative because an unusually large fraction of its internal energy is zero point energy. This energy is responsible for the very high molar volume and compressibility; its effects are most marked in the liquid phases where it prevents the helium from solidifying under its vapour pressure, even at the lowest temperatures (SIMON [1]). Nevertheless, the behaviour of the solids, and of the liquids at higher temperatures, turns out to be not greatly different from that of other simple solids and liquids. In this paper we review the measurements which have been made on the conductivity of condensed helium, and discuss the information which may be obtained from them.

2. - The solid phases.

The conductivity of dielectric solids is a matter of considerable theoretical interest, but there is rather a shortage of good crystals with a really simple structure. In principle, the condensed inert gases offer an interesting series of solids, but it is necessary to obtain crystals reasonably free from cracks and coarse grain structure, which would severely limit the heat flow. Helium is particularly favoured in this connection as owing to the peculiar form of

the melting curve, it is possible to obtain tolerably perfect single crystals by cooling the compressed liquid at constant volume (WEBB, WILKINSON and WILKS [2]). Even though the helium must be contained within a strong metal cylinder, the thermal conductivity of the condensed phase is so considerable that the heat flow through the helium is always much bigger than through the metal.

The thermal conductivity of solid ^4He contained in an 0.5 mm tube at a density of 0.194 g/cm^3 is shown in Fig. 1 which is taken from WEBB *et al.*; the form of the curve is typical of that for dielectric solids as discussed by BERMAN [3]. At the higher temperatures the conductivity is limited mainly by scattering processes of the three phonon Umklapp type which are

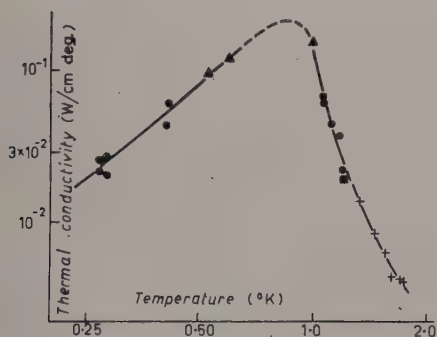


Fig. 1. — The thermal conductivity of solid ^4He at a density of 0.194 g/cm^3 , in a tube of internal diameter 0.5 mm. The crosses (+) represent earlier measurements in a 6 mm tube.

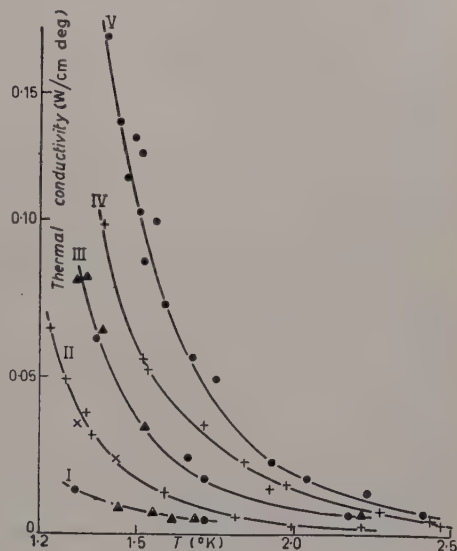


Fig. 2. — The variation of the thermal conductivity of solid ^4He in a tube of internal diameter 6 mm, as a function of temperature and density. I) 0.194; II) 0.203; III) 0.208; IV) 0.214; V) 0.218 g/cm^3 .

characteristic of a regular lattice with anharmonic forces. According to PEIERLS [4] the conductivity in this region should be of the form $AT^n \exp [\theta/bT]$, where n is of order unity, θ the Debye characteristic temperature, b approximately 2, and A a constant which is related to the anharmonicity and may be a function of density. The conductivity in this Umklapp region is very sensitive to the density as is shown in Fig. 2 (WILKINSON and WILKS [5]), and it turns out that the variation of θ with density is the most important parameter. These results cannot be compared directly with Peierls' expression for the conductivity as the value of θ for a given density varies appreciably with temperature (KEESOM and KEESOM [6]; WEBB *et al.* [2]), but one may proceed by writing,

in analogy with the usual gas kinetic relation, $K = \frac{1}{3}\lambda C v$, where C is the thermal capacity per cm^3 , v the velocity of sound, and λ the mean free path of the thermal waves between scattering processes which give rise to thermal resistance. It is thus found that λ is proportional to $\exp[\theta/2.3T]$ to within the accuracy of the experiments, and this behaviour is in good agreement with Peierls' theory of Umklapp processes (BERMAN, SIMON and WILKS, [7]).

The mean free path for Umklapp type processes increases rapidly as the temperature falls and eventually approaches the diameter of the specimen. Thermal resistance then arises only from the scattering of the thermal waves at the boundary of the specimen (CASIMIR, 1938), and the mean free path, λ , takes a value of the order of the diameter of the specimen. In this case the conductivity should vary as the specific heat of the crystal, and will therefore *decrease* as the temperature falls. The maximum in the conductivity-temperature curve (Fig. 1) occurs in the region where the mean free path for Umklapp processes is about equal to the diameter of the specimen (0.5 mm), at lower temperatures the conductivity varies approximately as T^3 , as does the specific heat. A more detailed analysis of these results shows that the mean free path slowly increases as the temperature falls, but even at the lowest temperatures is still at least a factor 2 less than the dimensions of the specimen. The reasons for this behavior are not fully understood but probably arise from the difficulty in obtaining good crystals in the narrower specimen tubes used in this particular experiment.

By extrapolating the results just discussed one may deduce that considerably larger changes in the conductivity will be observed at still higher

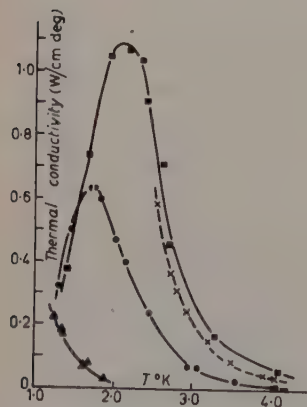


Fig. 3. — The thermal conductivity of solid ^4He at high densities. ▲: 0.218 g/cm^3 , ●: 0.262 g/cm^3 , ■: 0.282 g/cm^3 , x: 0.276 g/cm^3 .

densities and Fig. 3 shows results of WEBB and WILKS [4] at densities of .218, .262 and .282 g/cm^3 . The large variations observed both in the position and height of the maxima are again in general agreement with the behaviour postulated by PEIERLS and CASIMIR; at the higher densities the value of A appears to increase, implying that there is less anharmonicity in the more compressed material. Fig. 4 shows the conductivity of solid ^4He at two densities together with values for quartz and sapphire which have very different values of θ ; these results suggest that a reasonable estimate may be made of the conductivity of a dielectric crystal in the region of the maximum from a knowledge of θ alone.

No measurements have yet been made on solid ^3He but there is no reason to expect its behaviour to be very different from that of ^4He ,

except that it will have a considerably lower value of θ on account of its higher compressibility. The most interesting possibility concerning ^4He in the solid phase is with regard to the so-called isotope effect. It has been remarked for some time that most dielectric crystals do not have such a high maximum conductivity as would be expected on theoretical grounds, and BERMAN, FORSTER and ZIMAN [10] have proposed that the conductivity is in fact limited by scattering arising from the presence of different isotopes randomly distributed in the crystals. The ^4He used in the experiments described above contained probably no more than one part in 10^7 of ^3He ; this concentration of « foreign » isotope is much lower than that for the other crystals which have been measured, and BERMAN *et al.* remark that the maximum conductivity of solid helium comes closer to the theoretical value than that of any other material. The introduction of an appreciable concentration of ^3He into solid ^4He should have a very marked effect; the resistance produced by a second isotope is proportional to $(\Delta M/M)^2$, where M is the mass of the main constituent, and ΔM the difference in mass between the isotopes, and this ratio has a relatively large value in helium. The isotope concentration in solid helium may be easily varied, and it would obviously be desirable to measure the conductivity as a function of ^3He concentration.

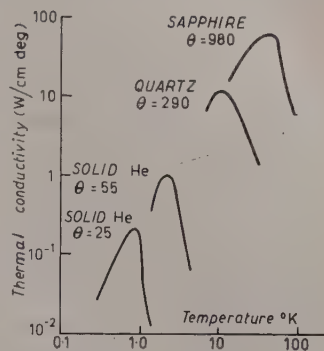


Fig. 4. — The thermal conductivities of various dielectric crystals.

3. — The liquid phases.

Before discussing the thermal conductivity of liquid ^3He and ^4He , it is useful to consider what is known about the conductivity of other simple liquids. The available information is rather meagre, and the most complete measurements are those of UHLIR [11] on argon and nitrogen; the results are rather similar, those for argon are shown in Fig. 5. (As the boiling point (87.4 °K) of argon is not far removed from its melting point (83.9 °K) it is necessary to apply considerable overpressures in order to make measurements over an appreciable temperature range). Ignoring the shaded region where convection may have occurred, it is seen that the conductivity in the liquid state rises steadily with falling temperature when measured at constant pressure. However, theoretical treatments usually lead to values of the conductivity at constant volume, and derived values for three different densities are

shown on the diagram. It is clear that a large part of the increase in conductivity with falling temperature is due to the change in volume; also the temperature dependence is less marked at the lower densities.

The viscosity of liquid argon has also been measured recently by ŽDANOVA [12] and her values for the viscosity are shown in Fig. 6. (Actually the curves show the fluidity or the reciprocal of the viscosity). The most striking factor of these results is that while at the higher densities the viscosity increases as the temperature falls, at the lowest densities it falls. This behaviour is accounted for by supposing that at low densities the liquid may best be described by an approach from a gas-like model and at higher densities from a solid-like model. The viscosity of a perfect gas decreases with falling T ,

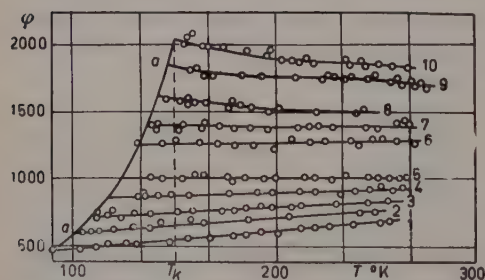


Fig. 6. — The fluidity (reciprocal of the viscosity) of liquid argon in c.g.s. units. (ŽDANOVA [12]). 1) $\rho = 1.37$; 2) 1.31; 3) 1.22; 4) 1.16; 5) 1.10; 6) 1.02; 7) 0.95; 8) 0.88; 9) 0.78; 10) 0.70 g/cm³. The continuous line gives the fluidity under the vapour pressure.

of the liquid under the vapour pressure using the same model; these are in fair agreement with the measurements of ŽDANOVA at the higher temperatures, but are too low at the lower temperatures. This discrepancy in the case of

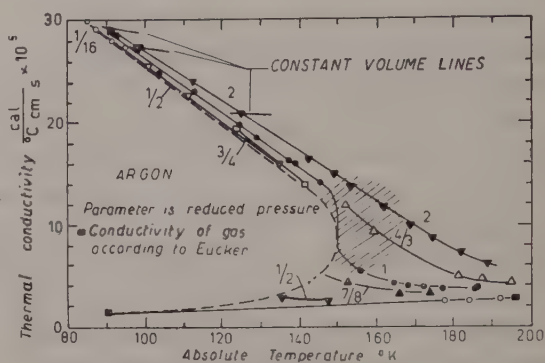


Fig. 5. — The thermal conductivity of argon under various pressures, expressed in units of the critical pressure of 48 atm. In the shaded region convection may have occurred. The dashed line represents extrapolations of constant pressure lines to the saturation temperatures (UHLIR [11]).

while the viscosity of a liquid with a quasi-lattice structure should rise exponentially with falling T , as is discussed by ANDRADE [13] and FRENKEL [14]. Of course a real liquid is neither a gas nor a solid, but the terms gas-like and solid-like are convenient provided it is understood that they represent asymptotic conditions never actually realized. As is discussed by UHLIR, it seems that a quantum mechanical treatment of a dense gas model can account for both the magnitude of the thermal conductivity and for its temperature dependence. UHLIR also gives calculated values of the visco-

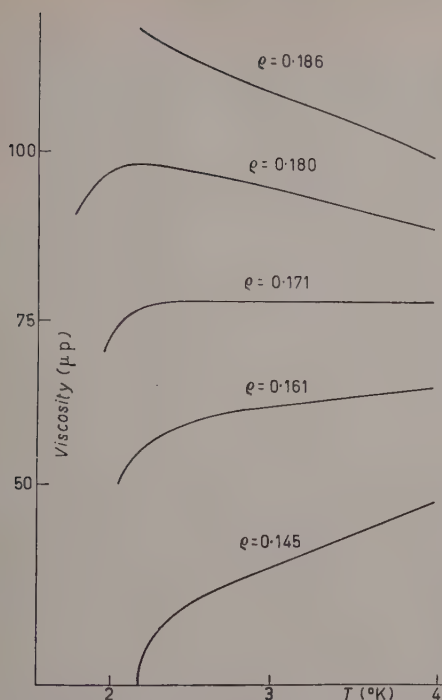


Fig. 7. — The viscosity of liquid helium I as a function of density (TJERKSTRA [15]).

results in a considerably greater molar volume. The thermal conductivity has been measured by GRENIER [16] (Fig. 8) and also by BOWERS [17]; these results were obtained under the vapour pressure, so that they correspond to molar volumes which increase considerably with rising temperature. GRENIER did not investigate the variation of the conductivity with density in any detail, but it did not appear to be very great. In any case the results in argon suggest that the effect of working at constant density would be to increase the

the viscosity underlines the limitations of the model but is not altogether surprising, as the viscosity unlike the thermal conductivity becomes very large when the liquid solidifies.

3.1. Helium I. — As is well known liquid ^4He exhibits a transition of the second order at 2.17 °K; the form of the liquid above this temperature (helium I) is not particularly remarkable, but at lower temperatures the fluid (helium II) exhibits quantum effects on a macroscopic scale. The viscosity of helium I has been measured at various densities by TJERKSTRA [15] and as shown in Fig. 7 exhibits a transition from gas-like to solid-like behavior as the density is increased. The viscosity at the lowest density decreases more rapidly with temperature than is the case for argon, and this may be associated with the relatively larger effect of zero point energy in helium which

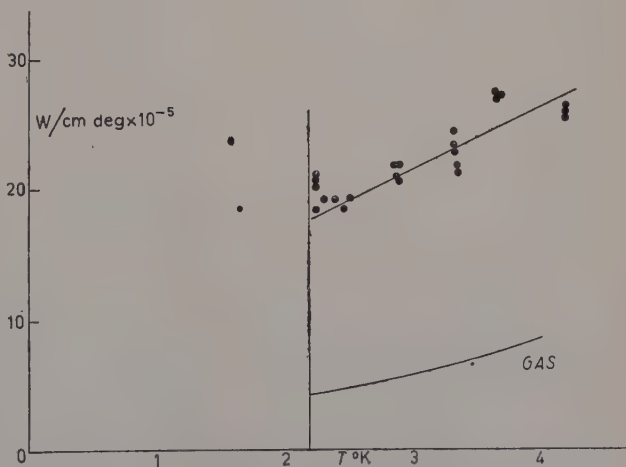


Fig. 8. — The thermal conductivity of liquid helium (GRENIER [16]). The values for the gas are taken from UBBINK and DE HAAS [30].

rate at which the conductivity falls with falling temperature; thus the behaviour of the conductivity, like that of the viscosity, suggests that a gas-like model is appropriate. Several authors have noted that the gas kinetic relation $K = 2.5 \eta C_v$ is approximately obeyed in helium I, and it is interesting to compute the ratio $K/\eta C_v$. The only complete data are for helium I along the vapour pressure line, and taking the results of DASH and TAYLOR [18] for the viscosity, of GRENIER for the conductivity, and extrapolated values of HILL and LOUNASMAA (to be published) for C_v , we find that $K/\eta C_v$ varies from 2.6 at 2.8 °K to 3.2 at 4.0 °K (CHALLIS, [19]). It is important to notice that there is a very considerable difference between C_v and C_{sat} in the region of 4 °K.

Although the viscosity of helium I depends considerably on pressure there is hardly any indication as to how the conductivity varies with it. Such results would be of interest as they would enable one to determine the dependence of the conductivity on temperature at constant density. A complete range of values of the conductivity and viscosity would offer good material to verify detailed calculations of the transport coefficients from a dense gas model or otherwise.

3.2. Helium II. — The behaviour of heat flow in helium II is so different from that in any other material that we do not propose to consider it in detail; for a survey of this region, see WILKS [20]. Here we only mention two aspects

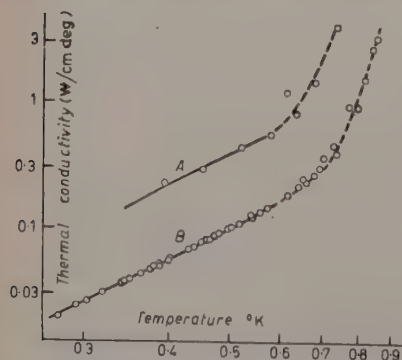


Fig. 9. — The thermal conductivity of liquid helium: A, in a tube 0.80 mm diameter; B, in a tube 0.29 mm diameter.

of its behaviour which underline its unique character. Although the behaviour of the thermal conductivity about 0.6 °K is complex, the results given in Fig. 9 (H. A. FAIRBANK and WILKS, [21]) show that below 0.6 °K the conductivity is proportional to the temperature gradient, to the specific heat and to the diameter of the specimen, as would be the case for solid helium. Thus the liquid appears to be as ordered as the solid, a conclusion in accord with the Third Law of Thermodynamics which states that the liquid has zero entropy at absolute zero. It is also of interest that at 0.6 °K the specific heat and entropy of the liquid begin to

increase rapidly indicating that the liquid is becoming more disordered; one might therefore expect the thermal conductivity to decrease at this temperature, but in fact it increases rapidly.

The complexity of helium II is also shown by the effect of adding impurity

atoms, which in fact means ^3He , for this is the only substance which will go into solution with ^4He . Quite small concentrations say 1 in 10^4 , are sufficient to reduce steady heat flows of about $10^2 \text{ W/cm}^2 \text{ deg}$ to about $10^{-3} \text{ W/cm}^2 \text{ deg}$. (BEENAKKER, TACONIS, LYNTON, DOKOUPIL and VAN SOEST, [22]). Helium II also has the unique property of transmitting true waves of temperature (second sound) which may be regarded as an oscillating flow of heat, but the addition of ^3He does not much decrease the amplitude of the waves (although it affects their velocity). To explain this seemingly contradictory behaviour we remark that an isotope produces thermal resistance in a solid because it acts as *fixed* scattering centre. In the liquid, however, the impurities are generally free to move about. Thus in the case of oscillating heat flows, they just drift to and fro with the heat flow. However, a steady flow carries the ^3He to the hot side of the vessel (LANE, FAIRBANK, ALDRICH and NIER, [23]), and there builds up a concentration gradient which effectively brings the ^3He atoms to rest. It is this stationary ^3He which is responsible for the increased thermal resistance (GORTER, TACONIS and BEENAKKER, [24]).

3.3. *Helium 3.* — Although it has been known for some time that ^3He does not have such strange properties as helium II, there have until recently been no measurements of the thermal conductivity. Fig. 10 shows recent values by CHALLIS and WILKS [26]; made with rather a small quantity of liquid; as discussed by the authors, the values may be about 10% low, because the resistance of the conductivity cell included the boundary resistances at its ends. The liquid also contained about 5% of ^4He , but as the conductivities of ^3He and ^4He are quite similar this should not make much effect. DONNELLY, FAIRBANK and LEE [27] have also reported values of the thermal conductivity including one point at 0.27°K which shows that the conductivity continues to fall at lower temperatures. Thus its

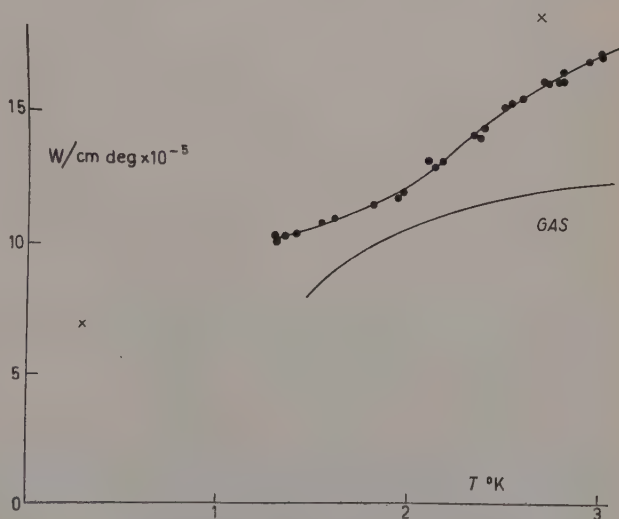


Fig. 10. - The thermal conductivity of liquid and gaseous ^3He (CHALLIS and WILKS [26]). As discussed by the authors the results for the liquid are probably about 10% too low. The two points \times are due to LEE, DONNELLY and H. A. FAIRBANK [27].

general behaviour is not unlike that of helium I. There is not really sufficient information available to calculate the ratio $K/\eta C_v$ as the specific heat has only been measured under the vapour pressure. However, if we take the values of T. R. ROBERTS and SYDORIAK [25] together with values of the viscosity given by DASH and TAYLOR [18] and the above conductivities the ratio comes out to be about 2.5.

It is also interesting to compare the conductivity of each liquid isotope with that of the corresponding gas, and these are also shown in Fig. 8 and 10. The conductivities of both gases and liquids decrease steadily with falling temperature, but the conductivities of liquid and gaseous ^3He are much closer together in magnitude than is the case for ^4He (CHALLIS and WILKS, [26]). ^3He has a much larger molar volume ($\sim 40 \text{ cm}^3$) than ^4He (28 cm^3) and this difference could be explained on the grounds that ^3He approximates more closely to the state of a gas.

As in the case of ^4He there is a need for more measurements to determine how the various parameters of the liquid vary with temperature when measured at constant volume. For example the viscosity rises with falling temperature but it is not clear how much of this may be associated with volume changes, as in the case of argon and ^4He . It is also desirable for measurements of the thermal conductivity and viscosity to be extended to still lower temperature to a region where the spin degeneracy of the liquid has been largely removed; that is the region below 0.1°K . In this connection it is interesting to note that SINGWI and KOTHARI [28] and POMERANČUK [29] have calculated that the conductivity of a Fermi-Dirac gas well below its degeneracy temperature should vary as $1/T$; in contrast the measured values of the liquid fall steadily down to 0.27°K .

REFERENCES

- [1] F. E. SIMON: *Nature*, **133**, 460, 524 (1934).
- [2] F. J. WEBB, K. R. WILKINSON and J. WILKS: *Proc. Roy. Soc.*, **A214**, 546 (1952).
- [3] R. BERMAN: *Advances Phys.*, **2**, 103 (1953).
- [4] R. PEIERLS: *Ann. der Phys.*, **3**, 1055 (1929).
- [5] K. R. WILKINSON and J. WILKS: *Proc. Phys. Soc.*, **A 64**, 89 (1951).
- [6] W. M. KEESOM and A. P. KEESOM: *Physica*, **3**, 105 (1936).
- [7] R. BERMAN, F. E. SIMON and J. WILKS: *Nature*, **168**, 277 (1951).
- [8] H. B. G. CASIMIR: *Physica*, **5**, 495 (1938).
- [9] F. J. WEBB and J. WILKS: *Phil. Mag.*, **44**, 663 (1953).
- [10] R. BERMAN, E. L. FOSTER and J. M. ZIMAN: *Proc. Roy. Soc.*, **A 237**, 344 (1956).
- [11] A. UHLIR: *Journ. Chem. Phys.*, **20**, 463 (1952).
- [12] N. F. ŽDANOVA: *Soviet Physics JETP*, **4**, 749 (1957).
- [13] E. N. ANDRADE da C.: *Phil. Mag.*, **17**, 497, 698 (1934).

- [14] J. FRENKEL: *Kinetic Theory of Liquids* (Oxford, 1946).
- [15] H. H. TIERKSTRA: *Physica*, **18**, 853 (1952).
- [16] C. GRENIER: *Phys. Rev.*, **83**, 598 (1951).
- [17] R. BOWERS: *Proc. Phys. Soc.*, A **65**, 511 (1952).
- [18] J. G. DASH and R. D. TAYLOR: *Phys. Rev.*, **106**, 398 (1957).
- [19] L. J. CHALLIS: *Thesis* (Oxford, 1957).
- [20] J. WILKS: *Reports on Progress of Physics* (London, 1957).
- [21] H. A. FAIRBANK and J. WILKS: *Proc. Roy. Soc.*, A **231**, 545 (1955).
- [22] J. J. M. BEENAKKER, K. W. TACONIS, E. A. LYNTON, Z. DOKOUPIL and G. VON SOEST: *Physica*, **18**, 433 (1952).
- [23] C. T. LANE, H. A. FAIRBANK, L. T. ALDRICH and A. O. NIER: *Phys. Rev.*, **73**, 256 (1948).
- [24] C. J. GORTER, K. W. TACONIS and J. J. M. BEENAKKER: *Physica*, **17**, 841 (1951).
- [25] T. R. ROBERTS and S. G. SYDORIAK: *Phys. Rev.*, **98**, 1672 (1955).
- [26] L. J. CHALLIS and J. WILKS: *Proceedings of Conference on ^3He at Ohio State University* (1957).
- [27] D. M. LEE, R. J. DONNELLY and H. A. FAIRBANK: *Bull. Amer. Phys. Soc.*, **2**, 64 (1957).
- [28] K. S. SINGWI and L. S. KOTHARI: *Phys. Rev.*, **76**, 305 (1947).
- [29] I. POMERANČUK: *Žu. Èksper. Teor. Fiz.*, **20**, 1919 (1950).
- [30] J. B. UBBINK and W. J. DE HAAS: *Physica*, **10**, 465 (1943).

INTERVENTI E DISCUSSIONI

— K. MENDELSSOHN:

Another interesting effect observable in heat conductivity measurements on solid ^4He with ^3He impurity would be the annealing of the crystal under its zero point energy. At low enough temperatures the stable condition of the He crystal will be a state in which the ^3He is in some form separated out and this should be apparent in the heat conduction. Hence if a specimen with random distribution of ^3He is made and its heat conductivity is measured at successive times while the crystal is kept at low temperature, a change due to the ordering of the solid system under its zero point motion should be apparent in the results. It will be of particular interest for the theories of the melting process if the rate of this change is observed in the proximity of the melting curve.

— J. WILKS:

This is an interesting possibility. However, our experience with pure ^4He suggests that to obtain annealing in the solid (and therefore mobility of ^3He atoms) one might have to go to temperatures higher than those where phase separation probably occurs.

— M. J. BUCKINGHAM:

One would only expect the viscosity and thermal conductivity of liquid ^3He to approach the low temperature behaviour in the region, so far not explored, where the specific heat is presumably linear with temperature namely below 0.2°K .

— L. J. CHALLIS:

If the measured values of the conductivity of liquid ^3He are to extrapolate to a pure phonon conductivity at sufficiently low temperatures, a very rough estimate indicates that the pure phonon conductivity would probably not be observed much above 0.01°K .

— M. J. BUCKINGHAM:

I do not agree that at low temperatures in liquid ^3He the excitations are mainly Debye type. They correspond much more to the particle excitations of an ideal Fermi gas — giving for example a linear rather than T^3 specific heat.

— J. WILKS:

I think there probably will be a T^3 component in the thermal conductivity although this will not be distinguishable until below 0.1°K or less. However, measurements in this temperature region will be quite difficult.

— A. MICHELS:

The discrepancy found between the experimental values of C_v and that found from the data of heat conductivity and viscosity $\lambda = \frac{5}{2}\eta C_v$ may be related to the following idea.

While η is measured at constant density as long as p and T are constant, during the determination of λ this is not exactly true.

During a measurement of λ a temperature gradient exists and thus a density gradient. This will lead to complications at these densities and with these gases, where a density dependent potential energy is present.

Effects of Translational Diffusion on Nuclear Spin Relaxation in Simple Condensed Systems (*).

H. C. TORREY

Department of Physics, Rutgers University - New Brunswick, N. J.

It is well known that translational diffusion may under certain circumstances be mainly responsible for nuclear spin relaxation and one expects this to occur especially in simple monoatomic condensed systems when complications due to molecular rotation, quadrupole effects and other competing processes are absent. The possibility exists therefore that in such systems a study of the relaxation time T_1 of the nuclear spins as a function of temperature, pressure and other parameters may throw some light on the internal dynamics of such systems.

The process of relaxation by translational diffusion was treated first by BLOEMBERGEN [1] (+) and later a more refined treatment was given by the author [2]. The latter paper will be referred to as A.

The relaxation time for a two spin system may be found from the fundamental result (generalized from A)

$$(1) \quad w_{ab} = \frac{1}{\hbar^2} \iiint P(\mathbf{r}, \mathbf{r}_0, t) \varrho(\mathbf{r}_0) H_{ab}^*(\mathbf{r}) H_{ab}(\mathbf{r}_0) \exp[i\omega t] dt d\mathbf{r} d\mathbf{r}_0.$$

Here w_{ab} is the probability per unit time for a transition between states a and b of relative spin orientation of two spins (1) and (2); H_{ab} is the matrix element of the term in the Hamiltonian inducing the transition; \mathbf{r}_0 the position vector of spin (2) relative to spin (1) at time $t = 0$; \mathbf{r} the same at time t ; $\varrho(\mathbf{r}_0)$ the radial density function (the number of spins per unit volume) at $t = 0$

(*) Research supported by the U. S. Air Force Office of Scientific Research.

(+) R. KUBO and R. TOMITA: *Journ. Phys. Soc. Japan*, **9**, 888 (1954) have pointed out that the effect of double transitions should have a weight twice that given by BLOEMBERGEN. The same error occurs also in A. The results of the present paper have been modified to correct this error.

relative to spin (1); $P(\mathbf{r}, \mathbf{r}_0, t) d\mathbf{r}$ the conditional probability that if spin (2) is at \mathbf{r}_0 at $t=0$ it is at \mathbf{r} in $d\mathbf{r}$ at time t ; and $\omega = |E_a - E_b|/\hbar$, where E_a and E_b are the energy eigenvalues of the two orientation states.

We shall first apply this result to the case of diffusion in which the elementary step is small compared with the molecular diameter a . (Strictly $\langle r^2 \rangle \ll 6a^2$). In this case as shown in A provided that one is on the high temperature side of the T_1 minimum which will be true except for very viscous liquids, one can use for $P(\mathbf{r}, \mathbf{r}_0, t)$ the solution of the diffusion equation

$$(2) \quad P(\mathbf{r}, \mathbf{r}_0, t) = (8\pi Dt)^{-3/2} \exp [|\mathbf{r} - \mathbf{r}_0|^2/8Dt],$$

where D is the self-diffusion coefficient.

For $\varrho(\mathbf{r}_0)$ we assume a simple step function: $\varrho = 0$, $r_0 < a$ and $\varrho = n$ (number of spins per unit volume) for $r_0 > a$. This amounts to taking $r_0 = a$ as the lower limit of integration over r_0 . A similar cut-off is made for the integration over r .

The result for T_1 for a system of like spins is

$$(3) \quad \frac{1}{T_1} = \frac{8\pi}{15} \gamma^4 \hbar^2 I(I+1) n/aD.$$

This expression is $\frac{4}{5}$ of the result for T_1^{-1} obtained by BLOEMBERGEN (corrected for the Kubo-Tomita effect).

If on the other hand the elementary step is large compared with the atomic diameter one must multiply the above result by $5D\tau/2a^2 = 5\langle r^2 \rangle/12a^2$, where τ is the mean jump time (see eq. (3b) of A). Since under actual circumstances in a liquid one has both processes occurring [3], the correct expression will be somewhere between. It is not possible to be more definite without making some assumptions as to the details of the microscopic diffusion process. Such details are most uncertain in liquids, but in certain solids where one is dealing with lattice diffusion it is possible to seek for a quantitative comparison between theory and experiment.

In searching for simple systems to which this relaxation theory can be applied one naturally thinks of the noble liquids and solids He and Xe. So far sufficient data are not available to test the theory for such materials. Other substances, less simple, are the alkali metals. HOLCOMB and NORBERG [4] have applied the diffusion theory with good results to Li, Na and Rb. In these cases one has complications due to quadrupole moments and interaction with conduction electrons.

Another type of system which one would not ordinarily consider simple are solid solutions of hydrogen in certain transition metals. If one fixes one's attention on the H in such systems, however, and assumes that the H is dissolved interstitially, is dissociated and ionized, the H system is almost ideally

simple. The protons are located at the interstitial sites in potential minima and jump by an activation process to neighboring sites. We have studied the relaxation of the proton spins in such materials, namely in $\text{PdH}_{.64}$, $\text{TiH}_{1.77}$, and $\text{TaH}_{.75}$.

It is known that there can be more than one phase existing in such materials. For small concentrations one has the so-called α -phase in which the hydrogen occupies the various interstitial sites at random. As the H concentration is increased a β -phase appears. For a range of concentrations the two phases coexist but for sufficiently high concentrations of H only the β -phase is present. The process is very analogous to the well-known continuity of liquid and gaseous states of matter exhibited by the Van der Waals isotherms. In fact the pressure-concentration isotherms have a remarkable resemblance to the Van der Waals isotherms; the α -phase corresponding to the gas and the β -phase to the liquid. The pressure is nearly constant over the concentration range in which both phases coexist and rises rapidly with concentration in the pure β -phase. LACHER [5] has treated this process as an order-disorder transformation; the β -phase corresponding to some ordered arrangement of the H in the interstitial sites. For the concentrations used in our nuclear resonance studies the β -phase is alone present. Presumably the H occupies a sub-lattice of the interstitial sites. This sub-lattice is incompletely occupied at the concentrations we used. There are present substantial number of vacancies into which the H can jump.

In these cases, then, we are dealing with diffusion in a lattice which has been treated in the theory of part IV of A. In the case of $\text{PdH}_{.63}$ and $\text{TiH}_{1.77}$ where the effects of the nuclear moments of the metal are almost negligible this theory can be taken over almost without change (except for the Kubo-Tomita effect). For $\text{TaH}_{.75}$ however, the large moment of ^{181}Ta (100% abundant) produces about $\frac{3}{2}$ of the total relaxation of the proton spins and appropriate modifications are required in the theory. These however are easy to make. T_1 for H in these materials has been measured over a wide temperature range and it is found that at low temperatures the relaxation is controlled by inter-

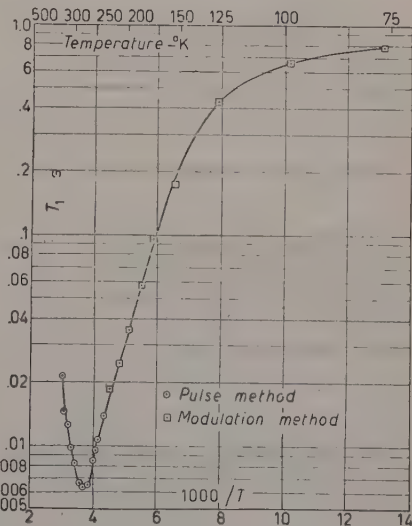


Fig. 1. - Spin-lattice relaxation time T_1 of H in $\text{TaH}_{0.75}$ as a function of temperature.

action with conduction electrons but at higher temperature diffusion relaxation is dominant. Fig. 1 shows the results for $\text{TaH}_{.75}$. A deep minimum in T_1 is found for a frequency of 9.25 MHz at $T = 268^\circ\text{K}$. The minimum T_1 is (6.3 ± 0.2) ms. Fig. 3 shows the details of the minimum; the solid line is theoretical. The minimum value of T_1 provides an excellent and sensitive

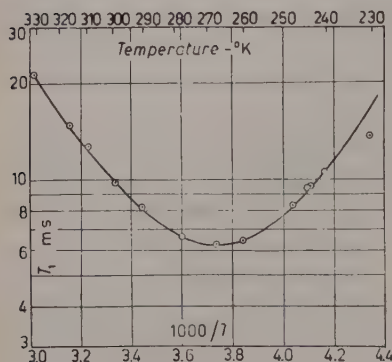


Fig. 2. — Detail of Fig. 1. near minimum in T_1 .

test of the theory, for the theoretical value of T_{1m} (see for example eq. (87) of A) depends only on the structure of the interstitial lattice and on the nuclear moments, the jump time at this temperature being simply related to the frequency, $\omega\tau = s$, where s is a constant of the order of unity and depends on the structure of the interstitial lattice occupied by the H. We have assumed that this lattice is b.c.c. since the stoichiometric composition TaH is approached for the highest concentration in the b.c.c. Ta lattice. Such a lattice can be formed from either the tetrahedrally or the octahedrally co-ordinated interstitial sites. The latter appears more

probable since such an interstitial lattice would account for the tetragonal distortion of the Ta lattice observed by STALINSKI [6] in the β -phase of H whereas this type of distortion would not be expected from a b.c.c. lattice formed from the tetrahedral sites. Actually we have used both possibilities to calculate the expected value of T_1 (min.). The theoretical value of this quantity depends on the value assumed for the Ta nuclear moment which contributes about $\frac{2}{3}$ of the whole relaxation; the remaining $\frac{1}{3}$ coming from the proton-proton interactions. The Ta moment is unfortunately known only from optical h.f.s. determinations. The latest and probably the most accurate measurement is that of BROWN and TOMBOULIAN [7] who give $\mu = 1.9$ n.m.; but taking into account corrections due to the finite size of the nucleus they change this to 2.1 n.m. The error in this result may however be as much as 20%. We obtain the following results for T_{1m} :

$\mu_{(\text{Ta})}$ (assumed)	interstitial lattice	
	octahedral	tetrahedral
1.9 n.m.	5.3 ms	6.0 ms
2.1	6.1	6.8
2.3	6.9	7.6
observed	(6.3 ± 0.2) ms	

An adequate test of the theory must await a further determination of the tantalum moment but if the octahedral lattice is assumed and the best value of 2.1 n.m. is taken the agreement is excellent.

The relaxation of protons in $\text{PdH}_{.64}$ resembles that in $\text{FeH}_{.75}$. Again there is a deep minimum in T_1 ; $T_{1m} = 13.6$ ms at a temperature of 277 °K. In this case the Pd moment plays an almost insignificant role. Only ^{105}Pd (23% abundant) has a moment and that is quite small ($\mu = 0.57$ n.m.; $I = \frac{5}{2}$). The interstitial lattice is almost certainly f.c.c. displaced from the f.c.c. Pd lattice. Again the interstitial lattice can be formed from octahedral or tetrahedral sites. The following results are obtained for T_{1m} :

octahedral sites	tetrahedral sites	observed
14.4 ms	14.2 ms	(13.6 ± 0.6) ms

The small difference in the first two is due to the small effect of the ^{105}Pd moment. The agreement with the experimental value is satisfactory and it is not possible to decide on the lattice on the basis of these results.

The activation energy for proton jumping in these hydrides can be obtained by plotting $\log \tau$ vs. $1/T$, where τ is the mean jump time. The latter can be obtained from the theoretical formula for T_1 as suggested in A. The results show that in $\text{TaH}_{.75}$ and $\text{PdH}_{.64}$ there are two activation energies for each material.

In $\text{TaH}_{.75}$ we find 0.25 eV above 240 °K and 0.11 eV below and in $\text{PdH}_{.64}$, 0.24 eV above 220 °K and 0.08 eV below. Their similarity in behavior is striking.

In $\text{TiH}_{1.77}$ as shown in Fig. 2 two minima in T_1 are found. The reason for this is still uncertain, but it would seem likely that there may be two activation processes perhaps associated with the two kinds of interstitial sites.

Pure Ti metal has a hexagonal close-packed structure but with this much hydrogen the Ti lattice is f.c.c. It would appear likely that the stoichiometric composition TiH_2 would have the fluorite structure as is known [8] to be

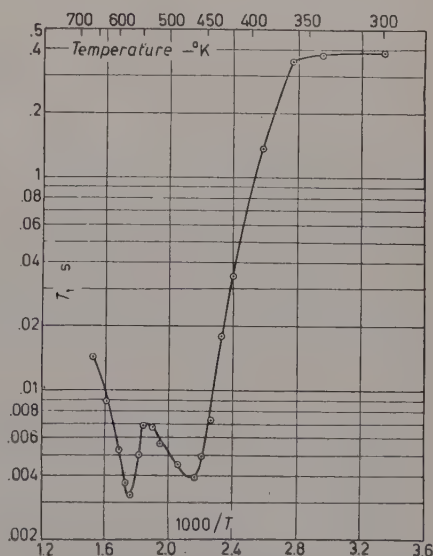


Fig. 3. — Spin-lattice relaxation time, T_1 of H in $\text{TiH}_{1.77}$ as a function of temperature.

the case for ThH_2 . In this case the H occupies the tetrahedral sites, but for the reduced hydrogen concentration of our sample it is possible that the octahedral sites are partially occupied. It is possible that competition between octahedral and tetrahedral sites may account alone for the two activation energies observed in $\text{TiH}_{.75}$ and $\text{PdH}_{.64}$. At any rate the calculated T_1 for the fluorite structure is 4.2 ms whereas the two minimal T_1 's have the observed values of 3.1 ms and 3.9 ms.

A more complete discussion of the interpretation of these data including the correlative interpretation of line width data as well as the low temperature relaxation due to interaction with conduction electrons will be published elsewhere.

* * *

The experimental work on which the paper is based was done by Drs. T. KOHANE, P. GREEBLER and E. APGAR. The samples were prepared by Drs. I. GINSBURG and P. GREEBLER.

REFERENCES

- [1] N. BLOEMBERGEN: *Thesis* (Leyden, 1948).
- [2] H. C. TORREY: *Phys. Rev.*, **92**, 962 (1953).
- [3] B. BROCKHOUSE: in this issue, pag. 45.
- [4] D. HOLCOMB and R. E. NORBERG: *Phys. Rev.*, **98**, 1074 (1955).
- [5] J. LACHER: *Proc. Roy. Soc., A* **161**, 525 (1937).
- [6] B. STALINSKI: *Bull. de l'Acad. Polonaise des Sci.*, Cl. III, vol. II, no. 5 (1954).
- [7] B. M. BROWN and D. H. TOMBOULIAN: *Phys. Rev.*, **88**, 1158 (1952).
- [8] R. E. RUNDLE, C. G. SHULL and E. O. WOLLAN: *Acta Cryst.*, **5**, 22 (1952).

Nuclear Magnetic Resonance and Molecular Association in Liquids.

L. GIULOTTO

Istituto di Fisica dell'Università di Pavia - Pavia

Recent observations on the diamagnetic shift of nuclear magnetic resonance lines in H-bonded systems have given some information about molecular associations. Another possibility to study H-bonding and molecular association in liquids by means of the technique of nuclear magnetic resonance exists, although on rather different grounds. The basic line we have pursued at Pavia is as follows: according to the theory of BLOEMBERGEN, PURCELL and POUND [1] we can expect that in mixtures of two liquids, at different concentrations and constant temperature, the product $T_1\eta$ (T_1 = thermal relaxation time, η = viscosity) should vary linearly with concentration. If deviations from this law are observed, one is allowed to think that molecular association occurs. As a matter of fact, clustering does affect the rotational motion of the molecules, thus causing a variation of T_1 .

Molecular associations in liquids and in liquid mixtures can be investigated also by observing, at different temperatures T and at constant concentration, possible deviations from the relationship $T_1\eta/T = \text{const}$, which is also allowed for by the theory.

In order to carry out that kind of research, one needs to operate so as to measure nuclear relaxation times of liquids with good precision. Oxygen in solution, which causes a diminution of T_1 , must be removed. The measurement of T_1 can be performed by a sequence of signals due to fast and adiabatic passages through resonance (with the exclusion of transients). During one such passage the nuclear magnetization undergoes a complete reversal and then tends exponentially to the equilibrium value. The value of T_1 can be evaluated from the heights of successive signals and from the distance between them [2].

We report hereby some experimental data part of which have already appeared [3].

Fig. 1 shows the plot of $(1/T_1) \cdot (\eta_0/\eta)$ (η_0 = viscosity of the solvent, η = viscosity of the solution) versus concentration, for solutions of C_6H_5Cl in CCl_4 : The linear behaviour is in agreement with the assumption that no molecular

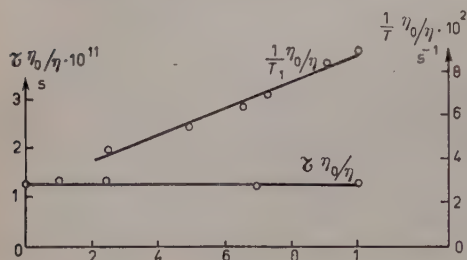


Fig. 1. — $(1/T_1) (\eta_0/\eta)$ and $\tau \eta_0/\eta$ in solutions of C_6H_5Cl in CCl_4 at different concentrations.

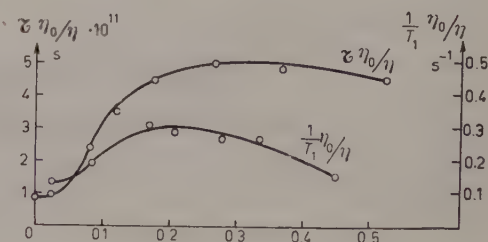


Fig. 2. — $(1/T_1) (\eta_0/\eta)$ and $\tau \eta_0/\eta$ in solutions of C_6H_5OH in CCl_4 at different concentrations.

association is present in such a solution. In the same figure data concerning the Debye time τ , obtained by other authors, are reported. $\tau \eta_0/\eta$ results to be independent of concentration, in agreement with our results on T_1 .

In Fig. 2 the analogous data are reported for solutions of C_6H_5OH in CCl_4 .

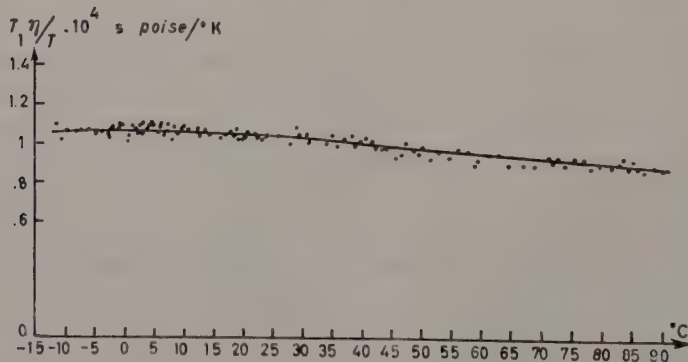


Fig. 3. — $T_1\eta/T$ in pure water at different temperatures.

The non-linear behaviour is in agreement with the assumption that in these solutions molecular associations are present.

Solutions of alcohols in CCl_4 show a similar behaviour.

In Fig. 3 the behaviour of $T_1\eta/T$ in pure water at various temperatures from $-12^\circ C$ to $95^\circ C$ is reported. One can see that $T_1\eta/T$ is only roughly independent of the temperature. In fact $T_1\eta/T$ decreases appreciably with increasing temperature, especially at the higher temperatures.

This behaviour does not seem to agree with the assumption that well de-

find molecular associations (such as $(\text{H}_2\text{O})_2$, $(\text{H}_2\text{O})_3$, ...) are present. Our results are in better agreement with the assumption of a quasi-crystalline structure of water, which is progressively collapsing as the temperature increases. The accuracy of our results does not allow us to decide if $T_1\eta/T$ has a maximum around 4 °C.

Measurements now on progress show that also in the case of ethyl alcohol $T_1\eta/T$ decreases with increasing temperature in the range explored so far.

REFERENCES

- [1] N. BLOEMBERGEN, E. M. PURCELL and R. V. POUND: *Phys. Rev.*, **73**, 679 (1948);
N. BLOEMBERGEN: *Nuclear Magnetic Relaxation* (The Hague, 1948).
- [2] G. CHIAROTTI, G. CRISTIANI, L. GIULOTTO and G. LANZI: *Nuovo Cimento*, **12**, 519 (1954).
- [3] G. CHIAROTTI, G. CRISTIANI and L. GIULOTTO: *Nuovo Cimento*, **1**, 863 (1955);
L. GIULOTTO, G. LANZI and L. TOSCA: *Journ. Chem. Phys.*, **24**, 632 (1956);
L. GIULOTTO: *Arch. de Sci.*, **9**, 212 (1956); L. GIULOTTO, G. LANZI and L. TOSCA:
Arch. de Sci., **10**, 250 (1957).

Magnetic Resonance Studies of Self-Diffusion in Simple Solids.

C. P. SLICHTER

University of Illinois - Urbana, Ill.

1. - Introduction.

The effect of atomic movement on the widths of nuclear magnetic resonance lines is dramatic and a familiar phenomenon to workers in the resonance field. This paper is concerned with the study of diffusion rates, primarily in simple solids, by measurements of the widths of nuclear resonance lines. We will begin with a brief review of the pertinent theoretical expressions, demonstrate their application to self-diffusion in several cases, and offer some speculations on a possible technique for extending the information to separate the energy of diffusion, E_d , into its two parts the energy of motion, E_M , and the energy of formation, E_F .

2. - Theory of motional narrowing.

A numbers of papers have been written on the subject of the effect of atomic motions on the width of resonance lines, the phenomenon of « motional narrowing » [1]. For our purposes, a simple argument will give the necessary results. The width of a nuclear resonance may be determined by a variety of effects, but the one which concerns us arises from the magnetic dipole interaction with the neighbors. A neighbor of magnetic moment μ a distance r away produces a magnetic field of magnitude

$$(1) \quad H_{\text{loc}} = \pm \mu/r^3,$$

where the plus and minus signs are to remind us that the direction may aid or oppose the field of our magnet. We expect, therefore, that the resonance width will be approximately H_{loc} where for r we use the nearest neighbor

distance. H_{loc} produces a shift in the precession angular frequency of amount $\Delta\omega_0$ given by

$$(2) \quad \Delta\omega_0 = \gamma H_{\text{loc}},$$

where γ is the nuclear gyromagnetic ratio.

The effect of nuclear motion can be seen by thinking of nucleus with one neighbor, which every so often is replaced. The distance r remains fixed, but the spin orientation of the successive neighbors are in general random. As result the local field at the fixed nucleus varies from $+H_{\text{oc}}$ to $-H_{\text{loc}}$. Let us define a time, τ_c , which is crudely the average time that the local field may be thought of as having one sign. It is then the mean time a given nucleus remains as a neighbor. Then in τ_c a phase angle $\pm \Delta\omega_0 \tau_c$ is accumulated, by the fixed nucleus, over and above that due to uniform precession in the applied field. After n such intervals, some with more rapid precession, some with less rapid, the mean square deviation from uniform precession is $\overline{\Delta\varphi^2} = n (\Delta\omega_0 \tau_c)^2$ since we have a random walk in angle. In a time ϑ , n is given by $n = \vartheta/\tau_c$, so that

$$(3) \quad \overline{\Delta\varphi^2} = (\Delta\omega_0)^2 \tau_c \vartheta.$$

When $\overline{\Delta\varphi^2} = 1$, sizeable dephasing has occurred. This dephasing time, usually called T_2 , is the inverse of the line-width, $\Delta\omega$, giving us

$$(4) \quad \frac{1}{T_2} = \Delta\omega = (\Delta\omega_0)^2 \tau_c.$$

We note that the smaller τ_c the narrower the line. This equation therefore describes motional narrowing. However making τ_c infinite cannot make the line infinitely broad of course, since the *maximum* breadth is clearly $\Delta\omega_0$. Thus we have that $\Delta\omega = \Delta\omega_0$ for $\Delta\omega_0 \tau_c > 1$. This result signifies that very slow motion has no effect. Above a critical threshold $\tau_c = 1/\Delta\omega_0$ the line becomes progressively more narrow.

Physically we are saying that in a rigid lattice a nucleus grinds away relentlessly either too fast or too slow to maintain phase with the other nuclei. Interchange of neighbors converts the dephasing to a random walk, a less efficient method of getting out of step. The interchange of neighbors does not help maintain phase memory, of course, if the nuclei have gotten out of phase before a step occurs.

If we write $1/\tau_c = \nu \exp[-E/kT]$ we note that

$$(5) \quad \Delta\omega = (\Delta\omega_0)^2 \frac{\exp[E/kT]}{\nu}$$

and that we can determine E by studying either 1) the temperature variation of $\Delta\omega$ in the narrowed region or 2) assuming a value for ν obtain E by finding the narrowing temperature at which $\nu \exp[-E/kT] = \Delta\omega_0$. The second method is similar to the proposal of NOWICK [2] for analyzing diffusion data by assuming D_0 .

The line-narrowing criteria can be used to determine the unknown energy E when the line narrows at temperature, T , from a rigid lattice width $\Delta\omega_0$ in terms of the corresponding quantities E_a , T_a , and $\Delta\omega_0^a$ of a resonance for which E_a is known. The formula we find is

$$(6) \quad E = E_a \left(\frac{T}{T_a} \right) + RT \ln \left(\frac{\Delta\omega_0^a \nu}{\Delta\omega_0 \nu_a} \right).$$

Since we do not know ν in general, we must use an estimate to get the logarithmic correction term. A simple guess is to say ν is proportional to the Debye Θ . Unfortunately when one goes from one type of lattice to another, or if the rigid lattice line shapes are quite different, one cannot hope for too great precision. In fact, there is some ambiguity in what to take as the narrowing temperature.

3. - Application.

The ideas of the previous section can be readily generalized to a more complicated motion such as that of self-diffusion. Although a rigorous theory can be set up, to date no one has carried through the entire analysis. A fairly satisfactory result can be obtained easily, however, for the case of a strongly narrowed line (fast motion). The result is $\Delta\omega = \alpha(\Delta\omega_0)^2\tau$, where α is a constant of order unity but not too well known, and τ is the mean time an atom spends on a lattice site. For purposes of comparison between different materials, one can often assume α will be the same in both.

A number of applications of the resonance techniques have been reported. The first figure shows the data of HOLCOMB and NORBERG [3] on sodium. The semi-log plot of T_2 ($\propto 1/\Delta\omega$) vs. $1/T$ should be a straight line with slope the energy of diffusion E_D . A line with the slope of 10.0 kcal/mole $^\circ\text{K}$, is drawn through the data. NACHTRIEB, WEIL, and CATALANO [4] find 10.4 kcal/mole $^\circ\text{K}$ by radioactive tracers. The second figure shows data for lithium also taken by NORBERG and HOLCOMB. The value of 13.2 kcal also agrees with that obtained from their spin-lattice relaxation measurements analyzed by Torrey's theory. Comparison of the line-narrowing temperatures gives 13.8 kcal for Lithium which is 4% greater. In both cases we see that at temperatures near the melting point the semi-log relationship fails. We will

discuss this point later. Several other metals have been studied. MASUDA [5] has studied Cd and found agreement with results of radio-active tracers. From the resonance view-point Masuda's results are very interesting because the line-breadth $\Delta\omega_0$ arises from the pseudo-exchange coupling between nuclei.

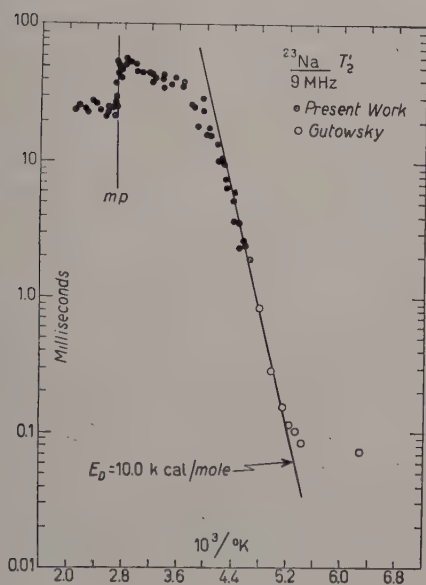


Fig. 1. — Log of spin phase-memory time in sodium (corrected for spin-lattice relaxation broadening) vs. $1/T$ from HOLCOMB and NORBERG, ref. [3].

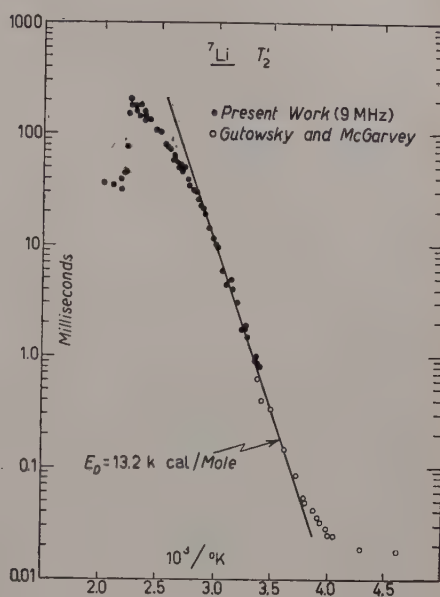


Fig. 2. — Log of spin phase-memory time in lithium (corrected for spin-lattice relaxation broadening) vs. $1/T$ from HOLCOMB and NORBERG, ref. [3].

The case of aluminium is more complicated. SEYMOUR [6] first observed the line narrowing, his data extending up to 450 °C. His measure of the width of the resonance was the distance between the points of maximum slope of the absorption line. He finds $D_0 = 10^{-3 \pm 1} \text{ cm}^2/\text{s}$ and $E_d = .91 \text{ eV}$. This value of D_0 is excessively small, and the activation energy differs markedly from the estimate of NOWICK [2] who predicted 1.43 eV from data on chemical diffusion. The activation energy also differs from the value $E_d = 1.2 \text{ eV}$ obtained by BRADSHAW and PEARSON [7] who measured the resistance of quenched aluminium.

SPOKAS [8] has extended the results of SEYMOUR to the melting point (650 °C). His data are shown in Fig. 3. The first thing that SPOKAS finds is that over most of the region of Seymour's data the line shape is changing from a nearly Gaussian low temperature line to a Lorenz shaped line at about 360 °C. Above 360 °C the shape is Lorentz, and it is in *this* region that the

theory of motional narrowing should apply with some precision. Over most of the range of Seymour's data (he begins to see narrowing at about 260 °C) the criteria of width are ambiguous since the shape is changing.

SPOKAS has developed a so-called phase coherent pulsed apparatus that enables him to work with the poor signals and narrow lines found at high temperatures. He finds that the aluminum line narrows until about 430 °C above which a leveling off sets in (see Fig. 3). We shall attribute the high temperature broadening to an electric quadrupolar interaction and discuss the evidence for this hypothesis in the next section. The fact that the high temperature line width is independent of temperature leads us to attribute it to a temperature independent

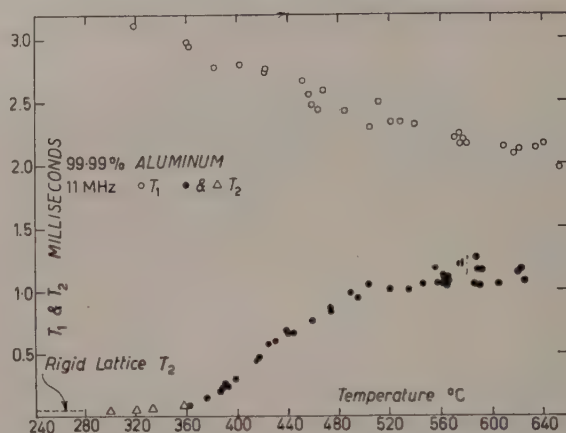


Fig. 3. — Spin phase-memory time, T_2 , and spin lattice relaxation time, T_1 , in aluminum vs. T from SPOKAS, ref. [8].

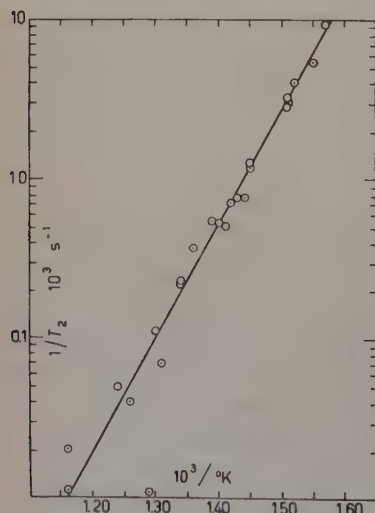


Fig. 4. — Log of dipolar contribution to the spin phase-memory time vs. $1/T$ in aluminum from SPOKAS, ref. [8].

mechanism. We then subtract this width, obtaining the plot of Fig. 4 which gives $\ln(1/T_2)$ vs $1/T$. The data now agree with a straight line of slope (1.4 ± 1) eV.

From the narrowing temperature, using a reasonable D_0 (such as given by NOWICK [2]) SPOKAS finds $E_D = 1.43$ eV. These results are at least internally consistent, and lead to the belief that the value of BRADSHAW and PEARSON may be a bit low.

4. — Broadenings below the melting point.

If a nucleus with an electric quadrupole moment is in a site of perfect cubic symmetry, there is no orientation dependence of the energy of interaction between its electric quadrupole moment and the surroundings. Thus, ideally there would be

no electric quadrupole effects observed in Li, Na, or Al. The presence of impurities, dislocations or strains will distort the symmetry, however, as has been observed for example by WATKINS and POUND for ionic crystals and by BLOEMBERGEN and ROWLAND for metals [9]. Since the quadrupolar coupling varies from nucleus to nucleus under these circumstances, the resonance line is to some extent broadened. There are no signs of such effects in Li, Na, or Al at low temperatures because the dipolar breadth masks them. We suppose however that they account for the high temperature residual widths. A detailed discussion of these effects is beyond the scope of this paper but we can remark that the shape of the high temperature resonance has features characteristic of a quadrupolar broadening. We note that the fact that the aluminum width is independent of temperature tells us about the characteristic «size» of the disturbance, since it implies that there is no motional narrowing of the quadrupolar broadening. If by $T_2)_Q$ we denote the quadrupolar breadth, we have the condition that no motional narrowing will be seen as long as $T_2)_Q \geq \tau_c$, where τ_c is the length of time for a significant change in the quadrupolar coupling to take place. Suppose we attribute a characteristic length, l , to the quadrupolar coupling. This might be the mean distance between impurities or dislocations, for example. Then we might say τ_c is given by the time for a nucleus to diffuse a distance comparable to l . Thus $\tau_c \sim \tau l^2/a^2$, where a is the lattice constant. Therefore we have

$$l^2 \geq a^2 \frac{(T_2)_Q}{\tau}.$$

For aluminium SPOKAS finds $l > 200a$. One can account for the magnitude of $T_2)_Q$ fairly easily.

5. - Liquid metals.

The line broadenings observed by NORBERG and HOLCOMB above the melting points are surprisings since liquid lines are characteristically narrow, due to the short correlation times τ_c . It is characteristic in the case of short τ_c (specifically $\omega_0 \tau_c < 1$, where ω_0 is the Larmor frequency) that any line-broadening mechanism also produces spin-lattice relaxation. In fact the spin phase memory time, T_2 , equals the spin-lattice time T_1 . The fact that T_2 is shorter than T_1 for liquid sodium and lithium is very difficult to understand since it implies a range of interaction comparable to the dimensions of the particle and an interaction which is *not* present in the solid. A line of investigation which seems promising is suggested by the fact that the diffusion times across the particles used by HOLCOMB and NORBERG are about $(10 \div 20)$ ms [10], comparable to or shorter than the $(20 \div 100)$ ms T_2 's observed. It seems

possible that surface relaxation is involved. One can show that to invoke a surface layer in which motion is slow, but in which the relaxation is still a « motionally narrowed » dipolar breadth will unfortunately not account for the observed widths [11]. (This case is an example of what TORREY has called the proportional case.) Perhaps quadrupole effects combined with long correlation times (to prevent spin-lattice relaxation) are responsible. Studies of size effects would be helpful in coming to a conclusion. In liquid aluminum SPOKAS found no extra broadening, but the natural line width given by spin-lattice relaxation via conduction electrons ($T_2 = 2$ ms) is too broad to expect much for his samples.

6. - Speculations.

Although, we see that magnetic resonance can determine the energy of diffusion, E_D , the question arises whether or not magnetic resonance can measure the two energies E_F and E_M separately. In principle the answer is yes. A simple way (conceptually) to measure E_F and E_M is to pulse heat the sample, and quickly measure the line width before the vacancy concentration has had time to change. (This experiment is similar to the quench experiments in which the presence of vacancies is detected by resistance measurements). The line-width will differ as a result of the different rate of motion of atoms into vacant sites, but the formation part will remain unchanged. The question which needs to be answered is how do the times work out. MIEHER and SIMMONS have performed exploratory measurements. A rise of 30 °C should give a readily observed difference between « transient » and steady state diffusion. It appears feasible to produce such heatings in times of the order of a fraction of a millisecond, and to complete the line-width measure within another millisecond. In this time and at appropriate temperatures for conducting the experiment a vacancy can make 10^8 jumps. BRADSHAW and PEARSON [7] estimate the vacancies made 10^{10} jumps in their samples before disappearing. Moreover, typical quench rates used in resistance experiments run about 50 °C/ms starting from temperatures which are higher than those at which the line narrows. A pulse-heating experiment may therefore be feasible.

REFERENCES

- [1] N. BLOEMBERGEN, E. M. PURCELL and R. V. POUND: *Phys. Rev.*, **73**, 1168 (1948); P. W. ANDERSON: *Journ. Phys. Soc. Japan.*, **9**, 316 (1954); R. KUBO and K. TOMITA: *Journ. Phys. Soc. Japan.*, **9**, 888 (1954).
- [2] A. S. NOWICK: *Journ. Appl. Phys.*, **22**, 1182 (1951).
- [3] D. F. HOLCOMB and R. E. NORBERG: *Phys. Rev.*, **98**, 1074 (1955).
- [4] N. H. NACHTRIEB, E. CATALANO and J. A. WEIL: *Journ. Chem. Phys.*, **20**, 1185 (1952).
- [5] Private communication. The author is indebted to Dr. MASUDA for sending the results prior to publication.
- [6] E. F. W. SEYMOUR: *Proc. Phys. Soc.*, A **66**, 85 (1953).
- [7] F. J. BRADSHAW and S. PEARSON: *Phil. Mag.*, Series 8, **2**, 570 (1957).
- [8] J. SPOKAS: *Thesis*, University of Illinois (1957).
- [9] G. D. WATKINS and R. V. POUND: *Phys. Rev.*, **89**, 658 (1953); T. J. ROWLAND: *Acta Metal.*, **3**, 74 (1955).
- [10] R. E. MEYER and N. H. NACHTRIEB: *Journ. Chem. Phys.*, **23**, 1851 (1955).
- [11] H. C. TORREY: *Phys. Rev.*, **104**, 563 (1956); *Bull. Am. Phys. Soc.*, Series 11, **1**, 216 (1956).

INTERVENTI E DISCUSSIONI

— G. CARERI:

Could a correlated motion of the molecules in the liquid explain the strange results at melting?

— C. P. SLICHTER:

It seems difficult to believe that the moments are less random in the liquid than in the solid.

P A R T E T E R Z A

Dense Gases.

The Statistical Mechanical Basis of the Enskog Theory of Transport in Dense Gases.

J. G. KIRKWOOD and S. A. RICE

Sterling Chemistry Laboratory, Yale University - New Haven, Connecticut

The theory of transport in a dense fluid of rigid spheres is developed from Liouville's equation with the use of distribution functions coarse grained in time by methods employed by ROSS and KIRKWOOD in the derivation of Maxwell-Boltzmann integro-differential equation for gases of low density. If the interval of time smoothing is chosen to be an arbitrarily small non-zero positive quantity, only binary encounters contribute to the collision term in the contracted Liouville equation satisfied by the probability density $f^{(1)}$ in μ -space (singlet phase space). When the collision term is evaluated under the assumption, which cannot be exact, that the correlation function $g^{(2)}(R_1, R_{12})$ pair space is independent of momentum, a modified Maxwell-Boltzmann equation is obtained, which differs only in minor respects from the intuitively derived Enskog equation.

The Enskog expressions for the stress tensor and heat flux are derived from first principles and the coefficients of shear viscosity and thermal conductivity are evaluated by means of the new theory. The shear viscosity turns out to be identical with that of ENSKOG, while the thermal conductivity exhibits minor differences.

The physical implications of short time coarse-graining are discussed. Due to the singular nature of the force between rigid spheres, the time smoothed distribution functions are never identical with the fine-grained distribution functions even when the interval of time smoothing becomes an arbitrarily small non-zero quantity. However, the identification of macroscopic observable with averages corresponding to distribution functions with short time smoothing is open to serious question.

The following expressions are obtained for the coefficient of shear viscosity η and the coefficient of thermal conductivity κ ,

$$\eta = \frac{5kT}{8\Omega^{(2,2)}} \left[\frac{1}{g^{(a)}} + \frac{8\pi a^3}{15v} + \left(\frac{4\pi a^3}{15v} \right)^2 g^{(a)} \right],$$

$$\kappa = \frac{75k^2T}{32m\Omega^{(2,2)}} \left[\frac{1}{g^{(a)}} + \frac{11\pi a^3}{15v} + \frac{8}{75} \left(\frac{\pi a^3}{v} \right)^2 g^{(a)} \right],$$

$$\Omega^{(2,2)} = \left(\frac{4\pi kT}{m} \right)^{\frac{1}{2}} a^2,$$

where v is the volume per molecule and a and m are the diameter and mass of the rigid spheres. $g^{(a)}$ is the equilibrium radial distribution function for a pair of spheres in contact.

INTERVENTI E DISCUSSIONI

— G. CARERI:

What about the self-diffusion coefficient?

— S. ONO:

Recently we (S. ONO and T. MURAKAMI) made the investigation on the mechanical basis of the Enskog-Chapmann. This is based on the variation principle just the same as Hirschfelder and Curtiss' one, and gives exactly the same as Enskog and Chapmann for viscosity and thermal conductivity. This is not the method based on the first principles of statistical mechanics. However, the result seems to have the relation to Prof. KIRKWOOD's results.

— I. PRIGOGINE:

I would like to ask Prof. KIRKWOOD the following two questions:

1) Is your result not identical to the lowest order in concentration to the result given by Bogoliubov in his book?

2) I do not understand your method of expansion. I understand that one may expand in power of interaction constant or in power of concentration, but what is here the expansion parameter?

This is as more obscure for me because the recent derivations of the Boltzmann equation, especially the Bogoliubov derivation show clearly that the higher order terms in concentration are closely related to the « N body problem ». I believe therefore that no two body theory can give reliable results for higher concentrations.

— G. UHLENBECK:

If you develop your results in a virial expansion, up to which order is there agreement with the Enskog theory?

— J. KIRKWOOD:

This has not yet been done, but will be done in the near future.

— M. TODA:

I am trying to see if one can derive the Uhlenbeck and the Boltzmann equations using quantum mechanics and Bogoljubov's method. So far I am restricted to weak interactions. So I would like to ask Prof. KIRKWOOD if I can see easily the change in your calculation when you use well-potential instead of rigid sphere.

The Transport Properties of Dense Assemblies of Rigid Spheres.

H. C. LONGUET-HIGGINS

University Chemical Laboratory - Cambridge

Summary. — A general method is described for the calculation of transport coefficients in dense fluids composed of rigid spheres. It is assumed that for uniform concentrations the spatial distribution function has its equilibrium value, but that the velocity distribution is a product of Maxwellian single-particle functions chosen to give correctly the local temperature and hydrodynamic velocity. The following assemblies are investigated: 1) The single-component assembly of smooth rigid spheres for which the shear and bulk viscosities, the thermal conductivity and the self-diffusion coefficient are calculated explicitly. 2) The two-component mixture of spheres of different mass and the same radius; for this assembly the heat and matter transport coefficients are calculated and are found to satisfy Onsager's theorem. 3) The multi-component assembly. The diffusion constants are calculated and are also found to satisfy Onsager's theorem. 4) The one-component assembly of rough spheres. The viscosity and thermal conductivity are found to be greater than in the smooth sphere assembly. 5) A one-component assembly of spheres each of which possesses two internal energy levels, excitable by collision. For this assembly a formula is obtained for the absorption of sound at high frequencies.

INTERVENTI E DISCUSSIONI

— R. EISENSCHITZ:

If the repulsive potential becomes very steep the limit of validity of classical mechanics may be reached. This should be taken into account when comparing rigid sphere models with experiment.

Molecular Dynamics Computations for the Hard Sphere System.

T. WAINWRIGHT and B. J. ALDER

University of California Radiation Laboratory - Livermore, Cal.

1. - Introduction.

Statistical mechanical theories of many-particle systems encounter difficulties on account of the complex mathematical nature of the problem. This difficulty is compounded by the complicated and not well established law of interatomic force between the particles. This latter uncertainty makes any comparison of the theory with experimental data on real gases and liquids doubly unsure. With fast electronic computers it is possible to set up artificial many-particle systems with interactions which are both simple and exactly known. Experiments with such a system can yield not only the equilibrium and transport properties at any arbitrary density and temperature of the system, but also any much more detailed information desired. With these « controlled » experiments in simple systems it is then possible to narrow down the problem as to what analytical scheme best approximates the many-body correlations. This is not to say that computations can not be performed on more realistic systems.

The main disadvantage of such an artificial system is that only rather small numbers of particles can be treated in a reasonable calculating time. This means that the inherent fluctuations in the artificial system will be more limited than the fluctuations in a very large system. Also the boundaries might have an influence on the bulk properties, however, there is at present no evidence of this, except possibly in transition regions.

2. - Description of the method.

In calculations described here a system of particles, ranging in number from 32 to 500, is considered to be located in a rectangular box. The position and velocity of each particle is stored in the memory of the calculating ma-

chine, and the changes of all positions and velocities are arrived at by numerical solution of the classical many-body problem [1]. The interaction potential is taken to be either that of smooth, rigid spheres or an attractive square well with a rigid core, but this report is concerned with only the former case.

The boundary conditions are such that a particle which passes out through one side of the box, re-enters with the same velocity through the opposite side [2]. Alternately, the system can be conceived of as an infinite array of identical boxes with penetrable walls. This is not unlike the cell model [3] of liquids, however, the cells here contain many more particles than one is analytically capable of handling and the boundaries are not fixed. More analogous to the cell model is a calculation now being carried out, where the particles are strictly confined to a box with hard walls.

At low densities, the number of particles in the box is unimportant, however, at high densities the number of particles in the box determines the kind of packing which is achieved. A few low-density calculations have been made with a cubic box and 100 particles. Both high and low-density calculations have been made with a cubic box and $4n^3$ particles (i.e. 32, 108, 256, and 500). In these cases the packing is necessarily face-centered cubic. A number of calculations have been made with 96 particles in a rectangular box whose edge lengths were such that the close-packed configuration is hexagonal.

Since the interaction potentials are such that particles exert forces on each other only at certain specified separations, the entire dynamic calculation can be done by considering a succession of two-body collisions. A tally of the number of collisions as a function of time and also the sum of the absolute values of the momentum changes are occasionally printed by the machine as the calculation proceeds so that the collision rate and the pressure can be determined. The latter is calculated from the growth-rate of the momentum sum by means of the virial theorem. The velocity changes of each particle are recorded on magnetic tape so that the history of the system can later be reconstructed in order to calculate such things as radial distribution functions, diffusion coefficients, velocity distributions, H -functions, and velocity autocorrelation functions.

3. - Non-equilibrium properties.

Nearly all of the systems so far studied have been started with a particular non-equilibrium velocity distribution. The particles all have equal kinetic energies with velocities in random directions. Fig. 1 shows the monotonic decrease of the Boltzmann H -function [4] for a system of 100 rigid spheres at $v/v_0 = 14.14$, where v is the specific volume and v_0 is the close-packed specific volume. The horizontal line represents the equilibrium value of H

(544.6 in the arbitrary units used). The H -function is seen to approach the equilibrium value in about 2 collisions per particle. Similar calculations have been made over a wide range of densities; in all cases the equilibrium value

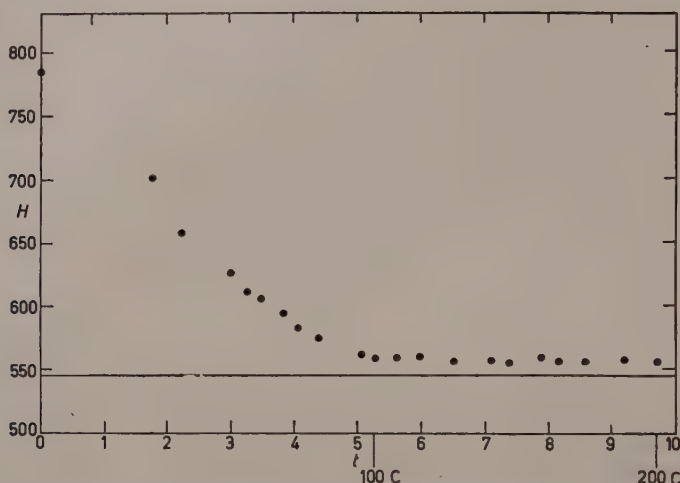


Fig. 1. — The behavior of the Boltzmann H -function with time, t , or collision number, C , for 100 hard spheres at $v/v_0=14.14$. The horizontal line represents the equilibrium H value.

is reached monotonically in from 2 to 4 collisions per particle. The rapidity with which the velocity distribution equilibrates is made possible by the fact that large amounts of momentum can be exchanged in single collisions. The

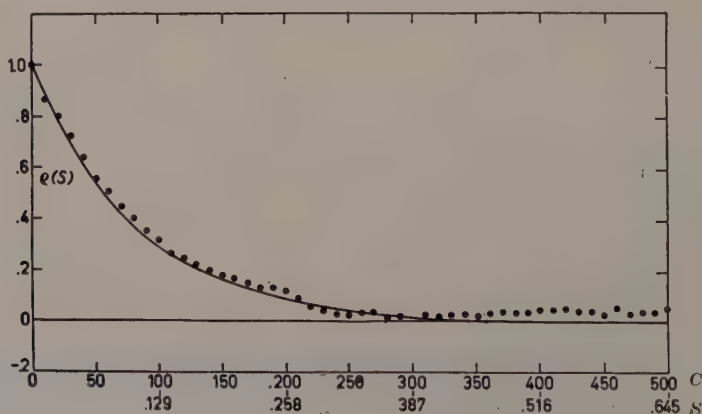


Fig. 2. — A comparison of the velocity auto-correlation function, $q(s)$, with an exponential decay (solid line) at $v/v_0=2.0$ for hard spheres. The abscissa is given in terms of collision number, C , and time, s .

reason the H -function levels out slightly higher than the computed equilibrium value is evidently that the finite size of the system precludes the existence of any energies far out on the tail of the Maxwell distribution.

Fig. 2 and 3 show the velocity auto-correlation function, $\varrho(s)$, for rigid spheres at low and high densities. It can be seen that for low densities the auto-correlation function is a simple exponential function of time characteristic

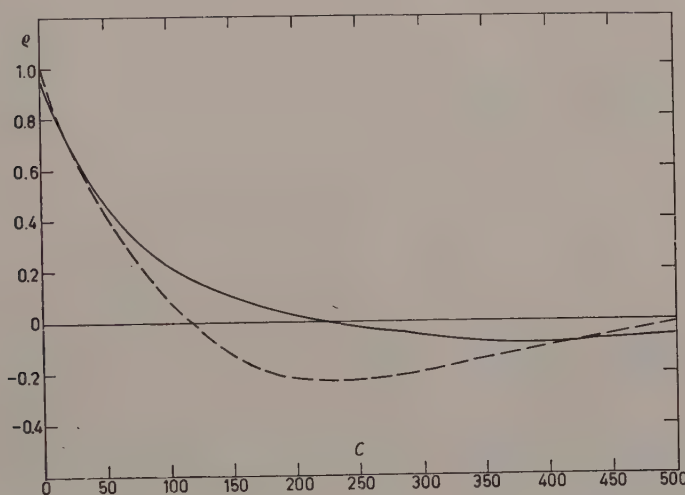


Fig. 3. — The velocity auto-correlation function, $\varrho(s)$, versus collision number for hard spheres at $v/v_0=1.60$ (solid line) and $v/v_0=1.03$ (dotted line).

of a Markoff process. For high densities, however, the function has undulations which indicate correlations with past behavior of the system. The auto-correlation function and the self-diffusion coefficient, D , are connected by

$$(1) \quad D = \frac{kT}{m} \int_0^{\infty} \varrho(s) \, ds ,$$

so that,

if $\varrho = \exp[-\beta s]$, then

$$(2) \quad D = kT/m\beta .$$

The values of β and, therefore, D have been calculated by BOLTZMANN [4] and, for higher densities, by ENSKOG [5]. Table I shows a comparison, for various hard-sphere densities, of the diffusion coefficient as calculated directly

from

$$(3) \quad D = \frac{\sum_{i=1}^N [\mathbf{r}_i(t+s) - \mathbf{r}_i(t)]^2}{6s},$$

with the values calculated from Eqs. (1) and (2) and the values according to BOLTZMANN and ENSKOG. For the Enskog theory the equation of state has to be known (see Sect. 4). At intermediate densities the Enskog correction

TABLE I. — *Comparison of the diffusion coefficients (*)*.

v/v_0	Eq. (2)	Eq. (1)	Eq. (3)	ENSKOG	BOLTZMANN
14.141	2.9(2)	—	3.2(2)	3.4(2)	3.9(2)
2.000	3.1(3)	3.4(3)	3.4(3)	3.3(3)	1.1(2)
1.767	2.4(3)	2.0(3)	2.0(3)	2.4(3)	—
1.600	1.9(3)	1.3(3)	1.3(3)	1.9(3)	—
1.031	1.7(4)	—	5(5)	1.9(4)	—

(*) The number in parenthesis is the negative power of 10 by which the accompanying number must be multiplied.

appears to be valid, however, at higher densities, where the non-Markoffian behavior becomes evident, the Enskog theory does not give the measured diffusion coefficient. It should be noted, however, that the Enskog theory does give the correct decay coefficient, β , even at quite high densities, i.e. if we consider the initial decay of the auto-correlation functions before the undulations take over, the curve is exponential with the Enskog coefficient as can be seen from the agreement between ENSKOG and Eq. (2) at the highest density in the table. This is as expected since it can be shown [6] by an expansion of the auto-correlation function in time that at any density for very short times a Markoff process is valid. The physical implication is that it takes a short time for the memory with past behavior to build up.

4. — Equilibrium properties.

The equation of state of systems of rigid spheres has been investigated rather intensively, especially in the density range $1.5 < v/v_0 < 1.7$ where there is a strong indication of a first order transition. Fig. 4 shows the number of collisions (circles) and the momentum sum \sum (triangles) for a system of 100 rigid spheres at $v/v_0 = 2$ as a function of time. \sum is defined as

$$(4) \quad \sum_i (\mathbf{r}_{a_i} - \mathbf{r}_{b_i}) \cdot \Delta \mathbf{v}_{a_i},$$

where \mathbf{r}_{a_i} and \mathbf{r}_{b_i} are the positions of particles a_i and b_i which are involved in collision i . $\Delta \mathbf{v}_{a_i}$ is the change of velocity of particle a_i which is the same, except for sign, as the change in velocity of particle b_i . The pressure is determined by

$$(5) \quad \frac{pv}{kT} - 1 = \frac{1}{N\bar{v}^2} \frac{\Delta \Sigma}{\Delta t},$$

where N is the number of particles in the system and \bar{v}^2 is the mean square velocity relative to the center of mass of the system. A straight line is drawn through the triangles and its slope measured to find $\Delta \Sigma / \Delta t$ and thus, $pv/kT - 1$. According to the theory of Enskog the collision rate is given by

$$(6) \quad \frac{\Delta C}{\Delta t} = \frac{N-1}{d} \sqrt{\frac{3\bar{v}^2}{\pi}} \left(\frac{pv}{kT} - 1 \right),$$

where d is the diameter of a sphere. The straight line through the circles is drawn with this slope. It is found that this Enskog relationship between pressure and collision rate holds good even for quite high densities. Table II shows a comparison of experimental collision rates with rates calculated according to ENSKOG for a variety of densities. Fig. 4 is typical of all systems regardless of density. It is thus evident that the non-Markoffian character has no apparent influence on the collision rate while it has a pronounced effect on the diffusion coefficient.

In a narrow intermediate range of densities the systems show a tendency to undergo spontaneous transitions between states of considerably different pressures. Thus, for all systems of $v/v_0 \geq 1.525$ and $v/v_0 < \text{about } 1.7$ which are

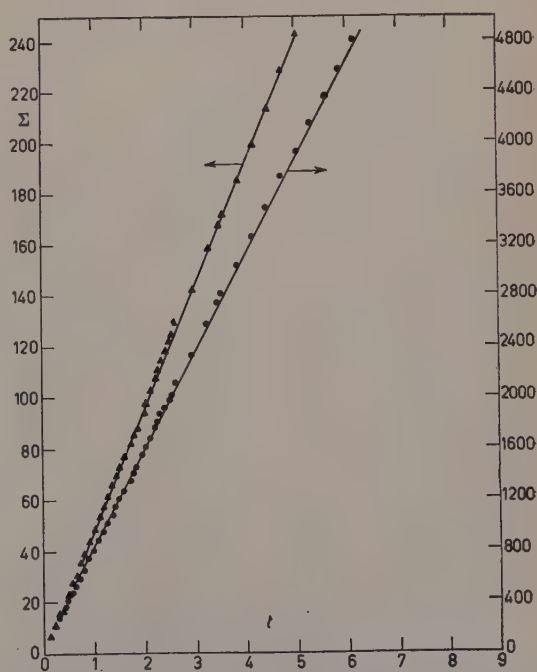


Fig. 4. — A plot of the virial (triangles), Σ , and the collision number (circle), C , as a function of time for a system of 100 hard sphere particles at $v/v_0 = 2.00$. The solid line for the collision rate is calculated from Enskog's theory.

started out in a face-centered cubic configuration, the pressure remains steady at a low value for a more or less long period of time and then suddenly the collision rate increases (see Fig. 5) and the Σ curve increases its slope indicating a transition to a higher pressure. The time required for the first such transition is as expected generally longer for the higher densities, however, there are large statistical variations. See Table III. For $v/v_0 = 1.525$ the transition occurs after about 93 000 collisions, then at 203 000 collisions the system spontaneously goes back to the low pressure state and stays there for about a 1000 collisions before returning to the high pressure state. It is not known whether systems at even higher densities would finally go to

TABLE II. — *Collision rate compared to Enskog theory.*

v/v_0 (+)	32 particles		108 particles	
	observed (*)	ENSKOG	observed	ENSKOG
1.030 1	2 650	2 530	13 950	14 040
1.250 0	391	378	2 079	2 064
1.344 8	—	—	1 681	1 639
1.400 0	277	269	—	—
1.420 0	—	—	1 481	1 452
1.500 0	246	240	1 320	1 310
1.525 0 (S)	242	235	—	—
1.525 0 (F)	342	328	—	—
1.530 0 (S)	241	233	—	—
1.530 0 (F)	323	311	—	—
1.355 0 (S)	239	231	—	—
1.535 0 (F)	315	307	—	—
1.540 0 (S)	239	238	—	—
1.540 0 (F)	313	305	—	—
1.550 0 (S)	234	228	1 338	1 328
1.550 0 (F)	308	304	1 647	1 628
1.600 0 (S)	233	229	1 334	1 364
1.600 0 (F)	283	273	1 485	1 480
1.650 0	263	256	1 370	1 380
1.700 0	246	238	1 270	1 270
1.750 0	225	221	—	—
1.767 8	—	—	1 160	1 140
1.800 0	208	204	—	—
2.000 0	164	159	—	—
3.000 0	79	78	—	—
14.142	14.4	14.3	—	—

(*) The root mean square deviation from a straight line has been evaluated in a few cases; at $v/v_0 = 1.4$ it is 5 collisions out of 277 collisions, at $v/v_0 = 1.031$ it is 8 collisions, and for the five densities clustered around $v/v_0 = 1.75$ it is in the neighborhood of 18 collisions.

(+) (S) and (F) refer to solid and fluid phases, respectively.

TABLE III. — *Collision number at which the first transition to a fluid took place.*

v/v_0	32 particles	108 particles	256 particles
	C	C	C
1.5250	93 000	—	—
1.5300	76 000	—	—
1.53125	4 000	—	—
1.5325	9 000	—	—
1.5350	2 000	—	—
1.5400	400	—	—
1.5500	25 000	3 000	—
1.6000	5 000	2 100	1 900
1.6500	—	800	—
1.7000	—	< 100	—
1.7678	—	1 200	4 600

the high pressure state if sufficient time were allowed. It is clear that configurational states can require extremely long times to equilibrate because the proper fluctuation among a set of particles may not occur frequently.

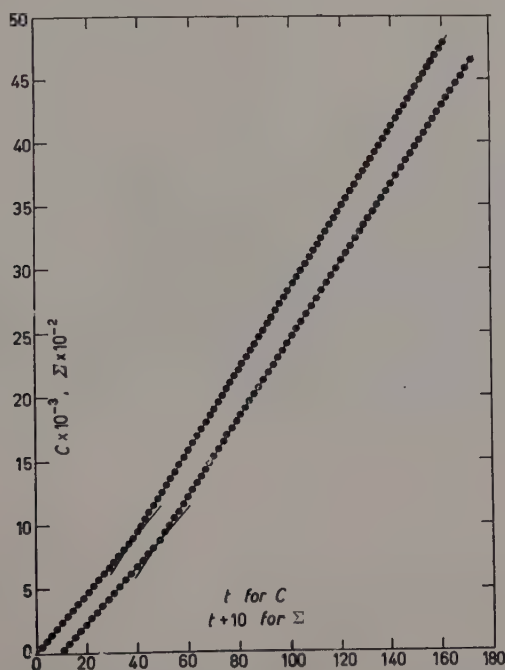


Fig. 5. — The collision rate, C , and the virial, Σ , as a function of time for 32 hard sphere particles at $v/v_0=1.5325$ showing a sudden jump at about 9000 collisions.

A Cathode-ray picture tube attached to the calculating machine was utilized to make traces in a plane projection of the positions of the centers of the particles in the 32 particle system $v/v_0 = 1.525$. Fig. 6 shows the traces from collision 202 000 to 203 000 where the system is in the high pressure state.



Fig. 6. — The traces made up by a succession of positions of a 32 particle hard sphere system at a density of 1.525 in a cubic box projected onto the xy plane. The periodic boundary condition allows the same particle to make traces on opposite edges of the graph. If the system were close packed, only 16 positions would be visible since in a planar projection two particles are right on top of each other. The above traces are evidently in the liquid state between collisions 202 000 and 203 000.

Fig. 7 depicts the traces of particles between 203 000 and 204 000 collisions. It is evident from this figure that with the system now in the low pressure state the particles have achieved the configuration of a crystal lattice. This

lattice, interestingly enough, is a crystal which is displaced relative to the original crystal, and hence the recrystallization took place at a different place in the melt. (Compare Fig. 7 and 10). Fig. 8 shows the traces between 204 000 and 205 000 collisions which includes the transition back to the high pressure state. Between 205 000 and 206 000 collisions the picture reverts back to one like Fig. 6. Thus we are able to identify the high and low pressure states as



Fig. 7. — As Fig. 6 except what is evidently a solid between collisions 203 000 and 204 000.

fluid and solid. Fig. 9 and 10 show the traces in the fluid and solid regions respectively for about 3 000 collisions. Evidently the system is not sufficiently large that the fluid and solid phases can exist in equilibrium, but rather a system in the appropriate density range exists part of the time in one phase and part of the time in the other.

An extremely long calculation would be required to establish a time average

over the two pressure states. Furthermore, the average pressure in the transition region thus obtained differs from the pressure of a large system which could contain crystals in equilibrium with fluid. We have, therefore, chosen to calculate pressures of the fluid and solid phases separately. Similar behavior has been found by WOOD, PARKER and JACOBSON [7] in their Monte Carlo cal-



Fig. 8. — As Fig. 6 except between collisions 204000 and 205000. The system has melted in that interval.

culations on hard sphere systems. Those calculations are described in an accompanying paper which includes a graph of the equation of state.

Table IV shows the pressures we have calculated for systems of various sizes and over a wide range of densities. In the transition region, both the high and low pressures are given except for most of the 500 particle systems which were not run long enough for the transition to the high pressure phase



Fig. 9. — As Fig. 6 except for 3000 collisions
in the middle of the liquid region.



Fig. 10. — As Fig. 6 except for 3000 collisions
in the middle of the initial solid region.

TABLE IV. — *The equation of state for hard sphere particles.*

N $v/v_0^{(*)}$	32		96		160		108		256		500	
	$pv_0/kT^{(a)}$	C^* ^(b)	pv_0/kT	C^*	pv_0/kT	C^*	pv_0/kT	C^*	pv_0/kT	C^*	pv_0/kT	C^*
30.43	—	—	—	—	.0363	3.2	—	—	—	—	—	—
14.142	—	—	—	—	.0875	2.8	—	—	—	—	—	—
3.000	1.03	39	—	—	—	—	—	—	—	—	—	—
2.722	—	—	—	—	1.27	2.0	—	—	—	—	—	—
2.000	2.95	5	2.87	2	2.90	5.6	—	—	2.90	3.0	—	—
1.800	4.22	15	—	—	—	—	—	—	—	—	—	—
1.7678 (S)	—	—	—	—	—	—	~4.1	1.2	4.15	4.6	4.14	2.8
1.7678 (F)	—	—	—	—	4.36	4.0	4.47	4.0	4.45	4.6	—	—
1.750	4.64	15	—	—	—	—	—	—	—	—	—	—
1.700	5.20	15	5.1	2	—	—	5.08	33	—	—	4.58	3.2
1.650 (S)	—	—	—	—	—	—	~5.2	0.8	—	—	4.96	3.0
1.650 (F)	5.70	50	—	—	—	—	5.68	4.0	—	—	—	—
1.600 (S)	5.36	5	—	—	—	—	5.37	2.0	5.38	1.9	5.42	3.2
1.600 (F)	6.29	53	—	—	—	—	6.28	34	6.27	8.6	5.95	8.6
1.550 (S)	5.57	25	—	—	—	—	5.94	3.0	—	—	—	—
1.550 (F)	7.11	196	—	—	—	—	7.12	30	—	—	—	—
1.540 (S)	5.66	0.4	—	—	—	—	—	—	—	—	—	—
1.540 (F)	7.29	47	—	—	—	—	—	—	—	—	—	—
1.535 (S)	5.72	2	—	—	—	—	—	—	—	—	—	—
1.535 (F)	7.36	50	—	—	—	—	—	—	—	—	—	—
1.530 (S)	5.80	76	—	—	—	—	—	—	—	—	—	—
1.530 (F)	7.50	124	—	—	—	—	—	—	—	—	—	—
1.525 (S)	5.85	93	—	—	—	—	—	—	—	—	—	—
1.525 (F)	7.55	170	—	—	—	—	—	—	—	—	—	—
1.500	6.08	42	6.12	4	—	—	6.12	14	6.20	3.0	—	—
1.420	—	—	7.28	2	—	—	7.22	2.6	—	—	—	—
1.400	7.3	6	—	—	—	—	—	—	—	—	—	—
1.3448	—	—	8.63	2	—	—	8.63	5.8	—	—	—	—
1.250	11.7	10	11.7	2	—	—	11.7	5.5	—	—	—	—
1.160	—	—	18.3	2	—	—	—	—	—	—	—	—
1.100	—	—	29.6	2	—	—	—	—	—	—	—	—
1.031	95.1	2	97.5	2	—	—	97.1	5.0	—	—	—	—

(^a) The root mean square deviation from a straight line for Σ versus t has been evaluated in a few cases: at $v/v_0=1.031$ the deviation for pv_0/kT is .20, at $v/v_0=1.40$ it is .14, at $v/v_0=1.70$ and 1.75 it is respectively .24 and .31.

(^b) C^* is the number of 1000 collisions the problem has been run.

(*) (S) and (F) refer to solid and fluid phases, respectively.

to take place. For larger systems because of larger possible fluctuations the transition should take place in fewer collisions per particle (Table III).

The effect of the number of particles on the pressure is most noticeable in the transition region. For a larger and larger number of particles the system

should approach more and more a horizontal line in the equation of state. Though no noticeable difference between 32 and 108 particles was obtained in the two branches, the true average between the two pressures may be different. From very preliminary results it may be possible that for 500 particles the system can partially contain the two coexisting phases simultaneously and thus yield a partially averaged pressure.

Outside the two phase region no difference can be detected in the equation of state for various sized samples and this includes the 96 particle system with the hexagonal close packed structure in a rectangular box. In fact, it can be shown [8] that the second, B , and third, C , virial coefficients have the following dependence on the number of particles, N , in a periodic system

$$(7) \quad B_N = B_\infty (1 - 1/N),$$

$$(8) \quad C_N = C_\infty (1 + \frac{1}{5}N - \frac{6}{5}N^2),$$

where the subscript ∞ is the ordinary virial coefficient for an infinite system. Hence, this is a small correction for even 32 particles.

The pressure has also been calculated by means of the radial distribution function. The comparison with Eq. (5) is within the accuracy of the calculation. The radial distribution functions disagree somewhat, however, with the ones calculated from the superposition theory [9] at intermediate densities although that theory predicted a transition for hard spheres at $v/v_0 = 1.48$.

* * *

We wish to acknowledge the splendid co-operation of the computing group; in particular Dr. S. FERNBACH for making time available and Mrs. S. CAMPBELL, Mr. N. HARDY, and Mrs. M. SHEPHERD for their coding help.

REFERENCES

- [1] Proceedings of the I.U.P.A.P. Symposium on Statistical Mechanical Theory of Transport Properties in Brussels (to be published).
- [2] B. J. ALDER, S. P. FRANKEL and V. A. LEWINSON: *Journ. Chem. Phys.*, **23**, 417 (1955).
- [3] R. J. BUEHLER, R. H. WENTORF, J. O. HIRSCHFELDER and C. F. CURTISS: *Journ. Chem. Phys.*, **19**, 61 (1951).
- [4] S. CHAPMAN and T. COWLING: *The Mathematical Theory of Non-uniform Gases* (Cambridge, 1939).
- [5] J. O. HIRSCHFELDER, C. F. CURTISS and R. B. BIRD: *Molecular Theory of Gases and Liquids* (New York, 1954).

- [6] C. LONGUET-HIGGINS and J. A. POPLE: *Journ. Chem. Phys.*, **25**, 884 (1956).
[7] W. W. WOOD, F. R. PARKER and J. D. JACOBSON: in this issue, pag. 133.
[8] I. OPPENHEIM and P. MAZUR: *Physica*, **23**, 197 (1957).
[9] J. G. KIRKWOOD, E. K. MAUN, and B. J. ALDER: *Journ. Chem. Phys.*, **18**, 1040 (1950).
-

INTERVENTI E DISCUSSIONI

— G. S. RUSHBROOKE (to Dr. W. W. WOOD):

With regard to the curve labelled 5 virial coefficients in the last slide of Dr. ALDER's paper, I presume these are the 5 known virial-coefficients for a gas of hard spheres. It is remarkable that this curve fits the more-condensed phase data rather than those for the less-condensed phase.

— W. W. WOOD:

This is misleading and if the estimated 6-th virial coefficient is used, the curve follows the less condensed phase quite closely.

— A. MUNSTER (to Dr. W. W. WOOD):

It seems from the slide, that the Kirkwood superposition is a poorer approximation than the free volume theory. This is a little surprising, because the Kirkwood approximation represents a superposition in the triplet space, whereas the free volume theory, as shown by KIRKWOOD, is in fact a superposition in the space of molecular pairs.

— W. W. WOOD:

The Kirkwood superposition approximation is a much better approximation than the free volume theory at densities lower than those shown on the slide.

— H. C. LONGUET-HIGGINS (to Dr. B. ALDER):

Would Dr. ALDER express a view as to whether the condensed phase should be regarded as a solid or a liquid phase?

— B. ALDER:

The pictures we have made will make it evident that the condensed phase is definitely a solid phase.

— H. TEMPERLEY (to Dr. B. ALDER):

Can you see any analogy between the behaviour of your condensed system and of the system of coupled oscillators studied in the older work at Los Alamos? The striking property of the latter assembly was that it often returned approximately to its initial configuration after going through a small fraction of the configurations theoretically accessible to it.

— B. ALDER:

I am only slightly familiar with the results of Dr. ULAM. If I remember correctly only a very few cases have been studied and it is possible that the statistics were not very extensive.

— J. DE BOER (to Dr. B. ALDER):

Is it possible, by changing the initial configurations to facilitate that the system comes in the «high pressure»-phase, instead of in the «low pressure» phase. One might get from such attempts more insight in the «structure» of the different phases.

— B. ALDER:

This would indeed be interesting. WOOD and we have exchanged positions at various stages of the calculation and have started our system out in the high pressure phase. It would be enlightening to make a further study of the time necessary to go to the high pressure phase as a function of the initial configuration.

— H. EISENSCHITZ (to Dr. B. ALDER):

Would the oscillations in the correlation function variate in the limit $N \rightarrow \infty$?

— B. ALDER:

We have not made a study of this as yet.

— J. L. CHALLIS:

I should like to ask if it would be possible to carry out thermal conductivity experiments using, say, a hard sphere model, by accelerating particles at one end of the imaginary box?

Recent Monte Carlo Calculations of the Equation of State of Lenard-Jones and Hard Sphere Molecules (*).

W. W. WOOD, F. R. PARKER and J. D. JACOBSON
Los Alamos Scientific Laboratory - Los Alamos, New Mexico

1. - Introduction and method.

The investigations reported at this symposium are in the process of publication elsewhere [1, 2]; since the latter papers are rather detailed, we will content ourselves here with a rather brief survey of the work, with only a few additional results.

The term « Monte Carlo » has come into use to designate numerical methods in which specifically stochastic elements are introduced, in contrast to the whole body of classical numerical techniques which consist of numerical evaluations of completely determinant algebraic expressions. The particular Monte Carlo method used here was devised by METROPOLIS *et al.* [3]; its essential feature is that it produces a Markov chain [4] in which the individual Markov states are points in the usual configuration space of statistical mechanics, for a system of N molecules confined at a temperature T in a volume V . The transition probabilities characterizing the Markov chain are determined in such a way that the value of any function of configuration state, averaged over all states developed in the Markov chain, approaches the petit canonical ensemble average value of the same function.

It should be noticed that the present method does *not* consist in an evaluation of the configurational phase integral by means of a random selection of points in configuration space. A method of the latter sort, which may be compared with a sequence of independent throws of a die, is indeed

(*) Work performed under the auspices of the United States Atomic Energy Commission.

a frequently used Monte Carlo technique, but is inappropriate to the study of reasonably dense molecular systems.

The method is also essentially classical-mechanical in its applicability: it could be used with a quantum-mechanical system provided one had beforehand an enumeration of the energy-states of the system; but that, of course, is the fundamental question in the quantum-mechanical many-body problem.

By use of the theory of Markov chains with time-independent transition probabilities, it can be shown that the conditions to be satisfied by the Markov process, in order for it to be equivalent to the petit ensemble, are the following:

$$\text{I) } p_{jk} \exp[-\beta U_j] = p_{kj} \exp[-\beta U_k], \quad \text{all } j \text{ and } k.$$

$$\text{II) } \sum_k p_{jk} = 1, \quad \text{all } j.$$

III) The class of all configuration states must be ergodic.

The transition probability p_{jk} is the conditional probability, if at time t the system is in state j , that at time $t+1$ it may be in state k . Note that we are following the usual Markov terminology in which the chain is thought of as being developed over successive instants of time; but this is in no way related to a real physical time associated with molecular velocities, which do not appear in our problem at all. The potential energy of state j is U_j ; $\beta = 1/kT$, where k is Boltzmann's constant. A prescription for the calculation of U_j is assumed to be given. For Lennard-Jones molecules

$$(1) \quad U = \frac{1}{2} \sum_{m=1}^N \sum_{\substack{n=1 \\ (n \neq m)}}^N u(r_{mn}),$$

$$(2) \quad u(r_{mn}) = \epsilon^* [(r^*/r_{mn})^{12} - 2(r^*/r_{mn})^6].$$

We use ϵ^* to denote the depth, and r^* the radius, of the well of the Lennard-Jones 12, 6 potential; r_{mn} is the distance between molecules m and n . For hard spheres, equation (2) becomes

$$(2') \quad u(r_{mn}) = \begin{cases} \infty & r_{mn} > \sigma; \\ 0 & r_{mn} < \sigma; \end{cases}$$

where σ is the molecular diameter.

For convenience, we are supposing the class of configuration states to be discrete and finite in number, corresponding to some suitably fine subdivision of space into cells. Such a subdivision (an extremely fine one) is of course introduced by the use of digital calculators; provided it is small enough, we

may be sure that the results obtained by means of it will closely approximate those obtained from a continuum analysis.

Condition I) takes the form of a requirement of microscopic reversibility between any two states j and k .

Condition II) is just the normalization condition for the rows of the single-step transition matrix.

Condition III), the ergodicity condition, is subtle. One can see that it will follow if I) is satisfied, for any potential energy function U_j whose singularities are a set of zero measure. Such is the case with Lennard-Jones molecules, but not for hard spheres, where at high densities by far the larger volume in configuration space corresponds to infinite values of U . Here we will only point out that this equation is closely related to the general question of accessibility in statistical mechanics.

Finally, we emphasize that except for the ergodic question, for given intermolecular interactions, and given N , V , T , the Monte Carlo method as here described is exact. There is no systematic error. There will be after any finite development of a chain, of course, some statistical error in the calculated averages. Of course, however, it is out of the question to calculate with values of N of the order of 10^{23} ; in fact N cannot, with present calculators, be greater than a few hundred at most, and in most of the present work $N = 32$. In order to make some correspondence with macroscopic or thermodynamic systems, we have employed the usual periodic boundary conditions; see reference [1] for a more extensive discussion. Further, summations such as those in equation (1) must be truncated at some point, rather than extended over all the molecules of the large system. In practice, they are carried out only over the 12 to 54 nearest j molecules for each i . Contributions of more distant interactions to the thermodynamic properties are estimated by approximate means [1]; the corrections are frequently quite large, but we believe they are reliably estimated so that the error from this source is not great. The effect of approximating the macroscopic system by a small number of degrees of freedom plus the periodic boundary condition can be studied by varying N ; in the present work two values, 32 and 108, have been examined for Lennard-Jones molecules. For hard spheres, the calculations to date have used only 32. Although additional calculations with larger N would be desirable, there is at present no indication that the error thus introduced is appreciably greater than the small statistical errors.

2. - Lennard-Jones molecules.

It is well-known that the Lennard-Jones potential is capable of representing the interaction of argon atoms reasonably well, although not with perfect accuracy of course. For purposes of comparing the Monte Carlo calculations

with experimental data on argon, the parameters ε^* and r^* were given the values determined by MICHELS *et al.* [5] from second virial coefficients: $\varepsilon^*/k = 119.76^\circ\text{K}$, $r^* = 3.822 \text{ \AA}$. The most extensive calculations were made for various volumes on an isotherm with $kT/\varepsilon^* = 2.74$. The comparisons are

made in terms of a reduced volume v/v^* , where v is the actual molar volume, and $v^* = N_0 r^{*3}/\sqrt{2}$, N_0 being Avogadro's number. For argon, $v^* = 23.79 \text{ cm}^3/\text{mole}$.

In Fig. 1 the Monte Carlo p - v results at this temperature are compared with experimental observations on argon (the corresponding temperature is about 55°C) by BRIDGMAN [6] and MICHELS *et al.* [5], as well as with two other more approximate theories, the Lennard-Jones-Devonshire cell theory as modified by WENTORF *et al.* [7], and the triplet-superposition approximation to the Kirkwood-Born-Green integral equation [8, 9]. The agreement between the Monte Carlo values and Michels' data is very good throughout the range of the calculations which extends from about 150 to 2000 atm. This agreement suggests both that the approximations involved in the Monte Carlo work are not severe, and also that the Lennard-Jones model is reasonably good for argon in this region. The data used by MICHELS to determine the potential parameters are of course predominantly at lower pressures than this range, so that the agreement is in no sense forced. The agreement with BRIDGMAN is quite poor; it is possible [1] that at least part of the disagreement may be due to errors in the experimental data.

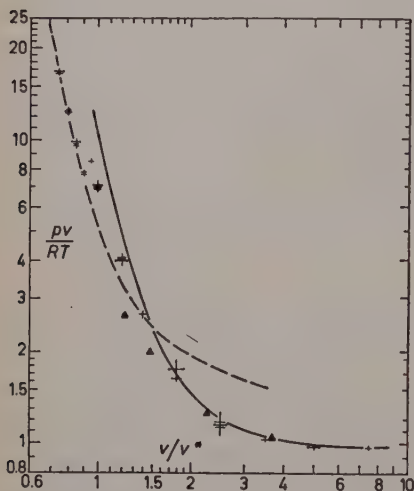


Fig. 1. — Compressibility factor versus reduced volume, for Lennard-Jones molecules at the reduced temperature $kT/\varepsilon^* = 2.74$ (for argon, $T = 328^\circ\text{K}$). In the multiple cross symbols, each horizontal bar represents the average value from one Markov chain; those having the small dots at their extremities were from 108-molecule systems; the others are from 32-molecule system. The extent of the vertical line is a probably over-conservative estimate of reliability. The upper and lower solid curves represent Bridgman's and Michels's experimental data for argon, respectively. The dashed curve represents the Lennard-Kirkwood integral equation in the triplet superposition approximation.

From the standpoint of a study of intermolecular forces in argon, a reinvestigation of the behavior of argon from 2000 to 15000 atm would be very valuable.

Between $v/v^* = 0.90$ and 0.95 there is a distinct break in the p - v isotherm,

and also in the E' - v isotherm [1] (E' being the imperfection internal energy), which we have identified with the fluid-solid transition. It occurs at about the values of p and v expected from experimental observations at lower temperatures. It is also noteworthy that if one studies the diffusion of individual molecules during the course of the development of the chains, at volumes on the solid side of the break the molecules remain in essentially their original arrangement (on the sites of a regular face-centered-cubic lattice), while on the fluid side the arrangement has become chaotic. The behavior of the Markov chains through the coexistence region has not been investigated in detail. The available results suggest that it would be quite similar to that of hard sphere molecules which will be described below. Should this be the case, an order of magnitude or so improvement in calculator speed would be necessary before really meaningful calculations in this region could be carried out.

The cell theory is seen to give remarkably good results for the solid, but is nowhere good in the fluid region. It is really, of course, a theory of the solid state of the Einstein single frequency type, but with corrections for anharmonicity. Its failure for the fluid is probably not too surprising.

The superposition approximation of the Kirkwood-Born-Green theory, when corrected empirically [9] to correspond to the unmodified Lennard-Jones potential, gives good agreement at the larger volumes, but diverges as volumes comparable to liquid volumes are approached.

Fig. 2 compares three radial distribution functions at $v/v^* = 2.5$ on this same isotherm. The Monte Carlo result for the Lennard-Jones potential is quite different from that obtained [8] using the superposition approximation to the Kirkwood-Born-Green theory and a modified Lennard-

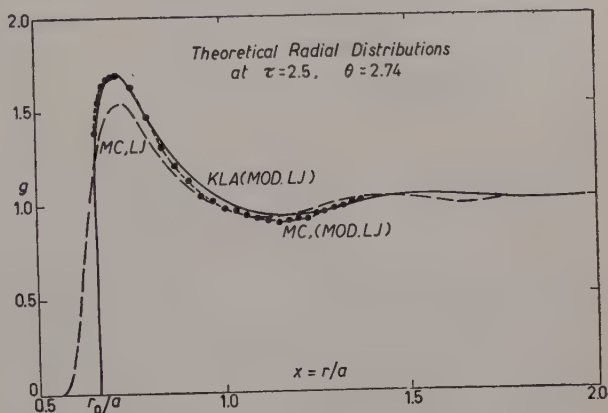


Fig. 2. — Radial distribution functions g versus $x = r/a$ at $\tau = v/v^* = 2.5$, and $\theta = kT/\epsilon^* = 2.74$. Here r is the distance from the center of the dummy molecule, and a is the nearest-neighbor separation in a face-centered cubic lattice at the same density. MC, LJ is the Monte Carlo curve obtained using the ordinary Lennard-Jones potential, while MC (MOD. LJ) is the Monte Carlo result from the modified potential, which was also used in Ref. [8]. The latter's result is shown as KLA (MOD. LJ).

Jones potential, which has a hard core ($u = \infty$) inside the usual cross-over point. The third curve, a Monte Carlo calculation using the modified potential, was calculated in order to determine whether the discrepancy between the first two was due more to the superposition approximation, or to the difference in the interaction laws used. Clearly, most of the difference is due to the latter, although a small difference remains between the curves using the same potential. The residual difference is presumably due to the superposition assumption. The thermodynamic results are compared in Table I, from which we see that the agreement of the energy values is much improved when they are calculated for the same potential. No great improvement is obtained in pv/RT ; however, perhaps half of the discrepancy may be due to statistical uncertainty in the Monte Carlo results.

TABLE I.

	pv/RT	E'/RT
Monte Carlo, LJ	1.17	.86
Monte Carlo, mod. LJ . .	1.46	.98
Superposition, mod. LJ .	1.31	.99

In Fig. 3 radial distribution functions for liquid argon under its own vapor pressure (18.3 atm) at 126.7 °K are compared. The experimental points are those obtained by EISENSTEIN and GINGRICH [10] by Fourier transform of

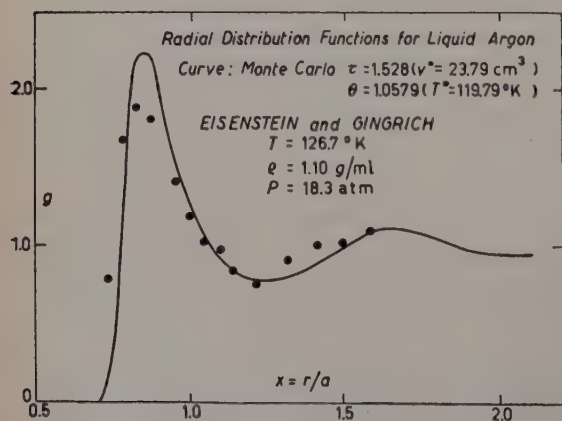


Fig. 3. — Experimental (●) and calculated (smooth curve) radial distribution functions for liquid argon.

observed X-ray scattering intensities. The Monte Carlo curve was calculated by using the experimental molar volume v and temperature T to calculate the appropriate values of reduced volume and temperature. The agreement is qualitatively good, but quantitatively is rather poor. There are serious truncation errors in the Fourier transform involved in obtaining the experimental values. It would probably be better to reverse the process,

and compare the Fourier transform of the calculated radial distribution function with the observed scattering intensity. This has not been done as yet.

The present result for Lennard-Jones molecules should be of use in assessing the merits of various approximate analytical theories in addition to the two compared with it here; for instance, the improvements to the cell theory currently being developed by a number of authors. The method makes possible interpretation of high pressure data (in Bridgman's range) for suitably simple molecules, in terms of the intermolecular forces. Additional calculations for both higher and lower temperatures have been carried out and will be reported when complete.

3. - Hard sphere molecules.

The present Monte Carlo method was previously applied to hard spheres in two dimensions by METROPOLIS *et al.* [3], and in three dimensions by ROSENBLUTH and ROSENBLUTH [11]. The results later obtained by WAINWRIGHT and ALDER [12] using their numerical molecular dynamical method disagreed with those of the ROSENBLUTHS [11] in the intermediate density range. This fact led us to begin a reinvestigation using the Monte Carlo method: since that time our work has been carried out in close collaboration with that of ALDER and WAINWRIGHT. The investigation is not yet quite complete, but sufficient results are available to warrant discussion here.

For hard spheres we use the reduced volume v/v_0 , where $v_0 = N_0\sigma^3/\sqrt{2}$ is the molar close-packed volume, so that $v/v_0 = 1$ at close-packing. Because of the absence of long-range interactions, the error introduced in less singular cases by truncating the energy summations is not present here. Thus the only approximation involved is that introduced by the use of small N and the periodic boundary condition. The same approximation is used by WAINWRIGHT, and ALDER so that for hard spheres their method studies, from the standpoint of exact molecular dynamical

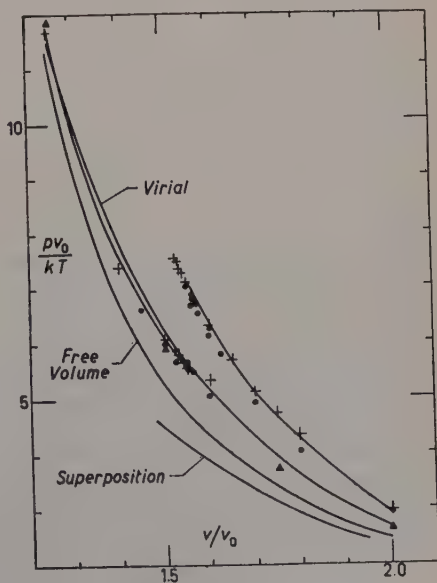


Fig. 4. - The equation of state of hard spheres. The heavy solid curve represents WAINWRIGHT and ALDER's [12] 108-molecule results; +, their 32 molecule results. • and ▲ represent the present and previous [11] Monte Carlo results. *Virial* = five term virial expression [11]. *Superposition* = Reference [13].

mics, the same system studied by exact statistical mechanics with use of the Monte Carlo method. Thus the two methods should give identical results if the quasi-ergodic theorem is valid for the dynamical system, in the sense that the latter spends equal times in equal volumes in the accessible region of configuration space, and further, provided that the accessible regions are the same in both methods. This equivalence has not, in fact, been demonstrated, so that one cannot assert that exact agreement should be obtained.

The present Monte Carlo calculations are all for the 32-molecule system. In Fig. 4 the resulting equation of state can be compared with that obtained by WAINWRIGHT and ALDER for both 32 and 108-molecule systems. It will be noticed that the calculated points are plotted on two distinct curves which overlap in the neighborhood of $v/v_0 = 1.55$. The reason for this presentation of the results is illustrated in Fig. 5, which shows the way in which the Monte

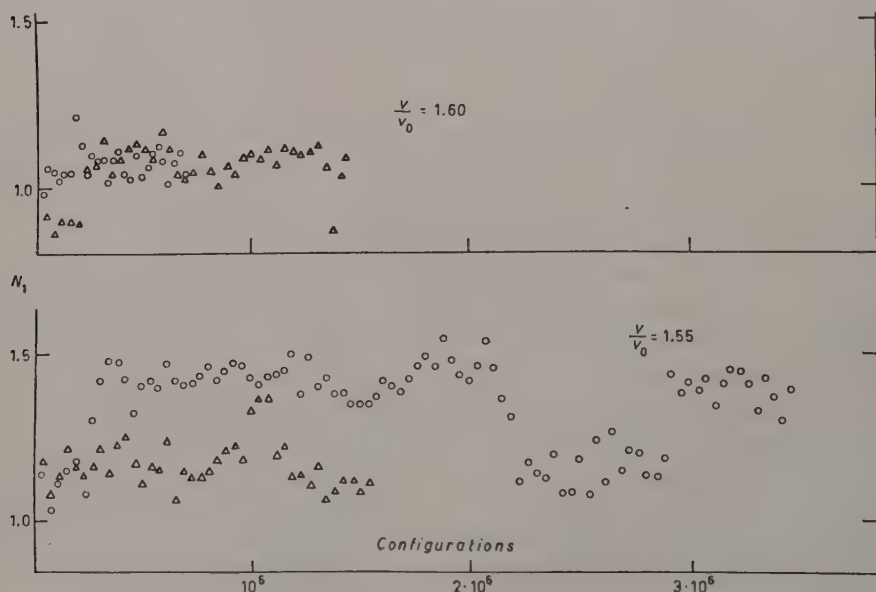


Fig. 5. — Convergence of Markov chains for 32 hard spheres in the apparent transition region. The abscissae are the length of the chains in configurations. The ordinate N_1 is the number of molecules in a spherical shell around a dummy molecule, of inner radius σ and outer radius r_1 . The latter is arbitrary, but is the same for each of the two chains shown for given v/v_0 . The points plotted are partial averages of N_1 , each point being the average over the configurations generated since the previous point. At $v/v_0 = 1.55$ the triangles represent a chain for which the initial configuration was a regular face-centered lattice, while the circles are a chain in which the initial configuration was a regular face-centered lattice but compressed towards one corner of the cube. At $v/v_0 = 1.55$, the circles have the same meaning as before, while the triangles are from a chain started from a configuration obtained by WAINWRIGHT and ALDER after several thousand collisions.

Carlo chains converge in this neighborhood. The quantity N_1 is qualitatively analogous to the pressure (which for hard spheres is proportional to the value of g at contact). The longer chain at $v/v_0 = 1.55$ is particularly striking, in that superimposed on the normal fluctuations there are three jumps between two different levels. The separation of these levels is sufficiently great and the number of jumps observed is so small, that the over-all average must be expected to be a very poor approximation to the correct value. The other chain at this volume is seen to oscillate exclusively around the lower of the two levels observed in the previous chain, except for one brief excursion to values near the higher level. Note that of the two chains, the over-all average of the first is close to the high level, while that of the second is close to the low level, confirming our previous remark that the chains are not long enough for good convergence. It should be mentioned that even if the class of Markov states should factor into separate ergodic classes, corresponding to the existence of two or more unconnected regions of phase space, the initial configurations of the two chains can easily be seen to be members of the same class. Thus the two chains must eventually give the same results; for this to occur, however, the chain would evidently need to be probably ten or more times longer than at present. Since the longer chain required about 40 hours for its development on IBM Type 704 calculators, such a program is not practicable. This being the case, we have instead adopted the policy of separately averaging, and plotting in Fig. 4, the low and high levels of each chain in which they both occur. A very similar behavior is observed in the ALDER and WAINWRIGHT method, and they have adopted the same procedure.

The agreement between the dynamical and statistical results is on the whole very good. We believe the Monte Carlo points at $v/v_0 = 1.7$ and 1.8 to be somewhat low, and in the future the agreement here will probably be somewhat improved. Aside from this, the only disagreement is that Alder and Wainwright's upper curve extends to slightly smaller volumes. If there is in fact any underlying difference in the ergodic behavior of the two methods, it would probably appear in just such a way. This may be the case, or it may be that the Monte Carlo chains in this region have not been long enough to observe the transition to the higher level (the usual starting configurations seem to produce initially the low level). As far as the Monte Carlo results alone are concerned, they would suggest that at $v/v_0 = 1.50$ the over-all average lies on the lower curve, while at $v/v_0 = 1.60$ it lies close to the upper curve, where the value of pv_0/kT is greater than at $v/v_0 = 1.50$ on the lower curve. This would suggest that a portion of the isotherm is mechanically unstable. If so, we then have a first-order phase transition; indeed the appearance of Fig. 4 strongly suggests this in any case.

In this connection, it is also worth mentioning that at volumes smaller than the apparent transition region, and during the persistence of the low level

states in chains in the transition region, diffusion is much restricted. Conversely, at greater volumes, and in the upper level states in the transition region, diffusion is very free.

Thus the present results strongly suggest the existence of a phase transition in hard spheres, as previously suggested from approximate considerations by KIRKWOOD and his co-workers [13].

The precise form of the isotherm expected from an exact treatment of the petit ensemble with finite N is somewhat uncertain. The arguments of HILL [14] suggest that loops, accompanied by regions of instability, are to be expected. As N increases the loops flatten out and the horizontal tie line of thermodynamics appears. It should be mentioned that when the periodic boundary condition is introduced, the system of N molecules is no longer calculated under conditions appropriate for the petit ensemble, if the molecules are considered to have the stated interaction potential, since interactions with molecules outside the cell volume are included. However, the potential energy, including these interactions, can be expressed in terms of the coordinates of just the N molecules confined in the cell of volume V , so that the method turns out to be exactly equivalent to the corresponding petit ensemble, but with a modified, somewhat singular, non-spherically symmetric pair potential. Unfortunately, for the reasons mentioned already, we are unable with present calculations to determine the complete canonical average which would connect the two curves of Fig. 4.

Also shown in Fig. 4 are the previous Monte Carlo results [11], the Lennard-Jones-Devonshire-Kirkwood cell or free volume theory [15], and the five-term virial expansion [11].

The previous Monte Carlo results are seen to lie approximately on the solid branch of the new equation of state, and on its rough extrapolation to larger volumes. We believe this to be related to the already mentioned tendency of the Monte Carlo chains to give initial levels which are low, and to the fact that the earlier work was done almost entirely with a system of 256 molecules on a somewhat slower calculator; both of the latter circumstances tend to prolong the lifetime of the initial low levels. Furthermore, the chains developed in the earlier work were much shorter than those presently used.

The new results increase the discrepancy of both the free-volume and superposition theories in the region covered by the figure. The virial curve shown is calculated from analytical values for the fourth and lower virial coefficients, and the ROSENBLUTHS' Monte Carlo value [11] for the fifth virial coefficient. Since convergence of the virial expansion in the solid region is not expected, there is no longer support for the earlier conjecture [11] that some high-order coefficients are negative.

REFERENCES

- [1] W. W. WOOD and F. R. PARKER: *Journ. Chem. Phys.*, **27**, 720 (1957).
- [2] W. W. WOOD and J. D. JACOBSON: *Journ. Chem. Phys.* **27**, 1207 (1957).
- [3] N. METROPOLIS, M. N. ROSENBLUTH, A. W. ROSENBLUTH, A. H. TELLER and E. TELLER: *Journ. Chem. Phys.*, **21**, 1087 (1953).
- [4] W. FELLER: *Probability Theory and Its Applications*, (New York, 1950) Chap. 15.
- [5] A. MICHELS, H. W. WIJCKER and H. K. WIJCKER: *Physica*, **15**, 627 (1949).
- [6] P. W. BRIDGMAN: *Proc. Am. Acad. Arts Sci.*, **70**, 1 (1935).
- [7] R. H. WENTORF, R. J. BUEHLER, J. O. HIRSCHFELDER and C. F. CURTISS: *Journ. Chem. Phys.*, **18**, 1484 (1950). The numerical values used here were calculated by Dr. WILSON FICKETT of this Laboratory (LASL), from the Lennard-Jones-Devonshire theory as modified by WENTORF *et al.*
- [8] J. G. KIRKWOOD, V. A. LEWINSON and B. J. ALDER: *Journ. Chem. Phys.*, **20**, 929 (1952).
- [9] R. W. ZWANZIG, J. G. KIRKWOOD, K. F. STRIPP and I. OPPENHEIM: *Journ. Chem. Phys.*, **21**, 1268 (1953). The values used here include the correction for the hard core, but not the empirical scale factor c introduced by ZWANZIG *et al.*
- [10] A. EISENSTEIN and N. S. GINGRICH: *Phys. Rev.*, **62**, 261 (1942).
- [11] M. N. ROSENBLUTH and A. W. ROSENBLUTH: *Journ. Chem. Phys.*, **22**, 881 (1954).
- [12] T. WAINWRIGHT and B. J. ALDER: in this issue, pag. 116.
- [13] J. G. KIRKWOOD, E. K. MAUN and B. J. ALDER: *Journ. Chem. Phys.*, **18**, 1040 (1950).
- [14] T. L. HILL: *Statistical Mechanics* (New York, 1956), Appendix 9.
- [15] W. W. WOOD: *Journ. Chem. Phys.*, **20**, 1334 (1952).

Note sur un calcul de perturbation en mécanique statistique.

J. YVON

Centre Études Nucléaires de Saclay - Gif-sur-Yvette (S. et O.)

1. — Principe de la méthode.

Un système thermodynamique en équilibre est soumis à un champ appliqué. On cherche à estimer les variations subies par ce système à la suite d'une variation infinitésimale du champ appliqué, lorsqu'il est revenu à l'équilibre. Le système est dans un thermostat, si bien que sa température demeure invariable.

L'auteur a déjà abordé [1] cette question, en considérant un système fermé. Il est bien préférable de considérer un système ouvert, c'est-à-dire un système qui peut échanger des particules avec un milieu ambiant.

Il n'est question ici que d'esquisser les idées essentielles de la méthode. Aussi l'étude sera-t-elle limitée au cas simple suivant:

- 1) Le système n'est pas quantifié.
- 2) les particules, disons les molécules, sont toutes identiques.
- 3) les molécules sont des centres de forces.

Le problème de la répartition des vitesses est entièrement résolu par la loi de distribution de Maxwell, il n'y a rien à en dire. Le problème à examiner est celui de la répartition dans l'espace.

Nous écrirons l'énergie potentielle du système lorsqu'il contient N molécules:

$$(1) \quad E_N = \sum_i V_i + \frac{1}{2} \sum_i \sum_j W_{ij},$$

V_i étant le potentiel appliqué sur la molécule: cependant que W_{ij} est l'énergie

potentielle du couple des molécules i et j . Nous admettons donc l'« additivité » des forces intermoléculaires.

Si on suppose le système fermé, la densité est fournie par l'intégrale

$$(1.2) \quad n_{N1} = \frac{1}{Z_N} \frac{1}{N!} N \int \exp[-\beta E_N] dr_2 dr_3 \dots dr_N,$$

où: dr_i est l'élément de volume relatif à la molécule i ;

β désigne $(kT)^{-1}$;

Z_N est la quantité qui assure que la somme de toutes les probabilités est égale à l'unité;

n_{N1} est la densité cherchée au « point » 1).

De même la densité relative aux couples de molécules s'écrit

$$(1.3) \quad n_{N12} = \frac{1}{Z_N} \frac{1}{N!} N(N-1) \int \exp[-\beta E_N] dr_3 dr_n \dots dr_N.$$

Passons aux systèmes ouverts. La probabilité d'avoir N molécules dans le système est

$$(1.4) \quad \Pi_N = \frac{Z_N Z^N}{\Xi},$$

Z étant l'activité chimique (suivant la convention des théoriciens) et Ξ une nouvelle quantité chargée d'assurer que la somme des probabilités soit encore égale à l'unité.

Dans le système ouvert, les densités simple et double s'écrivent respectivement

$$(1.5) \quad n_1 = \sum_N \Pi_N n_{N1},$$

$$(1.6) \quad n_{12} = \sum_N \Pi_N n_{N12}.$$

En différentiant membre à membre l'équation (2) par rapport au potentiel appliqué, on obtient la perturbation de la densité qui correspond à une perturbation infinitésimale du potentiel

$$(1.7) \quad \delta n_{N1} = -n_{N1} \beta \delta V_1 - \int n_{N12} \beta \delta V_2 d\tau_2 - n_{N1} \frac{\delta Z_N}{Z_N}.$$

On évalue δZ_N en multipliant par $d\tau_1$ et en intégrant

$$(1.8) \quad \int \delta n_{N1} d\tau_1 = -\beta \int n_{N1} \delta V_1 - \beta \int n_{N12} dV_2 d\tau_1 d\tau_2 - N \frac{\delta Z_N}{Z_N}.$$

Mais

$$(1.9) \quad \int \delta n_{N1} d\tau_1 = 0,$$

$$(1.10) \quad (N-1)n_{N2} = \int n_{N12} d\tau_1.$$

Il vient donc

$$(1.11) \quad \frac{\delta Z_N}{Z_N} = -\beta \int n_{N2} dV_2 d\tau_2.$$

Passons maintenant aux systèmes ouverts. La différentiation de l'équation (5) donne

$$(1.12) \quad \delta n_1 = \sum_N \Pi_N \delta n_{N1} + \sum_N \Pi_{N1} \delta \Pi_N.$$

Nous supposons l'activité chimique constante. Donc

$$(1.13) \quad \frac{\delta \Pi_N}{\Pi_N} = \frac{\delta Z_N}{Z_N} - \frac{\delta \Xi}{\Xi}.$$

Comme

$$(1.14) \quad \sum_N \delta \Pi_N = 0.$$

Il vient d'après (11) et (14)

$$(1.15) \quad \frac{\delta \Xi}{\Xi} = -\beta \int n_2 \delta V_2 d\tau_2.$$

Prenons maintenant la moyenne de l'équation (7) sur les systèmes ouverts. Il vient

$$(1.16) \quad \delta n_1 = -\beta n_1 \delta V_1 - \beta \int (n_{12} - n_1 n_2) \delta V_1 d\tau_2.$$

La densité double n_{12} peut avoir des propriétés plus ou moins compliquées, mais un de ses caractères essentiel est simplement que, dès que la distance 1-2 est grande du point de vue microscopique,

$$(1.17) \quad n_{12} = n_1 n_2.$$

Cette propriété, qui exprime l'absence de corrélations entre des molécules tant soit peu éloignées, n'est rigoureuses que dans les systèmes ouverts. Elle

entraîne que l'intégrale en $d\tau_2$ de (7) n'intéresse que le voisinage immédiat de la particule (1).

Il existe une autre manière d'établir une relation entre la perturbation du potentiel appliqué et la perturbation de la densité. Ecrivons en effet l'équation de l'ordre à grande distance

$$(1.18) \quad \log z - \beta V_1 = \log n_1 - \int g_{12} n_2 d\tau_2 - \int \frac{1}{2} g_{12} g_{13} g_{23} n_2 n_3 d\tau_2 d\tau_3 - \\ - \int \frac{1}{2} g_{12} g_{13} g_{24} g_{34} (1 + g_{14} + g_{23} + g_{14} g_{23}) n_2 n_3 n_4 d\tau_2 d\tau_3 d\tau_4 \dots,$$

qui permet d'estimer la répartition en densité des molécules sous l'effet d'un potentiel connu. Cette équation, à condition bien entendu d'adopter un nombre suffisant de termes dans le développement, est rigoureuse dans le cas d'un système ouvert. On a posé

$$(1.19) \quad g_{12} = (\exp [-\beta W_{12}]) - 1.$$

En la différentiant on obtient

$$(1.20) \quad -\beta \delta V_1 = \frac{\delta n_1}{n_1} - \int g_{12} \delta n_2 d\tau_2 - \int g_{12} g_{13} g_{23} n_3 \delta n_2 d\tau_2 d\tau_3 - \dots$$

Posons

$$(1.21) \quad H_{12} = g_{12} n_1 n_2 + \int g_{12} g_{13} g_{23} n_1 n_2 n_3 d\tau_3 + \dots$$

Il vient

$$(1.22) \quad -\beta \delta V_1 = \frac{\delta n_1}{n_1} - \frac{1}{n_1} \int H_{12} \frac{\delta n_2}{n_2} d\tau_2.$$

Nous avons obtenu deux transformations linéaires inverses: la première, équation (16), exprime δn en fonction de δV , la seconde exprime δV en fonction de δn . Il existe donc une relation entre H_{12} et $n_{12} - n_1 n_2$.

Examinons-la dans le cas homogène: avant la perturbation la densité ne dépendait pas des coordonnées d'espace. Nous traiterons le milieu comme un milieu infini. Les perturbations sont représentées par des ondes planes, que nous pouvons supposer complexes puisque les équations sont linéaires. A une perturbation de densité

$$(1.23) \quad \delta n_1 = A \exp [ikx_1]$$

correspond une perturbation de l'énergie potentielle

$$(1.24) \quad \delta V_1 = B \exp [ikx_1].$$

La relation (16) donne ici

$$(1.25) \quad A = - \left(1 + \frac{4\pi}{kn} \int (n_{12} - n^2) \sin kr \cdot r \, dr \right) n\beta B,$$

r représentant la distance 1-2. De même (18) donne

$$(1.26) \quad -n\beta B = \left(1 - \frac{4\pi}{kn} \int H_{12} \sin kr \cdot r \, dr \right) A.$$

Ainsi

$$(1.27) \quad 1 + \frac{4\pi}{kn} \int (n_{12} - n^2) \sin kr \cdot r \, dr = \frac{1}{1 - (4\pi/kn) \int H_{12} \sin kr \cdot r \, dr}.$$

Suivant les besoins cette relation pourra être résolue par rapport à n_{12} , ou par rapport à H_{12} . Résolvons-la par rapport à n_{12} :

$$(1.28) \quad n_{12} - n^2 = \frac{2}{\pi r} \int \sin kr \frac{\int H_{12} \sin kr \cdot r \, dr}{1 - (4\pi/kn) \int H_{12} \sin kr \cdot r \, dr} \, dk.$$

2. - Discussion.

La formule (1.21) exprime H_{12} à l'aide des g_{12} et de la densité. Il existe une formule analogue pour n_{12} . Je réécris la formule relative à H_{12} et j'écris celle relative à n_{12} dans la notation « géométrique » et dans le cas homogène

$$(2.1) \quad H_{12} = n^2 1 - 2 + n^2 \int_2^1 \rangle 3 \, d\tau_3 + \dots,$$

$$(2.2) \quad n_{12} = n^2 \exp \left[- \frac{W_{12}}{kT} \right] \left(1 + n \int_2^1 \rangle 3 \, d\tau_3 + \dots \right).$$

Le premier point à noter est que, compte tenu de ces deux développements, la formule (1.27) ou (1.28) n'est qu'une identité. Mais il est assez pénible de le vérifier directement. De plus on ne voit pas comment on aurait pu imaginer déduire (1.27) de la seule connaissance de (1) et (2). Il est donc permis de considérer (1.27) comme un complément très utile à (1) et (2).

Comparons maintenant la structure des développements (1) et (2). Ils présentent une différence essentielle: dans H_{12} les points 1 et 2 sont toujours doublement liés (sauf dans le premier terme) tandis que dans n_{12} ils sont simplement liés. Cette différence de structure apparaît en mettant en regard des

figures de même ordre

$$\triangleright \text{ pour } H_{12}, \quad > \text{ pour } n_{12}.$$

Or chaque trait représente une grandeur qui diminue rapidement avec la distance, dans l'hypothèse à laquelle nous nous tenons ici des forces à courte portée.

Une conséquence qualitative en résulte: H_{12} diminue beaucoup plus vite avec la distance que n_{12} : Une étude mathématique de cette question pourrait être utilement entreprise.

La formule (1.27) donne lieu à des relations particulières obtenues par identification terme à terme lorsqu'on suppose k assez petit pour qu'il soit permis de développer les deux membres en série entière par rapport à k . Pour alléger l'écriture nous poserons

$$(2.3) \quad \frac{4\pi}{(\alpha + 1!)n} \int H_{12} r^{2+\alpha} dr = L_\alpha,$$

$$(2.4) \quad \frac{4\pi}{(\alpha + 1!)n} \int (n_{12} - n^2) r^{2+\alpha} dr = M_\alpha.$$

L_α et M_α ont les dimensions d'une longueur élevée à la puissance α . Ceci dit, nous noterons les deux premières relations que cette méthode permet d'écrire

$$(2.5) \quad 1 + M_0 = \frac{1}{1 - L_0}$$

$$(2.6) \quad M_2 = \frac{1}{(1 - L_0)^2} L_2.$$

Une relation importante dans la théorie des fluctuations de densité permet d'introduire ici la dérivée isotherme de la pression P par rapport à la densité

$$(2.7) \quad 1 + M_0 = \left(\beta \frac{\partial P}{\partial n} \right)^{-1} (*).$$

Nous écrirons donc (5) et (6)

$$(2.8) \quad 1 - L_0 = \beta \frac{\partial P}{\partial n},$$

$$(2.9) \quad L_2 = \left(\beta \frac{\partial P}{\partial n} \right)^2 M_2.$$

(*) Faire attention qu'ici β désigne $1/kT$ et non pas, comme c'est aussi parfois l'usage, le coefficient de compressibilité isotherme.

Au point critique M_0 est une grandeur infinie. Il est probable qu'il en est de même de tous les M_λ . Par contre L_0 reste fini. Il est bien possible qu'il en soit de même des L_λ . Cette situation renforce l'opinion déjà exprimée suivant laquelle H_{12} est une grandeur à décroissance plus abrupte vis-à-vis de la distance que n_{12} .

3. - Application du comportement asymptotique des corrélations.

Nous retenons l'idée développée dans le paragraphe précédent que H_{12} est une fonction « abrupte ». Remplaçons alors dans l'équation (1.28) l'intégrale

$$\int H_{12} \sin kr \cdot r \, dr$$

par les premiers termes de son développement en série entière par rapport à k . L'équation (1.28) nous donnera — ainsi simplifiée — l'expression asymptotique — c'est-à-dire aux grandes distances — de

$$n_{12} - n^2.$$

Il vient, au quatrième ordre près

$$(3.1) \quad n_{12} - n^2 = \frac{n}{4\pi^2 i r} \int_{-\infty}^{+\infty} \exp[ikr] \frac{L_0 k - L_2 k^3}{1 - L_0 + L_2 k^2} dk.$$

L'approximation n'est satisfaisante que si L_2 est positif : vient alors

$$(3.2) \quad n_{12} - n^2 = \frac{n}{4\pi L_2} \frac{\exp[-r] \sqrt{(\beta/L_2)} (\partial \rho / \partial n)}{r}.$$

Ce type de décroissance par rapport à r avait été trouvé autrefois par ORNSTEIN et ZERNIKE [2]. La présente déduction précise la valeur des coefficients.

P. G. DE GENNES doit discuter dans une autre communication [3] les résultats obtenus dans ce paragraphe.

Il est clair que si L_2 est négatif, l'approximation est insuffisante. Il faut dans ce cas faire intervenir le paramètre L_4 . Il n'est pas difficile d'imaginer alors des valeurs des paramètres telles que le comportement asymptotique

soit du type sinusoïdal amorti. Il y a donc une possibilité de trouver un comportement asymptotique semblable à celui que l'expérience manifeste dans les liquides. Mais ce point n'a pas été approfondi.

R É F É R E N C E S

- [1] J. YVON: *Revue Scientifique*, Novembre-Décembre 1939, p. 662.
 - [2] Consulter L. VAN HOVE: *Phys. Rev.*, **95**, 249 (1954).
 - [3] P. G. DE GENNES: in this issue, pag. 240.
-

INTERVENTI E DISCUSSIONI

— J. A. PRINS:

Dans le cas des gaz comprimés, vous ne trouvez pas des oscillations?

— J. YVON:

Pas avec les deux premiers termes.

Some Remarks on Experiments in the Dense State.

A. MICHELS

Van der Waals Laboratorium, Gemeente Universiteit - Amsterdam,

The time allotted to me by the organizers of this colloquium shows clearly that I am not expected to give a description of the experiments carried out in recent years where the phenomena were to be studied under pressure. Even if the discussion is restricted to the field indicated by the title of this conference, the technical details of the methods used and the results obtained are too manifold to be compressed in a simple half hour. Moreover, I am convinced that such a summary would not be appropriate for this forum, where the scientists who have come to meet can well be expected to have read the papers which are for them of specific interest.

I am therefore convinced that I have understood the intention of the committee when I restrict myself to a more general description of what I consider to be the guiding principle of an experimentalist operating in the field under discussion, although I won't abstain from quoting as examples some specific experiments and results, so as to clarify my points of view.

As in any other problem of human life it is just reasonable that in the preparation of scientific research the path and the means to be chosen must match the target to be reached. To forestall unjustified criticism, I like to stress that with this adage I don't mean to disqualify the adventurer who by complete lack of information is inclined to carry out some experiments in the hope that he may find some phenomenon which may turn out to be worth his while. This sort of experiment just does not form the subject of this address. Neither do I intend to discredit the scientific worker in the field of applied research for industry who collects data necessary for technical application. Again this man has his target, and his effort is outside the scope of my present consideration. With these remarks the field has been cleared and the first question to be raised is: What does the physicist expect to learn about the condensed state from experiments carried out under pressure, how can he

arrange his methods to obtain the information desired, and what conditions must his instruments satisfy to be considered up to the standard?

Stating this question already indicates that the experimentalist must be versed enough in the theoretical problems to understand the language of the theorists and to co-operate with them in such a way that he can interpret their approach in terms of his own language, which is full of its own jargon of technical approaches. Some leeway must however be granted to him. His character leads in general to a more visual picture than a mathematical one, and this will provide him with a working hypothesis, which frequently can not stand the sharp criticism of the theoretical mind, but he knows it, don't fear. His visual conception is a beacon to light his course, and he is prepared to forget each beacon he has passed on the way to success. It has met its purpose.

But to come back to the question raised, what is the aim of the hunt for knowledge? First of all, it is to understand better the nature of the interaction between molecules, and the importance of the contributions of the different terms into which this interaction is usually separated: the dispersion term, permanent dipole and quadrupole terms, etc.; and secondly to study the effect of intermolecular forces on the structure of the dense phase and the effect of the kinetic properties on its general behaviour. In first instance it may be claimed that at the present status of theoretical physics it is possible in principle to calculate the interaction between two molecules. The practical results, however, are too scanty to be satisfying; very soon the calculations become so involved that definite conclusions can hardly be drawn. Even a rigid deduction of the second distribution function still lacks the proper foundation of the multibody interaction. Moreover, both for theorist and experimentalist the scientific doubt stays to be a salutary medicine.

I'm afraid I have again erred from the course initially taken, and must come back to my guns. If he wishes to learn more from our experiments about molecular interaction, the experimental physicist is inclined to consider the molecular field in itself of slight interest. A molecule free in space is a well-satisfied and well-determined animal. When another molecule approaches it something happens in the internal construction, and this change is coupled to an interaction which in mathematical terms can be described as a force field. It is therefore understandable that the doubt arises automatically whether the interaction of a third intruder can be considered to act as if the total interaction follows a rule of additivity. We can put this problem aside for the time being and assume non-additivity to be at least a second-order complication. However, we are not allowed to be surprised if later we find that this simplification turns out to be incompatible with the experimental results. The experimentalist must be on his guard and keep his eyes open.

A second assumption is inherent in the adiabatic approach. To avoid misunderstanding I like to describe this as the assumption that, notwithstanding

the acceptance of the permanent motion of the individual particles at each specific moment, the interaction is purely defined by the position of the interacting particles and not by the way they have obtained their respective positions or how they are going to leave them, so that their relative motion does not play a part in the interaction.

If this assumption is right it can be expected that normally all physical properties which are functions of the molecular interaction are more directly related to the density and temperature of a gas than to the pressure. Pressure only shows up in so far as this quantity also depends on the variables ϱ and T through what is called the equation of state.

It seems therefore reasonable to measure physical properties as a function of density and temperature. However, practical difficulties then obstruct our way. It is not easy to change temperature and keep density constant. A much simpler procedure is to work under constant pressure and allow the density to find its own value while the temperature varies. To circumvent the difficulty it is then necessary to determine first the equation of state $f(p, \varrho, T) = 0$, and to measure the quantity X we are interested in first as $\varphi(p, T)$. Elimination of p from these functions then yields the desired information.

Besides this, the equation of state gives some immediate information, although this information is mainly of a random character. Thermodynamic functions and variations in caloric values, e.g., c_v and c_p , can be deduced. Although these values depend on the molecular interaction and are related to the micro-structure of the system, they don't give a clear picture of the underlying phenomena. The only obvious direct information resulting from the equation of state is an approximation of the molecular interaction via the virial coefficients; in particular, in the expression

$$pv(RT)^{-1} = 1 + B\varrho + C\varrho^2 \dots,$$

B as function of T gives information on the potential field between two neighbouring molecules.

Before discussing another conclusion which can be drawn from the $f(p, \varrho, T) = 0$ measurement it is interesting to spend a few minutes with the experimentalist's worries and the test of his technological adequacy: « How accurate must the measurements be to satisfy the condition that they must be good enough to give the theoretical information for which they are initiated? » This question cannot be answered without previous experimental evidence. This evidence is, however, widely available.

In first approximation Boyle-Gay Lussac's law is valid; it is founded on the assumption of absence of molecular volume and interaction. A second approximation, which only assumes a rigid molecular volume and an attractive

field increasing rapidly with decrease of distance, leads to the Van der Waals equation.

This equation describes within a few per cent, the experimental results if appropriate values for the constants a and b are chosen. Apparently the picture as given by Van der Waals is right in principle, and the existence of an attractive field and a repulsive core can be accepted. However, to obtain information on the real molecular parameters accuracy much higher than a few per cent is required. This accuracy must be of the order of 1 part in 10000.

A similar conclusion can be drawn from the value of B , which is directly related to the molecular properties. Since B is of the order of 10^{-2} to 10^{-3} , $pV(RT)^{-1}$ must be measured at least to 0.01%.

A nice demonstration gives the c_v . As $(\partial c_v / \partial V)_T = T(\partial^2 p / \partial T^2)_V$ for any equation of state where p is a linear function of T (as is the case in the Van der Waals equation), c_v should be independent of density.

Fig. 1 shows that this is not true. The information presented could only be obtained by measurements so accurate that a quantity could be determined within about two per cent which, even in second approximation is negligible.

A final accuracy of 1 part in 10000 requires in general about 1 part in

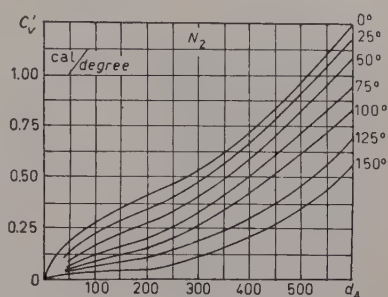


Fig. 1. — The increase in c_v of nitrogen by compression.

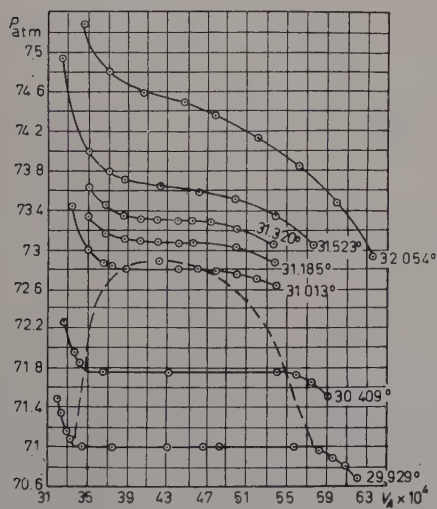


Fig. 2. — Some isotherms of carbon dioxide in the critical region.

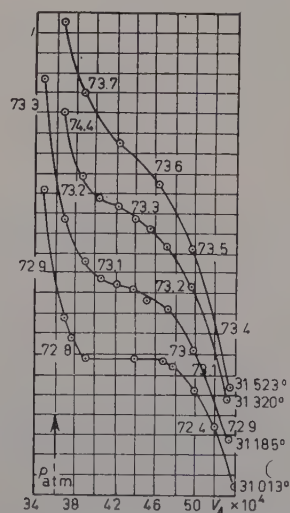


Fig. 3. — Four isotherms of carbon dioxide on a larger scale.

30 000 for each of the three parameters. However, frequently even this is not good enough. In the neighbourhood of the critical point, where $(\partial p/\partial V)_T$ and $(\partial T/\partial V)_p$ are abnormally small, higher precision is necessary in p and T determination, whereas in the range of liquid density where $(\partial p/\partial V)_T$ is large, V requires extra consideration, so that frequently 1 in 100 000 is not outside the claim put to the experimentalist. That these requirements lead to elaborate and time-consuming efforts

in measurements and standardization can easily be understood.

However, some results may show what is possible (Fig. 2, 3, 4). It may be added that data of the accuracy described have been obtained for several gases at pressures up to 3000 atm. and in the temperature range -180°C to $+300^\circ\text{C}$.

Discussion of how this accuracy is finally reached would require a too detailed description. However I will be only too pleased to answer any specific questions.

Contrary to what might be expected from earlier remarks some more information on the nature of the molecular interaction can be deduced from the experimental equation of state.

If an ensemble of molecules is considered as an ensemble of nuclei and electrons, as has been suggested by SCHOTTKY and later further developed by SLATER, the equation

$$3\Delta pV = \Delta U + \Delta K,$$

can be deduced for isothermal compression, where ΔpV denotes the change in pV by isothermal compression, ΔU the corresponding change in total energy and ΔK in kinetic energy.

As during compression the temperature is constant and the law of æquipartition is certainly valid, a large variation in K can only be attributed to a change in the kinetic energy of the electrons.

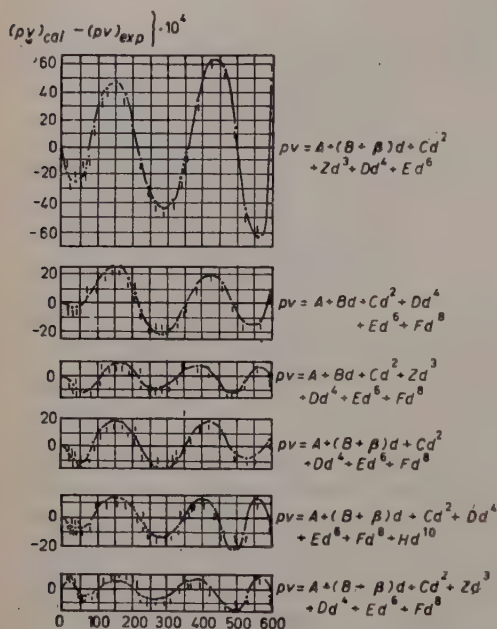


Fig. 4. — Differences between the experimental values of pV and those calculated from a series expansion for the 50°C isotherm of carbon dioxide.

Some specific experimental values of ΔK for compression at 425 °K from 1 ÷ 3000 atm are expressed in calories per mol:

H_2	3000	CO_2	9000
A	4000	C_2H_4	12000
N_2 and CO . .	6000	C_3H_6	14500

Calculations for the hypothetical atomic hydrogen by J. DE BOER, BIJL, DE GROOT, SOMMERFELD, TEN SELDAM and MICHELS on the assumption of the so-called « caged atom » have given values in line with these data. The results

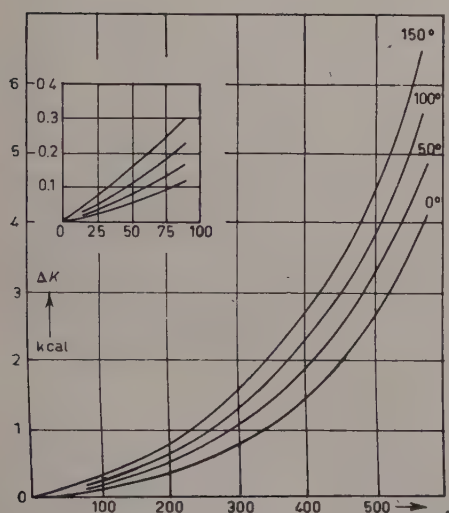


Fig. 5. — ΔK of nitrogen as a function of density at different temperatures.

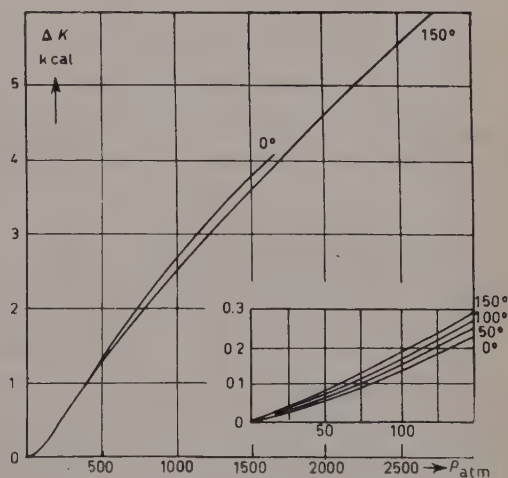


Fig. 6. — ΔK of nitrogen as a function of pressure at different temperatures.

show clearly that the interaction of molecules must be coupled with a disturbance in the electronic structure of the atom or molecule.

Special attention is called to the following two figures representing the value of ΔK for N_2 plotted respectively against density and pressure (Fig. 5, 6). These figures show clearly that the deformation of the electronic cloud is far more closely related to the pressure than to the density. Rightly or wrongly, the experimentalist is inclined to form a working hypothesis on the basis that the pressure is related to the total change in momentum of the molecules in his measuring equipment. He will realize that the increase of momentum by increasing temperature will allow two colliding molecules to penetrate deeper into each other's repulsive fields. The question then arises whether validity of the adiabatic assumption has to be reconsidered.

It may be of interest to draw attention to the fact that in the region where molecular attractive forces show up most clearly, namely in the neighbourhood of the critical point, ΔK has a negative sign, as can be seen from

Fig. 7.

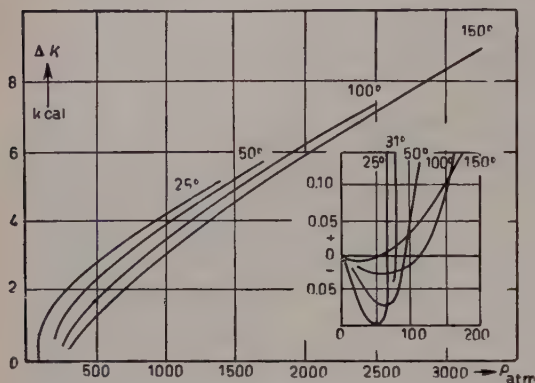


Fig. 7. — Pressure dependence of ΔK of carbon-dioxide at different temperatures.

The realization that during the interaction at small distances, most predominant at high density, a vigorous change occurs in the electronic cloud directly calls for experiments on the phenomena which are most closely related to the electrical structure of the molecule. This calls for measurement of optical quantities like refractive index, absorption and emission spectra, and measurement of the polarizability of compressed gases.

Although no high accuracy in the determination of the Lorentz-Lorenz and Clausius-Mossotti function can be claimed, there are reasons to believe that these functions have some relation to the same molecular phenomena which control ΔK as can be seen from Fig. 8.

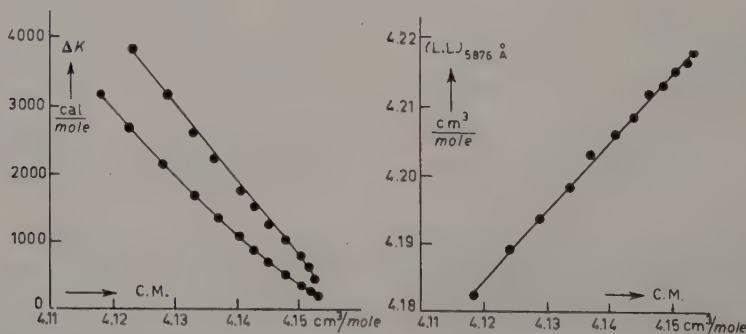


Fig. 8. — ΔK and the Lorentz-Lorenz function vs. Clausius-Mossotti function for argon.

New experiments on emission and absorption spectra have been described recently at the conference in Paris. As time is restricted I feel bound to leave them out of discussion for to-day and prefer to spend a few minutes on some remarks about an effect found in the transport properties (heat conductivity and viscosity) at elevated pressures.

It is generally well accepted that the isotherms of these properties as a

function of the density run nicely parallel (Figs. 9 and 10). Heat conductivity can be described as transport by migration or collision of random energy; viscosity, of momentum. It is therefore not unexpected to find $\lambda/c_v \propto \eta$.

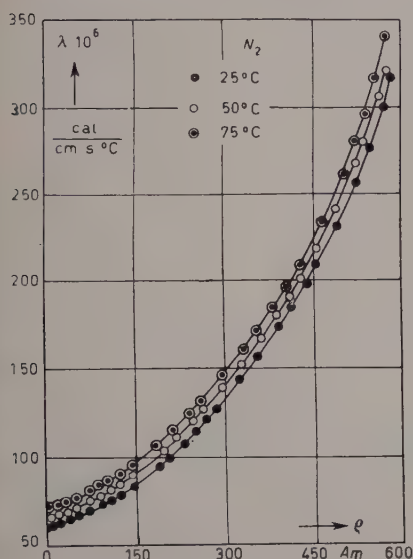


Fig. 9. — Thermal conductivity-density curves for nitrogen.

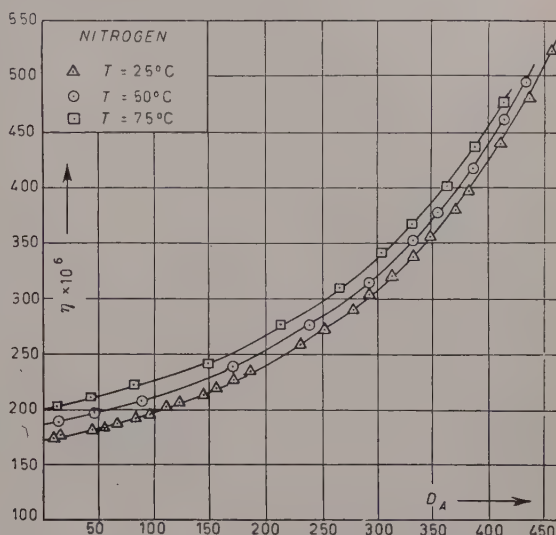


Fig. 10. — Viscosity-density curves for nitrogen.

A first exception was found when the heat conductivity of argon was measured. Whereas η versus ρ follows the normal pattern, λ versus ρ shows an unexpected overcrossing of the isotherms (see Fig. 11). Closer inspection discloses that the maximum separation between the isotherms is in the neighbourhood

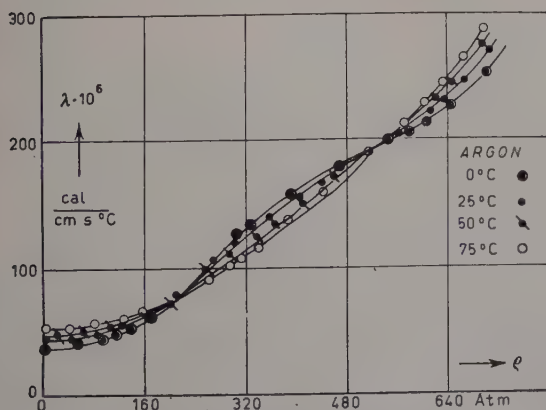


Fig. 11. — Thermal conductivity vs. density curves for argon.

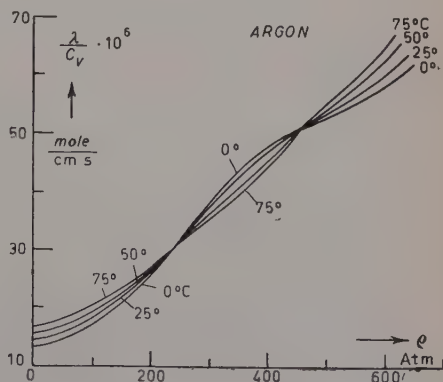


Fig. 12. — λ/c_v plotted as function of density.

of the critical density. Moreover if λ/c_v is plotted against density another unexpected phenomenon shows up (Fig. 12). The careful experimentalist is aware that in experiments run for the determination of λ the different layers are by necessity not at constant density but at constant pressure, and he

will ask whether a transport of potential energy must be accounted for, in addition to a transport of random or kinetic energy.

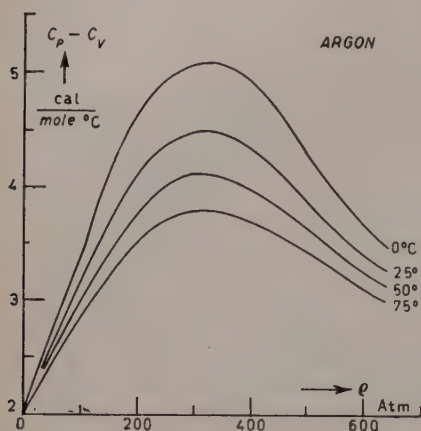


Fig. 13. — $c_p - c_v$ as a function of the density for argon.

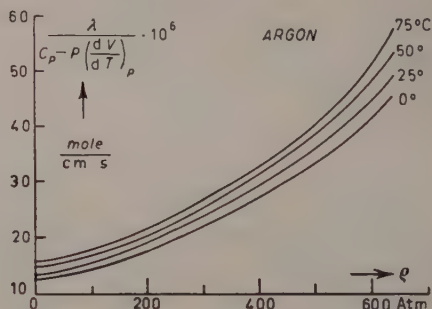


Fig. 14. — $\lambda/\{c_p - p(\partial V/\partial T)_p\}$ as a function of the density for argon.

The doubt is increased by considering the value of c_p as a function of ρ . Fig. 13 indicates that c_p shows a maximum in the range of the greatest anomaly in λ . The difference between c_p and c_v is twofold. There is contribution for external work $p(\partial V/\partial T)_p$ and a change in potential energy. It can hardly be expected that the former quantity will in reality play a role. Therefore $\lambda/\{c_p - p(\partial V/\partial T)_p\}$ has been plotted against density. The results are shown in Fig. 14.

Although a clear theoretical analysis is still lacking, the effect found has given an incentive to carry out some measurements with other gases in the region where $c_p - p(\partial V/\partial T)_p$ is high. Preliminary results of the work in progress confirm the picture formulated.

Finally, I would like to raise some criticism of the interpretation of the speed of sound in the critical region.

Some years ago it was asked whether an expansion of gas at extreme speed such as occurs in a popgun could be considered to be isentropic.

Assume (Fig. 15) a bullet is restricted in a barrel free of leak. Gas pres-

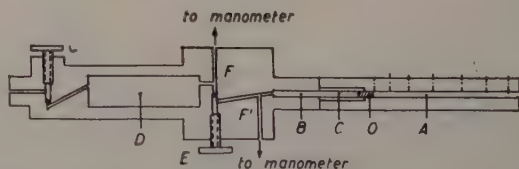


Fig. 15. — Schematic drawing of the expansion rate measuring apparatus. The bullet O is shot into the barrel A .

sure is built up behind the bullet to around 3 000 atm., pressure and temperature are measured and the bullet is released without friction. The bullet gains speed while the gas expands and the acceleration of the bullet is measured. Is the expansion of the gas isentropic; i.e., reversible adiabatic?

From the record of the position of the bullet versus time acceleration at any point could be deduced and thus the pressure. These figures could be compared with the known isentropes of the gas. The results confirmed the assumption of a reversible adiabatic expansion within the experimental accuracy of better than 1%. At first sight it may seem strange that this process should be reversible. However, this point is easily clarified if one considers the case in which the barrel is closed at the far end and some gas of lower pressure is left in front of the bullet. In its flight the bullet would then compress this gas until its velocity dies out and is reversed. Indeed, if no friction is present and no heat losses exist the bullet will from now on start moving backwards and forwards indefinitely, driven by an ideal gas spring.

The fact that during the process the entropy does not vary can be understood by interpreting the entropy as a measure of the probability. This probability is not only low when the gas is restricted to a section of the total available space, but also if the gas has obtained at the cost of its random motion a directed movement. An expanding gas only gains entropy when by collision directed motion is turned into random or heat motion.

Once it is found that the process is isentropic, it is possible to calculate the temperature the gas should have. If nitrogen with its 5 effective degrees of freedom is used everything works out nicely. For argon, however, where only 3 degrees of freedom are present, the cooling due to expansion proceeds to such a low temperature that the coexistence line is crossed and argon ought to liquify. At about -190°C the pressure, which should be 1 atm., is actually about 40 atm. This shows that the time was certainly not sufficient for the molecules to obtain their normal relative position before crossing the co-existence line. This can also be described by saying that the dynamic isentrope does not coincide with the static one.

If, however, this conclusion is true, it is questionable whether measurements of supersonic speed in the neighbourhood of the critical point can be employed to deduce properties which are defined for static conditions like c_p/c_v . In the region mentioned the distribution function changes so rapidly with temperature that no guarantee exists than the successive compressions and expansions can be described by a static isentrope.

I like to finish with a small psychological remark. Very frequently it can be observed in the approach of the experimentalist, who relies so much on his vision and intuition, how he often shows some relation to the artist. He enjoys elegant technical solutions and instruments, which give him the creative pleasure so much more apparent in the real artist.

INTERVENTI E DISCUSSIONI

— J. A. PRINS:

I understand there is no condensation in your rapid adiabatic expansion. As you know, in the atmospheric adiabatic expansions there is no condensation in supercooled air for many *days* in some cases! But surely this does not mean that the molecular distribution function needs many days to get adjusted.

So I think your observations in the two phase region do not give the slightest hint what to expect in the one phase region; the readjustment there is much smaller than the formation of droplets implies. Even in the two phase region I would expect the molecular distribution function to be adjusted very quickly to, say, the Van der Waals isentrope where the macroscopical density is homogeneous, though of course the formation of the inhomogeneous two phase system would take quite a long time, which has, however, nothing to do with the readjustment of the molecular distribution function of the homogeneous phase.

— A. MICHELS:

Deviation is already present above the coexistence line. Moreover, the process described lasted between 200 and 400 μ s, whereas by frequencies of 10^6 to 10^5 in sound velocity measurements an expansion is over between $\frac{1}{2}$ and 5 μ s.

The Equation of State of an Imperfect Gas of Elastic Spheres.

H. N. V. TEMPERLEY

Atomic Weapons Research Establishment - Aldermaston, Berkshire

FORD (1954) [1] has considered a « gaussian » model of an imperfect gas with purely repulsive interactions, in which the Mayer function is taken to be

$$(1) \quad f = \exp [-\varepsilon/kT] - 1 = -A \exp [-r^2/a^2],$$

which, with $A=1$, is a fair representation of an elastic sphere type of interaction. For *rigid* spheres, we have $f=0$ or -1 . In space of k dimensions, it is readily shown that the N -th virial coefficient is proportional to the sum

$$(2) \quad \sum_L \sum (-A)^L C^{-k/2},$$

where the inner summation is over all irreducible Mayer diagrams of L lines involving N points, and the quantity C is the « complexity » of the diagram, that is, the number of Cayley trees of order N that can be made from it by selecting $N-1$ of its lines. Thus, the gaussian model has consequences that can be described entirely in terms of the topological properties of the Mayer diagrams.

We compare (2) with the sum that occurs in the « restricted random-walk » problem, which is analytically simpler [3]. In this, we estimate the probability of a configuration in which molecules 1 and 2, 2 and 3, 3 and 4, etc., overlap, but overlapping of all other pairs is prevented, that is, we try to estimate the result of integrating the following product over the co-ordinates of N points:

$$(3) \quad f_{12}f_{23} \dots f_{N1}(1+f_{13})(1+f_{24}) \dots (1+f_{14}),$$

the terms in brackets preventing « overlaps » by non-neighbours in the ring. If we omitted these terms we should have the unrestricted random walk

problem, or the «ring» approximation to the virial coefficient. Expression (3) leads, when integrated, to a sum closely related to (2) when N is large. All the diagrams appearing in (3) are irreducible, but some irreducible diagrams are omitted. This difference between the two sums can be approximately allowed for by multiplying A by a factor of the order of $[(N-1)!]^{2/N^2}$ which approaches unity for large N . The relative weighting of the diagrams with large L is greater in (3) than it is in (2), that is steric effects are, for a given model, relatively more important in the restricted random walk problem.

It is known, from experience with the restricted walk problem on other models, that (3) should lead to a result proportional to

$$(4) \quad (-1)^N a^{kN} N^{-kl/2} [B(A, k)]^N,$$

where the first three factors are what we should get for the unrestricted walk, or the «ring» approximation, and the factor B^v corrects for self crossing paths. HAMMERSLEY [2] (1957) has proved the validity of this correction for a large class of models. The validity of (4) for this model has been independently checked, and an estimate of B can be made, in the following way.

A simple generating function has been found [4], which permits us to estimate C for any N and for any specified «structure» of the Mayer diagram (this term will be defined in a moment). The crude assumption that C can be regarded simply as a function of L , the total number of lines in the diagram, becomes inadequate for large N and has been dropped. We divide the lines into sets, one set corresponding to the «sides» 1 2, 2 3 ... $N1$ of a polygon, and $(N-3)/2$ other sets to the various possible types of «diagonal» of the polygon. Our estimate of C in any given case does involve averaging over diagrams which draw the same numbers of lines from *each* of the sets (two such diagrams being said to have the same structure), but is otherwise rigorous. Clearly this is very much more refined than averaging over all diagrams with the same L . (This generating function also has applications to polymer problems and the Ising model.)

The conclusion is that, for N large, the N -th virial coefficient should behave in the same way as (4), but various «small number effects» have been found which imply that the limiting behaviour is approached quite slowly. FORD (1954) has enumerated the complexities up to $N = 7$, and has, in fact, shown rigorously that the fourth and seventh virial coefficients are negative for spheres, contrary to the prevailing belief that they are all positive for a purely repulsive interaction. It is easy to show from (1) that PV remains finite as $V \rightarrow 0$ provided $A \leq 1$, while our present work indicates a singularity on the *negative* real axis of $1/V$, so that a «condensation effect» seems most unlikely for this model, a «soft» repulsion. This model is not directly comparable with the «hard» repulsion of rigid spheres.

It seems to be possible to use the above complexity estimates for a direct attack on (2), which would be more satisfactory than the indirect approach via (3). This question is being studied, but some details remain to be worked out. This work of FORD's seems to be the first application of circuit theory in statistical mechanics of phase changes.

REFERENCES

- [1] G. W. FORD: *Thesis*, University of Michigan, 1954.
- [2] J. M. HAMMERSLEY: *Proc. Camb. Phil. Soc.*, **53**, 642 (1957).
- [3] H. N. V. TEMPERLEY: *Trans. Farad. Soc.*, **43**, 1065 (1957).
- [4] H. N. V. TEMPERLEY: *Proc. Phys. Soc.*, **71**, 238 (1958).

INTERVENTI E DISCUSSIONI

— G. UHLENBECK:

Have you proved whether there is a transition point?

— H. TEMPERLEY:

There are gaps in the argument which prevent it from being completely rigorous. The absence of a transition point rests on the suggested alternation in sign of the higher virial coefficients which is only suggested, rather than rigorously proved by my work.

P A R T E Q U A R T A

Theory of Liquids.

Equation of State and Surface Tension of Liquids.

S. ONO

University of Tokyo - Tokyo

1. — As is well known the lattice theories of liquids are divided into two categories: the Lennard-Jones theory and the hole theory. In the present article I shall make some remarks on the relation between the above-mentioned two types of theories.

Several years ago ROWLINSON and CURTISS [1] made extensively analytical comparison between these theories. However, I shall here try to make clear the relation between these two types of theories from another point of view.

As is usual, we shall consider the partition function of the system consisting of N monatomic molecules with the mass m :

$$(1.1) \quad Z_N = \lambda^{-3N} Q_N,$$

$$(1.2) \quad Q_N = \frac{1}{N!} \int \dots \int \exp \left[\frac{-\Phi_N}{kT} \right] d\mathbf{r}_1 d\mathbf{r}_2 \dots d\mathbf{r}_N,$$

$$(1.3) \quad \lambda^{-1} = \frac{(2\pi m kT)^{\frac{1}{2}}}{h},$$

where Φ_N is the potential energy of the system and a function of the co-ordinates of the N molecules, $\mathbf{r}_1, \dots, \mathbf{r}_N$.

According to the usual procedure of the lattice theory, let us divide the co-ordinate space into L cells: $\Delta_1, \Delta_2, \dots, \Delta_N$. We assume that each cell is sufficiently small that the probability of multiple occupancy is negligible and at the same time sufficiently large that the interactions of molecules beyond immediately adjacent cells are regarded as only a small correction. Both of these conditions can be fulfilled only in the case of short-ranged intermolecular forces. Then L must be larger than N , and consequently there may exist in

general vacant cells, which we call « holes ». Thus the configuration integral (1.2) may be written in the form

$$(1.4) \quad Q = \sum_{\Delta l_1} \dots \int_{\Delta l_N} \exp \left[\frac{-\Phi}{kT} \right] d\mathbf{r}_1 d\mathbf{r}_2 \dots d\mathbf{r}_N,$$

where the summation is over all the $L!/N!(L-N)!$ arrangements which differ by more than a permutation.

The configuration integral expressed in the form of (1.4) is valid for gases as well as for liquids. In the present case, the volume of a cell, q , is different from $v = V/N$, the volume per molecule

$$(1.5) \quad q = V/L.$$

Further we shall consider the centers of these cells to form a space-lattice like structure.

Let us consider a lattice such that for each lattice point there are c nearest neighbors at a distance a : for the face-centered cubic structure this number is $c = 12$. We denote by ω_i the fraction of the nearest neighbor cells of the i -th molecule which are vacant, for a given configuration. Then, if the total number of pairs of nearest neighbor cells, one member of which is occupied and the other vacant, is denoted by cX , we obtain

$$(1.6) \quad X = \sum_{i=1}^N \omega_i.$$

Let us denote the intermolecular potential by $\varphi(r)$ as a function of the intermolecular distance r . When all of the molecules are at their own cells, the potential energy of the i -th molecules is $c(1 - \omega_i)\varphi(a)$, and the total potential energy is given by

$$(1.7) \quad \Phi_0 = \frac{c}{2} (N - X)\varphi(a),$$

the contribution from the second and more distant neighbors being neglected for the moment.

Then we assume that the force acting on the i -th molecule is given by the force which acts when $c(1 - \omega_i)$ neighboring molecules are located at the centers of their own cells. Although in this case the potential depends, not only on the distance, R , from the origin of this cell, but on the direction, we use the sphericalized potential given as

$$(1.8) \quad \overline{\Psi}(R, \omega) = c(1 - \omega) \left\{ \frac{1}{4\pi} \int \int \varphi(|\mathbf{a} - \mathbf{R}|) \sin \theta d\theta d\varphi - \varphi(a) \right\},$$

which depends only on the number of nearest neighbor molecules. For intermediate values of ω between 0 and 1, the cell potential may be less spherical.

If the sphericalized potential is used, the approximate total potential may be given by

$$(1.9) \quad \Phi = \frac{c}{2} (N - X) \varphi(a) + \sum_{i=1}^N \bar{\Psi}(R_i, \omega_i),$$

and substitution of (1.9) into (1.4) leads to

$$(1.10) \quad Q_N = \exp \left[\frac{-Nc\varphi(a)}{2kT} \right] \sum \{v(\omega^{(1)})v(\omega^{(2)}) \dots v(\omega^{(N)})\} \exp \left[\frac{Xc\varphi(a)}{kT} \right],$$

where v_f is a generalized free volume given by

$$(1.11) \quad v_f(\omega) = \int_A \exp \left[\frac{-\Psi(R, \omega)}{kT} \right] 4\pi R^2 dR.$$

To proceed further with the calculation we usually utilize the linear approximation

$$(1.12) \quad \ln v_f(\omega) = \ln v_f(0) + \omega \ln \left(\frac{v_f(1)}{v_f(0)} \right).$$

Substituting (1.12) into (1.11) we obtain

$$(1.13) \quad Q_N = \exp \left[\frac{-Nc\varphi(a)}{2kT} \right] \{v_f(0)\}^N \sum_X G(N, L, X) \exp \left[\frac{X\zeta}{kT} \right],$$

$$(1.14) \quad \zeta = \frac{c}{2} \varphi(a) + kT \ln \left(\frac{v_f(1)}{v_f(0)} \right),$$

where $G(N, L, X)$ is the number of the distinguishable arrangements of the N molecules in the L cells for a specified value X .

It is difficult to evaluate exactly $G(N, L, X)$. But, if we use the quasi-chemical approximation, we can carry out the calculation of the configuration integral and finally we have the following expression for the Helmholtz free energy:

$$(1.15) \quad F = nF_0^R + LkT \{x \ln x + (1-x) \ln (1-x)\} + \frac{1}{2} Lc kT \left\{ x \ln \frac{\beta - 1 + 2x}{x(\beta + 1)} + (1-x) \ln \frac{\beta + 1 - 2x}{(1-x)(\beta + 1)} \right\},$$

$$(1.16) \quad F_0^R = N_0 \zeta - N_0 kT \ln (\lambda^{-3} v_f(1)),$$

$$(1.17) \quad \beta = \{1 - 4\alpha x(1 - x)\}^{\frac{1}{2}}, \quad \alpha = \exp [-2\zeta/ekT],$$

$$(1.18) \quad x = \frac{N}{L},$$

n being the mole number.

2. — In the above derived expression of the Helmholtz free energy (1.15) the parameters $v_f(0)$ and $v_f(1)$ remain undetermined. As the choice of these constants the four types of approximation are well known: CERNUSCHI and EYRING [2], ONO [3], PEEK and HILL [4], and ROWLINSON and CURTISS [1].

However, we shall here determine these constants by the following conditions:

i) In the limit of infinitely dilute case the free energy agrees with that of a perfect gas which corresponds to the respective liquid.

ii) In high density limit the free energy (1.15) becomes identical with the one given by the Lennard-Jones theory, apart from the term corresponding to the so-called communal entropy, which is usually added in Lennard-Jones expression for the free energy [5].

iii) The cell size is determined to give a minimum value of the free energy for given values of N and V .

As will be seen later, in this method, the effect of the second and more distant neighbors are taken into account through the condition ii).

Let us consider the low density limit $x \rightarrow 0$. Then (1.15) reduces to

$$(2.1) \quad F \rightarrow -NkT \ln \frac{v_f(1)}{x} + 3NkT \ln \lambda - NkT.$$

According to the first condition, this expression must be identical with the free energy of a perfect gas. Then we have

$$(2.2) \quad v_f(1) = q = xv = x \frac{N}{V}.$$

In the high density limit, (1.15) becomes identical with nF_0^H given by (1.16). Then the second condition gives the relation $F^{LJ} = F_0^H + N_0kT$, where F^{LJ} is the free energy given by the Lennard-Jones theory including the communal entropy term. From (1.16) and the above relation, we find

$$(2.3) \quad F^{LJ} - F^0 = N_0kT,$$

where F^0 is the Helmholtz free energy of the perfect gas with the same T and V . The values of the difference $F^{1,j} - F^0$ can be calculated from the Table by HIRSCHFELDER and collaborators [6]. The relation (2.3) furnishes the physical significance of the parameter ζ , and, at the same time it enables us to take into account the effect of the second and more distant neighbors in the hole theory. This method seems to be approximated, but it may not be more than a linear approximation.

The Helmholtz free energy given by (1.15) is the function of q , x , and N . However, these three variables are not independent from each other, but they are connected by the relation

$$(2.4) \quad q = xv = x \frac{V}{N} = \frac{V}{L}.$$

Thus q is a function of x , if we keep V and N constant. Then, the third condition which is the condition of minimization [7] of the Helmholtz free energy, is

$$(2.5) \quad \left(\frac{\partial F}{\partial x} \right)_{N,V} = \left(\frac{\partial F}{\partial x} \right)_{N,q} + v \left(\frac{\partial F}{\partial q} \right)_{N,x} = 0.$$

On the other hand, the pressure is given by

$$(2.6) \quad p = - \left(\frac{\partial F}{\partial V} \right)_{N,T} = - \left(\frac{\partial F}{\partial q} \right)_{N,x,T} \left(\frac{\partial q}{\partial V} \right)_N - \left(\frac{\partial F}{\partial x} \right)_{N,q,T} \left(\frac{\partial x}{\partial V} \right)_N.$$

From (2.5), (2.6) and the relation $V = Nq/x$, we have the expression for the pressure

$$(2.7) \quad p = - \frac{kT}{q} \left\{ \ln(1-x) + \frac{Z}{2} \ln \frac{\beta + 1 - 2x}{(1-x)(\beta + 1)} \right\},$$

which happens to be identical with that in the usual hole theory.

If we use the relation (2.3) for ζ in (1.16), we can express the condition for the minimization of the free energy (2.5) in the form

$$(2.8) \quad \left(\frac{PV}{RT} \right)^u = \left(\frac{PV}{RT} \right)^{1,j} - \frac{2(1-x)\{4x(1-x) + 1 - \beta^2\}}{(\beta + 1)(\beta - 1 + 2x)(\beta + 1 - 2x)} \left\{ \left(\frac{PV}{RT} \right)^{1,j} - 1 \right\},$$

where $(pV/RT)^{1,j}$ and $(pV/RT)^u$ are the compressibility factors calculated respectively from the Lennard-Jones and the hole theories.

3. - The numerical computations have been carried out for the case of the Lennard-Jones potential:

$$(3.1) \quad \varphi(r) = 4\epsilon \left\{ \left(\frac{\sigma}{r} \right)^{12} - \left(\frac{\sigma}{r} \right)^6 \right\}.$$

The value of the reduced pressure $p^* = p\sigma^3/\epsilon$ calculated for the reduced temperature $T^* = kT/\epsilon = 0.8$ is shown in Fig. 1, together with the ones obtained from the Lennard-Jones and the simple hole theory in which the constant cell size has been chosen to be that at the low density limit, $q = 1.17\sigma^3$.

As expected, the present approximation agrees with the Lennard-Jones theory at high density and with the simple hole theory at low density, while it gives the results intermediate of the other two theories in the neighborhood of the minimum of the Van der Waals loop.

The calculated values of the reduced cell volume $q^* = q/\sigma^3$ and the value of x , the occupation probability, are shown in Table I. The cell size seems to be almost constant (*) for reduced molecular volume v^* larger than 1.6. The results are slightly different from de Boer's one [7], but it seems to be due to the effect of the second and more distant neighbors.

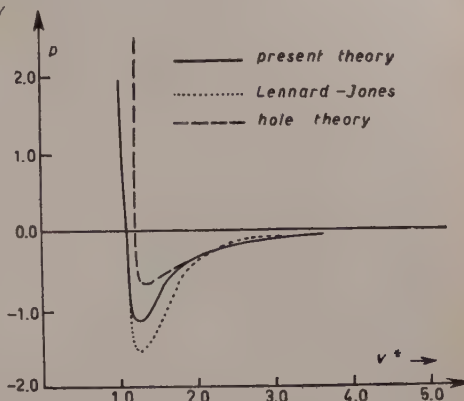


Fig. 1. — Calculated isotherm for $T^* = 0.8$.

TABLE I. — The values of the reduced cell size and the occupation probability as functions of the reduced molecular volume at the reduced temperature $T^* = 0.8$.

v^*	q^*	x
1.13	1.10	0.97
1.70	1.16	0.68
2.12	1.16	0.55
2.55	1.16	0.46
2.83	1.16	0.41
4.24	1.17	0.28
5.66	1.17	0.21

The estimated value of the reduced critical temperature is 1.05. The calculated values of the critical constants are shown in Table II, together with the results obtained from the other approximations.

(*) In Varenna some kind of peculiar change was reported, but it was due to a systematic error in interpolation from the Table.

TABLE II. — *Calculated values of critical constants.*

	$(pV/RT)_c$	T_c^*	p_c^*	V_c^*
Mean of experimental values for Ne, A and N ₂	0.293	1.28	0.119	3.15
LENNARD-JONES	0.591	1.30	0.434	1.77
CERNUSCHI-EYRING	0.342	2.74	0.469	2.00
ONO	0.342	0.75	0.128	2.00
PEEK and HILL	0.719	1.18	0.265	3.25
Present theory	0.330	1.05	0.136	2.55

The reduced cell size at the critical points is 1.28, which is slightly larger than the value at $T^* = 0.8$.

The results seem to be considerably better than those obtained from the other approximations.

4. — The hole theory developed in the above is extended here to an inhomogeneous system [3] consisting of two phases separated by a plane interface.

We shall consider a system confined to a rectangular parallelepiped vessel

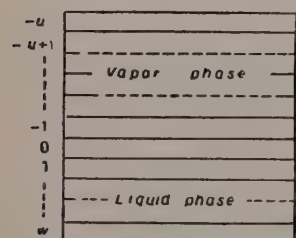


Fig. 2.

placed so that one of its edges points in the direction of the gravitational field. We assume that one of the principal planes of the hypothetical lattice is perpendicular to the gravitational force. We enumerate these planes $-1, -2, \dots$ upwards and $1, 2, \dots$ downwards, the 0-th plane being chosen arbitrarily, as shown in Fig. 2.

We shall indicate the properties referring to the t -th layer by a subscript t , for example, the number of molecules in the t -th layer is indicated by N_t ; and we shall indicate a set of the numbers, $N_u, \dots, N_1, N_0, N_1, \dots, N_w$ by $\{N_t\}$. Thus the configuration integral (1.10) can be expressed in the following form

$$(4.1) \quad Q_N = \sum_{N_u} \dots \sum_{N_0} \dots \sum_{N_w} Q(\{N_t\}),$$

$$(4.2) \quad \sum_{t=-u}^w N_t = N,$$

where $Q(\{N_t\})$ is the term corresponding to the given set $\{N_t\}$ and is given by

$$(4.3) \quad Q(\{N_t\}) = \exp \left[\frac{-Nc\varphi(a)}{kT} \right] \sum \{v_f(\omega_1) \dots v_f(\omega_N)\} \exp \left[\frac{Xc\varphi(a)}{2kT} \right],$$

the summation extending over all the configurations consistent with the given set $\{N_i\}$ of the numbers.

Inserting the linear approximation (1.12) in (4.3), we obtain

$$(4.4) \quad Q(\{N_i\}) = \exp \left[-\frac{Nc\varphi(a)}{kT} \right] (v(0))^N \sum_X g\{N\}X \exp \left[\frac{X\zeta}{kT} \right],$$

where $g(\{N_i\})$ is the number of the ways of arranging $N_{-u}, \dots, N_0, \dots, N_w$ molecules respectively in the cells of each of the corresponding layers with the given value of X .

Since it is rather complicated to use the quasi-chemical approximation for this inhomogeneous case, although it is actually possible, we shall use the Bragg-Williams approximation. Then, the statistical average of the total number of hole-molecule contact \overline{cX} is

$$(4.5) \quad \overline{cX} = \frac{1}{2}cAv \sum_{t=-u}^w \{2lx_t(1-x_t) + mx_t(1-x_{t+1}) + \\ + mx_{t+1}(1-x_t) + mx_t(1-x_{t-1}) + mx_{t-1}(1-x_t)\},$$

$$(4.6) \quad x_t = N_t/Av,$$

where A is the area of each layer and v the number of cells per unit area, lc the number of the nearest neighbor cells within the t -th layer, and mc the number of the nearest cells in one of the next layers $l+2m=1$.

Replacing X in (4.4) by the average \overline{X} as given in (4.5), we have

$$(4.7) \quad Q_N(\{x\}) = (v_f(0))^N \prod_{t=-u}^w \left\{ \frac{(Av)!}{(Avx_t)!(Av-Avx_t)!} \right\} \cdot \\ \cdot \exp \left[-\frac{Nc\varphi(a)}{2kT} - \frac{Av\zeta}{2kT} \sum_{t=-u}^w \{2lx_t(1-x_t) + mx_t(1-x_{t+1}) + \right. \\ \left. + mx_{t+1}(1-x_t) + mx_t(1-x_{t-1}) + mx_{t-1}(1-x_t)\} \right].$$

If we replace the logarithm of the configurational integral $\ln Q$ by the logarithm of its maximum term, $\ln Q^*$, in (4.1), we have the following expression for the Helmholtz free energy of the system:

$$(4.8) \quad F = nF_0^H + AvkT \sum_{t=-u}^w \{x_t \ln x_t + (1-x_t) \ln (1-x_t)\} + \\ + \frac{Av\zeta}{2} \sum_{t=-u}^w \{2lx_t(1-x_t) + mx_t(1-x_{t+1}) + mx_{t+1}(1-x_t) + \\ + mx_t(1-x_{t-1}) + mx_{t-1}(1-x_t)\},$$

where ζ and F_0^H are the parameters given by (1.14) and (1.16), respectively.

The condition of maximization for the terms of Q , which corresponds to minimization of the free energy as a function of set $\{x_i\}$ becomes

$$(4.9) \quad \zeta\{m(1 - 2x_{t-1}) + l(1 - 2x_t) + m(1 - 2x_{t+1})\} + kT \ln \frac{x_t}{1 - x_t} = A,$$

A being the Lagrange undetermined multiplier from the condition (4.2). The values of x_i 's determined from the above set of equations may be considered to correspond to the equilibrium distribution of molecules.

For a system composed of liquid and vapor phases, from the macroscopic point of view, layers of sufficiently large positive t lie in the interior of the liquid phase and those of sufficiently large negative t in the interior of the vapor phases; x_t approaches its values in the liquid and vapor phases, x_L and x_G , respectively

$$(4.10) \quad \left\{ \begin{array}{l} \lim_{t \rightarrow \infty} x_t = x_L, \\ \lim_{t \rightarrow -\infty} x_t = x_G, \end{array} \right.$$

Since the cell size is almost constant between the liquid and vapor densities under the orthobaric pressure as observed in Sect. 3, we may neglect the difference in the cell volume for liquid and vapor. Then, from the symmetry we have

$$(4.11) \quad x_L + x_G = 1.$$

Since (4.9) is valid for x_L and x_G , we obtain from (4.11) $A = 0$, i.e.

$$(4.12) \quad \zeta\{m(1 - 2x_{t-1}) + l(1 - 2x_t) + m(1 - 2x_{t+1})\} + kT \log \frac{x_t}{1 - x_t} = 0.$$

The value of x_L is given by

$$(4.13) \quad \zeta(1 - 2x_L) + kT \ln \frac{x_L}{1 - x_L} = 0, \quad (x_L > 1)$$

which is obtained from (4.10) and (4.12).

Let us introduce the notation for differences

$$(4.14) \quad \Delta x_t = x_{t+1} - x_t; \quad \Delta^2 x_t = \Delta x_{t+1} - \Delta x_t.$$

Then, using (4.12) we can rewrite (4.9) in the form

$$(4.15) \quad \Delta^2 x_{i-1} = \frac{1}{m} \left(\frac{kT}{\zeta} \ln \frac{x_i}{1-x_i} + \frac{1}{2} - x_i \right),$$

which is a non-linear difference equation.

We can solve this equation by the same method as for numerical integration of an ordinary differential equation. The boundary condition for the problem is given by (4.10).

Since the equation (4.9) and the boundary condition (4.10) are both invariant with respect to interchange x_i for $1-x_{i-1}$, we can see that the solution has the following symmetric property:

$$(4.16) \quad x_i + x_{1-i} = 1$$

if the 0-th layer is suitably chosen.

5. — Let us place the dividing surface between the 0-th and 1-st layers, the 0-th layer being so chosen that (4.16) may be satisfied. Then we shall denote the quantities referred to the liquid and vapor phases, which are considered to be homogeneous right up to the dividing surface, by subscripts L and G , respectively. According to (4.16) we obtain

$$(5.1) \quad N_L + N_G = N.$$

On the other hand, by the definition, we have

$$(5.2) \quad L_L = wAv, \quad L_G = (u+1)Av,$$

$$(5.3) \quad L = L_L + L_G.$$

From (4.8) we obtain

$$(5.4) \quad F_L = n_L F_0^H + L_L kT \{x_L \ln x_L + (1-x_L) \ln (1-x_L)\} + L_L x_L (1-x_L),$$

and

$$(5.5) \quad F_G = n_G F_0^H + L_G kT \{x_G \ln x_G + (1-x_G) \ln (1-x_G)\} + L_G x_G (1-x_G).$$

Then by the definition of the surface tension $\gamma = (F - F_L - F_G)/A$, we obtain from (4.8), (5.1), (5.4) and (5.5) the following expression for the surface

tension:

$$(5.6) \quad \gamma = v\zeta \sum_{t=1}^{\infty} [\{2lx_t(1-x_t) + mx_t(1-x_{t+1}) + mx_{t+1}(1-x_t) + \\ + mx_t(1-x_{t-1}) + mx_{t-1}(1-x_t)\} - 2x_L(1-x_L)\} + \\ + 2vkT \sum_{t=1}^{\infty} \{x_t \ln x_t + (1-x_t) \ln (1-x_t) - x_L \ln x_L - (1-x_L) \ln (1-x_L)\}],$$

where we have used the relations (4.11) and (4.16).

If we get the equilibrium distribution of x_t as the solution of the difference equation (4.15), we can calculate the value of the surface tension from (5.6).

The expression for the Helmholtz free energy given by (4.8) can be rewritten after some rearrangement as follows:

$$(5.7) \quad F = Av \sum_{t=-u}^v x_t f_t,$$

where

$$(5.8) \quad f_t = \frac{1}{N_0} F_0^H + kT \left\{ \ln \frac{x_t}{1-x_t} - \frac{1}{x_t} \ln (1-x_t) \right\} + \\ + \zeta \{m(1-x_{t-1}) + l(1-x_t) + m(1-x_{t+1})\},$$

which may be regarded as the Helmholtz free energy per molecule in the t -th layer, but a unique definition of f_t is impossible.

On the other hand, the chemical potential of a molecule in the t -th layer may be given by

$$(5.9) \quad \mu_t = \frac{1}{Av} \frac{\partial F}{\partial x_t} = \frac{1}{N_0} F_0^H + kT \ln \frac{x_t}{1-x_t} + \\ + \zeta \{m(1-2x_{t-1}) + l(1-2x_t) + m(1-2x_{t+1})\},$$

The condition for equilibrium, (4.12), is expressed in the following form

$$(5.10) \quad \mu_t = \mu,$$

μ being the chemical potential of the bulk phase. The above equation may correspond to the quasi-thermodynamic condition for equilibrium in Tolman's sense [8].

Meanwhile, from (4.8) we obtain the relation

$$(5.11) \quad \left(\frac{\partial F}{\partial A} \right)_{N,T} = vkT \sum_{t=-u}^v \ln (1-x_t) + v\zeta \sum_{t=-u}^v x_t (mx_{t-1} + lx_t + mx_{t+1}),$$

where we have used

$$(5.12) \quad kT \ln x_t = kT \ln (1 - x_t) - \zeta \{m(1 - 2x_{t-1}) + l(1 - 2x_t) + m(1 - 2x_{t+1})\},$$

which can be easily obtained from (4.12).

If the tangential pressure for the t -th layer is denoted by p_t^T , the elementary work done, due to the increase δA in the area at constant temperature, by the t -th layer of the system is

$$(5.13) \quad \delta W_t = P_t^T (\delta A) d,$$

where d is the thickness of the layer.

Thus the change in the Helmholtz free energy due to the change in the area A may be expressed as

$$(5.14) \quad \delta F = - \sum_t \delta W_t = - (\delta A) d \sum_t p_t^T.$$

Comparing (5.11) with (5.14), we obtain (*) the expression for the tangential pressure:

$$(5.15) \quad p_t^T = - \frac{1}{q} \{kT \ln (1 - x_t) + \zeta x_t (m x_{t-1} + l x_t + m x_{t+1})\}.$$

In the interior of the bulk phase, (5.15) reduces to

$$(5.16) \quad p = - \frac{kT}{q} \left\{ \ln \left(1 - \frac{q}{v} \right) + \left(\frac{q}{v} \right)^2 \frac{\zeta}{kT} \right\},$$

which can be derived in the same way as in the case of (2.7).

From (5.7), (5.8), (5.9) and (5.15) we really obtain the relation

$$(5.17) \quad \mu = \mu_t = f_{t1} + p_t^T \left(\frac{q}{x_t} \right).$$

Since $q^{-1}x_t$ is the number density of molecules in the t -th layer, (5.17) is identical in form with the formula which we find in the formulation of the quasi-thermodynamic theory of the surface tension [8].

Furthermore, we obtain, from (5.6), (5.16), (2.4) and (5.15),

$$(5.18) \quad \gamma = \sum_{t=-u}^w (p - p_t^T),$$

which corresponds to the mechanical definition of surface tension.

(*) This calculation was performed under the cooperation of Dr. S. KONDO.

Thus, it is seen that in the hole theory of surface tension relations identical in form with those of the quasi-thermodynamic theory have been found. The chemical potential expressed in the form of (5.9) depends, however, not only on x_i , but on x_{i-1} and x_{i+1} .

6. — The solution of the difference equation (4.15) has been obtained from various values of ζ/kT by ONO [3] and KURATA [10]. Some of the calculated results are shown in Fig. 3, where the (111)-plane of face-centered cubic lattice, for which $1 = \frac{1}{2}$ and $m = \frac{1}{4}$, is chosen as the exposed face. These density versus depth curves show strong resemblance with those obtained by HILL [11], based on the quasi-thermodynamic consideration.

From the values of x_i 's we can calculate the surface tension with the help of (5.6). Let us compare the calculated value with the experimental value for the case of liquid argon at 90 °K.

If we choose $\varepsilon/k = 116$ °K and $\sigma = 3.456$ Å as the constants of the Lennard-Jones potential (3.1), this temperature corresponds to $T^* = 0.776$ and the observed molar volume 28.1 cm³ to $v^* = 1.122$.

On the basis of the relation (2.3) we can calculate ζ from the table of HIRSCHFELDER *et al.* [6], by interpolation, obtaining the value $\zeta/kT = 4.78$ ($\zeta/\varepsilon = 3.71$).

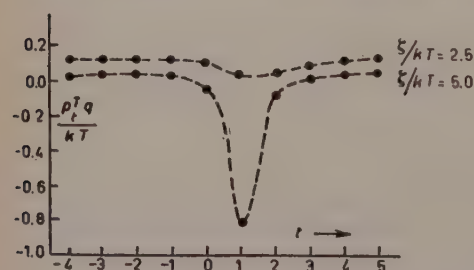


Fig. 4. — The variation of the tangential pressure around the interface layer.

Thus the calculated value of the surface tension of liquid argon at 90 °K is 9.04 dyn cm a little less than the observed value 11.9 dyn cm.

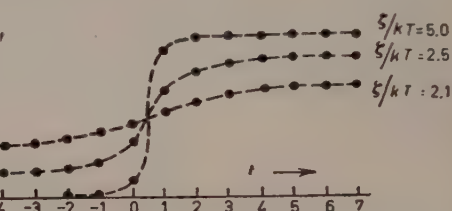


Fig. 3. — Change in the density around the interface layer calculated from the hole theory ($\zeta/kT_c = 2$).

Thus the calculated value of the surface tension of liquid argon at 90 °K is 9.04 dyn cm a little less than the observed value 11.9 dyn cm.

The variation of the tangential pressure within the interface layer has also been calculated from (5.15) and the values of x_i 's. In the case of liquid argon for the value of $\zeta/kT = 5.0$, which corresponds nearly to 85 °K, the minimum value of the

tangential pressure amounts to -280 atm. This enormous value of the negative pressure has been also expected from Kirkwood and Buff's theory of surface tension [12].

REFERENCES

- [1] J. S. ROWLINSON and C. F. CURTISS: *Journ. Chem. Phys.*, **9**, 1519 (1951).
- [2] F. CERNUSCHI and H. EYRING: *Journ. Chem. Phys.*, **7**, 547 (1939).
- [3] S. ONO: *Memoirs of the Faculty of Engineering, Kyushu University*, **10**, 195 (1947).
- [4] H. M. PEEK and T. L. HILL: *Journ. Chem. Phys.*, **18**, 1252 (1950).
- [5] Cfr., for example, R. H. FOWLER and E. A. GUGGENHEIM: *Statistical Thermodynamics* (Cambridge, 1939).
- [6] J. O. HIRSCHFELDER, C. F. CURTISS and R. B. BIRD: *Molecular Theory of Gases and Liquids* (New York, 1954).
- [7] This condition of minimization was already used by J. DE BOER: *Suppl. Nuovo Cimento*, **10**, 225 (1953).
- [8] R. C. TOLMAN: *Journ. Chem. Phys.*, **16**, 758 (1948).
- [9] T. L. HILL: *Journ. Chem. Phys.*, **20**, 141 (1952).
- [10] M. KURATA: *Busseiron-Kenkyu*, No. 39, 77 (1951).
- [11] T. L. HILL: *Journ. Chem. Phys.*, **20**, 141 (1952).
- [12] J. G. KIRKWOOD and F. P. BUFF: *Journ. Chem. Phys.*, **17**, 338 (1949).

Quantum Mechanical Effects on the Surface Tension of Simple Liquids.

I. OPPENHEIM

National Bureau of Standards - Washington, D.C.

Summary. — The differences in the surface tensions of the various isotopic species of a given simple substance are calculated. The surface tension is expressed in terms of the quantum mechanical pair distribution function and an expansion of the distribution function in powers of \hbar^2 is utilized. Calculations are made assuming a Lennard-Jones potential of interaction and the validity of the superposition approximation. An approximate theory of corresponding states is used to relate the surface tensions of the isotopes at different temperatures.

INTERVENTI E DISCUSSIONI

— G. BOATO:

Have you plotted the difference in surface tension of D_2 and H_2 versus your theoretical value?

— I. OPPENHEIM:

The differences in surface tensions of hydrogen and deuterium at the same temperature are due not only to quantum effects but depend more strongly on the density differences of the two liquid isotopes at the same temperature.

— J. DE BOER:

Could you explain how has been obtained, the $g(r)$ function used in the final expressions for the surface tension?

— I. OPPENHEIM:

The radial distribution function used was calculated by KIRKWOOD, LEWINSON and ALDER modified so as to apply to the complete Lennard-Jones potential. The results are not sensitive to the choice of the distribution function.

The Properties of Isotopic Liquids.

A. BELLEMANS

Faculté des Sciences, Université Libre de Bruxelles - Bruxelles

1. - Introduction.

The quantum theorem of corresponding states of DE BOER [1] permits to understand the difference between the thermodynamic properties of light isotopes such as ^4He , ^3He or H_2 , D_2 , T_2 , assuming that the intermolecular potential

$$(1.1) \quad \varepsilon(r) = \varepsilon\varphi(r/\sigma)$$

is a universal function and ε and σ are the same for all isotopic species of a given chemical compound. The quantum effects are measured by the so-called A parameter

$$(1.2) \quad A^2 = \frac{h^2}{M\varepsilon\sigma^2}$$

where M is the molecular mass.

This theory however fails in some cases. For example the vapor pressure of HT is larger than that of D_2 [2] although both molecules have the same A . Also it can be seen from Fig. 1 and 2 that the vapor pressure and the

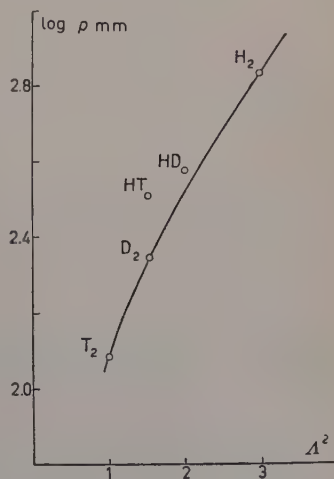


Fig. 1. - Vapor pressures of H_2 , HD , D_2 [12], HT [2] and T_2 [13] in function of A^2 at 20 °K. (The point corresponding to HT should be somewhat lowered because corrections for gas imperfection and non-ideality of the mixture HT-H_2 were neglected by BIGEISEN and KERR).

molar volume of HD are larger than the expected values interpolated from H_2 , D_2 and T_2 .

The case of heavy molecules is even worse because it generally appears that hydrogenocompounds have a lower vapor pressure than deuterocompounds in contradiction with de Boer's theory. The case of methanes is particularly interesting [3]. At low temperatures and at high temperatures one has respectively

$$p_{CH_4}/p_{CD_4} > 1 \quad \text{and} \quad p_{CH_4}/p_{CD_4} < 1.$$

It is also interesting to note that $^{13}CH_4$ and CH_3D though having the same molecular mass show markedly different properties [3, 4].

This last example and also the case $HT - D_2$ show that we must take into account the distribution of the total mass of the molecule among the constituting atoms. (De Boer's theory only cares for the total mass). The need of such a refinement has already been pointed out by BIGEISEN and KERR [2, 5]. We

think that two effects have to be introduced:

- 1) intermolecular forces slightly varying with isotopic substitution,
- 2) quantum rotational corrections.

The importance of these effects will be discussed in the next two sections.

2. - Differences in intermolecular forces.

Experiments have shown that the polarizabilities of hydrogenocompounds are somewhat larger than those of deuterocompounds. This is due to the zero-point energy of internal vibrations which depends on the reduced masses of the different bonds in the molecules. This effect has been studied theoretically by ISHIGURO *et al.* [6] in the case of hydrogen and by TODA and FRIEDMAN [7] in more general cases.

On account of this difference of polarizabilities (which is of the order of 1%) the intermolecular fields of hydrogeno- and deuterocompounds should be somewhat different. It seems however difficult to develop a quantitative theory of this effect. Measurements of second virial coefficients of CH_4 , CD_4 , $^{13}CH_4$ have been undertaken by Dr. THOMAS and Mr. VAN STEENWINKEL (at Brussels) which should afford some information on this problem.

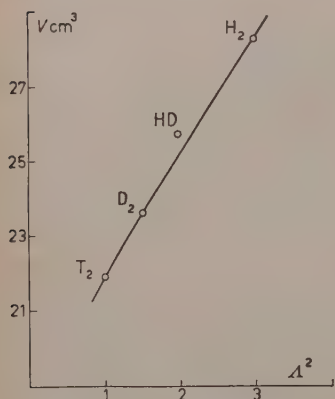


Fig. 2. - Molar volumes of H_2 , HD, D_2 [12] and T_2 [14] in function of A^2 at 20 °K.

We have tested our assumption of differences in intermolecular forces in the case of cyclohexanes C_6H_{12} and C_6D_{12} . Assuming that

- a) no quantum effects are present,
- b) C_6H_{12} and C_6D_{12} obey the same equation of state with somewhat different parameters ϵ_H , σ_H and ϵ_D , σ_D ,

we have determined the ratios

$$\epsilon_H/\epsilon_D \quad \text{and} \quad \sigma_H/\sigma_D$$

from two independent properties:

- i) the vapor pressures (in function of the temperature) [8],
- ii) the molar volumes (in function of the temperature) [9].

We find respectively

$$\text{i) } \epsilon_H/\epsilon_D = 1.006, \quad \sigma_H/\sigma_D = 1.005;$$

$$\text{ii) } \epsilon_H/\epsilon_D = 1.013, \quad \sigma_H/\sigma_D = 1.003.$$

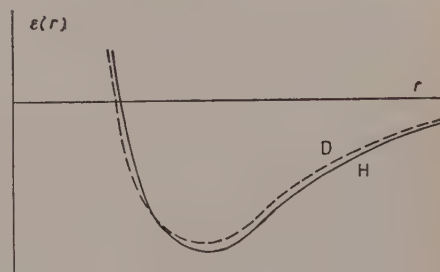


Fig. 3. — Schematic intermolecular potentials between hydrogeno- and deuterio-compounds (as expected from the discussion of cyclohexanes C_6H_{12} and C_6D_{12}).

The two sets of results are consistent with each other. They also suggest that the intermolecular potentials of hydrogenocompounds and deuterocompounds have the relative shapes shown on Fig. 3.

3. — Rotational effects.

The quantum rotational effects are of two types:

- a) an effect related to the angular dependency of the intermolecular potential; this effect depends on h^2/I , where I is the moment of inertia [10];
- b) a coupling effect between translation and rotation which is present for asymmetrical molecules such as HT, HD, CH_3D . In these molecules the center of mass does not coincide with the « center of interactions » which for HT and HD is the mid-point of the segment joining the atoms and which for CH_3D is the carbon nucleus.

A discussion of effects a) and b) will now be carried out by using elementary two-dimensional models which roughly reproduce the behavior of a molecule in a liquid or a solid.

Effect a): A diatomic molecule with moment of inertia I is rotating on a lattice point in a sinusoidal potential [10]. The classical Hamiltonian is

$$(3.1) \quad H = \frac{p_\varphi^2}{2I} - V_0 \cos q\varphi$$

and the quantum operator is

$$(3.2) \quad \mathcal{H} = -\frac{\hbar^2}{2I} \frac{\partial^2}{\partial \varphi^2} - V_0 \cos q\varphi,$$

(q is an integer). The classical partition function is

$$(3.3) \quad Z_{\text{cl}} = \frac{1}{h} \left(\frac{2\pi I}{\beta} \right)^{\frac{1}{2}} J_0(-i\beta V_0),$$

where J_0 is Bessel's function of zero order. The high temperature expansion of the quantum partition function is

$$(3.4) \quad Z_{\text{qu}} = Z_{\text{cl}} \cdot \left\{ 1 - \frac{\hbar^2 \beta^2 q^2}{24I} \frac{\partial}{\partial \beta} \ln J_0(-i\beta V_0) \right\}.$$

Expanding $J_0(-i\beta V_0)$ one has approximately for the free energy

$$(3.5) \quad F_{\text{qu}} - F_{\text{cl}} \simeq \frac{\hbar^2 \beta^2}{48I} q^2 V_0^2.$$

The quantum correction is inversely proportional to I . If one considers two isotopic molecules A and B with $I_A < I_B$, their molecular masses being identical, then

i) the vapor pressure of A is higher than that of B,

ii) if V_0 is interpreted as a mean field decreasing with increasing distances between molecules, the molar volume of A will be larger than that of B, at the same pressure and temperature.

Effect b): A rigid diatomic molecule with atoms of masses M_1 and M_2 at a distance d apart is linked to a fixed point (origin of the co-ordinates) by a harmonic central force. This force is applied to the mid-point of the segment joining the atoms. Let us call (x_1, y_1) and (x_2, y_2) the cartesian co-ordinates of the atoms. The potential energy of the molecule is

$$(3.6) \quad V = \frac{1}{2} K \left\{ \left(\frac{x_1 + x_2}{2} \right)^2 + \left(\frac{y_1 + y_2}{2} \right)^2 \right\},$$

where K is the restoring constant (which stands for the average potential exerted by neighbouring molecules and will determine the equation of state). Introducing the co-ordinates (x, y) of the center of mass of the molecule and the angle φ which gives its orientation in the plane we get for V

$$(3.7) \quad V = \frac{1}{2}K(x^2 + y^2) - K\alpha(x \cos \varphi + y \sin \varphi) + \frac{1}{2}K\alpha^2,$$

where

$$\alpha = \frac{d}{2} \frac{M_1 - M_2}{M_1 + M_2}.$$

The classical partition function is

$$(3.8) \quad Z_{\text{cl}} = \frac{1}{h^3} \left(\frac{2\pi I}{\beta} \right)^{\frac{1}{2}} \frac{M_1 + M_2}{\beta^2} \frac{1}{K},$$

where

$$I = \frac{M_1 M_2}{M_1 + M_2} d^2.$$

As K appears in factor the classical equation of state is independent of the masses M_1 and M_2 .

The quantum Hamiltonian operator is

$$(3.9) \quad \mathcal{H} = - \frac{\hbar^2}{2(M_1 + M_2)} \left\{ \frac{\partial^2}{\partial x^2} + \frac{\partial^2}{\partial y^2} \right\} - \frac{\hbar^2}{2I} \frac{\partial^2}{\partial \varphi^2} + V.$$

Considering terms in α of (3.7) as perturbation terms one finds the following results:

i) The lowest energy level is

$$(3.10) \quad \varepsilon_0 = \hbar\omega_0 \left\{ 1 + \frac{1}{16} \frac{(M_1 - M_2)^2}{M_1 M_2} \frac{\hbar\omega_0}{\hbar\omega_0 + (\hbar^2/2I)} \right\},$$

where $\omega_0^2(M_1 + M_2) = K$; it is clear that for asymmetrical molecules there is a supplementary term increasing the zero-point energy and involving K (through ω_0), thus acting on the equation of state.

ii) In the region of high temperatures

$$(3.11) \quad \beta(F_{\text{qu}} - F_{\text{cl}}) = \frac{1}{12} (\beta\hbar\omega_0)^2 + \frac{1}{96} (\beta\hbar\omega_0)^2 \frac{(M_1 - M_2)^2}{M_1 M_2}.$$

This last expression is especially interesting. The first term of the right-hand side is the usual quantum correction of an oscillator; it corresponds to the A effect of de Boer. The second term of the r.h.s. is only present for asymmetrical molecules. If we now consider two molecules A and B having the same molecular mass but one being asymmetrical and the other symmetrical it is clear from (3.10) and (3.11) that A will have a higher vapor pressure and a larger molar volume than B .

Hence both effects $a)$ and $b)$ act in the same direction. It is interesting to return now to the case of HT-D_2 considered in the first section. Both effects $a)$ and $b)$ will contribute to differentiate the properties of HT and D_2 . However we expect that $a)$ will be small because in the liquid state angular effects nearly cancel (in the absence of dipoles) on account of the symmetry of the neighborhood of a given molecule. Miss A. BABLOYANTZ has performed calculations on HT-D_2 molecules taking into account effect $b)$ alone. She has calculated a ratio for the vapor pressures in reasonable agreement with the experimental data [2]. The case of HD (cfr. Sect. 1) can also be interpreted in this manner [11].

* * *

The present note should be considered as a preliminary one. We hope to develop these ideas on a more quantitative basis and complete them by experimental investigations. We are greatly indebted to Professor PRIGOGINE, Miss A. BABLOYANTZ, Dr. TODA and Mr. H. FRIEDMAN for helpful discussions. This research has been made possible the support and sponsorship of the General Electric Co.

REFERENCES

- [1] J. DE BOER: *Physica*, **14**, 139 (1948).
- [2] J. BIGELEISEN and E. C. KERR: *Journ. Chem. Phys.*, **23**, 2442 (1955).
- [3] G. T. ARMSTRONG, F. G. BRICKWEDDE and R. B. SCOTT: *Journ. Res. NBS.*, **55**, 39 (1955).
- [4] T. F. JOHNS: *International Symposium on Isotope Separation* (Amsterdam, 1957).
- [5] J. BIGELEISEN: *Journ. Chem. Phys.*, **23**, 2264 (1955).
- [6] E. ISHIGURO, T. ARAI, M. MIZUSHIMA and M. KOTANI: *Proc. Phys. Soc.*, A **65**, 178 (1952).
- [7] M. TODA and H. W. FRIEDMAN: to appear *Journ. Chem. Phys.* (1957).
- [8] J. A. DIXON and R. W. SCHIESSLER: *Journ. Amer. Chem. Soc.*, **76**, 2197 (1954).
- [9] R. T. DAVIS and R. W. SCHIESSLER: *Journ. Phys. Chem.*, **57**, 966 (1953).
- [10] W. H. STOCKMAYER: *Journ. Chem. Phys.*, **27**, 321 (1957).

- [11] A. BABLOYANTZ: to appear in the *Journ. of Molecular Physics* (1958).
[12] H. W. WOOLEY, R. B. SCOTT and F. G. BRICKWEDDE: *Journ. Res. NBS*, **41**, 379 (1948).
[13] E. R. GRILLY: *Journ. Amer. Chem. Soc.*, **73**, 843 (1951).
[14] E. R. GRILLY: *Journ. Amer. Chem. Soc.*, **73**, 5307 (1951).

INTERVENTI E DISCUSSIONI

— G. BOATO:

1) Do you think you have to take into account also vibrational effects? From experimental data it seems that some isotopic molecules can have different vibrational frequencies in the liquid and gaseous state.

2) For the methanes, with ^{12}C and ^{13}C , one would expect a very small effect of the kind you have talked about. The vapour pressure difference must be principally determined by the Debye frequency spectrum as in rare gases (in the solid phase).

— A. BELLEMANS:

1) The incidence of internal vibrations has been discussed by BAERTSCHI and KUHN (*International Symposium on Isotopic Separation*, Amsterdam, 1957), on the basis of a simple model where molecules are assimilated to ensembles of oscillators, some having ultra-violet frequencies and some having infra-red frequencies. If the infra-red frequencies are active ones (i.e. a dipole moment is associated to them) then there will be a difference in the intermolecular forces of isotopic compounds. There is no such effect for hydrogen, and it seems to be small for a C—H or C—D bond. There will, however, be a relatively large effect for a C—Cl bond.

2) The difference of polarizability between $^{12}\text{CH}_4$ and $^{13}\text{CH}_4$ is related essentially to the difference of the reduced mass of $^{12}\text{C—H}$ and $^{13}\text{C—H}$ bonds. It is thus expected that the difference in polarizability will be much smaller for $^{12}\text{CH}_4$ — $^{13}\text{CH}_4$ than for $^{12}\text{CH}_4$ — $^{12}\text{CH}_3\text{D}$. Indeed the experimental data on $^{13}\text{CH}_4$ seem to indicate that there is no difference in intermolecular forces between $^{12}\text{CH}_4$ and $^{13}\text{CH}_4$ and that de Boer's theory is obeyed both in the liquid and in the solid state for this pair of isotopic molecules.

— J. DE BOER:

It does not seem to be quite meaningful to compare the properties of C_6H_{12} and C_6D_{12} by using the quantum mechanical principle of corresponding states and the corresponding quantum mechanical parameter $\lambda = h/\sigma\sqrt{m\epsilon}$. The latter is *only* intended to be helpful in describing quantum effects related to the *translational* degrees of freedom of spherical or quasi spherical molecules, but not for investigating the quantum effects occurring in internal (rotational, or vibrational) degrees of freedom.

— A. BELLEMANS:

On account of internal vibrations which are dependent on isotopic substitution, the polarizabilities of different isotopic molecules will be different, and this leads to somewhat different intermolecular forces. From the point of view of statistical me-

chanics this is a « classical effect » which does not disappear at high temperature. For two isotopic molecules such as $\text{CH}_4 - \text{CD}_4$ or $\text{C}_6\text{H}_{12} - \text{C}_6\text{D}_{12}$ differences in ϵ 's and σ 's would be of the order of one percent or less.

— E. A. GUGGENHEIM:

Comparison of the vapour pressures at the same temperature of two isotopic molecules seems an unfortunate basis for studying departures from the principle of corresponding states. The vapour pressure of each isotope depends in a known way on the molecular mass, the moments of inertia, the frequencies of the normal vibrational modes and above all on the energy of vaporization. To obtain convincing evidence that isotopic molecules, such as CH_4 and CD_4 , have significantly different mutual interaction energies it would be better to compare their energies of vaporization at the absolute zero corrected for nullpunktsenergie estimated from the Debye characteristic temperatures.

— H. C. LONGUET-HIGGINS:

Probably the best way of evaluating the ϵ and σ value for isotopic species such as CH_4 and CD_4 would be to compare their critical temperatures and volumes. Has Dr. BELLEMANS done this for any of the heavy molecules he studied, and has he compared the ϵ values with the polarizabilities?

— A. BELLEMANS:

To get a better insight on the incidence of isotopic substitution on intermolecular forces, it would be desirable to study in detail many of the thermodynamic properties of two well chosen isotopic compounds such as $\text{CH}_4 - \text{CD}_4$. However the data presently known are very fragmentary.

— B. WEINSTOCK:

In unpublished work about 10 years ago, I discovered that the coefficient of thermal diffusion of a mixture of $\text{H}_2 - \text{HT}$ was quite different from that of a $\text{T}_2 - \text{D}_2$ mixture. This appears to agree with your theory.

Integral Equation Method in the Theory of Liquids.

L. SAROLEA

Institut für Theoretische Physik - Heidelberg

Many equations are known, which give the pair distribution function in terms of integrals over the distribution functions for triples.

The whole problem is then to find a closure, and this is usually done by the superposition principle which assumes that the distribution function for triples is simply the product of the three pair distribution functions

$$F_3(123) = F_2(12) \cdot F_2(13) \cdot F_2(23).$$

Such an approximation is, however, quite arbitrary; besides, it has not always proved satisfactory.

Professor MAYER, of the University of Chicago, and myself, tried to find another approximation which would be logically suggested by the structure of the integral equations.

We first of all built up our own integral equations, roughly in the following way: we expressed the distribution functions in terms of the grand partition function and operated on both sides of the equation so obtained with a derivation operator $d/d\lambda$ (λ being an arbitrary variable). We got an equation which looks like this

$$(1) \quad \psi_m = \sum_n I_{mn} \psi_n^0,$$

where $\psi_m = dw_m/d\lambda$, w_m being the potential of averages forces for the group of m particles; ψ_n^0 is the corresponding quantity at infinite dilution; I_{mn} is a matrix depending on the density and on the distribution functions F_k ($k \leq m+n$).

Now, if one operates in the same way over the distribution functions at infinite dilution, one obtains another set of equations:

$$(2) \quad \psi_m^0 = \sum_n L_{mn}^0 \psi_n^0.$$

where L_{mn}^0 is the same matrix as L_{mn} except that it depends on the activity and on the distribution functions F_k^0 at infinite dilution.

Our λ is completely arbitrary. We can therefore select our ψ_n^0 as we please, but then of course our ψ_n are automatically uniquely determined.

Equations (1) and (2) are extremely general. Indeed, one can show that they contain the Kirkwood and Yvon-Born-Green integral equations as special cases, that is, for a special meaning attributed to λ . In order to obtain the Kirkwood and Yvon-Born-Green integral equations, equation (1) alone is necessary; equation (2) does not need to be considered. We therefore hoped that, from its consideration, something new might arise.

If we replace ψ_n^0 in equation (1) by its value given in equation (2), we obtain

$$\sum_k L_{mk} L_{kn}^0 = \delta_{mn}.$$

We can write down this equation explicitly because the matrices L_{mk} and L_{kn}^0 are, at least formally, known in terms of the distribution functions. If we do so, we obtain the following equation

$$(3) \quad \frac{\varrho}{z} \frac{F_2(\alpha\beta)}{F_2^0(\alpha\beta)} = \sum_k \frac{\varrho^k}{k!} \int \dots \int F_{1+k}(\alpha, k) \prod_1^k f_{i\beta} dk,$$

where ϱ is the density, z the activity, $f_{i\beta} = F_2^0(i\beta) - 1$.

This equation is rigorously correct. Furthermore, it converges: because for $k \approx 12$, either $F_{1+k}(\alpha, k) = 0$ if all the k molecules are close together, either $\prod_1^k f_{i\beta}$ drops out, if any of the k molecules is at a large distance from the others.

Unfortunately an equation with 12 terms is still far too difficult to be handled rigorously.

It seems attractive to try, as a first approximation, to retain the first term only (indeed, one can develop a plausibility argument which shows that this term should be the leading one). If we retain this term alone, we get

$$L_{11}(\alpha\gamma) \cdot L_{11}^0(\gamma\beta) = \delta_{\alpha\beta}.$$

If again we write this equation down explicitly, replacing the L_{11} , L_{11}^0 by their known values in terms of the distribution functions, and if we make a Fourier transformation, we obtain the following very simple equation

$$(4) \quad \varrho\gamma(t) = \frac{z\varphi(t)}{1 - z\varphi(t)},$$

where $\gamma(t)$ is the transform of $F_2(r) - 1$;
 $\varphi(t)$ is the transform of $F_2^0(r) - 1$.

Fourier inversion theorem then gives the pair distribution function. One can follow the behaviour of equation (4) with increasing activity. It turns out to have two second order poles, for two different activities. One would like to associate these activities with the activities corresponding to the phase changes, condensation and cristallization. Unfortunately they are far too high. We checked it for argon at 84 °K (which is argon triple point). The activity predicted by our equation for the condensation is about twenty times too high.

Equation (4) is thus too rough to describe properly the facts. Still, there are some positive points about it: it gives the correct answer for compressed gases, it shows two phase changes, although at the wrong place, it is simple enough to lead readily to numerical results, and one sees clearly which terms were neglected, so that one can use it as a convenient starting point towards better approximations.

Indeed there are still a lot of things one can do, starting from the correct equation (3). One can evaluate rigorously some parts of the sum, for instance the contribution of the configurations where only one molecule is directly connected to the α particle, the other particles being either independent, either bound in any cluster which does not include the α -particle.

One obtains in this way equations for the distribution function which are presumably better. However, none of these equations, except the simple one which was discussed above, gives the solution in an analytical form, so that it is by no means easy to tell how far they are good.

Saturation diélectrique et forces intermoléculaires dans les liquides.

A. PIEKARA

Institut de Physique, Académie Polonaise des Sciences. - Poznań.

L'effet de la saturation diélectrique, calculé par DEBYE pour les gaz [1] et pour les liquides [2], présente dans l'expérience une diminution de la constante diélectrique sous l'action d'un champ électrique extérieur. Cet effet, dit normal ou négatif, a été trouvé dans l'éther éthylique par HERWEG [3] et puis confirmé par KAUTZSCH [4]. En 1936 l'auteur en collaboration avec M. B. PIEKARA [5] a trouvé, que dans le nitrobenzène pur, soumis à l'action d'un champ électrique intense, la constante diélectrique augmente, c'est-à-dire que l'effet de la saturation est positif ou inverse. Ces résultats ont été corroborés en 1939 en commun avec M. A. ŁEMPICKI et après la guerre développés par M. A. CHEŁKOWSKI et l'auteur [6].

Dans cette étude nous avons mesuré le changement de la capacité d'un condensateur, rempli avec le liquid examiné, sous l'action d'un champ électrique appliqué sur les plaques. La méthode utilisée était celle de battements. Ils sont produits par deux générateurs de fréquences voisines, 1 MHz environ. Les battements ayant une fréquence sonore produisent avec un oscillateur basse fréquence des figures de Lissajous, sur l'écran d'une lampe oscillographique.

Nous avons utilisé deux type des condensateurs à liquide: l'un, à plaques cylindriques, et l'autre, plan, très robuste, dont la plaque interne était enfermée à l'intérieure d'un cylindre creux. Les résultats des mesures, à l'époque où elles étaient effectuées (A. PIEKARA et B. PIEKARA, 1936), nous ont frappé d'étonnement. Nous avons observé avec le nitrobenzène pur, très soigneusement purifié, l'effet inverse de la saturation diélectrique, c'est-à-dire l'augmentation de la constante diélectrique sous l'influence d'un champ électrique extérieur. Cet effet croît avec le carré de l'intensité du champ appliqué. Cependant, pour les solutions du nitrobenzène dans les solvants non polaires, d'une concentration plus petite qu'une concentration d'inversion (80 pour

cent en cas du benzène comme dissolvant, voir la Fig. 1), l'effet de la saturation est normale, c'est-à-dire négatif.

Dernièrement M. A. CHEŁKOWSKI [7] a trouvé l'effet « positif avec inversion » dans deux liquides polaires, notamment dans l'ortho-nitrotoluène et le m-nitrotoluène; la Fig. 2 montre la variation de cet effet avec la concentration, l'intensité du champ électrique appliqué étant de 49 kV/cm. Au contraire, dans l'ortho-nitroanisole, il a trouvé un effet purement négatif (voir la Fig. 1).

Un différent type de l'effet de la saturation diélectrique dans liquides polaires a été trouvé dans le 1,2-dichloroéthane et le 1,2-dibromoéthane [6]. C'est un effet, que l'on peut nommer « l'effet positif sans inversion », puisque pour le liquide pur, ainsi que pour les solutions dans un solvant non polaire (CCl_4) de concentration quelconque, l'effet $\Delta\epsilon$ reste constamment positif, ce que montre la Fig. 3.

L'existence de la saturation diélectrique positive, dans un liquide polaire, avec inversion dans les solutions, a été expliquée théoriquement par nous en 1937 [8]. Nous avons supposé que, dans un tel liquide polaire, comme le nitrobenzène par exemple, l'interaction moléculaire est plus considérable de la part de la molécule la plus proche d'une molécule envisagée. Les forces intermoléculaires tendent à coupler les molécules les plus voisines, de façon que la position du minimum d'énergie potentielle est celle des moments dipolaires antiparallèles. Dans le

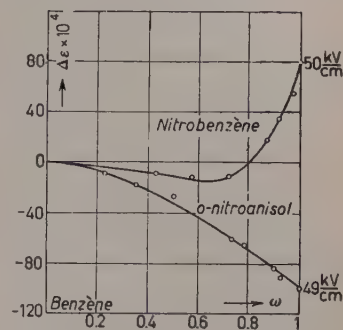


Fig. 1. — L'effet de la saturation diélectrique positive avec inversion dans le nitrobenzène et celui de la saturation négative dans l'o-nitroanisole (A. PIEKARA et A. CHEŁKOWSKI [6]; A. CHEŁKOWSKI [7]).

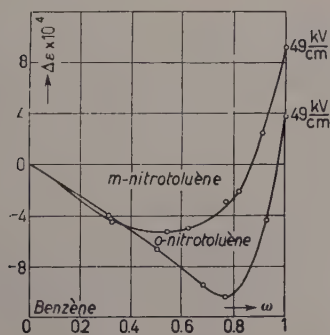


Fig. 2. — L'effet de la saturation diélectrique positive avec inversion dans l'ortho- et metanitrotoluène (A. CHEŁKOWSKI [7]).

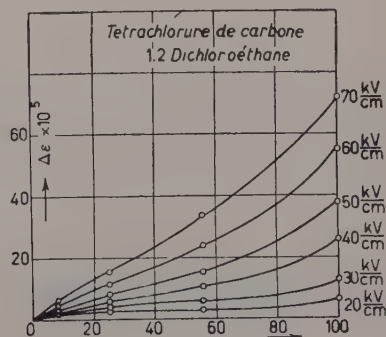


Fig. 3. — L'effet de la saturation diélectrique positive sans inversion dans le 1,2-dichloroéthane (A. CHEŁKOWSKI [7]).

champ électrique extérieur la valeur moyenne statistique du moment effectif d'un tel couple moléculaire augmente, ce qui entraîne une augmentation de la constante diélectrique. Si cet effet prévaut sur l'effet négatif de la saturation proprement dite, un effet positif apparaît. Cette hypothèse a été appliquée dans la théorie des autres phénomènes d'orientation moléculaire dans les liquides polaires, notamment dans la théorie de la polarisation diélectrique, de la biréfringence électrique et de la biréfringence magnétique [9]. Elle trouve un fort appui dans l'accord quantitatif avec les résultats expérimentaux pour les phénomènes d'orientation moléculaire mentionnés ci-dessus [10, 11], ainsi qu'avec les résultats des expériences cryoscopiques [12].

Récemment nous avons repris ce problème, M. S. KIELICH et moi [13], en généralisant cette théorie pour des interactions moléculaires quelconques et pour tous les phénomènes d'orientation moléculaire. On obtient ainsi, sous la condition que les molécules puissent être considérées comme ayant symétrie axiale, pour la valeur moyenne statistique de la composante du moment électrique d'une molécule suivant la direction du champ extérieur, une expression de la forme

$$(1) \quad \langle m_F \rangle = \left(a^e + \frac{\mu^2}{3kT} R_p \right) F + (\Delta_1^{ee} + 4\Delta_2^{ee} R_p + \theta_1^{ee} R_{CM} + 2\theta_2^{ee} R_K - \theta_3^{ee} R_S) F^3,$$

θ_1^{ee} , θ_2^{ee} et θ_3^{ee} représentent les termes bien connus de la théorie de Debye [1]; Δ_1^{ee} et Δ_2^{ee} sont les termes dûs à la déformation de la molécule dans un champ électrique; R_p , R_{CM} et R_K sont les facteurs de réduction qui paraissent dans la théorie de la polarisation diélectrique, de l'effet Cotton-Mouton et de l'effet Kerr ([13], voir aussi [14, 15]). Enfin, R_S représente le facteur de réduction de la saturation diélectrique, qui, d'une façon générale, s'exprime par l'expression:

$$(2) \quad R_S = \frac{1}{2} \left\{ 5 \left\langle \sum_{q=1}^N \cos \theta_{pq} \right\rangle \left\langle \sum_{r=1}^N \sum_{s=1}^N \cos \theta_{rs} \right\rangle - 3 \left\langle \sum_{q=1}^N \sum_{r=1}^N \sum_{s=1}^N \cos \theta_{pq} \cos \theta_{rs} \right\rangle \right\},$$

où θ_{pq} , etc., est l'angle entre les axes de deux molécules quelconques d'un volume V enfermant N molécules. Dans les cas très spécialisé d'un couplage deux-à-deux, où les moments dipolaires ont le minimum d'énergie potentielle dans la position antiparallèle, on obtient

$$(3) \quad R_S = 6 \frac{L}{y} - (1 - L)(1 + 5L),$$

où $L = L(y)$ représente la fonction de Langevin, $y = W/kT$ étant l'énergie d'interaction exprimée en unités sans dimensions. La Fig. 4 montre la variation de R_S avec y ; on voit que pour $y = 1.33$ R_S change de signe. Puisque l'énergie d'interaction de deux dipôles décroît comme r^{-3} (r , la distance entre les molécules voisines), nous voyons que y croît avec la concentration. De cette façon l'inversion de la saturation diélectrique dans les solutions du nitroben-

zène et des autres liquides trouve sa justification. Dans le cas du nitrobenzène, il-y-a encore, outre le couplage deux-à-deux, l'interaction avec un grand nombre des molécules entourantes. Cette interaction (du type Fowler-Debye) produit un certain relâchement des couples moléculaires, ce qui provoque un déplacement du point d'inversion de la saturation diélectrique vers des valeurs d' y plus grandes ($y \cong 3$, voir [11], II partie, Fig. 16).

Si le couplage deux-à-deux, comme dans le nitrobenzène, est quasiantiparallèle (c'est-à-dire, la valeur minimum de l'énergie potentielle correspond à une configuration antiparallèle des dipôles), on a $y = (\mu^2 / r_p') \cdot (1 / kT)$, r_p étant la distance moyenne des deux dipôles d'une paire moléculaire. En prenant au lieu de r_p une valeur trop grand, de r — la distance entre les molécules considérées comme ensemble de sphères tangentes — on obtient les valeurs de y , présentées par le tableau ci-dessous:

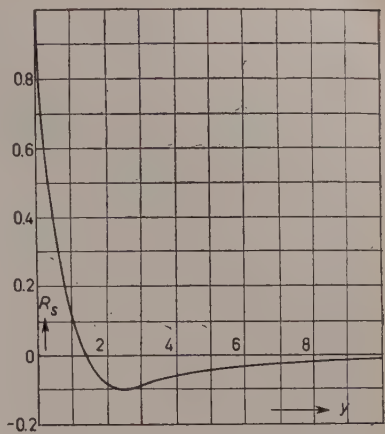


Fig. 4. — Facteur de réduction de la saturation diélectrique d'après la formule (3).

Liquide	Densité <i>d</i> (20 °C)	Poids mol. <i>M</i>	Nombre des molé- cules dans 1 cm ³ $n = \frac{N_A d}{M}$	$r^3 = \frac{1.41^{(*)}}{n}$	$\mu \cdot 10^{18}$	$y = \frac{\mu^2}{r^3 k T}$	$\frac{\Delta \epsilon \cdot 10^4}{\text{dans un champ de 60 kV/cm}}$
nitrobenzène <chem>c1ccccc1[N+](=O)[O-]</chem>	1.203 2	123.11	$5.89 \cdot 10^{21}$	$2.39 \cdot 10^{-22}$	4.23	1.85	+ 130
m-nitrotoluène <chem>Cc1cccc([N+](=O)[O-])c1</chem>	1.157 1	137.13	$5.08 \cdot 10^{21}$	$2.78 \cdot 10^{-22}$	4.17	1.55	+ 15
o-nitrotoluène <chem>Cc1ccccc1[N+](=O)[O-]</chem>	1.162 6	137.13	$5.11 \cdot 10^{21}$	$2.76 \cdot 10^{-22}$	3.66	1.20	+ 5
o-nitroanisol <chem>COc1ccccc1[N+](=O)[O-]</chem>	1.254 0	153.13	$4.93 \cdot 10^{21}$	$2.87 \cdot 10^{-22}$	4.82	2.01	— 160

(*) Voir [11], II partie, § 7.

Il est vrai que, pour les trois premières liquides, les valeurs calculées de γ décroissent successivement dans le même ordre que l'effet de la saturation positive $\Delta\epsilon$. Mais, ces valeurs sont trop petites et, avec une juste valeur de r_p , elles doivent être plus grandes que 3. Cela montre que la distance moyenne des molécules d'un liquide est beaucoup plus grande que la distance moyenne des deux dipôles d'un couple moléculaire ([11] et [1]). En ce qui concerne les molécules de *o*-nitroanisole, il paraît que la rotation des groupes $-\text{O}-\text{CH}_3$ rende le rapprochement des deux molécules, et par conséquent la formation de couples moléculaires, impossible; c'est pourquoi l'effet de la saturation diélectrique est fortement négatif.

Quant à l'effet positif sans inversion, il apparaît dans les molécules des 1,2-dichloroéthane et 1,2-dibromoéthane,



dans lesquelles il y a une rotation mutuelle des deux groupes ayant chacun un moment électrique. La théorie de couplage deux-à-deux s'applique ici, mais l'énergie d'interaction γ ne dépend plus de la concentration. Voici

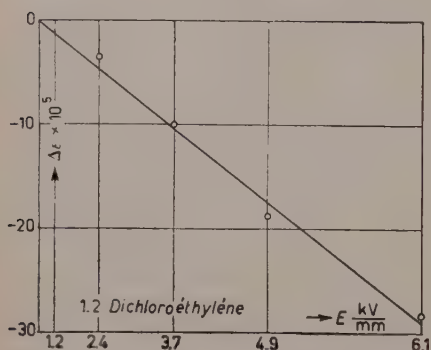
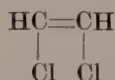


Fig. 5. — L'effet de la saturation diélectrique négative dans le 1,2-dichloroéthylène (A. CHEŁKOWSKI [7]).

pourquoi l'effet est positif sans inversion. Pour confirmer cette hypothèse nous avons examiné le 1,2-dichloroéthylène,



dans lequel une double liaison $\text{C}=\text{C}$ fait la rotation impossible. L'expérience montre, qu'en effet, $\Delta\epsilon$ pour 1,2-dichloroéthylène pur est négatif, c'est qui est représenté sur la Fig. 5.

Une autre confirmation de notre hypothèse se trouve dans les résultats des mesures cryoscopiques. Les écarts de la loi de Raoult,

$$j = \frac{\Delta T_d}{T_{id}} \cdot T$$

d'après les mesures de BURY et JENKINS [16], son représentés graphiquement sur les Fig. 6-8. Nous voyons, que la valeur de $(\partial j / \partial m)_{m=0}$, constituant une certaine mesure de l'énergie d'interaction entre les molécules dissoutes pour

une concentration infiniment petite, est assez grande pour le nitrobenzène (Fig. 6) — ce qui est en accord quantitatif avec la théorie (voir [12]) — tandis

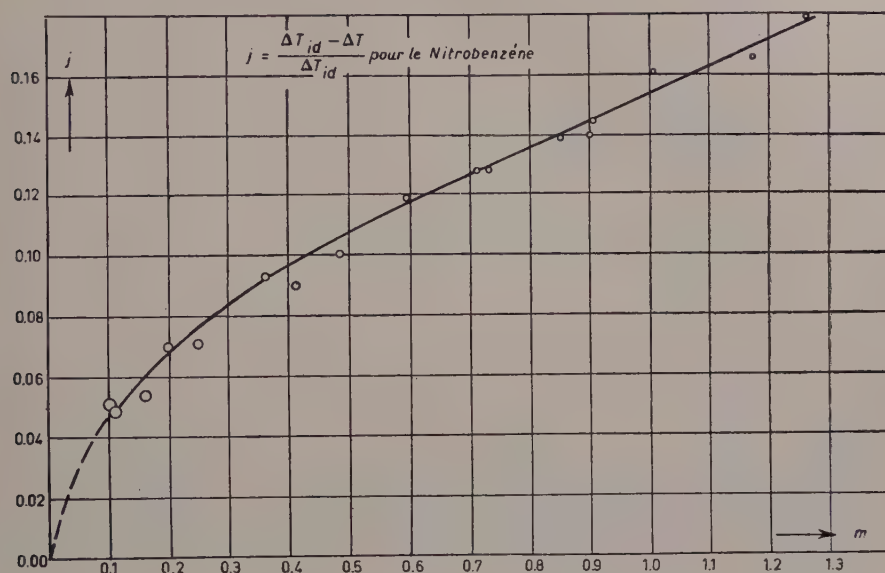


Fig. 6. — Les écarts de la loi de Raoult pour les solutions du nitrobenzène dans le benzène, d'après les mesures de BURY et JENKINS [16]; $\Delta \epsilon$ positif avec inversion (Fig. 1).

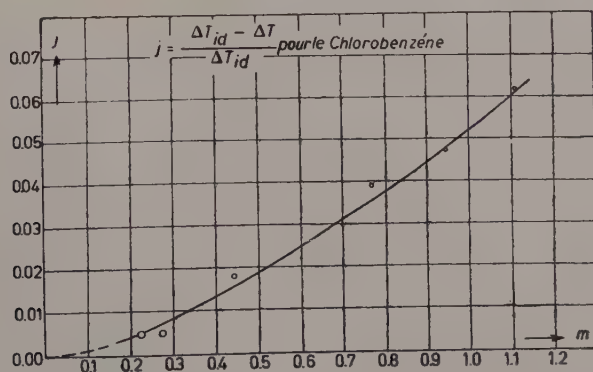


Fig. 7. — Les écarts de la loi de Raoult pour les solutions du chlorobenzène dans le benzène [16]; $\Delta \epsilon$ négatif [4].

qu'elle est nulle pour le chlorobenzène, dans lequel l'effet de la saturation est négatif (Fig. 7). De même $(\partial j / \partial m)_{m=0}$ est nul pour 1,2-dichloroéthane (Fig. 8),

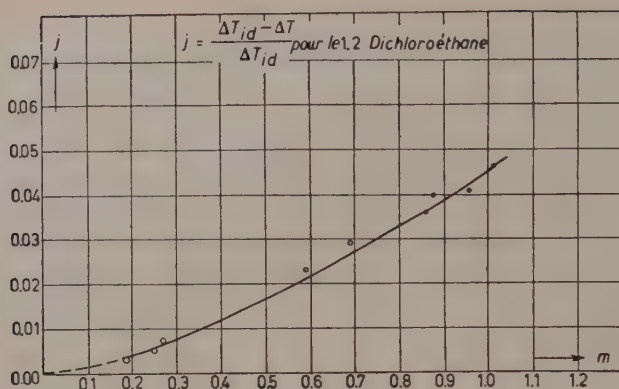


Fig. 8. — Les écarts de la loi de Raoult pour le 1,2-dichloroéthane dans le benzène [16]; $\Delta\epsilon$ positif sans inversion (Fig. 3).

dans lequel l'effet de la saturation est positif sans inversion, ce qui montre que dans ce liquide l'effet positif ($\Delta\epsilon > 0$) n'est pas dû à l'action intermoléculaire, mais plutôt à une action intramoléculaire.

RÉFÉRENCES

- [1] P. DEBYE: in *Handb. d. Radiologie*, 7 publié par E. MARX, **6**, 633 (1925).
- [2] P. DEBYE: *Phys. Zeits.*, **36**, 193 (1935).
- [3] J. HERWEG: *Zeits. f. Phys.*, **3**, 36 (1920); J. HERWEG et W. PÖTZSCH: *Zeits. f. Phys.*, **8**, 1 (1921).
- [4] F. KAUTZSCH: *Phys. Zeits.*, **29**, 105 (1928).
- [5] A. PIEKARA et B. PIEKARA: *Compt. Rend. Acad. Sci.*, **203**, 852, 1058 (1936).
- [6] A. PIEKARA et A. CHEŁKOWSKI: *Journ. Chem. Phys.*, **25**, 794 (1956); voir aussi: A. PIEKARA, A. CHEŁKOWSKI et S. KIELICH: *Zeits. Phys. Chem.*, **206**, 375 (1957).
- [7] A. CHEŁKOWSKI: *Acta Phys. Pol.*, en préparation; *Journ. Chem. Phys.*, **28**, 1249 (1958).
- [8] A. PIEKARA: *Compt. Rend. Acad. Sci.*, **204**, 1106 (1937).
- [9] A. PIEKARA: *Proc. Roy. Soc., A* **172**, 360 (1939); *Compt. Rend. Acad. Sci.*, **208**, 990, 1150 (1939).
- [10] A. PIEKARA: *Nature*, **159**, 337 (1947).
- [11] A. PIEKARA: *Acta Phys. Pol.*, **10**, 37, 107 (1950).
- [12] A. PIEKARA: *Acta Phys. Pol.*, **11**, 99 (1951).
- [13] A. PIEKARA et S. KIELICH: *Journ. Phys. et Rad.*, **18**, 490 (1957).
- [14] A. PIEKARA et S. KIELICH: *Acta Phys. Pol.*, sous presse.
- [15] S. KIELICH: *Acta Phys. Pol.*, sous presse.
- [16] C. R. BURY et H. O. JENKINS: *Journ. Chem. Soc.*, 688 (1934).

PARTE QUINTA

Review Papers on Helium 4

Liquid Helium as a Quantum Liquid.

J. DE BOER

Institute for Theoretical Physics, University of Amsterdam - Amsterdam

1. - Introduction.

Liquid helium is the only substance known, which has the property that it remains liquid down to the absolute temperature zero. This gives liquid helium already an exceptional position amongst the various substances. In addition to this, however, liquid helium has quite a number of other remarkable properties, which altogether makes the properties of this substance the object of an increasing number of theoretical and experimental investigations. It cannot be the object of this conference on the condensed state in general, to attempt in this introductory lecture to survey all the properties of liquid helium. Instead we will make a choice: first outline the position of liquid helium amongst other liquids (Sect. 2), then give a somewhat more detailed discussion of the ground state at $T=0$ (Sect. 3), the equilibrium theory of the thermal excitations (Sect. 4), the hydrodynamics of these (Sect. 5) and finally some remarks about the theoretical difficulties encountered in describing these thermal excitations.

2. - Liquid helium as a quantum liquid.

2.1. *Principle of corresponding states.* - If one wants to investigate the position of liquid helium amongst the substances and thus if one wants to compare its properties with those of other condensed substances like condensed hydrogen, deuterium, neon, argon, krypton and xenon, one should use a common « language » for describing the properties of these various substances. Such a common language is offered by expressing the physical properties in terms of units derived from the constants of the intermolecular forces which are characteristic for each particular substance. It has been

found that a reasonable description of many of the properties of monoatomic substances like He, Ne, Ar, Kr, Xe and also of the hydrogens H_2 , D_2 , T_2 can be given by assuming an intermolecular field of the form:

$$(1) \quad \varphi(r) = 4\varepsilon[(\sigma/r)^{12} - (\sigma/r)^6],$$

in which ε is the depth of the potential field and σ is the value of r for which $\varphi(\sigma) = 0$ (often one introduces also the value $r_0 = 2^{1/6}\sigma$, r_0 being the value of r at which the minimum of energy occurs $(d\varphi/dr)_{r_0} = 0$). The forces are assumed to be additive, which assumption seems to be satisfied surprisingly good. This conclusion can be drawn from the fact that although in many cases the constants of the potential field ε and σ have been determined from the properties of the dilute gas (second virial coefficient or gas viscosity), they offer a very good description (to within a few percent) of the condensed state (solid density and heat of sublimation). It should be mentioned that some authors have criticized the form of the 12-6 potential and instead prefer the introduction of an exponential-six potential. Two remarks have here to be made:

1) The potential field (1) is not pretending to give the accurate theoretical formula for the interaction but only a mathematical curve, which represents in effect a reasonable approximation to the true interaction curve whatever its mathematical expression will be.

2) It is questionable whether in the region where the exponential repulsion differs from the 12th power repulsion, the exponential repulsion is theoretically the better one: undoubtedly the quantum-mechanical perturbation treatment leads to exponential types of formulae, but the fact that one has to superpose the non-convergent contributions proportional to r^{-6} , r^{-8} and r^{-10} of the attractive field makes the outcome of the theoretical calculation rather questionable and in particular it is unknown whether the final interaction curve which would be the result of an improved theoretical calculation not suffering from these non-convergencies, is in effect better represented by an exp-6 or exp-6-8 curve than by the above mentioned 12-6 potential. In any case there is little doubt that the 12-6 curve allows a very satisfactory description of many of the properties of these substances and because nothing very much better can be done at this moment, we will base the discussion on this field.

The values of the constants $N\sigma^3$ and ε/k , which seem to be the best values at present [27], are given in Table I. One can express all physical quantities in terms of molecular units derived from the constants as explained in Table II.

In *classical* theory it is then easy to prove from dimensional considerations the validity of a *classical principle of corresponding states*:

$$(2) \quad P^* = f_1(V^*, T^*), \quad S^* = f_2(V^*, T^*), \quad \eta^* = f_3(\rho^*, T^*),$$

TABLE I. — *Values of molecular constants.*

substance	ε/k ($^{\circ}\text{K}$)	$N\sigma^3$ (cm^3/mole)
^3He , ^4He	10.22	10.06
H_2 , D_2 , T_2	37.0	15.12
Ne	35.60	12.51
A	119.8	23.79
Kr	166.1	29.35
Xe	229.8	36.74

TABLE II. — *Molecular units.*

Q u a n t i t y	Molecular unit	Reduced quantity
<i>Equilibrium properties:</i>		
molar volume	$N\sigma^3$	$V^* = V/(N\sigma^3)$
temperature	ε/k	$T^* = kT/\varepsilon$
molar energy	$N\varepsilon$	$U^* = U/N\varepsilon$
pressure	ε/σ^3	$P^* = P\sigma^3/\varepsilon$
density	m/σ^3	$\rho^* = \rho\sigma^3/m$
molar entropy	$Nk = R$	$S^* = S/R$
heat capacity	$N\varepsilon/(\varepsilon/k) = R$	$C^* = C/R$
surface tension	ε/σ^2	$\gamma^* = \gamma\sigma^2/\varepsilon$
<i>Non equilibrium properties:</i>		
viscosity	$(\sigma^2/m\varepsilon)^{\frac{1}{2}}$	$\eta^* = \eta(m\varepsilon)^{\frac{1}{2}}/\sigma$
heat conductivity		

where f_1 , f_2 , f_3 , etc., are universal functions valid for all substances and depending only on the fact that a 12-6 potential has been used for characterizing the potential field.

In *quantum theory* the additional constant h , the constant of Planck comes into the picture, which allows to define a new dimensionless constant:

$$(3) \quad \Lambda^* = \frac{\Lambda}{\sigma} = \frac{h/(m\varepsilon)^{\frac{1}{2}}}{\sigma} = \frac{h}{\sigma(m\varepsilon)^{\frac{1}{2}}},$$

which has a very simple physical meaning: $\Lambda = h/(m\varepsilon)^{\frac{1}{2}}$ is a kind of characteristic de Broglie wavelength and $\Lambda^* = \Lambda/\sigma$ is the reduced value of this quantity, i.e. this quantity Λ expressed in terms of the molecular unit of length: σ . The values of this constants are given in Table III.

The occurrences of this new dimensionless constant in quantum-mechanics

TABLE III. - *Values of quantum-mechanical parameter.*

Substance	$A^* = \hbar/\sigma(m\varepsilon)^{\frac{1}{2}}$
^3He	3.08
^4He	2.67
H_2	1.73
D_2	1.22
Ne	0.59
A	0.186
Kr	0.102
Xe	0.064

forces to extend the principle of corresponding states, formulated in (2) into a *quantum-mechanical principle of corresponding states* [1]

$$(4) \quad P^* = g_1(V^*, T^*, A^*), \quad S^* = g_2(V^*, T^*, A^*), \quad \eta^* = g_3(\varrho^*, T^*, A^*)$$

in which again g_1 , g_2 , g_3 , etc., are universal functions which now, however, depend also on the constant A^* .

Two remarks have to be made:

a) The principle of corresponding state considerations in (2) and (4) *only* applies, strictly spoken, to *monoatomic* substances. When more-atomic substances are considered in which internal vibrations or rotations play a role, it is essential that these internal motions should not influence appreciably the force law (1) and that their contribution to the thermodynamic quantities (e.g. U , S and C) is an additive contribution which can be subtracted *before* applying the principle of corresponding states. This seems, at least approximately, the case for such molecules like H_2 , D_2 and T_2 . For the case of HD and HT the difficulty exists already that the rotation of the molecule round an asymmetrically placed centre of mass makes the average spherical potential field probably different from that of H_2 and D_2 , making it impossible to apply the principle of corresponding states or at least making it necessary to correct for these differences.

b) In the principle of corresponding states the symmetry effects are neglected and also it should be mentioned that the functions g_1 , etc., need not always be smooth functions of A^* . In particular an abrupt change in this function might occur in case a small change of A^* causes a large change in structure of e.g. the condensed phase. Thus for instance all substances including the hydrogens have a close packed solid lattice structure at the absolute zero, but helium has a liquid structure with a much smaller co-ordination number. Thus the curve of the reduced molar volumes V^* for different

substances at $T = 0$ can be expected to show, when plotted as a function of Λ^* , at least somewhat a discontinuity between helium and hydrogen (see Fig. 1). Also ^3He and ^4He having different statistics, need not necessarily be on the same curve.

2.2. Diagram of states. — The influence which the quantum effects have on the diagram of state is shown in Fig. 2, which gives the diagram of states for a « classical » system and that for ^4He and ^3He . The diagram for a « classical » system, i.e. the experimental diagram of states of the heavy noble gases Ne, Ar and Kr which all practically coincide, is taken as the prototype of a classical system, whereas ^3He and ^4He are representing the most extreme cases of a « quantal » system. The cases of H_2 , D_2 and T_2 are lying in between these two extremes, the shift being a monotomic function of the values of the quantum-mechanical parameter Λ^* .

The most important difference between He and the classical substances

is that for the case of He at least two phases are possible at $T = 0$. This is because the melting line, and the vapour pressure line, which usually cross each other in the triple point, do not intersect, thus leading to the possibility of going in the liquid state down to $T = 0$. In the case of ^4He this transition to $T = 0$ is not continuous, there being a phase transition on the λ -line which separates the He-I liq. from the He-II liq. region. In the case of ^3He so far no such transition has been found experimentally although at very low temperatures $T \approx 0.3^\circ\text{K}$ the heat capacity shows a strange behaviour.

There are at present measurements showing that also in the solid phase of ^4He and ^3He phase transitions occur, but they will not be

considered here at this moment where only the gross quantal effects are important.

We now concentrate on the situation at $T = 0$ and consider in more detail the explanation for the existence of more stable phases in the case of helium, quite opposite to the classical system where only one stable phase exists. The stability of the different condensed phases at $T = 0$ can be com-

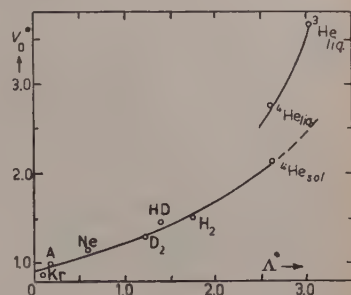


Fig. 1. — Values of V_0^* , the molar volume, expressed in molecular units, of the condensed state at $T = 0$ as function of Λ^* .

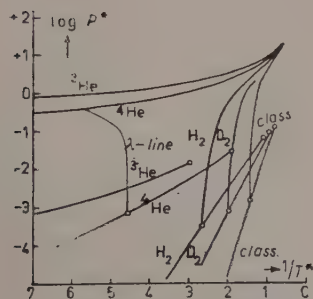


Fig. 2. — The P^*-T^* diagram for a classical substance, compared with those of D_2 , H_2 , ^4He and ^3He constituting a series of substances with increasing values of Λ^* .

pared by plotting the molar energy as a function of molar volume because, at $T=0$, the energy U and the free energy F are equal.

In *classical mechanics* the energy of the condensed phase at $T=0$ is equal to the *potential energy* of the system in which the molecules are placed on the positions corresponding to a definite crystalline lattice structure. One can evaluate the energies of a set of different lattices:

close packed (c.f.c. or hex.)	co-ordination number: 12
cubic body centered (c.b.c.)	» » 8
simple cubic (s.c.)	» » 6
T_d^2 (half occ. c.f.c.)	» » 6
diamond (half occ. c.b.c.)	» » 4

For simplicity we will identify the energies of the two possible close packed structures, which only differ very slightly in energy. It is then obvious that the structure with the largest co-ordination number has the lowest energy and therefore all classical substances crystallize in the close packed structure (leaving aside the matter of *which* close packed structure; cubic face centered or hexagonal, as this is irrelevant for the present considerations). The other structures are all meta stable at $T=0$ and therefore not realized in nature.

In *quantum mechanics* the energy of the condensed state at $T=0$ is the sum of the *potential energy* and the *zero-point energy* due to the zero-point motion of the atoms round their equilibrium positions (at least as long as the zero-point motion is so small that the separation into these additive contributions makes sense). Now the zero-point energy is equal to $(9/8)R\Theta_D$, for the case that the vibrations round the equilibrium positions have a small amplitude and the Debye theory is a good approximation in the theory of the solid state. When the zero-point vibrations have larger amplitudes it might be

expected that a good approximation is obtained by taking the average zero-point energy per molecule equal to the kinetic localization energy: $\hbar^2/8m(a-d)^2$ (where $a^3 = (V/N)\sqrt{2}$ and where d is an effective hard sphere diameter being roughly equal to 0.8 or 0.9σ). In Fig. 3 we have added the reduced zero-point energy $U_z^* = U_z/N\varepsilon = \hbar^2/m\varepsilon\sigma^2 8(a^* - d^*)^2$ (with $d^* = d/\sigma = 0.9$) for two

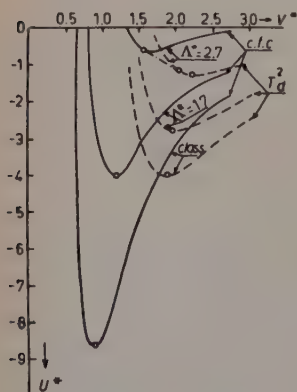


Fig. 3. - Schematic comparison of the total energy of a solid phase having a close packed lattice and that having a T_d^2 -structure (with co-ordination number = 6) for the classical case, for a substance with $\Lambda^* = 1.7$ (H_2) and for $\Lambda^* = 2.7$ (4He), showing the stability of the T_d^2 -structure for large values of Λ^* .

different values of $\Lambda^{*2} = \hbar^2/m\epsilon\sigma^2$, corresponding to hydrogen and helium respectively) to the curves for the reduced potential energy corresponding to the different structures. The first effect is, that because the zero-point energy decreases when the molar volume increases, this «blows up» the equilibrium volume of the substance to a larger value. This effect increases with increasing value of Λ^* and is, in agreement with the experimental findings, presented in Fig. 3. However a second remarkable result, first noted by LONDON [2], is that for large values of Λ^* more phases are stable at $T=0$ and that in fact the structure with the lowest total energy is no longer the close packed structure, but a structure with a smaller co-ordination number: the T_d^2 structure. Thus under zero pressure helium should be in the T_d^2 -phase corresponding to a small co-ordination number. At higher pressure $P = -dU/dV$ there occurs a transition, indicated by a broken line, at a pressure

$$P_m = [U(\text{c.f.c.}) - U(T_d^2)]/[V(T_d^2) - V(\text{c.f.c.})]$$

into the close packed phase. The pressure at which the transition occurs has to be identified with the melting pressure ($P_m = 25$ atm for ^4He). The two phases between which the transition occurs need not necessarily be the T_d^2 and close packed phase indicated above (although these are the most probable ones for ^4He) and in particular for ^3He it might be possible that *two* such transitions (from the ^3He (liq) in the ^3He (solid- α) phase and from the ^3He (solid- α) into the ^3He (solid- β) phase) occur at $T=0$. In fact it is not at all difficult to explain such a situation on the basis of a figure like Fig. 3.

It now has to be explained why the low co-ordination phase which exists under zero pressure is liquid and not solid. The stability requirements for a solid are:

$$a) \text{ the compression modulus: } K > 0 \qquad P = -K \cdot \Delta V/V,$$

$$b) \text{ the (rigidity) coefficient: } c_{44} > 0 \qquad X_y = -c_{44}x_y.$$

a) The compression modulus as the ratio of the hydrostatic pressure P and the relative volume change $\Delta V/V$ which results from this hydrostatic pressure is given by $K = -V dP/dV = V d^2U/dV^2$. This compression modulus can thus be written as a sum $K = K_p + K_z$, where K_p is the compression modulus corresponding to the potential energy alone and K_z is that corresponding to the zeropoint energy. If, as is explained above, the condensed phase «blows up» as a result of the zeropoint energy, the new equilibrium molar volume under zero pressure is found by determining the minimum of the total energy $U = U_p + U_z$ as a function of volume V . It is clear that in this new minimum $K = V d^2U/dV^2 > 0$ and that the first stability condition is satisfied.

For any lattice without zero-point energy the coefficient c_{44} can be evaluated without difficulty and the curve obtained is in general qualitatively very similar to that for the compression modulus, being positive for small values of V and turning negative and going through a minimum at roughly the same values of molar volume as the compression modulus K_v does. We now have to consider the contribution of the zero-point motion to this coefficient. In

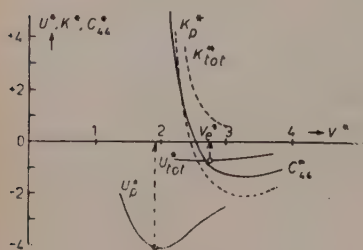


Fig. 4. — The potential energy U_v^* and the corresponding compression modulus K_v^* and the elastic, or rigidity coefficient c_{44}^* for a T_d^2 lattice together with the total energy U_{tot}^* and compression modulus K_{tot}^* , showing the change of the equilibrium-position from $V^* = 1.9$ to $V^* = 2.75$ as a result of the zero-point motion into the region where c_{44}^* is negative.

the region of larger molar volumes to which liquid helium is blown up as a result of the zero-point motion, we may assume that the zero-point energy is more or less structure independent and depends only on the density of the system. However, in the shearing deformation x_y under the influence of a shearing stress X_v , the density remains constant in first approximation and thus the rigidity coefficient c_{44} gets in first approximation (and as long as the zero-point energy depends only on density) no contribution from the zero-point energy. The situation then becomes as has been drawn in Fig. 4. As a result of the zero-point energy liquid He «blows up» from $V^* \approx 1.9$ being the volume at which the energy minimum of the T_d^2 lattice occurs to the experimental value $V^* \approx 2.75$. The compression modulus which would be negative in this region if only the contribution K_v^* from the potential energy were considered turns out to be positive as a result of the additional positive contribution K_z^* of the zero-point motion: $K^* = K_v^* + K_z^*$. However, the coefficient c_{44} which becomes negative in the same region $V^* > 2.5$ where also K_v^* becomes negative, is not made positive as a result of a compensation due to the zero-point motion and thus remains negative. The conclusion then is that the blown up T_d^2 phase of helium behaves as a liquid and not as a solid.

As a conclusion to this section we may thus summarize that the large zero-point energy, present in the case of helium, has the following consequences:

a) A phase with a much smaller co-ordination number (6) becomes more stable than the close packed structure, the volume being about 2.5 times and the energy only 0.1 of that of the close packed structure.

b) It can be understood at least qualitatively that this low co-ordination phase has a negative value of the «rigidity» coefficient c_{44} and thus is a liquid and not a solid.

3. - The ground state of liquid helium.

We now like to discuss briefly whether the qualitative discussion of the last Sect. 2 can be made quantitative to explain the energy and density relationship of the ground state of solid and liquid helium. In Fig. 5 the theo-

retical curves for U_p^* , i.e. the potential energy curves for different lattices, have been drawn, together with the experimental curves for the total energy U_{tot}^* for solid ^4He and liquid ^4He . The difference between U_{tot}^* and U_p^* has thus to be explained as the zero-point energy (if the addition of the two contributions is a reasonable approximation). In Fig. 6 the difference between the U_p^* curve for

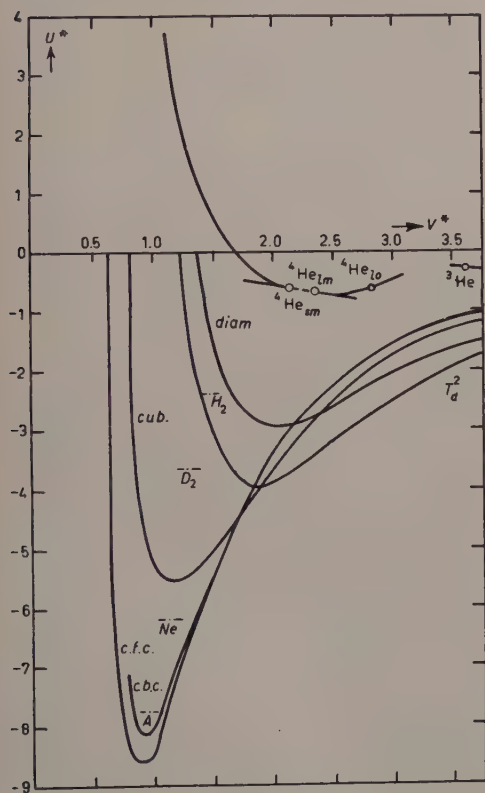


Fig. 5. - Experimental values for total energy of solid and liquid helium compared with the theoretical values for the potential energy contribution U_p^* from the close packed lattice and several other lattices of smaller co-ordination number.

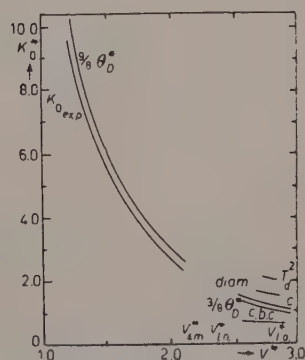


Fig. 6. - Experimental values of the zero-point energy, obtained from Fig. 5. compared with $\frac{8}{9}R\Theta_D$ in the solid phase and $\frac{3}{8}R\Theta_D$ in the liquid phase.

the close packed structure and the experimental curve for U_{tot}^* for solid ^4He has been plotted, as well as the difference between the liquid experimental curve for U_{tot}^* and a set of different U_p^* curves corresponding to different structures with low co-ordination number: diamond ($z=4$), T_d and cub. ($z=6$) and c.b.c. ($z=8$).

In the solid phase the values of the Debye temperature Θ_D are known from

the work of DUGDALE and SIMON [3]. If one calculates the zero point energy according to the Debye model, being $U_z = \frac{3}{8} R\Theta_D$, then one finds a reasonable agreement with the experimental curve. In the liquid state, where the Θ_D values are known also, but only the longitudinal waves can be propagated,

the zero-point motion due to these Debye waves would be $U_z = \frac{3}{8} R\Theta_D$ which value is obviously too small.

A different approximation for the zero-point energy can be obtained by comparing liquid He with a hard sphere gas with uniform attraction field. Hard spheres, which would be equivalent to the interacting He atoms, should have a diameter d being smaller than σ , the distance where the real potential field goes through zero. Therefore values of $d^* = d/\sigma$ varying from 0.8 to 1.0 will be considered. For the evaluation of the zero-point energy of a hard sphere gas one might assume that at high densities the zero-point energy, calculated with the cell model, i.e. $U_z = N \cdot h^2/8m(a-d)^2$ would be a good approximation, where a , the diameter of each of the cells is given by $a^3 = (V/N)\sqrt{2}$.

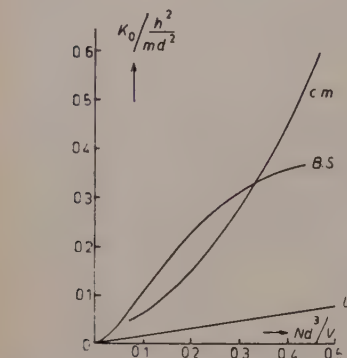


Fig. 7. — Comparison of zero-point energy K_0 of the cell model (c.m.) and that according to the theory of Brueckner and Sawada (B.S.) for hard spheres with diameter d as a function of the density: Nd^3/V . The lower straight line is that for the expression by Lenz.

At very small densities there is a well known approach by LENZ [4] leading to $(N/V)h^2d/2\pi m$, being proportional to the density. Recently YANG, LEE and HUANG [5] and BRUECKNER and SAWADA [6] have considered in much detail the ground state of the gas of hard spheres. The resulting value for the zero-point energy as a function of the density is plotted in Fig. 7 together with the value obtained with the cell model. The figure shows that in the intermediate region of $V/Nd^3 \approx 3$ which is of interest for the case of liquid helium

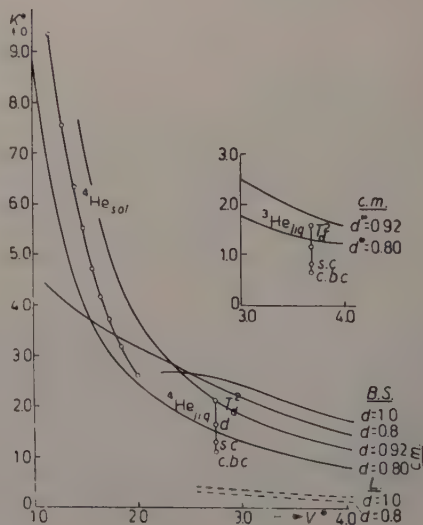


Fig. 8. — Experimental values of the zero-point energy, obtained from Fig. 5, compared with the values obtained from Fig. 7 for values of $d^* = d/\sigma$ varying between 0.8 and 1.0.

BRUECKNER and SAWADA get a result which is of the same order of magnitude as that obtained with the cell method. At higher densities, their result is much smaller than the one obtained with the cell theory. In Fig. 8 we have plotted the values of the total zero-point energy for liquid ^4He obtained by using values for the diameter d^* between 0.8 and 1.0, showing that these calculations for hard spheres give the right order of magnitude for the zero-point energy which is needed in the case of liquid helium.

4. - Thermal excitations in liquid helium.

4.1. *Experimental facts, thermal excitations.* - Direct information about the thermal excitations of liquid helium can be obtained from the measurements of the heat capacity and thermal expansion coefficient. For a description of these measurements the temperature range has to be divided into two regions:

- a) the temperature range below 0.6°K ;
- b) the temperature range between 0.6°K and T_λ .

In the *low temperature range* the heat capacity is proportional to T^3 in agreement with Debye's law (see Fig. 9). The value of the Debye temperature Θ_D can be calculated from the velocity of sound: $c = 239 \text{ m/s}$ to be $\Theta_D = 20.0^\circ\text{K}$. Insertion of this value in the expression for Debye's T^3 -law then shows that only one third of the possible modes in a solid, i.e. only the longitudinal or compressional modes, are excited in liquid helium. In agreement with the principles of thermodynamics also the thermal expansion should approach a T^3 -law [7] (see also [8]) and this appears to be confirmed by experiment (see Fig. 10). Thus in this low temperature range only longitudinal or elastic compressional waves are excited.

In the *temperature range above 0.6°K* the heat capacity gets a new contribution which increases very much and goes over into the λ -anomaly of the phase transition. Parallel to this there is the negative contribution to the thermal expansion coefficient which also starts to be important at temperatures above 0.6°K and finally makes even the thermal expansion coefficient negative up to the λ -point. For this behaviour at temperatures above 0.6°K another type of excitations are responsible in which most probably one or a small group of molecules is excited.

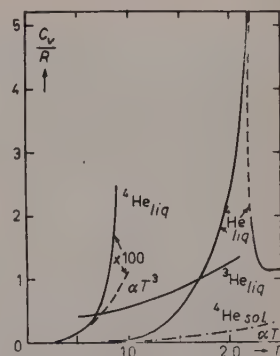


Fig. 9. - Molar heat capacity of liquid ^4He showing low temperature contribution proportional to T^3 and steep rise for $T > 0.6^\circ\text{K}$. Note also the large heat capacity of ^3He .

The difference in behaviour between ^3He and ^4He is rather remarkable: In ^3He the heat capacity remains very large even down to the lowest temperatures where measurements have been carried out. We will come back to this point in Sect. 6.

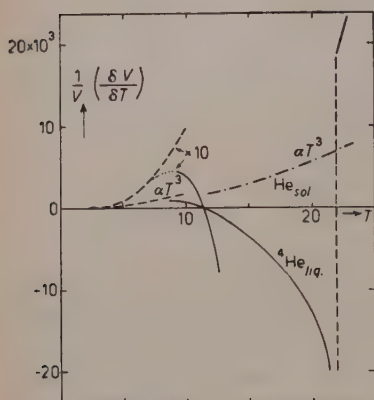


Fig. 10. — Thermal expansion coefficient of ^4He showing low temperature contribution proportional to T^3 and anomalous behaviour for $T > 0.6^\circ\text{K}$.

Summarizing one may conclude that at least for a phenomenological description of the thermal behaviour of liquid helium it is useful to distinguish provisionally between two different types of excitations:

a) Collective excitations, i.e. excitations in which large groups of molecules are moving in phase and which are properly described as compressional waves. It is well known that quanta of these compressional waves are indicated as « phonons ». These « phonons » carry energy $\varepsilon = \hbar\nu$ and momentum $\mathbf{p} = \hbar\boldsymbol{\sigma}$, where $|\boldsymbol{\sigma}| = 1/\lambda$ is the wave number. For long elastic waves the relation between ε and p is given by $\varepsilon = c \cdot p$,

where c is the velocity of sound. This leads to the relation $v = c\sigma$ between frequency and wave number. The spectrum of these excitations is thus a nearly continuous spectrum starting from $\sigma = 0$ upwards. The upper limit for the wave vector $\boldsymbol{\sigma}$ is given by $|\boldsymbol{\sigma}_0| = (3N/4\pi V)^{1/3}$, corresponding to N values of σ in total.

b) Molecular excitations, i.e. excitations in which only a small number of molecules, may be even only one molecule, is involved. It is assumed that these excitations require a finite excitation energy corresponding to about 10°K . These excitations may also move through the medium. In 1941 LANDAU [9] assumed that these excitations have a rotational character (« rotons ») and he proposed that these excitations have an energy $\varepsilon = \Delta + p^2/2\mu$ giving $v = (\Delta/\hbar) + \hbar\sigma^2/2\mu$. Thus from the group velocity $w = dv/d\sigma = \hbar\sigma/\mu$ and their momentum $p = \hbar\sigma = \mu w$ it follows that μ may be called the effective mass of these « rotons ». Later on (1947) LANDAU [10] modified this picture somewhat by changing the energy-momentum relation into $\varepsilon = \Delta + (p - p_0)^2/2\mu$ or $v = \Delta/\hbar + \hbar(\sigma - \sigma_0)^2/2\mu$ which formula should be valid for $\sigma \approx \sigma_0$ or $p \approx p_0$. From the fact that $w = dv/d\sigma = \hbar(\sigma - \sigma_0)/\mu$, whereas $p = \hbar\sigma$ one sees that now μ has no longer the simple meaning of an effective mass and that the nature of the excitations described by this formula is more complicated. In the next section we will come back to these points.

4.2. *Thermodynamic quantities.* — For the purpose of describing the thermal behaviour one may consider the system of thermal excitations moving round in liquid helium as a gas, a dilute gas, the distribution function giving the number of excitations per unit volume and in the range $d\sigma$, $f(\sigma)d\sigma$, being given by [9]

$$(5) \quad f_0(\sigma) = \frac{1}{\exp [\beta \varepsilon(\sigma)] - 1}.$$

Using the methods of statistical mechanics one finds [9, 8] for the specific thermodynamic functions:

$$(6) \quad \tilde{F} = \frac{F}{V} = -kT \int \ln (1 - \exp [-\beta \varepsilon(\sigma)]) d\sigma = -\frac{1}{3} \int f_0 \sigma \frac{\partial \varepsilon}{\partial \sigma} d\sigma,$$

$$(7) \quad P = \frac{1}{3} \int f_0 p w d\sigma = \frac{1}{3} \int f_0 \sigma \frac{\partial \varepsilon}{\partial \sigma} d\sigma = -\tilde{F},$$

$$(8) \quad \tilde{U} = \int f_0 \varepsilon d\sigma,$$

$$(9) \quad \tilde{S} = \frac{1}{T} \int f_0 \left[\varepsilon + \frac{1}{3} \sigma \frac{\partial \varepsilon}{\partial \sigma} \right] d\sigma.$$

The expression for P is obtained in the usual way by taking the diagonal terms from the pressure tensor, which is obtained by evaluating the transport of momentum. The momentum transported per phonon is equal to p and the velocity with which it is transported is the group velocity w of the phonons. The average number of excitations per unit volume n_{exc} is given by:

$$(10) \quad n_{\text{exc}} = \int f_0(\sigma) d\sigma.$$

according to the definition of $f_0(\sigma)$, given by (5). The gas of excitations behaves as a degenerate gas or a radiation gas: the number of excitations n_{exc} is only a function of temperature and the thermodynamic potential $\tilde{G} = G/V = \tilde{U} - T\tilde{S} + P = 0$.

If now we introduce the $\varepsilon(\sigma)$ relation corresponding to the *phonon type of excitation* one finds that:

$$(11) \quad P_{\text{ph}} = -\tilde{F}_{\text{ph}} = \theta \pi_5^4(4) \frac{k^4}{h^3 c^3} T^4 = \frac{4\pi^5}{45} \frac{k^4}{h^3 c^3} T^4,$$

$$(12) \quad \tilde{U}_{\text{ph}} = \frac{4\pi^5}{15} \frac{k^4}{h^3 c^3} T^4,$$

$$(13) \quad \tilde{S}_{\text{ph}} = \frac{16\pi^5}{45} \frac{k^4}{h^3 c^3} T^4,$$

which is in agreement with the experimental findings at low temperatures ($T < 0.6^\circ\text{K}$). The number density of phonons per unit volume becomes:

$$(14) \quad n_{\text{ph}} = 8\pi\zeta(3) \frac{k^3}{h^3 c^3} T^3,$$

where $\zeta(3) = \sum n^{-3} = 1.202$. In all these formulae the upper limit of the integration σ_D has been replaced by ∞ which is a good approximation as long as $kT \ll \varepsilon(\sigma_D)$. Using the definition of σ_D this may also be expressed by requiring that $6\zeta(3) \cdot n_{\text{ph}} \ll N/V$ or $n_{\text{ph}} \ll 0.14 N/V$. It should be noted that from (11) and (14) it can be derived that the pressure satisfies the relation:

$$(15) \quad P_{\text{ph}} = \frac{\zeta(4)}{\zeta(3)} n_{\text{ph}} kT \approx 2.7 n_{\text{ph}} kT,$$

which expression is the analogue of the corresponding expression $P = [\zeta(3/2)/\zeta(1/2)] n_{\text{ph}} kT$ for the degenerate ideal Bose-Einstein gas (*).

For the *molecular type of excitations* one finds [9] with the Landau (1940) expression $\varepsilon = \Delta + \hbar^2 \sigma^2 / 2\mu$

$$(16) \quad n_{\text{mol}} \approx (2\pi\mu kT / \hbar^2)^{3/2} \exp[-\beta\Delta]$$

and

$$(17) \quad P_{\text{mol}} = -\tilde{F}_{\text{mol}} = n_{\text{mol}} \cdot kT,$$

$$(18) \quad \tilde{U}_{\text{mol}} \xrightarrow{T \rightarrow 0} n_{\text{mol}} \Delta,$$

$$(19) \quad \tilde{S}_{\text{mol}} \xrightarrow{T \rightarrow 0} n_{\text{mol}} \Delta / T.$$

For the type of excitations described by the modified expression $\varepsilon = \Delta + \hbar^2(\sigma - \sigma_0)^2 / 2\mu$ the same expressions (17)–(19) for the thermodynamic for-

(*) For the degenerate B.E. gas we have for the number of molecules per unit volume n_{th} which still takes part in the thermal motion:

$$n_{\text{th}} = \zeta \left(\frac{5}{2} \right) \left(\frac{2\pi m kT}{h^2} \right)^{3/2}.$$

The corresponding pressure is:

$$P = \zeta \left(\frac{5}{2} \right) \left(\frac{2\pi m kT}{h^2} \right)^{3/2} \cdot kT = \frac{\zeta(\frac{5}{2})}{\zeta(\frac{3}{2})} n_{\text{th}} kT,$$

with $\zeta(\frac{3}{2}) = 1.342$ and $\zeta(\frac{5}{2}) = 2.612$ appear instead of $\zeta(3) = 1.202$ and $\zeta(4) = \pi^4/90$ because of the relationship $\varepsilon = p^2/2m$ which replaces $\varepsilon = cp$ for the case of gas molecules.

mulae hold, in which, however,

$$(20) \quad n_{\text{mol}} \approx (2\pi\mu kT/h^2)^{\frac{1}{2}} 4\pi\sigma_0^2 \exp[-\beta\Delta]$$

replaces the formula (16) for n_{mol} . This second type of excitations thus gives an exponential contribution to the thermodynamic quantities, because of the exponential rise of the average number of molecular excitations n_{mol} per unit volume. Contrary to the case of the phonons, the pressure due to these molecular excitations is simply given by $n_{\text{mol}} \cdot kT$ as is the case for an ideal gas, which is *not* degenerate. For temperatures above 0.6 °K the contribution due to these molecular excitations becomes more important than that due to the phonons. The general behaviour of the heat capacity: at low temperatures proportional to T^3 and an experimental rise for $T > 0.6$ °K can thus be explained on the basis of this picture. In Fig. 11 the most recent data about the constants Δ and σ_0 of the thermal excitations have been plotted. These data have been obtained by combining the measurements on the heat capacity with those of second sound to be discussed later.

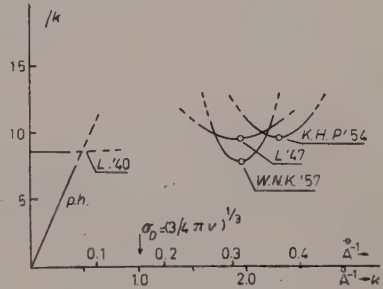


Fig. 11. — Most recent values of the character of the thermal excitations, according to LANDAU (1947), DE KLERCK and PELLAM (1954) and WIEBES, NIELS-HAKKENBERG and KRAMERS (1957).

If we assume in agreement with experiment that the velocity of sound c increases and thus n_{ph} decreases with pressure we find a positive thermal expansion coefficient at low temperatures proportional to T^3 . In order to make the thermal expansion coefficient negative at higher temperatures one has to assume that $n_{\text{ph}} \cdot \Delta$ becomes larger under increasing pressure. For a more detailed discussion of the properties of the thermal excitations we refer to a recent survey given by the author [8].

5. — Hydrodynamics of liquid helium.

5.1. Phenomenological theory. — In the previous section we have considered the equilibrium properties of liquid helium. In this section we will discuss the hydrodynamical properties of liquid helium. We start with showing the importance of the phenomenological relations introduced by LANDAU [9].

The well known experiment by ANDRONIKAŠVILI, in which a pile of circular discs oscillates in liquid helium II, shows that only part of the liquid

is taken with the oscillating discs. This part of the density, which is called the « normal fluid » density ϱ_n , thus shows normal viscous behaviour, whereas the remaining part ϱ_s , the « superfluid », shows no viscosity. The normal fluid density increases from $\varrho_n = 0$ at $T = 0$ to $\varrho_n = \varrho$ at $T = T_\lambda$.

The second experiment which gave important information about the behaviour of these two fluids is the famous experiment of KAPICA in which liquid helium is forced to flow isothermally through a capillary from a vessel I to a vessel II. This flow appears to be practically without friction, but on the entry of the capillary an amount of heat is developed in vessel I which has to be withdrawn from vessel I in order to keep the whole process going on at constant temperature. This same heat has to be applied to vessel II into which the helium flows through the capillary. Careful measurements have shown that when Q is the amount of heat supplied per mole flowing through the capillary, $Q = TS$, where S is the entropy per mole of helium. It is assumed that the fluid which flows through the capillary is the « superfluid », as the normal fluid is prevented to flow because of its viscosity. This experiment then shows that the *superfluid carries no entropy*.

One thus arrives at the two fluid pictures of LANDAU [9]. If the local velocities of the two fluids are given by \mathbf{v}_s and \mathbf{v}_n one may write for the bulk velocity \mathbf{V} of the liquid and the relative velocity of the two fluids \mathbf{v} :

$$(21) \quad \mathbf{v} = \mathbf{v}_n - \mathbf{v}_s,$$

$$(22) \quad \varrho \mathbf{V} = \varrho_n \mathbf{v}_n + \varrho_s \mathbf{v}_s,$$

all these quantities \mathbf{v}_n , \mathbf{v}_s , \mathbf{V} and \mathbf{v} are here supposed to be « local values », i.e. to depend on x , y , z and t .

The motion of the bulk liquid satisfies the continuity equation and the equation of motion:

$$(23) \quad \frac{\partial \varrho}{\partial t} = -\varrho \operatorname{div} \mathbf{V},$$

$$(24) \quad \varrho \frac{\partial \mathbf{V}}{\partial t} = -\operatorname{grad} P$$

if we linearize and leave out the viscosity terms, so as to simplify the formulae. The normal fluid is assumed to satisfy the following equations:

$$(25) \quad \frac{\partial \tilde{S}}{\partial t} = -\tilde{S} \operatorname{div} \mathbf{v}_n,$$

$$(26) \quad \varrho_n \frac{\partial \mathbf{v}}{\partial t} = -\tilde{S} \operatorname{grad} T.$$

The first equation is the conservation equation of the normal fluid expressing the fact that the normal fluid exclusively carries the entropy. The last equa-

tion is the equation of motion for the two fluids relative to each other equivalent to that suggested by LANDAU [9]. This shows that the relative motion of the two fluids with respect to each other is the result of a temperature gradient, just as the bulk flow results from a pressure gradient. In the equations (23) to (26) the intensive quantities ϱ , T , P and \tilde{S} are all considered to be the local values, i.e. they may depend on \mathbf{r} and t .

By differentiating (23) to t and (24) to x and eliminating V_x , one is able to derive:

$$(27) \quad \frac{\partial^2 \varrho}{\partial t^2} = \frac{\partial^2 P}{\partial x^2} \quad \text{or} \quad \frac{\partial^2 \varrho}{\partial t^2} = \left(\frac{dP}{d\varrho} \right) \frac{\partial^2 \varrho}{\partial x^2},$$

leading to

$$(28) \quad c_s^2 = \frac{dP}{d\varrho}$$

being the velocity of ordinary sound waves. In the same way one can obtain from the second two equations (25) and (26):

$$(29) \quad \frac{\partial^2 \tilde{S}}{\partial t^2} = \frac{\varrho_n}{\varrho_s} \tilde{S}^2 \frac{\partial^2 T}{\partial x^2} \quad \text{or} \quad \frac{\partial^2 \tilde{S}}{\partial t^2} = \left(\frac{\varrho_n}{\varrho_s} \tilde{S}^2 \frac{dT}{d\tilde{S}} \right) \frac{\partial^2 \tilde{S}}{\partial x^2},$$

using $\varrho_n \mathbf{v}_n + \varrho_s \mathbf{v}_s = 0$. This gives

$$(30) \quad c_{s2}^2 = \frac{\varrho_n}{\varrho_s} \tilde{S}^2 \frac{dT}{d\tilde{S}} = \frac{\varrho_n}{\varrho_s} \frac{T \tilde{S}^2}{\tilde{C}},$$

which is the velocity of second sound. Similar to the ordinary sound waves representing waves in which the density and the pressure oscillate round the equilibrium values, the second sound waves represent waves in which the temperature and the entropy density oscillate round their equilibrium values. A better name for these waves would have been entropy waves, just as the ordinary sound consists of density waves, but the name «second sound» can also be defended with good arguments.

An important consequence of Landau's formula for second sound (30) is that by measuring the velocity of second sound one can determine $\varrho_n/(\varrho - \varrho_n)$ as a function of temperature for liquid helium, thus

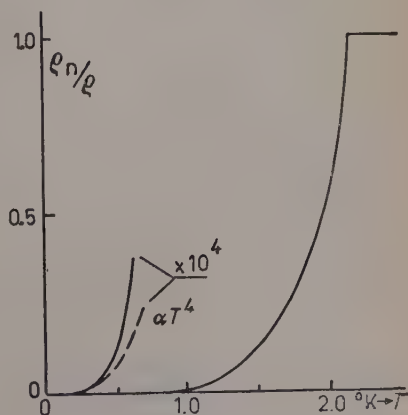


Fig. 12. - Values of the normal fluid density as a function of temperature showing the low temperature contribution proportional to T^4 (multiplied by 10^4) and the steep rise for temperature $T > 0.6$ °K.

obtaining new information about this important thermodynamic quantity: the normal fluid density ϱ_n . The measurements (see Fig. 12) showed that at very low temperatures the normal fluid density is proportional to T^4 , but that above 0.6°K a sharp rise of ϱ_n occurs up to the value $\varrho_n = \varrho$ which is reached at $T = T_\lambda$. In the temperature region above 1°K close agreement is obtained with the direct measurements of ϱ_n according to the method of ANDRONIKAŠVILI. It is interesting that this quantity ϱ_n shows such a different behaviour in the two temperature regions below and above 0.6°K , which appeared also in the heat capacity and the thermal expansion.

5.2. Theoretical basis of the two-fluid model. — The two-fluid hypothesis can be given a more quantitative foundation on first principles following a method originating in the concepts of LANDAU and in the work of H. A. KRAMERS [11] and of R. KRONIG [12] and HALATNIKOV [13]. In Sect. 4 we explained the equilibrium properties of liquid helium in terms of a gas of excitations moving round in the liquid and distributed according to the distribution law (5). In this section we will show that also the non-equilibrium properties can be explained quantitatively on this same basis.

The liquid viscosity is supposed to be due to collisions of the thermal excitations with each other and with the walls and in fact a very nice qualitative and quantitative description of many experimental facts has been obtained on this basis by LANDAU and his collaborators. Thus in Andronikašvili's experiment the gas of excitations does not move as a whole because of the friction which would be caused with the parallel plates and similarly the excitations do not move through the capillary in Kapica's experiment. What moves in these two cases is the background fluid in which all the excitations move round and on which no frictional forces are exerted by the walls (at least when the velocity is not too large). This background fluid thus should be identified with the «superfluid» and its local velocity with \mathbf{v}_s , whereas the gas of excitations is identified with the «normal fluid» responsible for the frictional forces and with a local average velocity $\mathbf{v}_n(\mathbf{r}, t)$. The meaning of ϱ_n and ϱ_s will become clear later on.

The distribution function $f(\boldsymbol{\sigma}; \mathbf{r}, t)$ for the excitations becomes also a local quantity depending on \mathbf{r} and t as parameters. When the average local velocity of the thermal excitations relative to the background-fluid is indicated by $\mathbf{v}(\mathbf{r}, t) = \mathbf{v}_n(\mathbf{r}, t) - \mathbf{v}_s(\mathbf{r}, t)$, then the expression for the distribution function is:

$$(31) \quad f(\boldsymbol{\sigma}; \mathbf{r}, t) = \frac{1}{\exp[\beta(\varepsilon'(\boldsymbol{\sigma}) - \mathbf{v}_n \cdot \hbar \boldsymbol{\sigma})] - 1}.$$

Here $\varepsilon'(\boldsymbol{\sigma})$ is the energy of the excitations measured in a system at rest in

which the average (local) velocity of the excitations is given by \mathbf{v}_n . Here T is considered to be the local temperature $T(\mathbf{r}, t)$ and for simplicity we will assume that local variations of the density $\varrho(\mathbf{r}, t)$, which might have an influence on the curve $\varepsilon'(\sigma)$, can be neglected. Because of the Doppler-effect we find for the frequency as measured in a co-ordinate system moving with the local velocity $\mathbf{v}_s(\mathbf{r}, t)$ of the background fluid (or superfluid): $\nu = \nu' - \mathbf{v}_s \cdot \boldsymbol{\sigma}$ leading to the expression for the energy as measured in the moving co-ordinate system $\varepsilon(\nu) = \varepsilon'(\nu) - \mathbf{v}_s \cdot \hbar \boldsymbol{\sigma}$. Substitution in (31) then leads to:

$$(32) \quad f(\boldsymbol{\sigma}; \mathbf{r}, t) = \frac{1}{\exp [\beta(\varepsilon(\sigma) - \mathbf{v} \cdot \hbar \boldsymbol{\sigma})] - 1} \approx f_0(\boldsymbol{\sigma}; \mathbf{r}, t) - \mathbf{v} \cdot \hbar \boldsymbol{\sigma} \frac{df_0}{d\varepsilon},$$

when $f_0(\boldsymbol{\sigma}; \mathbf{r}, t)$ is the local equilibrium distribution function (5), having $T = T(\mathbf{r}, t)$.

The excitations may collide during their motion through the background or superfluid and it is assumed that in these collisions total energy and momentum of the excitations is conserved. We may therefore apply the conservation laws:

$$(33) \quad \frac{\partial}{\partial t} \int f \varphi d\boldsymbol{\sigma} + \frac{\partial}{\partial \mathbf{r}} \cdot \int f \varphi \frac{\partial \varepsilon'}{\partial \mathbf{p}} d\boldsymbol{\sigma} = 0,$$

where for φ we may substitute $\varphi = \varepsilon'(\sigma)$ and $\boldsymbol{\varphi} = \mathbf{p} = \hbar \boldsymbol{\sigma}$. This leads to the following expressions:

$$(34) \quad \frac{\partial}{\partial t} (\varrho_n \mathbf{v}) = - \text{grad } P,$$

$$(35) \quad \frac{\partial}{\partial t} \tilde{U} = - \text{div} (\tilde{U} + P) \mathbf{v}_n,$$

where P and \tilde{U} , the pressure and the energy density, are given by the integral expressions (7) and (8) and where ϱ_n is written for the following integral:

$$(36) \quad \varrho_n = - \frac{1}{3} \int \frac{df_0}{d\varepsilon} p^2 d\boldsymbol{\sigma}.$$

We will see later on that ϱ_n can be identified with the normal density. Linearizing the equations (34) and (35) one obtains:

$$(37) \quad \varrho_n \frac{\partial \mathbf{v}}{\partial t} = - \text{grad } P,$$

$$(38) \quad \frac{\partial \tilde{U}}{\partial t} = - (\tilde{U} + P) \text{div } \mathbf{v}_n.$$

If now we make use of the fact that the thermodynamic potential density $\tilde{G} = \tilde{U} + P - T\tilde{S} = 0$ one may write $P = -\tilde{F}$ and $\tilde{U} + P = T\tilde{S}$ (equations which can be verified immediately from the expressions (6) to (9)). Thus one may write:

$$(39) \quad \varrho_n \frac{\partial \mathbf{v}}{\partial t} = + \text{grad } \tilde{F},$$

$$(40) \quad \frac{\partial \tilde{U}}{\partial t} = - T\tilde{S} \text{div } \mathbf{v}_n.$$

Also it follows from $\tilde{G} = 0$ that $d\tilde{F} = -\tilde{S}dT$ and $d\tilde{U} = Td\tilde{S}$ giving finally:

$$(41) \quad \varrho_n \frac{\partial \mathbf{v}}{\partial t} = -\tilde{S} \text{grad } T,$$

$$(42) \quad \frac{\partial \tilde{S}}{\partial t} = -\tilde{S} \text{div } \mathbf{v}_n.$$

These two equations which thus have been obtained by successive transformations of the conservation equations, involving linearization and the fact that $\tilde{G} = 0$, are identical with the two equations postulated by LANDAU.

As a byproduct of this foundation of the equations of Landau in the excitation picture we have obtained a formal theoretical expression for the *normal fluid density* ϱ_n , defined in terms of the distribution function for the excitations. This expression for the normal fluid density may be transformed by partial integration into:

$$(43) \quad \varrho_n = \int f_0 \cdot h^3 \frac{4\sigma \partial \varepsilon / \partial \sigma - \sigma^2 \partial^2 \varepsilon / \partial \sigma^2}{3(\partial \varepsilon / \partial \sigma)^2} d\sigma.$$

Substituting $\varepsilon = pc$ one finds:

$$(44) \quad S_{n,ph} = \int f_0 \frac{4\varepsilon}{3c^2} d\sigma = \frac{4}{3c^2} \bar{U} = \frac{16\pi^5}{45} \frac{k^4}{h^3 c^5} T^4,$$

which formula explains the low temperature behaviour of ϱ_n as has been found from second sound measurements. If we substitute the expression for the molecular type of excitations: $\varepsilon = h^2 \sigma^2 / 2\mu + \Delta$ one finds:

$$(45) \quad \varrho_{n,mol} = \int f_0 \mu d\sigma = n_{mol} \cdot \mu = \mu \left(\frac{2\pi\mu kT}{h^2} \right)^{\frac{3}{2}} \exp[-\beta\Delta].$$

This explains the experimental rise of the normal fluid density ϱ_n at temperatures greater than 0.6 °K which has been found experimentally.

The expression under the integral which has to be integrated in order to obtain the normal fluid density, thus has in the two cases the meaning: $\frac{1}{3}\epsilon/c^2$ and the effective mass μ for the two type of excitations respectively. Summarizing this Sect. 5 one may say that the picture in which the thermal motion is described in terms of thermal excitations, offers not only a quantitative understanding of the equilibrium properties of liquid helium, i.e. of the quantities $\tilde{U}(T)$ and $\tilde{S}(T)$, but also of the hydrodynamic properties described by the equations of Landau and the equation for the normal fluid density ϱ_n .

The picture has been extended, in particular also by LANDAU and HALATNIKOV [13, 14], to include the *irreversible* processes going on in the gas of excitations and giving rise to viscosity and heat conductivity terms in the conservation equations and explaining the experimental fact about heat conductivity and viscosity in a satisfactory manner, but these phenomena will not be considered here.

It should be mentioned, however, that the whole picture is valid only at those temperatures where the density of excitations is relatively small, because at higher temperatures the distinction between a background fluid (= superfluid) in which the gas of excitations (= normal fluid) is moving, becomes illusory.

The question of how to explain the λ -point in this picture remains open. LANDAU takes the λ -point at *that* temperature, where ϱ_n as defined by (36) attains the value ϱ , but it is obvious that on the basis of the *present* picture of the normal fluid density in terms of the gas of excitations such an extrapolation of expression (36) for ϱ_n is difficult to justify. We will not give, however, a more detailed discussion of the λ -point as the main intention of this survey is to draw attention to these properties of liquid helium for which a satisfactory explanation has been found, this being the case in particular for the properties in the low temperature region.

6. - Theoretical description of the excitations in liquid helium.

6.1. *Introduction.* - From the discussion of the experimental data in terms of « thermal excitations » propagating through liquid helium, it follows that two types of thermal excitations are of particular importance:

1) excitations of elastic waves or « *collective excitations* », quantized in the form of « phonons »;

2) *molecular type of excitations*, which do not have this « collective » character. These represent probably localized excitations of one or more excited molecules. These excitations have been given the name « rotons », but we will speak of molecular excitations.

For a theoretical description of these different types of excitations an approach has been made from a purely hydrodynamical point of view by attempting to quantize the hydrodynamical equations of a non-viscous liquid. KRONING and THELLUNG [15] did this for the irrotational motions corresponding to phonon type excitations, whereas THELLUNG [16] and also ZIMAN [17] extended the theory by including vortex motions of a special type which could be treated with the usual Lagrangian formalism. The difficulty of this method lies in the fact that it starts as a pure continuum treatment of the condensed state in which the molecular structure enters indirectly via cut-off procedures, which are often not without arbitrariness, as explained in detail recently by THELLUNG [18].

It has been indicated previously [19, 8] by the present author that the existence of the two different types of excitations can also be understood on the basis of an extension of the well known «cell model» for the condensed state. The results obtained showed that further investigation along this line may be promising.

In fact the situation with respect to the collective motions possible in liquid helium is very similar to that existing in the case of the nucleus with the collective nuclear motions. Here, i.e. in the nuclear model of BOHR and MOTTELSON [20], one introduces collective (rotational) motions of the nucleus as a whole which, in addition to the individual particle motions, give a separate contribution to the Hamiltonian of the system. Although the results of this picture are extremely good, the theoretical basis for separating off the collective motions is still unsatisfactory and leaves many questions unanswered.

A generalization of the cell model for condensed helium which includes longitudinal elastic motions as collective modes, has been made in close analogy with the procedure used by BOHR and MOTTELSON in the nuclear model.

In the *usual cell model* for the condensed state the volume is divided up in a close packed system of N spherical cells of diameters $a^3 = (V/N)\sqrt{2}$, the centres R_1, R_2, \dots of which are located on the sites of a close packed lattice structure with smallest distance a . Each cell is supposed to contain one molecule and each molecule is moving in its cell in a potential field which is the average potential field due to the molecules in neighbouring cells, their average positions being the centres of their cells.

6'2. Generalization of the cell model. — The *generalization* proposed combines two different new features. The *first* generalization is based on the fact that when one is concerned with investigating the statistics, it is not advantageous to divide the system in N cells each containing 1 molecule, because then the exchange effects which occur between two or more molecules, cannot be treated at all. Instead one can combine the cells two by two or three by three in a certain regular way depending on the lattice and consider each such a cell-

cluster (composed of a group of two or more neighbouring cells) as one unit in which a corresponding group of two or more molecules moves, again under the influence of the average potential field of the groups of molecules located in neighbouring cell clusters. The *second* generalization includes the possibility of allowing the centres $\mathbf{R}_\alpha, \mathbf{R}_\beta, \dots$ of the cells to be displaced in such a way that these values correspond to the values of a given set of normal co-ordinates $Q_\sigma = \sum_\alpha \exp [2\pi i \boldsymbol{\sigma} \cdot \mathbf{R}_\alpha]$.

The quantum-mechanical formulation of the problem can then be made on the basis of the *adiabatic method* of Born and Oppenheimer: the collective motions are assumed to be slow compared with the molecular motions of the molecules in their respective cells. This assumption seems to be justified at least for collective motions with small values of the wave number σ : the spectrum of the collective excitations is a continuous spectrum starting from $E=0$, whereas the molecular excitations require a finite excitation energy corresponding to roughly 10 °K. According to the principles of the adiabatic method we thus first determine the eigenvalues $W(\mathbf{R}_\alpha, \mathbf{R}_\beta, \dots)$ corresponding to a given (deformed) lattice structure $\mathbf{R} = (\mathbf{R}_\alpha, \mathbf{R}_\beta, \dots)$, the corresponding eigenfunctions being

$$(46) \quad \Phi_n(\mathbf{p}; \mathbf{R}) = \prod_\alpha \varphi_{n_\alpha}(\mathbf{p}_\alpha; \mathbf{R}),$$

where the co-ordinates $\mathbf{p}_\alpha, \mathbf{p}_\beta$, etc., indicate the position vectors of the molecules in the cells α, β , etc., with respect to the origin of these respective cells and n_α indicates the set of quantum numbers indicating the state of the molecule in the cell α .

(It should be noted that the eigenfunctions in which the cell α is excited and others are in the ground state is not yet a proper eigenfunction because of the necessity to allow for the motion of such an excitation through the whole system [8, 21]).

The ground state energy $W_0(\mathbf{R})$ (as a function of the values of $\mathbf{R} \equiv (\mathbf{R}_\alpha, \mathbf{R}_\beta, \dots)$ corresponding to a certain set of values of Q_σ, \dots) now serves as potential energy in the equation for the eigenfunctions of the collective modes

$$(47) \quad \Omega_v(Q) = \prod_\sigma \Omega_{v_\sigma}(Q_\sigma),$$

where $\Omega_{v_\sigma}(Q_\sigma)$ is the eigenfunction of the collective modes $\boldsymbol{\sigma}$ with vibrational quantum number v_σ .

The total eigenfunction of the system can then be written as

$$(48) \quad \Psi_{n,v}(Q, \varrho) = \prod_\sigma \Omega_{v_\sigma}(Q_\sigma) \cdot \prod_\alpha \varphi_{n_\alpha}(\mathbf{p}_\alpha)$$

and the total energy

$$(49) \quad E_{v,n} = E_0 + \sum_{\sigma} v_{\sigma} \cdot \hbar c \sigma + \sum_{\alpha} (\varepsilon_{n\alpha} - \varepsilon_0),$$

when E_0 is the ground state energy of the system.

For a full exposition of the whole method we may refer to a recent survey article [8] and to a publication on the use of collective co-ordinates in the case of liquid helium [21]. It may be important to make one more remark about the fundamental difficulty in all theories which use collective co-ordinates: i.e. how to make the introduction of collective co-ordinates in compliance with the total number of degrees of freedom. In [8] this was established by using all the centres of mass of the groups of molecules in different cells as co-ordinates which were determined by a set of collective co-ordinates equal in number to the total number of centres of mass in the different cell clusters and treating the relative motions in the cells as « molecular » motions. Then of course no difficulty with the number of degrees of freedom arises. The procedure does not seem entirely satisfactory, however, because obviously the cell model with N cells in which each cell contains only one molecule, cannot be treated in this way, because then no possibility for molecular motions is left. If, however, one introduces a redundant set of co-ordinates Q_{σ} to describe the collective motions it is necessary to introduce simultaneously a set of subsidiary conditions to suppress the redundant degrees of freedom (*). In fact these subsidiary conditions can here be *satisfied approximately* by using the cell model in which the motion of the molecules has to satisfy certain constraints set by the deformation of the cell model which is imposed upon the system. Speaking quantum-mechanically one may say that the expectation values for the co-ordinates in the deformed cell system, which can be obtained from the wave function $\varphi_{n\alpha}(\mathbf{p}_{\alpha})$ for each molecule practically coincides with the centre of its cell and that thus these expectation values are approximately in agreement with the values set for these co-ordinates by the values of the collective co-ordinates Q_{σ} .

The method followed here thus leads to a molecular picture of the two types of excitations:

1) the collective excitations associated with the collective co-ordinates occurring in the wave functions $\mathcal{Q}(Q_{\sigma})$ with excitation energies $v_{\sigma} \cdot \hbar c \sigma$;

2) molecular excitations associated to internal cell motions described by the wave functions $\varphi(\mathbf{p}_{\alpha})$.

(*) See e.g. the nice review article by D. TER HAAR [23] in which different methods of dealing with collective co-ordinates are treated. See in particular also [22] Y. WATANABE's discussion based on classical mechanics and the paper of W. BRENIG [24] on the application of such concepts in the case of liquid helium.

6'3. *Collective modes.* — As far as the *collective modes* are concerned it has to be remembered that the wave number σ should always be kept small compared with the reciprocal lattice distance in the system, because for too large values of σ the assumption on which the collective model is based, i.e. that the collective motions can be considered to be slow compared with the internal cell motions, is no longer valid. Therefore the expression $\nu = c\sigma$ for the frequency wave number relation with constant c is probably a fairly good approximation. In fact our calculations for the contribution which these collective excitations give to the thermodynamic quantities of liquid helium were based on this assumption.

It is of interest, however, to investigate what would be the effect of the molecular structure on the $\nu(\sigma)$ relation, i.e. what dispersion relation results from the molecular structure of liquid helium. Unfortunately a theoretical treatment for the dispersion relation in the liquid state is not a simple matter. In order only to get an impression of what may happen we will satisfy ourselves with the dispersion which would occur in solid structure of the density of liquid He. In Fig. 13 the frequency-wave number curve has been presented calculated for a very simplified model (simple cubic structure) for waves propagating in the (100)-, the (110)- and (111)-direction. Making the appropriate average over different directions one finds the curve with maximum and minimum as presented in the figure. It is of interest that the curve as a whole shows qualitatively the same features as the overall dispersion curve assumed by LANDAU to exist for excitations in liquid helium. The part of the excitation curve in the region of small σ -values has to be associated with the phonon type of excitations in which the relation $\varepsilon = h\nu = hc\sigma$ is valid. In the range of large σ -values, i.e. near the maximum and minimum in the range of the reciprocal Debye wave length $\sigma_D = 1/\lambda_D \approx 0.62/\bar{a}$ (when $\bar{a} \approx 3.6 \text{ \AA}$ is the average distance between the molecules), the approach is no longer valid and the excitations are no longer collective, but on the contrary molecular

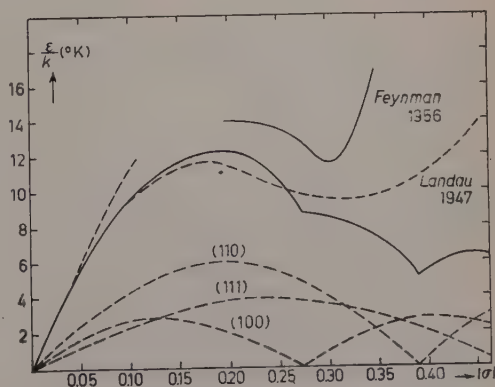


Fig. 13. — Relation between $\varepsilon = h\nu$ and σ according to a very simplified calculation for a cubic structure of ^4He . The three interrupted curves represent $\varepsilon(\sigma)$ for the (100)-, (110)- and (111)-direction respectively, the drawn curve represents the average curve (averaged over all directions). The curves are compared with the experimental curve and that obtained by FEYNMAN and COHEN.

and that obtained by FEYNMAN and COHEN.

in character. In fact near the maximum the wave length is such that neighbouring molecules are moving *in opposite phase* ($\lambda_{\max} \approx 6 \text{ \AA}$), whereas in the region of the minimum they are moving *in phase* ($\lambda_{\min} \approx 3.2 \text{ \AA}$).

These very qualitative considerations may show once more that the $\varepsilon(\sigma)$ curve as found by experiment can be understood as a whole by considering only the longitudinal elastic modes: the long wave-length part gives the phonons, the short wave-length part in the dispersion region is associated to molecular vibrations of a very short wavelength for which the collective description seems to be not appropriate and for which a molecular description would be more promising.

The present considerations throw also another light on the physical meaning of the results obtained by FEYNMAN [25] and by FEYNMAN and COHEN [26] for the dispersion relation in liquid helium. In fact these results were obtained with a variational method in which the trial wave function for the excitations was assumed to be of the form:

$$\Psi_{\sigma} = \Psi_0 \cdot \sum_{i=1}^N \exp [2\pi i \sigma \cdot \mathbf{r}_i] \approx \Psi_0 \cdot Q_{\sigma}.$$

Now for a harmonic oscillator the wave function for the first excited state: $\Omega_1(Q) = Q \exp [-\frac{1}{2}\alpha Q^2]$, can be obtained from that for the ground state: $\Omega_0(Q) = \exp [-\frac{1}{2}\alpha Q^2]$, by multiplication with Q , which makes the wave function $\Psi_{\sigma} \cdot Q_{\sigma}$ a reasonable guess for the excited states at long wave lengths. In fact also here one obtains, by using this same wave function in the region of small wave lengths a curve with a maximum and a minimum (given also in Fig. 13), the physical origin of which is undoubtedly the same as that for the qualitative dispersion curve evaluated from the mechanics of the lattice.

6.4. Molecular excitations. — We now finally would like to come back to the nature and excitation energies of the *molecular excitations* which follow from the cell model. If we consider a cell model in which the cells are all considered separately and in which every cell is occupied by one particle only, the first excited state is of the order of magnitude of 18°K . There is, however, little doubt that in these molecular excitations the exchange between particles, i.e. the symmetry effects play an important role. Therefore it is more promising to combine the cells of the cell model in a regular way to cell clusters, as mentioned in the beginning of this section. As a more detailed report on these aspects of the cell treatment has been given elsewhere, we will only shortly explain the results which are summarized in Fig. 14. When we combine the cells into cell clusters of two neighbour cells containing two molecules each, the excitation energies are approximately those of a rigid «dumbbell» rotator in which the molecules are on the average distance a . This distance is somewhat different for ^3He and ^4He , making the excitation

energies somewhat different also. However, the symmetry properties make that in the case of ^4He the odd levels are forbidden leaving a first excitation energy of roughly 6.75°K for ^4He and 2.5°K for ^3He . Moreover the states have entirely different weights due to the nuclear spin of ^3He . If one makes the cell clusters larger than two cells, one finds for the « plane rotators » in the cell clusters composed of three neighbouring cells (arranged in an equilateral triangle) and for the « spherical rotators » in the cell clusters composed of four neighbouring cells (arranged in a tetrahedron) in the T_a^2 -lattice a very similar behaviour because of the symmetry properties. It is illuminating to see the difference between ^4He and ^3He : in the case of ^4He there remains a finite excitation energy for all models of about $6 \div 7^\circ\text{K}$, however in the case of ^3He

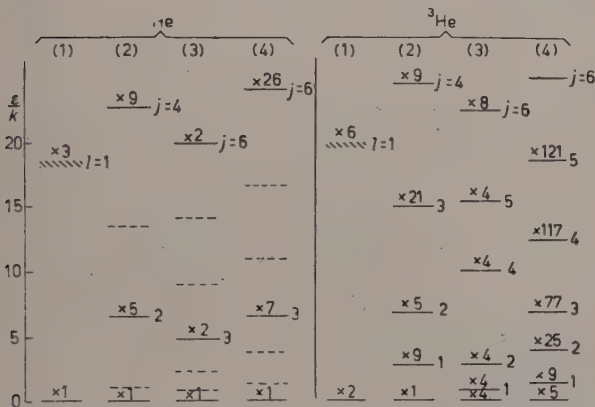


Fig. 14. — Energy levels of molecules (or groups of molecules) in their cells (or cell clusters) according to the cell model. The figures 1 to 4 indicate the number of molecules per cell, $\times 5$, $\times 9$, etc. indicate the multiplicity and $j=2, 4$, etc. indicate the rotational quantum numbers.

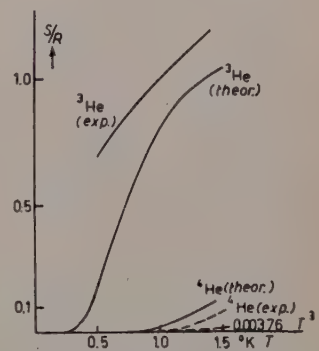


Fig. 15. — Entropy of liquid ^4He and ^3He as calculated from the cell model using cell clusters of two cells, each containing two molecules.

the excitation energy becomes smaller and smaller the larger the cell cluster becomes and also the lowest state becomes degenerate. All this points to an enormous difference in the behaviour of the entropy due to the molecular excitations in ^4He and in ^3He . For the case of cell clusters with two molecules the entropy curve has been plotted in Fig. 15 for ^4He and ^3He . The large values for ^3He at low temperatures are due to the small excitation energies and large statistical weights which make the contribution of the low lying excited states to the thermodynamic properties in ^3He very different from those of ^4He , where the molecular excitations only start to contribute at temperatures $T \approx 0.6^\circ\text{K}$. For the case of more molecules per cell cluster the difference is even more striking because here the entropy for ^3He would ap-

proach a finite non-zero value. Of course the interaction of the groups of molecules in different cell clusters lifts the degeneracy and would make the entropy fall to zero at much lower temperatures.

Summarizing we may conclude that the cell model thus offers a description for some of the features of the thermal excitations of liquid helium and in particular leads to an explanation of the striking difference in entropy between the two isotopes of helium.

REFERENCES

- [1] J. DE BOER: *Physica*, **14**, 139 (1948).
- [2] F. LONDON: *Proc. Roy. Soc., A* **153**, 576 (1936); *Superfluids*, vol. II (Amsterdam, 1957) p. 1.
- [3] J. S. DUGDALE and F. E. SIMON: *Proc. Roy. Soc., A* **218**, 291 (1953).
- [4] W. LENZ: *Zeits. f. Phys.*, **56**, 778 (1929).
- [5] K. HUANG and C. N. YANG: *Phys. Rev.*, **105**, 767 (1957); T. D. LEE, K. HUANG and C. N. YANG: *Phys. Rev.*, **106**, 1135 (1957); F. J. DYSON: *Phys. Rev.*, **106**, 20 (1957).
- [6] K. A. BRUECKNER and K. SAWADA: *Phys. Rev.*, **106**, 1117, 1128 (1957).
- [7] K. R. ATKINS and M. H. EDWARDS: *Phys. Rev.*, **97**, 1429 (1955).
- [8] J. DE BOER: in *Progress in Low Temperature Physics*, vol. II (Amsterdam, 1957). Ch. I.
- [9] L. LANDAU: *Journ. Phys. USSR*, **5**, 71 (1941).
- [10] L. LANDAU: *Journ. Phys. USSR*, **11**, 91 (1947).
- [11] H. A. KRAMERS: *Physica*, **18**, 653 (1952).
- [12] R. KRONIG: *Physica*, **19**, 535 (1953).
- [13] I. M. HALATNIKOV: *Žu, Eksp. Teor., Fiz.*, **23**, 8 (1952).
- [14] L. LANDAU and I. M. HALATNIKOV: *Žu. Eksp. Teor., Fiz.*, **19**, 637, 709 (1949).
- [15] R. KRONIG and A. THELLUNG: *Physica*, **18**, 749 (1952).
- [16] A. THELLUNG: *Physica*, **19**, 217 (1953).
- [17] J. M. ZIMAN: *Proc. Roy. Soc., A* **219**, 257 (1953).
- [18] A. THELLUNG: *Helv. Phys. Acta*, **29**, 103 (1956).
- [19] J. DE BOER and E. G. D. COHEN: *Physica*, **21**, 79 (1955); *Proc. Intern. Conf. Low Temp. Phys.* (Paris, 1955), p. 113.
- [20] A. BOHR and B. R. MOTTELSON: *Dan. Mat. Fys. Medd.*, **27**, no. 16 (1953).
- [21] J. DE BOER: to be published in *Physica* (1958).
- [22] Y. WATANABE: *Proc. Theor. Phys.*, **16**, 1 (1956).
- [23] D. TER HAAR: *Rep. on Progr. Phys.*, **20**, 130 (1957).
- [24] W. BRENIG: *Zeits. f. Phys.*, **144**, 488 (1956).
- [25] R. P. FEYNMAN: *Phys. Rev.*, **91**, 1301 (1953); **94**, 262 (1954).
- [26] R. P. FEYNMAN and M. COHEN: *Phys. Rev.*, **120**, 189 (1956).
- [27] R. LIMBECK: *Dissertation Amsterdam* (1951), in Dutch; for ^3He , ^4He see: J. DE BOER: in *Progress in Low Temperature Physics*, vol. I (Amsterdam, 1955), Ch. 18; for H_2 see: E. G. D. COHEN, M. J. OFERHAUS, J. M. J. VAN LEEUWEN, B. W. ROOS and J. DE BOER: *Physica*, **22**, 791 (1956).

INTERVENTI E DISCUSSIONI

— C. DOMB:

1) I should like to ask Professor DE BOER how he calculated the zero-point energy of the solid for different crystal structures for large λ^* .

2) The assumption that $C_{44} < 0$ for solid helium at absolute zero means that the solid phase is unstable. An alternative possible interpretation is that the solid phase is metastable.

— J. DE BOER:

1) The zero-point energy is for all structures assumed to be the same function of the density, viz. that calculated for a close-packed cell-model.

Recent Experiments on Superfluidity.

K. MENDELSSOHN

Clarendon Laboratory - Oxford

In the first experiments on the passage of He II through narrow slits and capillaries it was noted that, besides the astonishingly high flow rate, the transport of liquid also appeared to be highly independent of pressure head. This phenomenon was even more pronounced in the transfer of liquid by means of the film where it completely dominates the flow pattern. These latter observations led to the concept of a «critical» rate of transport below which no dissipation will occur and which is somewhat analogous to the critical current in a superconductor. On the other hand, early observations on He II transport in wider capillaries did not at all support this idea and in particular by an analysis of the heat conductivity measurements of KEESOM and his co-workers, GORTER was able to show that friction in liquid helium seemed to set in gradually, the force depending on the cube of the relative velocity between normal and superfluid component. In order to investigate this question further, flow experiments through narrow slits and compressed powder were carried out at Oxford [1, 2] which showed clearly the existence of a critical velocity in the latter case and in slits of 10^{-4} cm diameter if the flow took place under a thermal gradient. It was also demonstrated that, when the slit width was increased to 10^{-3} cm the phenomena became obscured by the motion of normal fluid which was carried in the flow. Subsequent experiments by WINKEL and others [3] in Leiden, using counterflow in narrow slits, too, have demonstrated the existence of a critical velocity.

Experiments on the transfer of helium by films in contact with the unsaturated vapour [4] showed with regard to the critical velocity much the same pattern as the saturated film. Superflow was observed to occur, at a given temperature and percentage saturation, up to a sharply defined critical rate. In view of the wide discrepancies between the experimental values of the adsorption isotherms, it is difficult to express these critical rates rigorously

as functions of film thickness. However, the results indicate that, whereas for the saturated film the rate becomes largely temperature independent below 1.5 °K, in the case of the unsaturated films the rate rises progressively as the temperature is lowered. A similar observation has recently been made by CHAMPENEY [5] when measuring the flow rate of liquid helium through porous glass with an average channel size of $\sim 10^{-7}$ cm. Although in one of his experiments the rate increased with falling temperature by a factor of 10^5 the curve showed no sign of becoming concave against the temperature axis.

Thus, while the existence of a critical velocity could be clearly demonstrated in films and in narrow slits, no evidence for it could be found in channels larger than 10^{-3} cm because in these normal flow becomes predominant and does not permit a clear analysis of superfluidity. Another difficulty arises from the fact that, as the channel size is increased, the critical volume flow rate appears to diminish. This fact in itself makes it harder to observe critical rates in larger capillaries.

In principle, a straightforward heat conductivity experiment, such as shown in Fig. 1, should allow a decision as to the existence of a critical rate in wider tubes. C is a capillary which connects a bulb with the helium bath B . The bulb which is thermally isolated from the bath carries a thermometer T and a heater H . As heat is supplied by H , normal fluid is excited in the bulb and passes through the capillary into B , while an equal amount of superfluid must flow from B into the bulb in order to maintain constant density. If, for velocities smaller than the critical, the transport of superfluid takes place without dissipation against either the walls or the normal fluid, then the thermal resistance along the capillary $\Delta T/\dot{Q}$, is entirely due to the viscous drag of the normal fluid. The heat \dot{Q} is given by the heat of transport as

$$\dot{Q} = \rho \dot{V} S T,$$

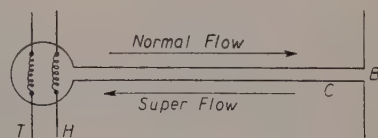


Fig. 1. - Arrangement for measuring the thermal resistance of liquid helium in a capillary.

where S is the total entropy of the liquid and \dot{V} the volume flow rate. For a capillary of radius a and length l , Poiseuille's law requires

$$\dot{V} = (\pi a^4 / 8 \eta l) \Delta p,$$

with the pressure difference Δp given by H. London's formula as

$$\Delta p = \rho S \Delta T,$$

from which the thermal resistance derives as

$$\Delta T/\dot{Q} = \eta (8l/\pi a^4)(1/\rho^2 S^2 T).$$

It is significant that in the subcritical region the thermal resistance should be independent of the heat current and the onset of dissipation can therefore be observed as a rise in the thermal resistance for a critical value of \dot{Q} . However, it was impossible in the earlier experiments on the heat conduction of He II in capillaries to apply this criterion because slight temperature fluctuations of the bath completely obliterate the predicted phenomenon which is confined to the region of small values of \dot{Q} .

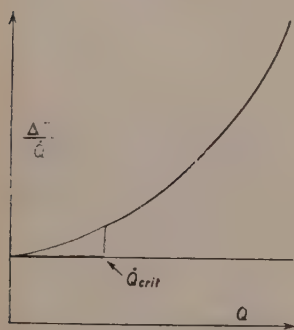


Fig. 2. - The thermal resistance $\Delta T/\dot{Q}$ of He II as function of the heat current \dot{Q} .

increase. A discussion of the exact form of the latter lies outside the scope of this paper and we are here only concerned with the *onset* of mutual friction. It is, however, important to note that above this onset the thermal resistance follows a curve which extrapolates back to the same value for $\dot{Q} = 0$ as in the case without mutual friction. The results thus seem to indicate that two distinct types of flow mechanism can occur in the capillary, one in which the superfluid suffers no dissipation whereas it does encounter friction in the other. While for small velocities the former is stable, the latter is the stable flow mechanism for high velocities. At a given critical velocity the mechanisms pass over into each other almost discontinuously.

Recently BREWER and EDWARDS in Oxford have perfected a cryostat in which the temperature of the helium bath below the lambda-point can be kept constant within $\sim 2 \cdot 10^{-5}$ deg and they have used the arrangement shown in Fig. 1 to determine the value of η . They found that indeed for small values of \dot{Q} the thermal resistance was independent of the heat current and thus proved the existence of a sub-critical velocity region for capillaries of 10^{-2} cm diameter [5]. The onset of non-linear friction in the capillary is shown diagrammatically in Fig. 2 where the thermal resistance is plotted against the heat current. While for small values of \dot{Q} the resistance remains constant, a sudden rise occurs at a given heat current which is followed by a more gradual

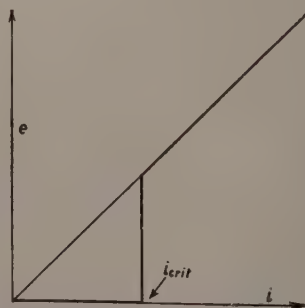


Fig. 3. - The electric field e as function of the current i in a superconductor.

The situation in liquid helium is therefore somewhat analogous to the well known behaviour in superconductors where, as shown in Fig. 3, a current will flow under zero electric field, i.e. without dissipation until, at a definite value of the current density, the electric field rises suddenly. The onset of dissipation is marked by a discontinuous transition from superconductivity to Ohm's law. It is well known that this region is in superconductivity marked by hysteresis phenomena and the analogy is strengthened by the fact that in liquid helium, too, very pronounced hysteresis can occur at the transition. It was found that, as \dot{Q} was gradually increased, the thermal resistance would remain constant up to remarkably high values of the heat current. Then suddenly a completely discontinuous transition to a state of high heat resistance would take place. On reducing \dot{Q} again, the thermal resistance would drop gradually and the transition to frictionless superflow would not occur until a fairly low value of \dot{Q} has been reached. Reducing the heat flow now to zero and then increasing it again will, however, not result in a similar hysteresis phenomenon. On the contrary, the transition would now take place close to the value of \dot{Q} at which it occurred when the heat current was reduced. It was noticed that a very considerable time (of the order of one hour) had to elapse between successive experiments; in order to reproduce a large hysteresis. Furthermore, when the heat current in the tube was larger than the equilibrium critical value but no transition had occurred owing to this hysteresis phenomenon, mechanical disturbance, such as tapping the cryostat, would produce a discontinuous transition to the dissipative flow mechanism.

Our observation of a discontinuous transition from superfluidity to dissipative flow has recently been corroborated by observations of VINEN [6] in Cambridge who found a sudden rise in attenuation of second sound which was radiated across a tube of liquid helium carrying a heat current. The observation seems to indicate the existence of a sharply defined critical velocity.

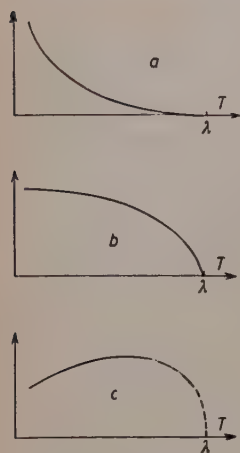
It is possible that the wide scatter of result obtained in work where attempts have been made to determine critical velocities may be due to the occurrence of hysteresis phenomena, such as the one described above, which may easily falsify the observations. Combining our data and those of VINEN with the critical velocities obtained in films and narrow slits, it appears that they can best be represented by the expression

$$v_{\text{crit.}} = \text{const } d^{-\frac{1}{2}},$$

where d is the diameter of the capillary. This type of law has been proposed by MOTT [7] and also by DASH [8].

The variation of the critical rate with temperature is well known for the saturated film, at least down to 1 °K. There is some uncertainty concerning the lower temperatures. The behaviour in sub-saturated films and in wide

capillaries is less well established and at our present state of knowledge little more can be done than sketching the qualitative behaviour for these two cases



which are shown in Fig. 4. It is evident that our information on these phenomena is very incomplete and that further and more reliable data will have to be obtained before conclusions as to the nature of the transition phenomenon can be drawn. In particular, it will be necessary to have a much clearer picture of the manner in which vorticity is established and destroyed. Perhaps experiments similar to those reported by Professor CARERI may be able to elucidate these processes.

Fig. 4. — Diagrammatic sketch of the variation of the critical velocity $\dot{V}_{\text{crit.}}$ as function of the absolute temperature between 1 °K and the λ -point in (a) the unsaturated film and pores of 10^{-7} cm diameter, (b) the saturated film and (c) capillaries of $\sim 10^{-2}$ cm diameter.

REFERENCES

- [1] R. BOWERS and K. MENDELSSOHN: *Proc. Roy. Soc., A* **213**, 158 (1952).
- [2] B. S. CHANDRESEKHAR and K. MENDELSSOHN: *Proc. Roy. Soc., A* **218**, 18 (1953).
- [3] P. WINKEE, A. M. DELSING and F. D. POLL: *Physica*, **21**, 331 (1955).
- [4] R. BOWERS, D. F. BREWER and K. MENDELSSOHN: *Phil. Mag.*, **42**, 1445 (1951).
- [5] D. C. CHAMPENEY: *Proc. Int. Conf. on Low Temp. Physics* (Madison, 1957).
- [6] W. F. VINEN: *Proc. Roy. Soc., A* **240**, 114 (1957).
- [7] N. F. MOTT: *Phil. Mag.*, **40**, 61 (1949).
- [8] T. C. DASH: *Phys. Rev.*, **94**, 825, 1091 (1954).

INTERVENTI E DISCUSSIONI

— J. C. DASH:

I was very pleased to see that these measurements appear to agree with the square-root law $V_c \propto d^{-\frac{1}{2}}$ for the variation of critical velocity with channel size. I would draw attention to the further agreement of the observed variation of V_c with the predicted temperature dependence. This variation is predicted by my model to be proportional to $\rho_s^{-\frac{1}{2}}$, which yields a gradual increase with temperature of V_c at low temperatures, the increase accelerating as the λ point is approached.

— A. VAN ITTERBEEK:

May I ask Dr. MENDELSSOHN if the picture of the change transition in capillary tubes has not to be approached to the superconductivity in thin films?

— K. MENDELSSOHN:

The conditions seem to be similar to those in superconductors where resistance hysteresis has been found to occur. However, just as in superconductors, we are not quite clear why hysteresis effects in helium occur in some capillaries and not in others.

— L. ONSAGER:

- 1) Has an analogue of the intermediate state been observed in helium?
- 2) What do you think of the rotating bucket experiments?

— K. MENDELSSOHN:

While it is true that above the onset of friction dissipation occurs in the superfluid, the state is clearly different from He I. However, it is doubtful whether one should equate this state with the intermediate state in superconductors since, owing to the magnetic effects, the latter is a true mixture of phases in co-ordinate space. There may well exist a similarity between the vortex formation in the rotating bucket and in our tubes but so far we know too little about either to form useful conclusions.

— H. C. LONGUET-HIGGINS:

Do you consider that the waiting period necessary to reproduce the hysteresis is due to diffusion of the vortex in the superfluid to the walls of the vessel?

— K. MENDELSSOHN:

Expansion of a vortex ring and its absorption on the wall of the tube would appear the most likely process responsible for hysteresis but it is difficult to see why the time involved should be so long.

— G. CARERI:

Dr. THOMSON and Dr. SCARAMUZZI in our Laboratory have found anomalous changes in a steady state conjugation current produced by γ -ray ionization in liquid He II upon application of large heat flows. It is conceivable that some of the effects noted could be due to turbulence since they occur roughly at the critical velocities observed by you and Hall and Vinen. These effects are now under further investigation.

— W. FAIRBANK:

In a liquid helium bubble chamber built at Duke University we have observed the formation of bubbles without the presence of ionizing radiation in liquid helium below the λ point. The bubbles are formed when the liquid is expanded by means of a piston in contact with the liquid to a negative pressure of about 100 mm. From experiments above the λ point this appear to be too small a change in pressure to cause bubble tracks along the ionizing path of radiation. The question is raised as to whether the nuclei for the bubbles observed below the λ point are quantized vortex lines. If so this might be another method of observing vortex lines.

PARTE SESTA

Statistical Mechanics of Quantum Systems.

The Equilibrium Phase Transition in Liquid Helium.

E. MAYER

The E. Fermi Institute for Nuclear Studies, University of Chicago - Chicago.

Summary. — In collaboration with H. AROESTE and S. BALDURSSON we have attempted an investigation of the properties of a Bose-Einstein liquid. The essential feature of the treatment is to express the properties of the Bose-Einstein liquid in terms of those of an hypothetical Boltzmann liquid for which the density matrix has not been symmetrized. The pair and higher distribution functions of the Boltzmann liquid enter the equations. The X-ray diffraction pattern of He I is used to obtain the necessary function for two atoms, and the Kirkwood closure assumed for the higher functions. The parameters necessary to reproduce some of the features observed in the transition are all reasonable.

INTERVENTI E DISCUSSIONI

— M. J. BUCKINGHAM:

What is in fact the order of the transition you find in your approximation and what is the asymptotic dependence of the cluster integrals on size of cluster?

— J. E. MAYER:

With the crude approximation which we have so far used, the integrals β_n for n particles go as

$$\beta_n = \beta_0^n u^{-\frac{n}{2}},$$

as the equivalent integrals in the perfect gas theory do. The integrals enter the equations for the thermodynamic properties in a different way than in the perfect gas theory and the transition is found to be third order.

Quantum Statistics of Interacting Particles.

E. W. MONTROLL and J. C. WARD

Department of Physics University of Maryland - College Park

Summary. — A systematic generalization of the Mayer cluster integral theory has been developed to deal with the quantum statistics of interacting particles. The grand partition function appears in a natural way and the cluster integrals are integrals over propagators which are derived from the Green's function solution of the Bloch equation (which follows from the Schrödinger equation by replacing $i\hbar$ by $\beta = 1/kT$). Every cluster integral can be represented by a hybrid of a Mayer graph and a Feynman diagram. The indistinguishability of particles causes each particle (or vertex) in a Mayer cluster integral to be replaced by a «toron» which can be described in the following manner through a Feynman diagram. Consider an (r, β) space in the form of a torus of tubal circumference β . A toron of order n is represented by a closed path which loops the torus n times so that a cut at constant β' (with $0 < \beta' < \beta = 1/kT$) on the torus identifies the position of n particles at β' but which in the absence of a cut gives no indication of where one particle ends and another begins. The grand partition function is a sum over all graphs in which torons are connected by interaction lines that represent quanta of energy and momentum exchanged through collisions. Self interaction lines on torons must be included. The cluster integrals associated with rings of torons have been analyzed. It is shown that in the case of the electron gas the classical limit of the contribution of these integrals to the grand partition function yields the Debye-Huckel theory while the low temperature limit leads to the Gell-Mann Brückner equation for the correlation energy of the ground state. A prescription was given for the construction of the cluster integral associated with any given diagram.

A complete account of this work is published in the Jan. 1957 issue of *Journ. of Fluid Physics*.

INTERVENTI E DISCUSSIONI

— G. UHLENBECK:

If your method is applied to a Bose gas of hard spheres, would you still end up with a development in a/λ ?

— J. C. WARD:

I think so, but I am not yet sure.

— O. PENROSE:

Can interactions with hard cores be treated by this method?

— J. C. WARD:

Yes, although one has first to solve the two body problem, and so on, for the particular diagram that one wishes to treat.

Note sur les corrélations dans un fluide quantique en équilibre.

J. YVON

Centre d'Études Nucléaires. de Saclay - Gif-sur-Yvette (S. et O.).

1. - L'opérateur densité double.

Dans un fluide non quantique les corrélations spatiales entre les molécules considérées deux à deux sont définies par la densité double n_{12} .

Rappelons à ce sujet quelques formules simples. Il est commode pour l'exposé de supposer qu'un champ appliqué écarte les molécules de la répartition uniforme.

D'abord l'expression de la densité en fonction de l'activité z (definition de Guggenheim):

$$(1) \quad n_1 = z \exp \left[-\frac{V_1}{kT} \right] \left\{ 1 + z \int \left(\exp \left[-\frac{W_{12}}{kT} \right] - 1 \right) \exp \left[-\frac{V_2}{kT} \right] d\tau_2 + z^2 \times \dots + \dots \right\}.$$

Ensuite celle de la densité double

$$(2) \quad n_{12} = z^2 \exp \left[-\frac{V_1 + V_2 + W_{12}}{kT} \right] (1 + z \times \dots + \dots).$$

Il s'agit de développements en série entière par rapport à z dont seuls les premiers termes sont écrits. La convergence est assurée d'une part tant que z n'est pas trop grand, d'autre part par la courte portée des forces intermoléculaires. Les forces sont, pour simplifier, supposées essentiellement binaires.

Dans un mémoire paru dans *Nuclear Physics* (Août 1957) l'auteur a tenté d'obtenir des formules analogues pour un fluide quantique. La présente note est destinée à en donner un rapide commentaire.

Le difficulté réside:

- 1) dans l'impossibilité de séparer les problèmes de l'espace ordinaire des problèmes de l'espace des impulsions;

représentés par ε , seraient partiellement rejetés aux termes d'ordre supérieur et fortement estompés. Nous préférons conserver les développements (3) et (4), mais sans dissimuler les faiblesses de cette manière de faire.

Quand il n'y a pas d'interaction du tout, les formules (3) et (4) deviennent respectivement

$$(5) \quad \frac{\mu_1}{1 + \varepsilon\mu_1} = j_1 \quad \text{ou} \quad \mu_1 = \frac{j_1}{1 - \varepsilon j_1},$$

$$(6) \quad \mu_{12} = (1 + \varepsilon P_{12})\mu_1\mu_2.$$

Ces résultats, qui conviennent au gaz parfait, n'ont d'original que les notations.

2. — Condensation de Bose-Einstein.

Considérons un système de bosons sans interaction. A température constante et à volume constant la densité croît avec z . La condensation de Bose-Einstein survient pour $z=1$.

Supposons maintenant qu'il y ait une interaction. Pour fixer les idées supposons que cette interaction n'entraîne pas l'existence d'état lié. La plus basse valeur propre de l'énergie d'un couple de bosons est alors 0. La plus grande valeur propre de l'opérateur j_{12} est, corrélativement, z^2 . Il en résulte une anomalie des corrélations pour $z=1$ — d'après le dénominateur de la formule (4) — qui retentit sur μ_1 à travers le terme du second ordre et qui peut avoir un certain rôle dans le phénomène de condensation que les théoriciens admettent généralement survenir aussi bien dans un fluide avec interaction que dans un gaz parfait.

C'est avec intention que dans la formule (4) on a maintenu un ε^2 qui aurait bien pu être remplacé par 1. L'intention était de marquer que l'anomalie qui peut se produire avec des bosons peut se produire aussi avec des fermions. Elle n'est pas de même nature puisque — pour μ_1 — elle n'apparaît pas au premier ordre. Disons seulement ici qu'il sera peut-être intéressant de rechercher si dans un système de fermions de grandes valeurs de z — de l'ordre de 1 — n'entraînent pas un changement de structure.

Note sur les corrélations dans les gaz comprimés.

P. G. DE GENNES

Centre d'Études Nucléaires de Saclay - Gif-sur-Yvette (S. et O.).

1. - Introduction.

Nous utiliserons la formule démontrée par YVON [1] pour un fluide classique sous la forme

$$(1.1) \quad -k_B T \frac{\delta n}{\delta V} = 1 + \int d\mathbf{R}_2 \frac{n_{12} - n^2}{n} \exp[i\mathbf{k} \cdot \mathbf{R}_{12}].$$

Les notations sont celles de [1] : n_k est l'amplitude d'une modulation sinusoïdale de densité due à la perturbation sinusoïdale d'énergie potentielle, d'amplitude δV_k . La longueur d'onde de la perturbation est $2\pi/k$.

Pour déterminer la fonction de corrélation n_{12} on se propose d'utiliser des formes approchées de n_k / V_k .

La méthode suggérée par YVON [1] consiste à utiliser un développement en série d'Ursell qui exprime le potentiel à appliquer en chaque point pour stabiliser une distribution donnée de densité.

Le résultat s'écrit

$$(1.2) \quad \frac{1}{k_B T} \frac{\delta V_i}{\delta n_i} = -1 + \frac{1}{n} \int d\mathbf{R}_2 H_{12} \exp[i\mathbf{k} \cdot \mathbf{R}_{12}],$$

où H_{12} est donné sous forme d'un développement en série de puissances de la densité n .

Il y a d'ailleurs d'autres façons d'évaluer $\delta V_k / \delta n_k$ (ou H_{12}): par exemple, dans l'approximation cellulaire on écrira l'équilibre de chaque atome dans une cellule un peu déformée par la perturbation sinusoïdale δV_k . Nous avons appliqué une technique de ce genre au problème analogue des corrélations de spin dans un cristal ferromagnétique [2].

Toutefois, ces approximations cellulaires, par leur nature même, ne couplent

que les valeurs de la densité entre des points voisins. La fonction H_{12} qui en résulte n'est différente de 0 que lorsque R_{12} est inférieur au rayon de la cellule: la portée de H_{12} est ainsi *artificiellement limitée*. (Ceci n'empêche pas d'ailleurs les corrélations n_{12} que l'on en déduit, de s'étendre aux longues distances, comme le montre (1)). Mais on peut espérer, d'après la structure du développement d'Ursell de H_{12} [1], que H_{12} est effectivement une fonction à portée limitée; nous allons illustrer cette remarque, sur un exemple, par l'étude des premiers termes du développement.

2. - Résultats pour l'argon.

Plutôt que d'étudier toute la fonction H_{12} nous nous bornerons à envisager

$$(2.1) \quad L_2 = \frac{1}{6n} \int d\mathbf{R}_2 R_{12}^2 H_{12}.$$

Comme l'intégrale de H_{12} sur tout l'espace est connue, (et positive pour les densités inférieures à la densité critique)

$$(2.2) \quad \frac{1}{n} H_{12} d\mathbf{R}_2 = 1 - \frac{1}{k_B T} \frac{\partial p}{\partial n},$$

la connaissance de L_2 permet d'avoir une idée sur la « portée » de H_{12} . Le calcul de L_2 a été fait pour une interaction du type Lennard-Jones

$$(2.3) \quad W(R) = 4\varepsilon \left[\left(\frac{\sigma}{R} \right)^{12} - \left(\frac{\sigma}{R} \right)^6 \right].$$

On s'est limité aux deux premiers termes du développement d'Ursell-Yvon pour H_{12} , la contribution du premier étant calculée à la main, celle du second sur une machine IBM 650. Les températures choisies étaient $T_c = 1.3 \varepsilon/k_B$ (valeur qui correspond à la température critique pour l'argon) et $T_1 = 2\varepsilon/k_B$. Les résultats sont les suivants:

$$(2.4) \quad L_2(T_c, n) = \frac{2\pi}{3} n\sigma^3 [2.50 - 0.17 n\sigma^3] + O(n^3),$$

$$(2.5) \quad L_2(T_1, n) = \frac{2\pi}{3} n\sigma^3 [1.64 - 0.33 n\sigma^3] + O(n^3).$$

La conclusion essentielle, valable dans les limites de validité du développement utilisé, est la suivante:

1) Pour les températures étudiées et même pour les densités comparables à la densité critique ($n_c \sigma^3 = 1/3.16$ pour l'argon) L_2 est positif.

2) Dans les conditions critiques, le deuxième terme du développement de L_2 ne représente encore que 2% environ du premier: ceci est un indice favorable quant à la convergence générale de la méthode.

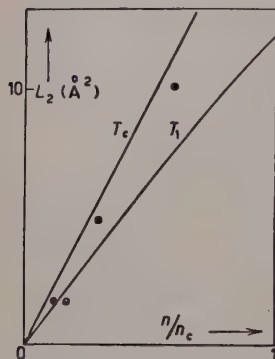


Fig. 1. — Valeurs numériques de L_2 pour l'argon. Trait plein: valeurs théoriques pour $T = T_c$ et $T = T_1 = 1.54 T_c$. Points: valeurs estimées d'après les mesures de EISENSTEIN et GINGRICH pour $T = 1.02 T_c$.

Les résultats obtenus pour l'argon sont représentés sur la figure.

Il est possible en principe de déduire L_2 des mesures de diffusion faites avec les rayons X: lorsque l'angle de diffusion est petit, l'intensité diffusée prend la forme asymptotique

$$(2.6) \quad I(k) = |F(k)|^2 \frac{1}{(1/k_B T)(\partial p / \partial n) + L_2 k^2},$$

k est la longueur du vecteur de diffusion; $|F(k)|^2$ est un facteur de forme.

Lorsque L_2 est positif (3.6) prévoit un maximum de diffusion vers l'avant. Ce maximum a été effectivement observé au voisinage de la température critique: il est très apparent sur les courbes d'Eisenstein et Gingrich relatives à l'argon [3]. Toutefois, en raison des difficultés inhérentes à la diffusion aux petits angles, les déterminations de L_2 par ce procédé sont très imprécises (quelques points sont représentés sur la Fig. 1). Des résultats plus détaillés pourraient être obtenus par l'emploi de neutrons de grande longueur d'onde.

Les calculs numériques ont été effectués par Madame D. PILLARD et M. J. LECLERC.

REFERENCES

- [1] J. YVON: in this issue, pag. 237.
- [2] P. G. DE GENNES et A. HERPIN: *Compt. Rend. Acad. Sci.*, **243**, 1611 (1956).
- [3] A. EISENSTEIN et N. S. GINGRICH: *Phys. Rev.*, **62**, 261 (1942).

PARTE SETTIMA

Helium 4

Quantum Hydrodynamics and the Theory of Helium II.

A. THELLUNG

Department of Mathematical Physics, University of Birmingham - Birmingham

The development of quantum hydrodynamics is closely connected with the theory of He-II, and in particular Landau's theory. In 1941 and 1947 LANDAU postulated his famous energy spectrum for a liquid near absolute zero [1, 2], from which he was able to derive and predict many of the properties of He-II. Quantum hydrodynamics has mainly been set up as an attempt to explain this energy spectrum.

1. - Landau's energy spectrum.

According to LANDAU, every weakly excited state of a liquid can be considered as an aggregate of a number of so-called elementary excitations. He postulated two kinds of such excitations:

a) Phonons or quantized (longitudinal) sound waves. It is assumed that a phonon carries a momentum \mathbf{p} , which is related to the wave vector \mathbf{k} of the sound wave through

$$(1) \quad \mathbf{p} = \hbar \mathbf{k}.$$

\hbar is Planck's constant, divided by 2π . The energy of a phonon of momentum \mathbf{p} is then given by

$$(2) \quad \varepsilon(\mathbf{p}) = cp.$$

c is the velocity of sound, p is the magnitude of \mathbf{p} .

b) Rotons. In LANDAU's first paper [1] they were supposed to be quantized vortex motions. In a later paper [2] they were associated with longi-

tudinal waves of short wave lengths. A roton is also assumed to carry a momentum \mathbf{p} , characterizing it, and its energy is given in LANDAU's two papers by

$$(3) \quad e(p) = \Delta + \frac{p^2}{2\mu} \quad \text{or} \quad \Delta + \frac{(p - p_0)^2}{2\mu}$$

respectively, where Δ , μ and p_0 are constants.

The lowest energy eigenvalues of the liquid are then additively composed of the excitation energies, i.e. they are of the form

$$(4) \quad E(..., n_p, ...; ..., N_p, ...) = \sum_p n_p \varepsilon(\mathbf{p}) + \sum_p N_p e(\mathbf{p}),$$

where n_p and N_p may take any positive integer or zero values and are the number of phonons and rotons of momentum \mathbf{p} . Similarly, the corresponding momentum eigenvalues of the liquid are

$$(5) \quad \mathcal{P}(..., n_p, ...; ..., N_p, ...) = \sum_p n_p \mathbf{p} + \sum_p N_p \mathbf{p}.$$

Once the energy spectrum (4), (2), (3) is given, one can apply the methods of statistical mechanics to calculate the partition function and all the thermodynamic quantities of the liquid. Furthermore, from the above energy spectrum and the momentum spectrum (5) one can deduce the equations of the two-fluid model [1, 3], from which the phenomena of superfluidity and second sound etc., can be derived [1, 4]. With a suitable choice of Δ , μ and p_0 in (3) excellent agreement between the theory and the experimental data on the specific heat of He-II and the velocity of second sound is obtained [5]. In order to get the customary form of the two-fluid equations it is essential that the excitations carry momenta as expressed in (5 *).

LANDAU had found his energy spectrum in a rather intuitive way. He did not give an actual derivation. Therefore the exact nature of rotons was left rather obscure. The existence of phonons in a liquid can be understood, because the situation is analogous to what one has in a crystal. However, there have been some doubts whether a phonon carries a momentum.

The great success of Landau's theory suggested that his assumptions were right, and ever since the main purpose of most theories of He-II has been to derive his energy and momentum spectrum.

(*) *Note added in proof:* This statement does no longer seem to me to be correct. At least for phonons it is mainly a question of convention and convenience whether one defines them as carrying momenta or not. A careful analysis (in particular of the term «velocity of the bearer fluid») shows that the two-fluid equations turn out to be the same in both cases.

2. - The idea of quantum hydrodynamics.

In order to give a rigorous derivation of the energy spectrum of a liquid from first principles, one would have to solve the Schrödinger equation for about 10^{23} particles with interaction, which is a hopeless undertaking. Instead, one can try to introduce some kind of collective variables, i.e. simpler variables which give only a rough and approximate description of the system, but which, one hopes, still retain at least some of its essential features.

One possibility is to describe the liquid by means of the hydrodynamic equations, thereby neglecting the atomistic structure. The variables used are the velocity and the density. One can then apply the general rules of quantum mechanics to this system and see what energy spectrum one obtains. There is of course no *a priori* justification for replacing the actual liquid by a continuous one. To a certain extent, the whole procedure is therefore rather a game of chance, but it is interesting to see what comes out.

An argument in favour of the hydrodynamical description can be given as follows: From experiments on specific heat one knows that in He-II at low temperatures only phonons are excited and their wavelengths are large with respect to the interatomic distance. For such sound waves it does not matter if the discrete masses of the atoms are smeared out to a continuous mass distribution and the atomic forces are replaced by certain elastic properties. At higher temperatures the rotons come into play. If the rotons are oscillations of very small wave length, the hydrodynamical variables will not describe them adequately. On the other hand, if they are some kind of vortex motions on a larger scale, as LANDAU originally thought, hydrodynamics will probably provide reasonable results.

It might be that hydrodynamics works quite well for Bosons of spin zero but not for Fermions. Particles with spin probably have motions that cannot be accounted for in terms of hydrodynamic variables. In this case, the hydrodynamic picture is either wrong or in any case very incomplete. This is indicated by the work of BRUECKNER and SAWADA [6] and LEE, HUANG and YANG [7].

The classical hydrodynamic equations of a non-viscous fluid in Eulerian variables are

$$(6) \quad \dot{\mathbf{v}} + (\mathbf{v} \cdot \nabla) \mathbf{v} + \frac{1}{\rho} \nabla P = 0,$$

$$(7) \quad \dot{\rho} + \operatorname{div}(\rho \mathbf{v}) = 0,$$

$$(8) \quad P = P(\rho).$$

The velocity \mathbf{v} and the density ϱ are functions of position $\mathbf{x} = (x_1, x_2, x_3)$ and time t . The dot denotes local differentiation with respect to the time. (6) is Euler's equation of motion and (7) the equation of continuity. In (8) we assume the pressure P to be a function of the density alone. The problem whether one has to take the adiabatic or the isothermal law does not arise here because at the lowest temperatures there is no difference. In fact we want to start from the equations of the fluid at absolute zero. For this reason no viscous terms have been included in (6). In this mechanical system various types of motion can become excited, and the idea is that at higher temperatures application of the methods of statistical mechanics will give the changes in the equation of state and other thermodynamic properties and that the interaction between the excitations will automatically produce dissipative effects.

3. – Canonical formalism and quantization.

In order to apply the rules of quantum mechanics to this system one would like to have the equations in a canonical form. However, so far it has proven impossible to obtain Euler's equation of motion (6) directly in a canonical form. One can, however, find a set of canonical equations from which (6) follows by taking the gradient. Quantization is then straightforward. We show this first for the simpler case of irrotational motion (*a*). The results for the general case (including vortex motions) will be given afterwards (*b*).

a) Irrotational motion. – In this case the velocity field can be derived from a potential $\varphi(\mathbf{x}, t)$,

$$(9) \quad \mathbf{v} = -\nabla\varphi.$$

We then start from a simpler set of hydrodynamic equations, namely Bernoulli's equation

$$(10) \quad \dot{\varphi} = \frac{1}{2} (\nabla\varphi)^2 + \int_{P_0}^P \frac{dP'}{\varrho'}$$

and the equation of continuity

$$(11) \quad \dot{\varrho} = \operatorname{div} (\varrho \nabla\varphi).$$

The integral in (10) is to be taken between the equilibrium pressure P_0 , corresponding to the equilibrium density ϱ_0 , and the actual pressure $P(\varrho)$. Euler's equation (6) is obtained by taking the gradient of (10) and remembering (9). (10) and (11) are two equations for the two variables φ and ϱ . (P is a given function of ϱ). Together with the initial and boundary conditions they determine the irrotational motion of the fluid completely.

Equations (10) and (11) can now be obtained from a canonical formalism, as was shown by KRONIG and THELLUNG [8]. It turns out that the Hamiltonian is

$$(12) \quad \mathcal{H}_{\text{ph}} = \int_V d^3x H_{\text{ph}}, \quad H_{\text{ph}} = \frac{1}{2} \varrho (\nabla \varphi)^2 + E_p(\varrho),$$

where

$$(13) \quad E_p(\varrho) = \varrho \int_{\varrho_0}^{\varrho} (P' - P_0) \frac{d\varrho'}{\varrho'^2},$$

and that φ and ϱ are canonically conjugate variables. As $E_p(\varrho)$ is the potential energy per unit volume and $\frac{1}{2}\varrho(\nabla\varphi)^2$ the kinetic energy, H_{ph} in (12) is the energy density and \mathcal{H}_{ph} the total energy of the fluid of volume V .

The canonical equations of motion are then

$$(14) \quad \dot{\varphi} = \frac{\delta \mathcal{H}_{\text{ph}}}{\delta \varrho}, \quad \dot{\varrho} = -\frac{\delta \mathcal{H}_{\text{ph}}}{\delta \varphi},$$

$\delta \mathcal{H}_{\text{ph}}/\delta \varrho$ and $\delta \mathcal{H}_{\text{ph}}/\delta \varphi$ meaning functional derivatives, e.g.

$$(15) \quad \frac{\delta \mathcal{H}_{\text{ph}}}{\delta \varphi} = \frac{\partial H_{\text{ph}}}{\partial \varphi} - \sum_{i=1}^3 \frac{\partial}{\partial x_i} \frac{\partial H_{\text{ph}}}{\partial (\partial \varphi / \partial x_i)}.$$

(Since the variables φ and ϱ are labelled by a continuous variable \mathbf{x} one has to apply the formalism of field theory; see e.g. WENTZEL [9]). An integration by parts shows that

$$(16) \quad \frac{dE_p}{d\varrho} = \int_{\varrho_0}^{\varrho} \frac{dP'}{\varrho'},$$

and it is then readily verified that the two equations (14) yield (10) and (11).

In quantum theory, φ and ϱ become operators fulfilling the commutation relations (in the Schrödinger representation)

$$(17) \quad \begin{cases} [\varrho(\mathbf{x}), \varphi(\mathbf{x}')] = \frac{\hbar}{i} \delta(\mathbf{x} - \mathbf{x}'), \\ [\varphi(\mathbf{x}), \varphi(\mathbf{x}')] = [\varrho(\mathbf{x}), \varrho(\mathbf{x}')] = 0, \end{cases}$$

where δ is the 3-dimensional Dirac δ -function. (See e.g. WENTZEL [9], § 1). In order to find the eigenvalues of \mathcal{H}_{ph} we observe that classically the deviation of the density ϱ from its equilibrium value ϱ_0 is extremely small compared with ϱ_0 for weakly excited states. Hence it is a good approximation to

replace ϱ by ϱ_0 in the expression for the kinetic energy and to expand $E(\varrho)$ in powers of $(\varrho - \varrho_0)$, thereby neglecting terms of higher than second order, viz.

$$(18) \quad E_p(\varrho) = \frac{c_0^2}{2\varrho_0} (\varrho - \varrho_0)^2 + \dots$$

c_0 means the velocity of sound at density ϱ_0 (see e.g. [8]). The approximate Hamiltonian

$$(19) \quad \mathcal{H}_{\text{ph}}^0 = \int d^3x \left(\frac{1}{2} \varrho_0 (\nabla \varphi)^2 + \frac{c_0^2}{2\varrho_0} (\varrho - \varrho_0)^2 \right)$$

is then quadratic in the field variables and its eigenvalues can be found according to the standard methods of field theory. Imposing periodic boundary conditions, we decompose φ and ϱ into Fourier series

$$(20) \quad \begin{cases} \varphi = \frac{1}{V^{\frac{1}{2}}} \sum_{\mathbf{k}} \sqrt{\frac{c_0 \hbar}{2\varrho_0 k}} (a_{\mathbf{k}} + a_{-\mathbf{k}}^*) \exp[i\mathbf{k}\mathbf{x}], \\ \varrho - \varrho_0 = \frac{1}{V^{\frac{1}{2}}} \sum_{\mathbf{k}} \sqrt{\frac{\varrho_0 \hbar k}{2c_0}} i(a_{\mathbf{k}}^* - a_{-\mathbf{k}}) \exp[-i\mathbf{k}\mathbf{x}]. \end{cases}$$

Here we have introduced at once the operators $a_{\mathbf{k}}^*$ and $a_{\mathbf{k}}$ [8], which are seen from (17) to obey the commutation relations characterizing creation and annihilation operators, i.e.

$$(21) \quad [a_{\mathbf{k}}, a_{\mathbf{k}'}^*] = \delta_{\mathbf{k}, \mathbf{k}'}, \quad [a_{\mathbf{k}}, a_{\mathbf{k}'}] = [a_{\mathbf{k}}^*, a_{\mathbf{k}'}^*] = 0.$$

Then $\mathcal{H}_{\text{ph}}^0$ becomes

$$(22) \quad \mathcal{H}_{\text{ph}}^0 = \sum_{\mathbf{k}} \hbar c_0 k (a_{\mathbf{k}}^* a_{\mathbf{k}} + \tfrac{1}{2}).$$

Further, the total momentum of the fluid becomes

$$(23) \quad \mathcal{P} = - \int d^3x \varrho \nabla \varphi = \sum_{\mathbf{k}} \hbar \mathbf{k} a_{\mathbf{k}}^* a_{\mathbf{k}}.$$

As the eigenvalues of $a_{\mathbf{k}}^* a_{\mathbf{k}}$ are 0, 1, 2, ... we have obtained Landau's energy and momentum spectrum for phonons (apart from a zero point energy), and we interpret $a_{\mathbf{k}}^* a_{\mathbf{k}} = n_{\mathbf{k}}$ as the number of phonons of wave vector \mathbf{k} . The momentum spectrum (23) is exact, whereas the anharmonic terms in \mathcal{H}_{ph} will modify the energy spectrum (22), but for the weakly excited states occurring at low temperatures this is an extremely small effect.

b) *General motion (including vortices)*. — In this case a canonical formalism is also possible if one represents the velocity field in terms of the Clebsch variables,

$$(24) \quad \mathbf{v} = -\nabla\varphi + \lambda \nabla\psi,$$

where φ , λ and ψ are in general functions of \mathbf{x} and t . CLEBSCH [10] has shown that this can always be done and that furthermore it is possible to choose φ , λ and ψ so that the surfaces $\lambda = \text{const}$ and $\psi = \text{const}$ move with the fluid, i.e.

$$(25) \quad \frac{D\lambda}{Dt} = \dot{\lambda} + \mathbf{v} \nabla \lambda = 0,$$

$$(26) \quad \frac{D\psi}{Dt} = \dot{\psi} + \mathbf{v} \nabla \psi = 0.$$

One can then write all terms in Euler's equation (6) as gradients of scalar functions, and integration leads to the generalized Bernoulli equation [10]

$$(27) \quad -\dot{\varphi} + \lambda \dot{\psi} + \frac{1}{2} v^2 + \int_{P'}^P \frac{dP'}{\varrho'} = 0.$$

Besides, we have the equation of continuity

$$(28) \quad \dot{\varrho} + \text{div}(\varrho \mathbf{v}) = 0.$$

Expressing \mathbf{v} by means of (24) and remembering that P is a given function of ϱ , we have in (25)–(28) four differential equations for the four functions ϱ , φ , λ and ψ . Together with the initial and boundary conditions they determine the motion of the fluid.

Clebsch's transformation is rarely used for practical purposes, because it introduces a non-linear expression for the velocity (24). It, however, transforms the equations of motion so that a canonical formalism becomes possible. We only state the results. For more details see. e.g. THELLUNG [11]. Introducing a new quantity

$$(29) \quad \pi = -\varrho \lambda,$$

we write, instead of (24),

$$(30) \quad \mathbf{v} = -\nabla\varphi - \frac{\pi}{\varrho} \nabla\psi.$$

It turns out that ϱ , φ and π , ψ are pairs of canonically conjugate variables

with the Hamiltonian

$$(31) \quad \mathcal{H} = \int_V d^3x \left(\frac{1}{2} \varrho v^2 + E_p(\varrho) \right),$$

where \mathbf{v} is to be expressed by (30) and $E_p(\varrho)$ is given by (13). It is easy to verify that the canonical equations

$$(32) \quad \dot{\varphi} = \frac{\delta \mathcal{H}}{\delta \varrho}, \quad \dot{\varrho} = -\frac{\delta \mathcal{H}}{\delta \varphi}, \quad \dot{\psi} = \frac{\delta \mathcal{H}}{\delta \pi}, \quad \dot{\pi} = -\frac{\delta \mathcal{H}}{\delta \psi},$$

in view of (29), are equivalent to (25)–(28). It is satisfying that also in this more general case \mathcal{H} is just the ordinary energy of the fluid.

In quantum theory, ϱ , φ , π and ψ become operators, fulfilling the commutation relations

$$(33) \quad [\varrho(\mathbf{x}), \varphi(\mathbf{x}')] = [\pi(\mathbf{x}), \psi(\mathbf{x}')] = \frac{\hbar}{i} \delta(\mathbf{x} - \mathbf{x}'),$$

all other commutators vanishing. It is then a well-defined mathematical problem to find the eigenvalues of \mathcal{H} (31). These results were found independently by ITÔ [12], THELLUNG [11] and ZIMAN [13]. The problem of finding the energy spectrum could however not be solved in the form stated above.

4. – The energy spectrum.

A big step towards a solution was made by ZIMAN [13] who introduced a new complex variable Ψ and its conjugate Ψ^* (Hermitian adjoint in the quantized theory), which are rather complicated functions of π and ψ . In terms of these quantities the velocity takes the form

$$(34) \quad \mathbf{v} = -\nabla\varphi - \frac{i\hbar}{2\varrho} \{ \Psi^* \nabla\Psi - \nabla\Psi^* \Psi \}$$

and Ψ and Ψ^* fulfil the simple commutation relations

$$(35) \quad [\Psi(\mathbf{x}), \Psi^*(\mathbf{x}')] = \delta(\mathbf{x} - \mathbf{x}'), \quad [\Psi(\mathbf{x}), \Psi(\mathbf{x}')] = 0.$$

Substituting (34) in (31) and expanding all quantities in powers of $(\varrho - \varrho_0)/\varrho_0$, we obtain

$$(36) \quad \mathcal{H} = \mathcal{H}_{\text{ph}}^0 + \mathcal{H}_{\text{rot}} + \mathcal{H}_{\text{int}} + \dots,$$

where the terms of lowest order in $\varrho - \varrho_0$ are

$$(37) \quad \mathcal{H}_{\text{rot}} = \int_V d^3x \left(-\frac{\hbar^2}{8\varrho_0} \right) \{ \Psi^* \nabla \Psi - \nabla \Psi^* \Psi \}^2,$$

$$(38) \quad \mathcal{H}_{\text{int}} = \int_V d^3x \frac{i\hbar}{2} \nabla \varphi \{ \Psi^* \nabla \Psi - \nabla \Psi^* \Psi \},$$

and $\mathcal{H}_{\text{ph}}^0$ as given by (19). Since Ψ, Ψ^* come into play only if the motion is rotational they are called roton variables, whereas the quantities ϱ, φ leading to the spectrum (22) for $\mathcal{H}_{\text{ph}}^0$ are called phonon variables. $\mathcal{H}_{\text{ph}}^0$ only depends on the phonon variables and \mathcal{H}_{rot} only on the roton variables. $\mathcal{H}_{\text{int}}^0$ contains both fields.

Although \mathcal{H}_{rot} is of the fourth degree in Ψ and Ψ^* , some of its eigenvalues can be found. Assuming periodic boundary conditions for Ψ, Ψ^* and decomposing them into Fourier series

$$(39) \quad \Psi(\mathbf{x}) = \frac{1}{V^{\frac{1}{2}}} \sum_{\mathbf{k}} b_{\mathbf{k}} \exp[i\mathbf{k}\mathbf{x}], \quad \Psi^*(\mathbf{x}) = \frac{1}{V^{\frac{1}{2}}} \sum_{\mathbf{k}} b_{\mathbf{k}}^* \exp[-i\mathbf{k}\mathbf{x}],$$

one finds from (35) that the b^* 's and b 's satisfy the commutation relations

$$(40) \quad [b_{\mathbf{k}}, b_{\mathbf{k}'}^*] = \delta_{\mathbf{k}\mathbf{k}'}, \quad [b_{\mathbf{k}}, b_{\mathbf{k}'}] = 0,$$

and can therefore be interpreted as creation and annihilation operators. ZIMAN has shown that then \mathcal{H}_{rot} takes the form

$$(41) \quad \mathcal{H}_{\text{rot}}^0 = \sum_{\mathbf{k}} (\Delta + Bk^2) b_{\mathbf{k}}^* b_{\mathbf{k}} + \frac{\hbar^2}{8\varrho_0 V} \sum_{\mathbf{k}, \mathbf{l}, \mathbf{m}, \mathbf{n}} (\mathbf{k} + \mathbf{n})(\mathbf{l} + \mathbf{m}) b_{\mathbf{n}}^* b_{\mathbf{m}}^* b_{\mathbf{k}} b_{\mathbf{l}} \delta_{\mathbf{k} + \mathbf{l}, \mathbf{m} + \mathbf{n}},$$

where

$$(42) \quad \Delta = \frac{\hbar^2}{8\varrho_0 V} \sum_{\mathbf{k}} k^2, \quad B = \frac{\hbar^2}{8\varrho_0 V} \sum_{\mathbf{k}} 1.$$

If one sums here over all values of \mathbf{k} permitted by the periodic boundary conditions, the expressions (42) are clearly divergent. It is at this point that one has to allow for the atomistic structure of the liquid by saying that quantities varying with a wavelength smaller than the order of the interatomic distance d do not make sense. One therefore has to cut-off the sums in (42) at a maximum wave number K_0 of the order of magnitude of $1/d$. Arguments that the number of degrees of freedom in this theory should be the same as for the real atomistic liquid lead to a similar cut-off. However, none of these

arguments are rigorous, and there remains a certain arbitrariness; consequently one can only expect to get the right order of magnitude for A and B in (42) [13, 14]. The arbitrariness does not only depend on the value of K_0 and whether one takes a sharp or a smooth cut-off; it is also possible not to cut off the Fourier components of Ψ and Ψ^* separately, but only the Fourier components of the expression $\{\Psi^* \nabla \Psi - \nabla \Psi^* \Psi\}$, which is the only form through which Ψ and Ψ^* occur in the physically observable quantities like v , \mathcal{H} , etc. A discussion of such cut-off procedures was given by THELLUNG [14].

As a consequence of (40), $b_k^* b_k = N_k$ has the eigenvalues 0, 1, 2, ... and is interpreted as the number of rotons of wave vector k . \mathcal{H}_{rot} (41) is diagonal for the states where the total number of rotons

$$(43) \quad N_{\text{rot}} \equiv \sum_k b_k^* b_k$$

(which is a constant of the motion) is 0 or 1. This has been found by ZIMAN. The writer has succeeded in finding the complete set of eigenvalues of \mathcal{H}_{rot} for $N_{\text{rot}} = 2$. Most of them are exactly

$$(44) \quad 2A + B(k^2 + k'^2)$$

(where k and k' are any wave vectors occurring in (41)), which one would expect if only the first term on the right-hand side of (41) were present. Almost all the rest of the eigenvalues are very close to the values given in (44), and only an extremely small fraction (of order $1/N_{\text{at}}$, where N_{at} is the number of atoms in the liquid) of the eigenvalues have a rather phonon-like spectrum, which depends strongly on the cut-off procedure used; however, they are of vanishing statistical weight. Quite generally, the influence of the second term on the right-hand side of (41) can be neglected as long as $N_{\text{rot}} \ll N_{\text{at}}$ (compare [14], p. 108). The remaining part in (41) has eigenvalues of the form postulated in LANDAU's first paper [1].

Further, the total momentum

$$(45) \quad \mathcal{P} = \int_V d^3x \rho v = \int_V d^3x \left\{ -\rho \nabla \varphi - \frac{i\hbar}{2} (\Psi^* \nabla \Psi - \nabla \Psi^* \Psi) \right\}$$

becomes

$$(46) \quad \mathcal{P} = \sum_k \hbar k a_k^* a_k + \sum_k \hbar k b_k^* b_k,$$

which shows that also the rotons carry a (linear) momentum $\hbar k$.

However, this does not mean that we have solved the problem. Although

we know the eigenvalues of $\mathcal{H}_{\text{ph}}^0$ and, to a good approximation, those of \mathcal{H}_{rot} , we actually need the eigenvalues of the total Hamiltonian (36). And it is easy to see that \mathcal{H}_{int} , the interaction between phonons and rotons, greatly influences the spectrum. This question has been looked into by ALLCOCK and KUPER [15] and by THELLUNG [14]. \mathcal{H}_{int} can be treated by conventional perturbation methods. This leads to an expansion of the energy eigenvalues of \mathcal{H} (36) in negative powers of c_0 . The dimensionless perturbation parameter in question is

$$(47) \quad \varepsilon = \frac{BK_0^2}{\hbar c_0 K_0}.$$

For He-II the order of magnitude of ε is 0.4 so that perturbation theory might be expected to give reasonable results. A second order perturbation calculation shows that the rest energy Δ of the rotons in (41) is exactly cancelled to order c_0^2 . One therefore has to go to order c_0^{-1} , which means a fourth order perturbation calculation on \mathcal{H}_{int} . Furthermore, the expansion (36) of \mathcal{H} (31) in powers of $\varrho - \varrho_0$ also means an expansion in negative powers of c_0 since $\varrho - \varrho_0 \sim c_0^{-\frac{1}{2}}$ (20). In order to be consistent one therefore has to take also terms of higher order in $\varrho - \varrho_0$ in the expansion (36). These results were first stated by ALLCOCK and KUPER [15]. Using a method somewhat similar to the Bloch-Nordsieck transformation [16] combined with perturbation theory, they gave an explicit expression for the rest energy of a roton to order c_0^{-1} , without however evaluating the integrals involved. They also set the anharmonic terms in the potential energy (18) (which now should be taken into account) equal to zero.

The full calculation has been carried out by THELLUNG [14], using perturbation theory throughout. The terms $\sim (\varrho - \varrho_0)^3$ and $\sim (\varrho - \varrho_0)^4$ in (18) were thereby taken into account. The result is the following: The phonon spectrum remains unchanged (in the approximation considered in [14]). The roton spectrum becomes

$$(48) \quad \sum_k N_k (\Delta' + A'k + B'k^2).$$

The exact values of Δ' , A' , B' depend on the cut-off procedure used. With certain cut-off methods A' becomes zero, others give $A' \neq 0$. In all cases Δ' is $\sim c_0^{-1}$ and positive. For He-II the constants in (48) have the right order of magnitude to fit the experimental data on the specific heat up to temperatures near the λ -point. The right order of magnitude is all we can expect in view of the uncertainties introduced by the cut-off.

These uncertainties are due to the fact that the hydrodynamic treatment is naturally limited by the atomistic structure of the liquid. It would therefore be most desirable to investigate the connection between the hydrodynamic

variables and the co-ordinates and momenta of the particles. It might perhaps be possible to obtain hydrodynamic variables as a kind of averages over microscopic variables. If this could be done, one would probably gain some information about the right way of cutting off.

REFERENCES

- [1] L. LANDAU: *Journ. Phys. USSR*, **5**, 71 (1941).
- [2] L. LANDAU: *Journ. Phys. USSR*, **11**, 91 (1947).
- [3] R. KRONIG: *Physica*, **19**, 535 (1953).
- [4] For a comprehensive survey see R. B. DINGLE: *Phil. Mag. Suppl.*, **1**, 111 (1952).
- [5] D. DE KLERK, R. P. HUDSON and J. R. PELLAM: *Phys. Rev.*, **93**, 28 (1954).
- [6] K. A. BRUECKNER and K. SAWADA: *Phys. Rev.*, **106**, 1117, 1128 (1957).
- [7] T. D. LEE, K. HUANG and C. N. YANG: *Phys. Rev.*, **106**, 1135 (1957).
- [8] R. KRONIG and A. THELLUNG: *Physica*, **18**, 749 (1952).
- [9] G. WENTZEL: *Quantum Theory of Fields* (New York, 1949).
- [10] A. CLEBSCH: *Crelle's Journ.*, **54** (1857) and **56** (1859); see also H. LAMB: *Hydrodynamics* (Cambridge, 1932), Art. 167, p. 248.
- [11] A. THELLUNG: *Physica*, **19**, 217 (1953).
- [12] H. ITÔ: *Progr. Theor. Phys.*, **9**, 117 (1953).
- [13] J. M. ZIMAN: *Proc. Roy. Soc.*, A **219**, 257 (1953).
- [14] A. THELLUNG: *Helv. Phys. Acta*, **29**, 103 (1956).
- [15] G. R. ALLCOCK and C. G. KUPER: *Proc. Roy. Soc.*, A **231**, 226 (1955).
- [16] F. BLOCH and A. NORDSIECK: *Phys. Rev.*, **52**, 54 (1937); W. PAULI and M. FIERZ: *Nuovo Cimento*, **15**, 167 (1938).

INTERVENTI E DISCUSSIONI

— O. PENROSE:

Does the equation $\mathbf{v} = -\nabla\varphi + \lambda\nabla\psi$ uniquely specify φ , λ , ψ ? If not, is the decomposition of \mathcal{H} into

$$\mathcal{H}_{\text{ph}} + \mathcal{H}_{\text{rot}} + \mathcal{H}_{\text{int}},$$

invariant against a transformation to new φ , λ , ψ ?

— A. THELLUNG:

φ , λ , ψ are not uniquely specified by a given \mathbf{v} , although they are severely restricted by the conditions (25) and (26). Various authors [12, 13, 15] have studied the question of gauge transformations to new variables φ' , λ' , ψ' . The decomposition of \mathcal{H} is not

gauge invariant, but \mathcal{H} itself is. Therefore its eigenvalues are invariant and if we expand them in negative powers of c_0 , this expansion is still invariant. No faster convergence can therefore be gained by choosing a different gauge.

— L. ONSAGER:

Can you make such an election that $\nabla \cdot (\lambda \nabla \psi) = 0$?

— A. THELLUNG:

This is in general not possible.

— R. EISENSCHITZ:

Is the approach by TYABJI (S. F. B. TYABJI: *Proc. Cambr. Phil. Soc.*, **50**, 449 (1954)) (transverse waves) justified?

— A. THELLUNG:

Unfortunately, there is a mistake in Tyabji's paper and the «transverse waves» in a fluid are due to this mistake. But I would like to mention that in the first part of his paper, TYABJI got the interesting result that the hydrodynamic equations in Lagrangian variables (in contrast to the Eulerian variables used in our approach) can also be brought into a canonical form.

— A. PRINS:

What comes out if you apply, just as a mathematical exercise, the same calculations to the problem in two dimensions? It might be easier, though of course it would have a little physical meaning.

— A. THELLUNG:

I have never tried.

Bose-Einstein Condensation in Liquid Helium.

O. PENROSE

Imperial College - London.

In keeping with the title of this conference, I shall talk about the peculiar « condensed state » of liquid helium below its lambda-transition.

We treat liquid helium as a system of spinless Bose-Einstein (B.E.) particles with binary interactions, that is, with a Hamiltonian of the form

$$(1) \quad H = \sum_j (\mathbf{p}_j^2/2m) + \sum_{ij} U(\mathbf{q}_i - \mathbf{q}_j).$$

With such a general model, one cannot obtain numerical results, but one can obtain general results which appear to correspond to some of the peculiar properties of liquid helium.

Eq. (1) is not the exact Hamiltonian; it can be derived from the Hamiltonian of a system of electrons and ^4He nuclei by assuming that electrons move much faster than nuclei (Born-Oppenheimer approximation) and then neglecting three-body and higher types of interaction in the resulting effective potential for motion of the nuclei. These approximations, however, are much less crude than those leading to the ideal-gas, ideal-fluid, and cell models.

The most striking experimental fact about liquid helium is that it does not obey the ordinary laws of hydrodynamics. It has its own hydrodynamic laws, which are not fully understood yet, but which simplify under suitable conditions to the two-fluid equations proposed by LANDAU (ref. [1]). The aim of the present work has been to understand better why helium II requires these special hydrodynamic laws.

An essential difference between two-fluid and ordinary hydrodynamics is that we need more variables in the two-fluid case. For ordinary hydrodynamics, the state of the liquid can be completely described by giving the value, at each point in the liquid, of two scalar fields and one vector field, for example the (mass) density, energy density, and momentum density. For two-fluid

hydrodynamics, however, we need a second vector field before the liquid is completely described. The new vector field may conveniently be taken to be the superfluid velocity \mathbf{v}_s .

Since hydrodynamics can be derived, in principle, from the quantum mechanics of the particles comprising our model, the above hydrodynamical considerations should have a counterpart in the quantum mechanics. For ordinary hydrodynamics, the mass density, energy density, and momentum density can be defined in terms of the quantum state (or the density matrix) and the hydrodynamic equations correspond roughly to the conservation laws for mass, momentum, and energy (ref. [2]). Before we can understand why He II has special hydrodynamic equations, therefore, we must know the answers to two questions:

i) What feature in the quantum-mechanical description distinguishes He II from a « classical » liquid such as He I?

ii) What quantity in the quantum description corresponds to \mathbf{v}_s in the hydrodynamical description?

Landau's theory (ref. [1]), which treats liquid helium in terms of an assembly of phonons and rotons, does not give a real answer to these questions. It does not answer i) because it does not explain clearly why superfluidity should disappear above the lambda-transition. Its answer to ii) is that \mathbf{v}_s is the velocity of a « moving ground state » from which the actual quantum state is built up by adding excitations. This works well in many cases, but has two defects. First, it is based on the approximation of independent thermal excitations and therefore may lose its meaning for temperatures near the lambda-point, where this approximation breaks down. Secondly, it can lead to difficulties for non-uniform states (*).

Though it may be possible to overcome these objections, an easier approach is to use the analogy between liquid helium and an ideal B.E. gas, in the spirit of F. LONDON's work (ref. [4]). Below its transition temperature the ideal gas has the characteristic property of « B.E. condensation »: a finite

(*) For example, consider the wave function

$$\exp[i\alpha \sum_j \cos \mathbf{k} \cdot \mathbf{q}_j] \psi \simeq \{1 + \frac{1}{2}i\alpha \sum_j (\exp[i\mathbf{k} \cdot \mathbf{q}_j] + \exp[-i\mathbf{k} \cdot \mathbf{q}_j])\} \psi,$$

where $\psi(\mathbf{q}_1 \dots \mathbf{q}_N)$ is the ground-state wave function and α is small. According to the left-hand side, this represents (see ref. [3]) a « locally moving ground state » with velocity field $\nabla(\hbar/m)\alpha \cos \mathbf{k} \cdot \mathbf{x}$ at the point \mathbf{x} ; according to the right-hand side it is a linear combination of the ground state with two states built by adding one phonon to the ground state (ref. [3]). Thus it is not clear from the definition whether \mathbf{v}_s should be taken as $\nabla(\hbar/m)\alpha \cos \mathbf{k} \cdot \mathbf{x}$ or 0.

fraction of the particles condense into one single-particle quantum state. F. London's ideas suggest, then, that the answers to our two questions are:

- i) He II is the only liquid with the property of B.E. condensation.
- ii) \mathbf{v}_s is the velocity field of the condensed particles.

To make these speculations useful, we must show how to extend the concept of B.E. condensation to a system with interactions and show that He II is the only liquid with this property; then we must define a velocity field for the condensed particles and show that this definition is consistent with Landau's when both are applicable.

We first re-examine the concept of B.E. condensation of an ideal gas, in order to find a natural generalization applicable in the presence of interactions. To simplify this task as far as possible, we shall take periodic boundary conditions. In consequence, the single-particle stationary states are « plane waves » and may be labelled by their momentum eigenvalues. For thermal equilibrium below the transition temperature T_0 , the number of particles with momentum \mathbf{p} in an ideal B.E. gas of N particles is given by

$$\langle n_{\mathbf{p}} \rangle = (\exp [p^2/2mkT] - 1)^{-1} \quad (\mathbf{p} \neq 0)$$

$$\langle n_0 \rangle = N(1 - (T/T_0)^3) .$$

The characteristic feature distinguishing these mean occupation numbers from the occupation numbers above the transition, or for an F.D. gas, is the factor N in the expression for $\langle n_0 \rangle$, indicating that a finite fraction $1 - (T/T_0)^3$ of the particles have zero momentum. We may express this property of *B.E. condensation* in symbols by

$$(2) \quad \langle n_0 \rangle = O(N) .$$

In contrast, all the $\langle n_{\mathbf{p}} \rangle$'s are infinitesimal fractions of N for a non-condensed gas.

The criterion (2) can be generalized to a system with interactions, even though single-particle energy levels are not defined in the presence of interactions. We take $\langle n_{\mathbf{p}} \rangle$ to be the expectation of the number of particles with momentum \mathbf{p} . This expectation value can be defined in terms of the momentum $\varphi(\mathbf{p}_1, \dots, \mathbf{p}_N)$ representative of the quantum state of the system:

$$\langle n_{\mathbf{p}} \rangle = N \sum_{\mathbf{p}_1} \dots \sum_{\mathbf{p}_N} |\varphi(\mathbf{p}, \mathbf{p}_2, \dots, \mathbf{p}_N)|^2 .$$

Alternatively, it can be defined as the expectation of an operator which counts the number of particles with momentum \mathbf{p} , or in terms of the eigenvalues of

the one-particle reduced density matrix (ref. [5]). Having defined the $\langle n_p \rangle$'s for a system with interactions, we again take eq. (2) as our criterion for B.E. condensation.

The next step is to show that He II actually satisfies this criterion. A partial solution to this problem is given by the following theorems, which were derived in collaboration with Professor ONSAGER (refs. [5, 6]).:

Theorem I. *B.E. condensation is present in He II at absolute zero.* The proof depends on the B.E. symmetry of the atoms (one can show, in fact, that B.E. condensation is impossible in a Fermi system, such as liquid ^3He) and the presumption that He II remains liquid at absolute zero. There is also the special assumption that there is no « long-range configurational order » at absolute zero; this means that the configurations in widely separated parts of the liquid are assumed to be statistically independent.

This result needs extending to finite temperatures (since a two-dimensional B.E. gas, for example, shows B.E. condensation at absolute zero but not at finite temperatures.) Two such extensions are the following:

Theorem II. *The approximations of Feynman's theory of the lambda-transition (ref. [7]) imply that B.E. condensation is present for thermal equilibrium below the lambda-transition but not above.* Feynman's approximations are quite crude (for example, they imply a third-order transition instead of the observed (ref. [8]) logarithmic singularity); nevertheless the result does indicate that B.E. condensation is the characteristic property of He II sought in i) above.

Theorem III. *B.E. condensation is present at thermal equilibrium if the phonon theory is valid* — that is, if all the important stationary states can be constructed by adding phonons to the ground state using the formalism of ref. [9]. Experiment (especially specific heat measurements (ref. [10])) indicates that the phonon theory is valid below 0.5 °K unless the helium is rotating. Theorem III is more rigorous than theorem II in application to He II, but it tells us nothing about temperatures above 0.5 °K.

An interesting feature of Theorem III is that it combines Landau's idea of phonons with London's idea of B.E. condensation. Previously such a synthesis had been achieved only for the case of weak interactions (ref. [11]).

To discuss the question of defining \mathbf{v}_s , we must now generalize eq. (2) to moving systems. For spatially uniform states, the appropriate generalization is

$$(3) \quad \langle n_{\mathbf{p}'} \rangle = O(N) \quad \text{for some } \mathbf{p}'.$$

If (3) is satisfied we shall say that B.E. condensation is present and that the condensed particles have velocity $\mathbf{v}_c \equiv \mathbf{p}'/m$. From Theorem I it is easily shown that if He II is in a « moving ground state » then \mathbf{v}_c equals the velocity

of the moving ground state. Thus, for $T = 0^\circ\text{K}$, our suggested definition of \mathbf{v}_s (by $\mathbf{v}_s \equiv \mathbf{v}_c$) is consistent with Landau's definition (by $\mathbf{v}_s \equiv$ velocity of the moving ground state). The two definitions can also be consistent at finite temperatures:

Theorem IV. *If an equilibrium assembly of phonons with drift velocity \mathbf{v}_n is built upon a moving ground state of velocity \mathbf{v}_s , then B.E. condensation is present with $\mathbf{v}_c = \mathbf{v}_s$. Thus our proposed answer to ii) — to define $\mathbf{v}_c \equiv \mathbf{v}_s$ — is consistent with Landau's for any temperature below 0.5°K provided the system is spatially uniform.*

The definition of \mathbf{v}_c given in eq. (3) can be extended further, to non-uniform states. As shown in refs. [5, 12], one can define a wave function $\Psi(\mathbf{x})$ for the condensed particles. Then the velocity field of the condensed particles is (ref. [12])

$$(4) \quad \mathbf{v}_c = (\hbar/m) \nabla \varphi,$$

where $\varphi = \frac{1}{2}i^{-1} \log(\Psi/\Psi^*)$ is the phase of the wave function Ψ . Note that eq. (4) implies a quantization of circulation for \mathbf{v}_c , of the type discussed by ONSAGER and FEYNMAN ref. [13]).

We conclude that the theory of B.E. condensation can provide answers to the two questions asked here. On the other hand, it has not yet been possible to derive the two-fluid hydrodynamic equations using this point of view.

REFERENCES

- [1] L. D. LANDAU: *Journ. Phys. USSR*, **5**, 71 (1941).
- [2] J. H. IRVING and J. G. KIRKWOOD: *Journ. Chem. Phys.*, **18**, 817 (1950).
- [3] R. P. FEYNMAN: *Phys. Rev.*, **94**, 262 (1954).
- [4] F. LONDON: *Superfluids*, vol. II (New York, 1954).
- [5] O. PENROSE and L. ONSAGER: *Phys. Rev.*, **104**, 576 (1956).
- [6] O. PENROSE: *Proc. Int. Conf. on Low Temperature Physics* (Madison, 1957).
- [7] R. P. FEYNMAN: *Phys. Rev.*, **91**, 1291 (1953).
- [8] W. M. FAIRBANK, M. J. BUCKINGHAM and C. F. KELLERS: *Proc. Int. Conf. on Low Temperature Physics* (Madison, 1957).
- [9] O. PENROSE: *Phil. Mag.*, **45**, 80 (1954).
- [10] H. C. KRAMERS, J. D. WASSCHER and C. J. GORTER: *Physica*, **18**, 329 (1952).
- [11] N. N. BOGOLJUBOV: *Journ. Phys. USSR*, **11**, 23 (1947).
- [12] O. PENROSE: *Phil. Mag.*, **42**, 1373 (1951).
- [13] L. ONSAGER: *Suppl. Nuovo Cimento*, **6**, 249 (1949); R. P. FEYNMAN: *in Progress in Low Temperature Physics*, vol. I (Amsterdam, 1955), p. 36.

INTERVENTI E DISCUSSIONI

— G. UHLENBECK:

Have I understood the theorems you mentioned rightly by saying that the B.E. condensation follows given some phenomenological information like that He is a liquid at $T = 0$, or that the excitation spectrum is given at low temperatures by the phonons? Is it possible to turn the theorems around?

— O. PENROSE:

For absolute zero, we can show that B.E. condensation does not occur in a solid, so that B.E. condensation does imply the system is liquid.

For finite temperatures, I do not at present see any way to follow up your suggestions.

— O. PENROSE to a question by Dr. MENDELSSOHN:

Surely the frictionless flow you observed in your film experiment is perfectly compatible with the standard two-fluid picture?

The condensed particles all have the same momentum value $m\mathbf{v}_s$, which is not necessarily zero. Although there is no normal fluid at $T = 0^\circ\text{K}$, only about 10% of the particles are condensed. The zero-point energy is the kinetic energy of the remaining 90%.

— L. ONSAGER to Dr. K. MENDELSSOHN:

We do not identify the background of condensed particles with the superfluid portion; in a system of interacting particles only a fraction of them can belong to the background and yet the entire liquid can be superfluid. An observation made by Huang, Lee and Yang suggests that the zero point motion which results from the interaction actually makes it more difficult to mix liquids of different background velocities. This is related to the well-known fact that in a system of non-interacting Bose particles the (q -space) density fluctuations correspond a random distribution when all particles have the same momentum; but these fluctuations are substantially greater when particles of different momenta are put together. In a liquid such density fluctuations give rise to a considerable increase of the energy. We feel that a background of condensed particles is an almost indispensable feature of a theory for superfluid motion; unless the velocity of the superfluid part can be identified with a background velocity it seems extremely difficult to find a definition in microscopic terms.

Contribution to the Phonon Theory of Fluids.

R. EISENSCHITZ and A. CROWE

Department of Physics, Queen Mary College, University of London - London

Quantized sound waves in fluids—as distinct from solids—are by now familiar as a means for interpreting properties of liquid helium. So far this concept has no clear foundation in the principles of atomic dynamics. A deduction of the phonon energy spectrum in an assembly of interacting Bose-Einstein particles was first made by BOGOLJUBOV [1]. He was followed by a number of other authors; the latest contributors are BRUECKNER and SAWADA [2] who established a phonon and roton spectrum.

The knowledge of the energy spectrum is, however, not sufficient for identifying the relevant micro-physical processes or for deducing transport properties of a fluid. In connection with the transport theory the flow of momentum and energy was investigated (EISENSCHITZ [3]); it appeared that the picture of phonons carrying their momentum and energy with the velocity of sound was only partly valid.

In the present note the phonon concept is applied to the propagation of sound.

Following BOGOLJUBOV, let $T = \hbar^2 k^2 / 2m$ be the kinetic energy of a particle, \mathbf{k} being a vector the components of which are integer multiples of $(1/V)^{1/3}$. The potential energy of interaction of a pair of particles is denoted by $U(r)$ and its volume average is

$$(1) \quad \langle U \rangle = (4\pi/V) \int_0^\infty U(r) r^2 dr.$$

Let $b_{\mathbf{k}}$ and $b_{\mathbf{k}}^\dagger$ be the quantized Bose amplitudes,

$$b_{\mathbf{k}} b_{\mathbf{k}'}^\dagger - b_{\mathbf{k}'}^\dagger b_{\mathbf{k}} = \delta_{\mathbf{k}\mathbf{k}'}.$$

In the neighbourhood of the lowest energy level the amplitudes b_0 and b_0^+ are asymptotically commutative and equal to $N^{\frac{1}{2}}$, N being the total number of particles in the fluid. In this limit the equations of motion obtain the form

$$(2) \quad \begin{aligned} i\hbar(db_k/dt) &= A_{11}b_k + A_{12}b_{-k}^+, \\ i\hbar(db_{-k}^+/dt) &= A_{21}b_k + A_{22}b_{-k}^+, \end{aligned}$$

where the matrix A is defined as

$$\begin{bmatrix} T(k) + N\langle U \rangle & N\langle U \rangle \\ -N\langle U \rangle & -[T(k) + N\langle U \rangle] \end{bmatrix}.$$

By diagonalizing this matrix the energy levels are found to be

$$E(k) = [2T(k)N\langle U \rangle + T(k)^2]^{\frac{1}{2}},$$

which, in the limit of low energies, is equal to

$$(3) \quad E(k) = \hbar k[N\langle U \rangle/m]^{\frac{1}{2}}.$$

If these energy levels are interpreted as the energies of phonons it follows that the velocity of sound is equal to

$$(4) \quad c = [N\langle U \rangle/m]^{\frac{1}{2}}.$$

On account of this relation the velocity of sound is proportional to the square root of the density ($\rho^{\frac{1}{2}}$).

On account of equations (4) and (1) the velocity of sound depends on the interaction of particles at extremely short distances which would not be reached by real atoms. This apparent difficulty is resolved by BOGOLJUBOV by showing that the definition of $\langle U \rangle$ should be modified in such a way that the intermolecular repulsion is taken into account. Equation (1) is accordingly replaced by

$$(5) \quad \langle U \rangle = (4\pi/V) \int_0^\infty U(r) w(r) r^2 dr.$$

In this expression $w(r)$ is a solution of the Schrödinger equation for the relative movement of a pair of particles, subject to the condition that $\lim_{r \rightarrow \infty} w(r) = 1$.

Even if due account is taken of the intermolecular repulsion, equation (4)

is difficult to reconcile with our present knowledge of the fluid state. By applying the virial theorem it follows that the pressure is equal to

$$(6) \quad P = (2N/3V)[\langle T \rangle + (N/4)\langle \mathbf{r} \cdot (\partial U / \partial \mathbf{r}) \rangle].$$

In this expression the mean values are equal to the diagonal components of the T and $\mathbf{r} \cdot (\partial U / \partial \mathbf{r})$ matrix in the energy representation. The adiabatic bulk modulus is determined by the differential coefficients of the matrix elements with respect to the volume so that the velocity of sound is equal to

$$(7) \quad c = V[\partial P / mN \partial V]^{\frac{1}{2}}.$$

If the velocity of sound as derived from equation (4) is to agree with the results of equations (7) and (6) the matrix elements and volume averages appearing in these equations would have to comply with conditions for which there is, so far, no indication whatever. It should therefore be worth while to test the validity of equation (4) against experiment. This can be done by calculating the energy of interaction for a pair of helium atoms and by deriving $\langle U \rangle$, at first in accordance with equation (1).

In calculating the energy of interaction the state of the electrons in a helium atom was specified by hydrogenic wave functions corresponding to an

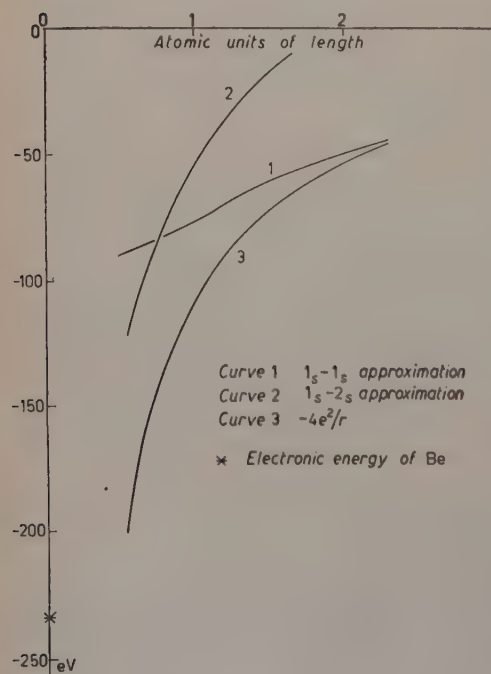


Fig. 1.

effective nuclear charge of 27/16 electrons. The interaction was derived under two different assumptions. Either the electrons in an atom were assigned $1s-1s$ orbitals or they were assigned $1s-2s$ orbitals with antiparallel spins. In the latter approach an allowance was made for the excitation energy of the separated atoms. By either method the energy of interaction is obtained as the sum of a large number of Coulomb—and exchange—integrals. The values of these quantities as functions of the interatomic distance were taken from tables (KOTANI [4]; PREUSS [5]) either directly or by the way of auxiliary functions. In the present approximations the difference $U(r) - U(\infty)$ is very likely to be too high. For this reason the

lower energy values were finally adopted, the 1s-1s values for distances larger than 0.75 atomic units and the 1s-2s values for smaller distances. For $r = 0$ the energy of the electrons was set equal to the energy of the beryllium atom.

In Fig. 1 the calculated energy of the electrons is plotted against the distance. The total energy is arrived at by adding the nuclear repulsion of $4e^2/r$.

In calculating the mean interaction $\langle U \rangle$ it was found that the main contributions arise from the distances between 0.5 and 1.5 atomic length units. The shorter distances and distances larger than 5 atomic units make only negligible contributions.

The calculated velocity of sound is equal to

$$c = 5.5 \cdot 10^5 \text{ cm/s},$$

whereas experiment yields $0.24 \cdot 10^5$. The calculated differential coefficient $\partial c / \partial (\rho^{1/3})$ is equal to $1.445 \cdot 10^6 \text{ cm}^{2/3} \text{ g}^{1/3} \text{ s}^{-2}$. Plotting the experimental velocity of sound against the square root of the density a straight line is found the slope of which is equal to $3.65 \cdot 10^5$. Here the discrepancy is not as large as in the absolute values but still appreciable.

The present method of calculating the energy of interaction cannot claim high accuracy and by improving the methods of calculation the gap between theory and experiment can be reduced. The amount of this reduction is, however, very limited since the result is remarkably insensitive towards arbitrary modifications of the interaction curve.

This result shows clearly the difficulty of reconciling the concept of phonons in fluids with the fundamental theory of matter.

* * *

We wish to Dr. R. A. BUCKINGHAM who kindly showed us his unpublished results on the interaction of helium atoms.

— — — —

REFERENCES

- [1] N. BOGOLJUBOV: *Journ. Phys. USSR*, **11**, 23 (1947).
- [2] K. A. BRUECKNER and K. SAWADA: *Phys. Rev.*, **106**, 1117, 1128 (1957).
- [3] R. EISENSCHITZ: *Proceedings of the Colloque International sur les phénomènes de transport en mécanique statistique* (in print).
- [4] M. KOTANI A. AMEMIYA, E. ISHIGORO and T. KIMURA: *Tables of Molecular Integrals* (Tokyo, 1955).
- [5] H. PREUSS: *Integraltafeln zur Quantenchemie* (Berlin, 1956).

INTERVENTI E DISCUSSIONI

— J. WILKS:

How do you interpret the Debye-like specific heat at liquid ^4He below 0.6°K ?

— R. EISENSCHITZ:

Specific heat is derived from energy spectrum and independent of any interpretation of the energy spectrum.

— H. TEMPERLEY:

Are the excitations specified by your relation between E and K physically present in the liquid or not? If they are not, what is wrong? If they *are*, they ought to check with the observed specific heat. If this is not the case, surely this points to the theories being too crude rather than to the invalidity of the phonon concept?

— L. ONSAGER:

If one allows the assumption—strong on the force of it but amply verified by experiment—that there are no low energy excitations other than phonons, then one can build the whole phonon theory in unique fashion from first principles.

Energy Fluctuations in Liquid Helium and its Flow Properties (*).

O. K. RICE

Department of Chemistry, University of North Carolina - Chapel Hill, N. C.

In another paper [1] we have discussed the relation between the elementary theory of the excitations in helium based on a cell model and the theory of Feynman [2], and it was concluded that these theories could be well correlated with each other. In the theories of Feynman and Landau [3], however, the energy levels are closely associated with specific values of the momentum, while in my view they may possibly not be so closely connected. If this latter view is correct a re-examination of the mechanism of the flow of superfluid with respect to the normal fluid and the nature of superfluidity is required. It will be the purpose of the present paper to consider this problem. After a preliminary discussion of some of the properties of the rotons and the superfluid, we shall show that energy fluctuations are capable of producing local temperature gradients which are much greater than any which are likely to be superimposed in experiments on second sound. There will thus be localized flow phenomena which will play an important role in determining the properties of the rotons, and we shall attempt to discuss some of the factors involved.

1. - Mass of the rotons.

We have shown [1] how to calculate n/N , where n is the number of rotons and N the number of atoms per unit volume, from the roton part of the specific heat, in the temperature range from 0.8° to 1.7° K where the density of rotons is low enough so that their interactions should not be too important.

(*) Work supported in part by the Office of Ordnance Research, U.S. Army.

This information can be combined with results on the ratio $x = \rho_n/\rho$ of the density of normal fluid to the total density to give z , the effective number of atoms per roton. In Table I we give some estimated values of z . The first one is based on the values of x previously calculated [4] from second sound and specific heat data. The second one is based on the recent repetition of the Andronikashvili experiment by DASH and TAYLOR [5].

TABLE I.

T (°K)	z second sound	z DASH and TAYLOR	z , corr. second sound	z , corr. DASH and TAYLOR
0.8	28.7	—	23.0	—
1.1	15.8	11.8	14.5	10.8
1.4	11.3	10.0	10.8	9.6
1.7	9.9	9.1	9.8	8.9

The columns headed z , corr., were calculated in the same way, except that in calculating n/N the roton part of the specific heat was obtained by subtracting the value for the phonon specific heat more recently suggested by KRAMERS [6] from the same value of the total specific heat.

It will be noted that the value of z obtained from second sound differs rather markedly from that given by DASH and TAYLOR. Their values of x are systematically lower than those obtained from second sound; the absolute values of the differences change only moderately with temperature, but the percentage difference increases greatly at the lower temperature. The smaller the value of x , the greater will be the difficulty in determining it by the Andronikashvili experiment. Therefore, although DASH and TAYLOR consider their accuracy to be considerably greater than the differences between the results of the two methods, we are inclined to believe that the results obtained from the second-sound experiments are to be preferred, at least at low temperatures.

According to the theories of Landau and Feynman z should vary roughly inversely as T . This relation appears to hold fairly well, between 1.1° and 1.4°. Below 1.1° the variation of z appears to be somewhat more rapid, though this effect is considerably diminished when the corrected value of z is used. Above 1.4° the variation is somewhat less rapid. The work mentioned by KRAMERS [6] will also necessitate some correction in the entropy, and there is furthermore some possibility [7] that the values of the velocity of second sound originally involved in the calculation of z need some correction. This being the case, it is not absolutely certain that the variation of z is actually more rapid than that of T^{-1} at the lower temperatures.

The interpretation of these results on the basis of the ideas of the present paper will be given in Sect. 4.

2. - Forces causing flow of superfluid.

In a recent paper [4] I have advanced arguments to confirm an earlier suggestion that in liquid helium the normal and superfluid are separated not merely in momentum space, as is often assumed, but also on a microscopic scale in actual physical space. This idea certainly seems to be in accord with the picture of the rotons as localized excitations, at least in the region where they predominate over the phonon excitations, and in this paper we will not attempt to discuss the phonons. It was then noted that the reversible flow phenomena implied the existence of a pressure resident in the superfluid and tending to move the superfluid with respect to the rotons. The magnitude of this pressure was given by

$$(2.1) \quad P_s = \rho g,$$

where ρ was the density and g the free enthalpy (Gibbs free energy) per gram. Eq. 2 is based upon the equation

$$(2.2) \quad \partial \mathbf{v}_s / \partial t - \partial \mathbf{v}_n / \partial t = (\rho / \rho_n) s \text{ grad } T,$$

where \mathbf{v}_s and \mathbf{v}_n are velocities of superfluid and normal fluid, respectively, t is time, ρ_n is density of normal fluid, s is entropy per gram, and T is absolute temperature. A derivation of Eq. (2.2) was given by LONDON [8], following GOGATE and PATHAK [9]. This proof is based upon thermodynamic principles, assuming that work done by the transfer of heat from a higher to a lower temperature appears as relative velocity of superfluid and normal fluid.

It seems appropriate to give another proof of Eq. (2.1) which may throw further light on the physical picture. We suppose two portions of helium II, one thermostated at 0°K and one at T , to be separated by a porous plug which allows only superfluid to pass. Each portion is under pressure by a piston, and the pressure p_0 on the portion at 0°K is adjusted so that there is no tendency of superfluid to flow in either direction. Since liquid helium at 0°K is solely superfluid, this is the pressure on the superfluid, and if the superfluid is a freely flowing fluid subject to no external forces the same pressure will exist within the *superfluid* at temperature T , where the total pressure is p_T . Now suppose that, by movement of the pistons, one gram of helium is caused to flow from 0°K to T . The work done on the helium is $p_0/\rho_0 - p_T/\rho_T$, where ρ_0 and ρ_T are densities. The increase in energy of the entire system, helium and thermostats, is equal to $e_T - e_0 - Ts_T$, where e_T and e_0 are the respective energies per gram and s_T is the entropy per gram at T . The specific entropy of the liquid at 0°K is of course zero. Thus we may write

$$(2.3) \quad p_0/\rho_0 - p_T/\rho_T = e_T - e_0 - Ts_T.$$

If the liquid is incompressible $\varrho_0 = \varrho_T = \varrho$ and we may set $e_0 = 0$. Thus

$$(2.4) \quad P_s/\varrho = p_0/\varrho_0 = e_T - Ts_T + p_T/\varrho,$$

from which Eq. (2.1) follows. If the liquid is compressible so that e_0 depends upon the pressure, it would not be sensible to set $e_0 = 0$, and the equality of the ϱ 's would not hold. Thus Eq. (2.3) is somewhat more general than Eq. (2.4) or Eq. (2.1). In practice, however, the latter are excellent approximations.

This deduction rests upon the assumption that the heat absorbed from the thermostat is equal to Ts_T , despite the fact that there is heat conduction in the system, so that true equilibrium is not established. However, the heat is absorbed in an essentially isothermal region.

For the total pressure p_T at temperature T , we may write

$$(2.5) \quad p_T = x_s P_s + x_n P_n,$$

where the x 's are the mole fractions and P_s is the intrinsic pressure of the superfluid part and P_n that of the normal part. It may seem strange that P_s and P_n can be different, but the kinetic considerations to follow will indicate how this can occur. Actual acceleration of superfluid with respect to normal fluid is caused by gradients of P_s . The effective force *per unit volume* of the entire liquid is $-(\zeta_s/\varrho) \text{ grad } P_s$. The equation of motion to the first order (small velocities and pressure gradients) is

$$(2.6) \quad -(\zeta_s/\varrho) \text{ grad } P_s = (\varrho_s \varrho_n / \varrho) (\partial \mathbf{v}_s / \partial t - \partial \mathbf{v}_n / \partial t).$$

The last term in parentheses is the relative acceleration of superfluid with respect to normal fluid, and $\varrho_s \varrho_n / \varrho$ is the reduced mass per unit volume. No such simple relation exists for $\text{grad } P_n$ in the case where $\text{grad } p = 0$, for gradients of P_s and P_n occur together with gradients of x_s and x_n . It is not strange that such a dissymmetry should occur, since the possibility of an acceleration exists solely on account of the special properties of the superfluid.

The question remains as to how the pressure gradients in the superfluid are produced. The answer would seem to be that they are a result of interactions between the superfluid and the normal fluid. How this might come about can be most easily understood in the case of low temperatures, where the rotons can be considered as separate entities. Whether the roton be considered as an atom vibrating with excess energy, or as a hindered plane rotator [1], it is clear that it is exerting forces on the surrounding medium. Thus a roton can be said to exert a pressure on its surroundings greater than the same number of atoms would as superfluid. If there were a boundary beyond which no rotons existed, the superfluid between these rotons would have to be at a lower pressure than the superfluid beyond the boundary, if there is

to be no *overall* change of pressure at the boundary. Thus there would be a gradient (or, in the case considered, actually a discontinuity) in the pressure of the superfluid, tending to cause superfluid to move into the region in which there were more rotons.

At still lower temperatures one would have to take the effects of phonons into account, but this will not be discussed in this paper.

3. - Fluctuations in temperature.

In deductions of the equation for second sound the effect of temperature gradients on the flow of superfluid is considered, but no account is taken of temperature fluctuations. Though it may be shown that they do actually have no effect on the equation itself, it is easy to show that they must be deeply involved in the mechanism of transfer. The average of the square of the fluctuation, δE_{N_0} , of the energy of N_0 atoms is given by the formula [10]

$$(3.1) \quad \langle (\delta E_{N_0})^2 \rangle_{av} = kT^2 C_{v,N_0},$$

where k is the Boltzmann constant and C_{v,N_0} is the heat capacity (constant volume) of the N_0 atoms. If δE_{N_0} is interpreted as a fluctuation in temperature it is, if small enough, given by

$$(3.2) \quad \delta E_{N_0} = C_{v,N_0} \delta T.$$

Substituting in Eq. (31), we obtain

$$(3.3) \quad \langle (\delta T)^2 \rangle_{av} = kT^2 / C_{v,N_0} = RT^2 / N_0 C_v,$$

where R is the molal gas constant and where C_v is the molal heat capacity. For orientation, let us consider liquid helium at 2 °K, where C_v/R is already roughly 2. It is seen that the average fluctuation of a group of 500 000 atoms, large enough to act more or less like a macroscopic droplet, yet covering a very small extension in space, will be of the order of 0.1%. This will produce temperature gradients enormously greater than any attained in experiments on second sound. Thus the convection of superfluid in a second sound wave cannot be a steadily continuous process at all. It must be the result of the superposition of flows in all directions, the number or size of them in one particular direction predominating just a little in close analogy to an ordinary diffusion process, though very different as concerns the resistance encountered. It is also different, in that the driving force produces an average *acceleration* instead of an average velocity. It is because of this that a wave equation instead of a diffusion equation results.

This calculation will suffice to indicate the importance of fluctuations in the transfer process. It is clear that a certain amount of kinetic energy will be associated with these fluctuations, and it will be of interest to find out whether this can be comparable to the intrinsic roton energy. A very rough calculation will suffice, starting with a first approximation based on the assumption that the fluctuation energy is, indeed, negligible. It will facilitate this calculation to collect certain preliminary results.

At temperatures where rotons predominate over phonons but where the roton density is still not too great we may write approximately for the energy E_{N_0} of N_0 atoms

$$(3.4) \quad E_{N_0} = \varepsilon n_0,$$

where n_0 is the number of rotons associated with N_0 atoms. Neglecting the variation of ε with T and using the equation for N_0 constant,

$$d \ln n_0 / dT = \varepsilon / kT^2,$$

we may write

$$(3.5) \quad C_{v,N_0} \sim n_0 \varepsilon^2 / kT^2.$$

Then, since δE_{N_0} can be taken as approximately $\varepsilon \delta n_0$, Eq. (3.1) takes the interesting form

$$(3.6) \quad \langle (\delta n_0)^2 \rangle_{av} = n_0,$$

showing that the fluctuations in the number of rotons in a given volume behave like those of a gas.

We will also need an expression for the entropy S_{N_0} . In reference [1] it was shown by considering the partition function that the entropy associated with n_0 rotons is given by $n_0 k(\varepsilon/kT + 1) \sim n_0 \varepsilon / T$. Hence

$$(3.7) \quad S_{N_0} \sim C_{v,n_0} kT / \varepsilon.$$

Now let us suppose that our system is divided into cubic cells of volume V_0 each containing on the average N_0 molecules and n_0 rotons. Fluctuations will occur in these cells; if the temperature difference between one cell and its neighbor is δT , whose average value can be calculated roughly from Eq. (3.3), then $\text{grad } T$ will be equal to $\delta T / V_0^{1/3}$ and $\text{grad } n_0$ will be equal to $\delta n_0 / V_0^{1/3}$. As in Eq. (2.6) the effective force per unit volume due to these fluctuations will be $-(\rho_s / \rho) \text{grad } P_s$, and this will be capable of operating through a distance about equal to $V_0^{1/3} \delta n_0 / n_0$ since a flow through a distance of this order of magnitude would equalize the concentration gradient. The capacity of the

fluctuations to do work will thus be equal to about

$$(3.8) \quad \kappa \sim |(\varrho_s/\varrho)V_0^{\frac{1}{2}} \text{grad } P_s \delta n_0/n_0|$$

and this will be a rough measure of the kinetic energy per unit volume involved in the fluctuations. From Eq. (2.1)

$$(3.9) \quad \text{grad } P_s = \varrho \text{ grad } g = -\varrho s \text{ grad } T.$$

Now s is the entropy per unit mass, so ϱs is the entropy per unit volume and $\varrho s V_0$ is the entropy S_{N_0} per cell. By Eq. (3.2) $\text{grad } T = C_{v,N_0}^{-1} \text{grad } E_0 \sim C_{v,N_0}^{-1} \varepsilon \text{ grad } n_0$. Therefore by Eq. (3.7)

$$(3.10) \quad \left\{ \begin{array}{l} \text{grad } P_s = -(kT/V_0) \text{grad } n_0, \\ \phantom{\text{grad } P_s} = -(kT/V_0) V_0^{-\frac{1}{2}} \delta n_0 \end{array} \right.$$

The analogy to the perfect gas law is obvious; the negative sign occurs because we are considering the pressure within the superfluid rather than the apparent pressure exerted by the rotons. Substituting this in Eq. (3.8) we obtain

$$(3.11) \quad \kappa \sim (\varrho_s/\varrho)(kT/V_0)(\delta n_0)^2/n_0.$$

Since $\langle \kappa \rangle_{av}$ is the average kinetic energy per unit volume the kinetic energy per cell is $\langle \kappa \rangle_{av} V_0$ and $K = \langle \kappa \rangle_{av} V_0/n_0$ is the kinetic energy per roton. Making note of Eq. (3.6) and remarking that in the temperature region we are considering $\varrho_s/\varrho \sim 1$, we find

$$(3.12) \quad K \sim kT/n_0.$$

The value of K depends upon how large we choose the original cells. These should clearly be chosen as small as they can be so that the idea of fluctuations retains a meaning and Eq. (3.1) or (3.6) can be applied. It would be senseless to choose them so small that n_0 were less than 1, and so we see that the maximum amount of fluctuation energy is of the order of kT per roton. The size of the cells will depend on the temperature, but we are led to believe that the average energy per roton will be roughly proportional to kT and will be a substantial fraction thereof. Before considering this further, however, it will be well to turn to another aspect of the problem.

The transfer of rotons from place to place will not be solely by the type of bodily motion inferred from the fluctuations. An excitation can also pass from one atom or group of atoms to an adjacent one without transfer of mass;

this results in broadening of the energy levels, as previously discussed [1]. If a roton moves with energy kT at 1.4 °K, assuming from Table I that the roton involves 11 atoms, the velocity of bodily motion will be around 23 meters per second. The other type of transfer might be expected to occur with something like the velocity of sound, around 250 meters per second. If it actually were this fast transfer of energy from one molecule to the next would occur in about 10^{-12} s, which would by the uncertainty principle require a spread of roton energies of about 7° or 8° whereas we have assumed previously [1] that it was only about 2° . Since the energy of excitations (presumably corresponding to compressional waves) and hence the frequency, tends to level off, instead of increasing regularly with wave number as in the phonon range, the velocity (which is equal to the wave length times the frequency) must decrease and a transfer in $3 \cdot 10^{-12}$ s might be a reasonable estimate. Actually this is very close to \hbar divided by the energy of a roton, hence to the period associated with a roton. We can compare the effective diffusion current Γ_a , due to the motion of the excitations, with the current Γ_b arising from bodily motion. We will have [12]

$$|\Gamma_a| = D \text{ grad } n,$$

where n is the number of rotons per unit volume and D is the diffusion constant, or

$$|\Gamma_a| = D \text{ grad } (n_0/V_0) \sim D \delta n_0/V_0^{\frac{1}{2}}.$$

Further it may be shown [12] that

$$D \sim \frac{1}{6} \lambda_0^2 / \tau,$$

where λ_0 is the distance and τ the time of a single energy transfer ($\lambda_0 \sim 3 \cdot 10^{-8}$ cm and $\tau \sim 3 \cdot 10^{-21}$ s).

Hence

$$|\Gamma_a| \sim \frac{1}{6} \lambda_0^2 \delta n_0 / \tau V_0^{\frac{1}{2}} = \frac{1}{6} v \lambda_0 n_0^{\frac{1}{2}} / V_0^{\frac{1}{2}} = \frac{1}{6} v \lambda_0 n^{\frac{1}{2}} / n_0^{\frac{1}{2}}$$

(where $v = \lambda_0 / \tau$), since $V_0 = n_0 / n$.

On the other hand Γ_b will be given by

$$\Gamma_b \sim (n_0/V_0)(u/n_0^{\frac{1}{2}}) = nu/n_0^{\frac{1}{2}},$$

where u is the velocity of a roton if its kinetic energy is kT (the velocity varies as $n_0^{-\frac{1}{2}}$). Therefore

$$\Gamma_a/\Gamma_b \sim \frac{1}{6} (v/u) \lambda_0 n^{\frac{1}{2}} n_0^{-\frac{1}{2}} \sim \frac{1}{6} (v/u) (\lambda_0/\lambda) n_0^{-\frac{1}{2}},$$

where λ is the distance between rotons. Now v/u is greater than 1, as we have seen, but certainly up to 1.4° we will have $\lambda/\lambda_0 > v/u$. Thus Γ_a is essentially negligible if $n_0 > 1$. If n_0 could be taken as 1, Γ_a would just be beginning to be comparable to Γ_b ; this conclusion is confirmed by considering the mean random-walk displacement of a single excitation, noting the time required for a displacement which is an appreciable fraction of the average distance between rotons, and comparing the apparent velocity found in this way with the bodily velocity corresponding to the energy kT . Since n_0 must probably be taken as greater than 1, however, the average velocity of bodily transfer of a roton (particularly the relative velocity between near neighbors) will be less than this; thus it seems probable that for very fine-grained fluctuations, where this velocity must be compared to that of *single* energy transfers, the energy-transfer mechanism will be most important, but for fluctuations involving a number of rotons, where the diffusion calculation is necessary, the mass transfer will be most important.

If n_0 could actually be taken to be about equal to 1, one might question whether the rotons do not actually act as gas particles, so that one would have a gas of excitations in a rather literal sense, as has often been assumed. In this case the fluctuations would be the source of the entire entropy, and it would be calculated as the entropy of a gas rather than as an entropy of location in an array of atoms. However, I believe that in actuality the fluctuations must be secondary phenomenon, superimposed upon the excitations, and it seems more reasonable to calculate the entropy as was done in reference [1].

A value of n_0 as small as 1 would lead to a curious situation in another respect. We have noted that the roton energies are broadened into a band whose width has been estimated [1] as 2° . At least, this must be true if the rotons can be considered to be approximately independent of each other at low concentrations. The nature of the fluctuations does indeed, in itself, imply some interaction between rotons even at low concentrations, introducing a perturbation which is not there in the case of an isolated roton. However, it hardly seems likely that it is sufficient to broaden the band of energy levels appreciably. The calculation of fluctuation energies must be at best an approximation. The actual range of energies excited at any temperature could be accurately calculated, if we knew the individual energy levels of the entire system, by use of a canonical ensemble. If n_0 could be close to 1 our approximation would clearly already be breaking down around 1°K . However, since n_0 is probably greater than this, it may be a reasonable approximation to assume that it is relatively constant over the range of temperatures we need to consider. This would mean that the average kinetic energy would be proportional to T . If there is any effect of the finite width of the energy band, it will show up as a decrease in the rate of increase of kinetic energy at higher temperatures, when the average kinetic energy begins to approach

the width of the band. This presumably implies an increase in the value of n_0 as this condition is approached. Clearly this situation raises some rather fundamental and difficult questions, which need further consideration, and at the present time we can only offer a guess as to the possible nature of the answers. The size of the cells which we can choose will be limited essentially by the fact that if the cells are too small Eq. (2.1), which was actually derived for a macroscopic system, loses its meaning. If the temperature is so high that the entire width of the band is excited, it may not seem strange that Eq. (2.1) would break down for a larger size of cell than it would at lower temperatures, for once such a high temperature is reached a system containing a given number of rotons will change less and less with temperature, so that the expected changes of P_s with temperature will not occur so readily. However, this will be less true for a portion of a system containing a very large number of rotons, because the total range of energies for this entire portion (as contrasted to the range of energies per roton) will still be large compared to kT . In the case of liquid ^4He the situation is complicated by the increase in the number of rotons with temperature, and by their interaction. These complications would not occur, at least to the same extent, in a dilute solution of ^3He in ^4He , which in some respects is similar to a solution of rotons in superfluid, a case which I have discussed in preliminary fashion elsewhere [12].

4. - Discussion of the roton mass.

We saw in Sect. 1 that the apparent mass of the roton varies between that of 9 to over 20 atoms between 1.7° and 0.8° . The smallest of these numbers is greater than the number of atoms we believe to be actually involved in the elementary excitations. The apparent excess of mass might result in part from the extra effective mass arising from the flow of surrounding atoms around the atoms actually involved in the excitation; this would be analogous to the situation occurring in the flow of a perfect fluid around a sphere [13], as suggested by FEYNMAN [2], in the case of an ^3He atom moving through liquid ^4He ; however, the excess mass is greater than we would expect to be contributed in this way. One possible cause of the large size of the rotons may arise from the transfer of energy without bodily transfer of mass, which we have just discussed. If this type of transfer occurs rapidly enough the roton will move over a considerable region before the fluid in its vicinity has a chance to change its velocity. Thus we may ask how long it will require for an atom from which the excitation has just departed to acquire the superfluid velocity, or, more precisely, how long a time will be needed for it to come to the velocity of the superfluid to within a certain fraction of the difference in velocity between the rotons and the superfluid. If, for example, this time, t_0 , should be in-

versely proportional to the relative velocity u_0 of the rotons with respect to superfluid, and if z is proportional to the number of jumps of the roton from one atom to another and this is proportional to t_0 , we may show that the average value of z will be inversely proportional to the temperature T . For the kinetic energy of a roton, relative to the superfluid, will be given by

$$(4.1) \quad K = \frac{1}{2} z m u_0^2,$$

where m is the mass of a helium atom. If t_0 and hence z are inversely proportional to u_0 we see that K is proportional to u_0 . So if the average value of K is proportional to T , then the average of u_0 will be proportional to T , and that of z inversely proportional to T .

To gain a better idea of the situation we shall attempt to understand what might happen if an atom were suddenly deserted by a roton and surrounded by atoms moving on the average at a different velocity. Naturally, in actuality the desertion would not be sudden, and one would have to consider also how the atom got started. But this crude calculation may suffice to give some insight into what may be expected.

For the time t_0 to be inversely proportional to u_0 , it will be necessary for the force, tending to bring the velocity of the atom thus deserted by a roton into coincidence with that of the superfluid, to be proportional to u^2 . Here u is the instantaneous relative velocity of the atom with respect to the superfluid. This is not an unreasonable proposal; it will be recalled that the force exerted by a gas on a wall is proportional to the square of the velocity of its molecules. If this hypothesis is correct,

$$(4.2) \quad du/dt = -au^2$$

where $-a$ is a proportionality constant. Integrating from time $t = 0$ when $u = u_0$ to the time t_0 when $u = bu_0$, where b is some fixed fraction, we will have

$$(4.3) \quad u_0^{-1}(b^{-1} - 1) = at_0$$

thus demonstrating the proportionality.

An inverse proportionality of z to T was anticipated in the Landau-Feynman theory, as we have noted in Sect. 1. The deviations from inverse proportionality exhibited empirically in Table I may not all be real, as was also noted in Sect. 1. They may also result from inexactness in the hypotheses from which such proportionality is derived. The deviation between 1.4° and 1.7° could possibly be due to diminution in the rate of increase of K at the higher temperatures, arising from an increase in n_0 as discussed at the end of Sect. 3.

Landau's theory [3] did a little more than indicate an inverse dependence of z on T . It also provided a constant, which when properly assigned, gave the actual value of ρ_n , hence of z . The theory of Feynman and Cohen [2] actually gives the values of this constant, in reasonable agreement with Landau's assignment. The values of z appear to be of an entirely reasonable magnitude, when investigated from the present point of view. We have estimated, at the end of Sect. 3, that the average time of transfer of a roton from one position to the next is $3 \cdot 10^{-12}$ s. To cover approximately 10 atoms, as at 1.4° , would then require $3 \cdot 10^{-11}$ s. If a roton had a kinetic energy of kT , then from Eq. (4.1) the velocity u_0 would be about $2.5 \cdot 10^3$ cm s $^{-1}$. In $3 \cdot 10^{-11}$ s, then, an atom would move about 7 Å. The velocity corresponding to an energy of kT is an overestimate, but probably not an extreme overestimate. So an atom which has been deserted by a roton, will catch up with the superfluid in something like the time it would require an atom of superfluid to go past it, which is about what might have been anticipated. This description is, of course far too mechanistic for a system in which quantum effects are important; it may be hoped, however, that it may tell what will happen on the average.

One remarkable result of the inverse dependence of the mass of a roton upon kinetic energy follows from Eq. (4.1). It may be readily seen that the momentum, which for our purposes we define as zmu_0 , is independent of kinetic energy. Since the statistics does not depend upon the momentum, this will introduce no difficulty.

5. - «Edge effects» and modification of the two-fluid theory.

If our picture of a roton moving through superfluid is correct, we might well expect certain «edge effects», arising from differences in the velocities of the various atoms moving as part of the roton. It is possible to treat this problem only upon the basis of certain assumptions, so that what follows must be considered merely as a possible description. There is a large random motion of both superfluid and normal fluid, but we can suppose that there is a net drift of the main body of superfluid with velocity, \mathbf{v}_s and a net bodily motion of the excitations with velocity \mathbf{v}_n . Any particular roton is moving with some velocity \mathbf{v}_r with respect to the superfluid in its neighborhood, but at the edge of the roton we might well expect some atoms to be moving with a velocity relative to the superfluid which is somewhat different from this and may even be in the opposite direction. If there is no net drift ($\mathbf{v}_n = \mathbf{v}_s$) then we can match every roton with another one whose velocity is in exactly the opposite direction. We shall assume that, if the rotons as a whole receive a very small relative drift velocity \mathbf{v} ($= \mathbf{v}_n - \mathbf{v}_s$) in some particular direction,

it will be possible to match a roton with relative velocity $\mathbf{v}_r + \mathbf{v}$ with one with relative velocity $-(\mathbf{v}_r - \mathbf{v})$; this behavior is analogous to that of a gas which is drifting bodily. We shall further assume that in such a pair of rotons we can also match individual atoms. The relative velocity of the i -th atom will be changed by an amount \mathbf{v}_i , which will be the same for each atom of a matched pair of atoms, and is proportional to \mathbf{v} . Since the \mathbf{v}_r 's of matched pairs will cancel, the net transfer of material relative to the superfluid per unit cross section per unit time will be equal to $\sum_i m\mathbf{v}_i$, where the summation is taken over all atoms in a unit volume; \mathbf{v}_i is of course equal to zero for all atoms which have the velocity of the superfluid. We can define the density of normal fluid by the equation

$$(5.1) \quad \sum_i m\mathbf{v}_i = \rho_n(\mathbf{v}_n - \mathbf{v}_s).$$

If the velocity of the center of gravity is given by \mathbf{v}_0 we have

$$(5.2) \quad \left\{ \begin{aligned} \rho\mathbf{v}_0 &= \sum_i m(\mathbf{v}_i + \mathbf{v}_s) = \sum_i m\mathbf{v}_i + \rho\mathbf{v}_s \\ &= \rho_n(\mathbf{v}_n - \mathbf{v}_s) + \rho\mathbf{v}_s \\ &= \rho_n\mathbf{v}_n + \rho_s\mathbf{v}_s, \end{aligned} \right.$$

where $\rho_s = \rho - \rho_n$ is the density of superfluid. If the excitations do not move, $\mathbf{v}_n = 0$, and the rate of flow is given by $\rho_s\mathbf{v}_s$. This is the situation in a narrow capillary. Since the work done by a piston, as in the considerations of Sect. 2, depends upon the volume moved, the pressure P_s is properly considered as operating in a fraction of the liquid equal to ρ_s/ρ . The right-hand side of Eq. (2.6), however, will require some modification. This is true because the kinetic energy contributed by any single atom depends upon the square of its velocity, whereas its contribution to the *flow* depends upon the first power. If the superfluid is stationary the kinetic energy of a matched pair of atoms is equal to

$$(5.3) \quad \frac{1}{2}m(\mathbf{v}_i + \mathbf{v}_r)^2 + \frac{1}{2}m(\mathbf{v}_i - \mathbf{v}_r)^2 = m\mathbf{v}_r^2 + m\mathbf{v}_i^2,$$

where \mathbf{v}_i is proportional to \mathbf{v} , which in this case is equal to \mathbf{v}_n . In this case the kinetic energy is all kinetic energy of the normal fluid. It is seen that the extra kinetic energy (the second term on the right-hand side—the first term arises from the random motion of rotons) due to the drift of normal fluid,

which we will call K_n , is proportional to $v^2 = v_n^2$ and we may write

$$(5.4) \quad K_n = \frac{1}{2} \sum_i m v_i^2 = \frac{1}{2} f \rho_n v_n^2$$

where f is a constant of proportionality which will depend only on the thermodynamic variables such as temperature or pressure. If all of the atoms associated with a given roton moved in the same direction as the actual excitation and not more rapidly, then f would in general be less than 1, since velocities less than v_n would contribute proportionately less to the kinetic energy than they do to the rate of flow. But if some atoms participate in motion of the general character of that of a perfect infinite liquid through which a foreign body is moving, then they can make a contribution to the kinetic energy which is not connected with any contribution to the momentum whatsoever, as may readily be deduced from an integration over the angles of the component of the velocity of the liquid in the direction of motion of the body [14]. So we cannot say whether f is greater or less than 1.

If the superfluid is moving we must, since v_i has the character of a velocity relative to superfluid, add v_s to the velocity terms in Eq. (5.3). Thus the contribution of a pair of matched atoms to the kinetic energy will be

$$\frac{1}{2} m (v_i + v_r + v_s)^2 + \frac{1}{2} m (v_i - v_r + v_s)^2 = m (v_s + v_i)^2 + m v_r^2.$$

The total kinetic energy per unit volume will be obtained by summing over all atoms, and will be

$$\frac{1}{2} \sum_i m v_r^2 + \frac{1}{2} \sum_i m v_s^2 + v_s \cdot \sum_i m v_i + \frac{1}{2} \sum_i m v_i^2.$$

The first term is the kinetic energy due to the random motion of the rotons, i.e., the fluctuations, and will not be counted as part of the kinetic energy of drift of superfluid and normal fluid. From the first line of Eq. (5.2), the other three terms are given by

$$K = \frac{1}{2} \rho v_0^2 + \frac{1}{2} \sum_i m v_i^2 - \frac{1}{2} \rho^{-1} (\sum_i m v_i)^2.$$

By an obvious extension of Eq. (5.4), $\frac{1}{2} \sum_i m v_i^2 = \frac{1}{2} f \rho_n (v_n - v_s)^2$, and the last term can be evaluated from Eq. (5.1). We thus find

$$(5.5) \quad K = \frac{1}{2} \rho v_0^2 + \frac{1}{2} [1 + (f - 1) \rho / \rho_s] (\rho_s \rho_n / \rho) (v_n - v_s)^2.$$

The second term on the right-hand side of Eq. (5.5) is the relative kinetic energy. Now the rate at which a force operating between the superfluid and normal

fluid will do work will be equal to the scalar product of this force and $\mathbf{v}_s - \mathbf{v}_n$, and this will be equal to dK/dt . Therefore Eq. (2.6) should be replaced by

$$(5.6) \quad -(\rho_s/\rho) \operatorname{grad} P_s = f'(\rho_s \rho_n/\rho)(\partial \mathbf{v}_s/\partial t - \partial \mathbf{v}_n/\partial t),$$

where

$$(5.7) \quad f' = 1 + (f - 1)\rho/\rho_s,$$

and the left-hand side of Eq. (2.2) should also be multiplied by f' .

The equation for second sound is ordinarily derived by using the equation of continuity of entropy

$$(5.8) \quad \partial \rho s / \partial t + \operatorname{div}(\rho s \mathbf{v}_n) = 0,$$

which states that the entropy follows the rotons, together with Eq. (2.2) or its equivalent, and the equation obtained by setting $\mathbf{v}_0 = 0$ in Eq. (5.2). If this derivation be carried out with the altered form of Eq. (2.2) the equation for the velocity of second sound turns out to be

$$(5.9) \quad u_{\text{II}}^2 = (\rho_s/\rho_n f') s^2 T / c_p.$$

Here c_p is the heat capacity at constant pressure per unit mass. The entropy is also reckoned per unit mass. It will be seen that the velocity of second sound yields a value of $f'\rho_n/\rho_s$ rather than ρ_n/ρ_s directly. One attempts to calculate $\rho_n/\rho = 1/(1 + \rho_s/\rho_n)$ and it is found then that the calculation gives

$$(5.10) \quad \frac{f'\rho_n}{\rho_s + f'\rho_n} = \frac{f'\rho_n/\rho}{f' + (1 - f')\rho_s/\rho} = \frac{1 + (f - 1)\rho/\rho_s}{1 + (f - 1)\rho/\rho_s + 1 - f} \frac{\rho_n}{\rho} = f'' \frac{\rho_n}{\rho},$$

instead of ρ_n/ρ . Thus we come to the conclusion that second sound will not give ρ_n/ρ directly, but rather a somewhat involved function.

A similar conclusion will hold for the Andronikašvili oscillating disk experiment. This experiment involves the transfer between the potential energy of a fiber and the kinetic energy of the oscillating disk and the normal fluid, the superfluid remaining stationary. Eq. (5.4) will be applicable to this case. If the normal fluid all moves together it contributes to the kinetic energy an amount equal to $\frac{1}{2}I\omega^2$, where I is the moment of inertia and ω is the angular velocity. If some of the atoms move with velocity different from \mathbf{v}_n the apparent moment of inertia will be changed by a factor f , and we will measure $f\rho_n/\rho$ instead of ρ_n/ρ .

We will now be interested in comparing f with the factor f'' which appears in Eq. (5.10), for this will allow us to compare the results obtained by second sound and by the Andronikašvili experiment. We really have little idea of the possible range of f , but we have made some calculations with f not too

far removed from 1, as shown in Table II. It will be seen that the deviations amount to only a few percent. up to relatively high values of ϱ_n/ϱ where there will be coalescence of rotons and more tendency of superfluid to slip around the normal fluid without involving too many of its atoms. Thus at large ϱ_n/ϱ

TABLE II. — Values of f'' for given values of f and ϱ_n/ϱ .

$f \backslash \varrho_n/\varrho$	0.8	0.9	1.1	1.2
0.25	0.786	0.897	1.097	1.187
0.50	0.750	0.889	1.091	1.167
0.75	0.500	0.857	1.078	1.125

we expect f to be closer to 1. On this basis, it seems reasonable to suppose that differences between the determinations from second sound and the Andronikašvili experiment need not become very serious. Since f is always greater than f'' , the apparent ϱ_n/ϱ obtained from the Andronikašvili experiment should be greater than that obtained from second sound, so this effect cannot be related to the discrepancies discussed in Sect. 1.

6. — Exchange of energy and approach to equilibrium.

In my earlier discussion of the second-sound equations, I showed that it was necessary to suppose that change of superfluid to normal fluid occurred during the passage of the wave. A mechanism, by means of which equilibrium, can be maintained, can readily be visualized in terms of the fluctuations we have discussed. There will always be some fluctuations involving large kinetic energies. We can imagine, therefore, that two rotons with sufficient relative kinetic energy between them could come together and form a third roton. In the reverse process, a triple collision (*) of three rotons, one roton will disappear and the two remaining ones will have a high kinetic energy. If the kinetic energy of a roton is as high as the intrinsic energy of the roton, very few atoms will be involved in the motion, so the roton will be highly localized. Therefore, it seems likely that such a collision would be reasonably effective.

There is no obvious way in which the mechanism described would tend to change the kinetic energy of a steady drift into rotons. In a triple collision, the rotons involved would themselves have an average drift and this

(*) The mechanism of collision which we have in mind here involves the coming together of rotons through energy transfer from one atom to another (energy-transfer mechanism) rather than that occurring due to bodily motion of the rotons (bodily-motion mechanism).

would presumably be preserved in the collision. However, if superfluid or normal fluid are accumulating in any region of space, as happens in second sound, there is no longer a *steady* drift; kinetic energy of relative motion could then presumably be transferred into fluctuation energy and ultimately converted into rotons in the way we have described, or vice versa

It is possible to estimate the rate at which three-roton collisions can occur. At the end of Sect. 3 we estimated that the time required for a roton to pass from one position in the liquid to the next will be about $3 \cdot 10^{-12}$ s. The chance that a roton has another roton next to it will be about $4n/N$, assuming four nearest neighbors, where there are n rotons per N atoms and the chance that the two will have still another neighbor will be about $6n/N$. It will, therefore, take about $3 \cdot 10^{-12}/(4n/N \times 6n/N)$ or $1.25 \cdot 10^{-13}(N/n)^2$ s for a given roton to make a successful collision; since three rotons are involved the number of collisions per roton per second will be $1.3 \cdot 10^{12}(n/N)^2$. From Table II of reference [1] this means about $1.2 \cdot 10^6$ possibly effective collisions per second at 1.1° , which should be amply sufficient to maintain equilibrium at the frequencies at which second sound is generally investigated. At 0.8° , however, there are only about $1.4 \cdot 10^3$ effective collisions per second, which may be more questionable. There is, however, apparently little dispersion in attenuation of second sound down to 0.8° at frequencies around 10^4 Hz. We may have underestimated the number of effective collisions, since we assumed in the calculation that a roton involves only one atom. But probably more important is the fact that at 0.8° phonons furnish the greater part of the energy, though only a small part of ϱ_n . In the discussion of the attenuation of first sound [14], it has been assumed that the number of rotons (and of phonons) can change in processes involving phonons, and that may be of importance, though just how effective such processes would be in effecting transfer between fluctuations energy and roton energy is difficult to see.

The energy-transfer mechanism of collision would seem to be the appropriate one to use for consideration of the exchange of energy between fluctuations and rotons. For a discussion of viscosity, on the other hand, a bodily motion mechanism must be involved. Though details of earlier calculations would be altered, it would seem that our picture of the motion of the rotons even if they tend to move in small groups, would make them sufficiently gas-like so that the results would not be greatly altered. For transfer of relative energy of drift to thermal energy, resulting in friction between superfluid and normal fluid and being connected with a critical velocity, collisions of rotons with quantized vortices may be especially important [15]. Again the results should not be greatly altered. The energy-transfer mechanism we have described may even in these cases be of some importance for the ultimate transfer of drift energy (through fluctuation energy) into rotons.

REFERENCES

- [1] O. K. RICE: *Phys. Rev.*, **108**, 551 (1957).
- [2] R. P. FEYNMAN: *Phys. Rev.*, **94**, 262 (1954); R. P. FEYNMAN and M. COHEN: *Phys. Rev.*, **102**, 1189 (1956).
- [3] L. LANDAU: *Journ. Phys. USSR*, **5**, 71 (1941); **11**, 91 (1947).
- [4] O. K. RICE: *Phys. Rev.*, **103**, 267 (1956).
- [5] J. G. DASH and R. D. TAYLOR: *Phys. Rev.*, **105**, 7 (1957). The value of x at 1.1° was obtained by extrapolation, using the curve given by DASH and TAYLOR. Their actual data may indicate a slightly lower value at 1.1° .
- [6] H. C. KRAMERS in *Progress in Low Temperature Physics*, vol. II, (Amsterdam 1957), p. 65. See note added to reference [1].
- [7] H. C. KRAMERS, T. VAN PESKI-TINBERGEN, J. WIEBES, F. A. W. VAN DEN BURG and C. J. GORTER: *Physica*, **20**, 743 (1954).
- [8] F. LONDON: *Superfluids* (New York, 1954), Vol. 2, pp. 77 ff, 83.
- [9] D. V. GOGATE and P. D. PATHAK: *Proc. Phys. Soc.*, **59**, 457 (1947).
- [10] R. C. TOLMAN: *Principles of Statistical Mechanics* (Oxford, 1938), p. 632.
- [11] See E. H. KENNARD: *Kinetic Theory of Gases* (New York, 1938), pp. 186, 272, 287.
- [12] O. K. RICE: to be published in the *Proceedings of the Symposium on Liquid and Solid ^3He* , Ohio State, (1957).
- [13] See, e.g., R. A. HOUSTOUN: *Introduction to Mathematical Physics* (London, 1920), pp. 54 ff.
- [14] I. M. HALATNIKOV: *Žu. Ėksper. Teor. Fiz.*, **20**, 243 (1950); **23**, 21 (1952).
- [15] See H. E. HALL and W. F. VINEN: *Proc. Roy. Soc.*, A **238**, 204, 215 (1956); W. F. VINEN: *Proc. Roy. Soc.*, A **240**, 114, 128 (1957).

INTERVENTI E DISCUSSIONI

— A. R. UBBELOHDE:

Would you expect the relaxation time of these rather large fluctuations to be of the same order as your estimate of the vibrational time? (about $3 \cdot 10^{-12}$ s).

— O. K. RICE:

The time of relaxation for transfer of energy without transfer of mass is of the same order of magnitude as the period to be associated with a roton, but this is sufficient to produce a spread in roton levels of only 2° as compared with the energy of around 10° . The spread of 2° seems consistent with thermodynamic data.

— M. TODA:

May I ask your opinion as to the superfluidity in liquid helium, how can it be interpreted from cell model, not from excitation spectrum?

— O. K. RICE:

Transfer of energy of drift motion of superfluid with respect to rotons into roton energy is difficult because of the energy gap. The fluctuation energy can perhaps be changed into roton energy via high-energy fluctuations, but as far as I can see this is independent of any relative drift. Another mechanism must be involved in the frictional forces between superfluid and normal fluid.

On the Structure of Liquid ^4He .

S. FRANCHETTI

Istituto di Fisica dell'Università - Firenze

Some years ago [1] the present author proposed an expression for the eigenfunctions of liquid ^4He based on the idea of « local eigenfunctions ». These—assumed spherically symmetrical for simplicity—should represent the motion of any atom in the field of its neighbours. An empirical evaluation of the local eigenfunction $\varphi(r)$ was given in [1]. It is essentially based on the amount of zero point energy. This function $\varphi(r)$ corresponds to the fundamental state for a potential well which has to take into account the *correlations* between the movements of the atoms. This effective potential is therefore different (in particular, flatter) than that which would be obtained averaging on any suitable distribution of *fixed* neighbours. (However, the next energy level is sufficiently higher so as to be practically unoccupied at the low temperatures in question).

The most natural way—and perhaps the only self-consistent one—to build one-particle eigenfunctions, starting from local ones, is to suppose that these can be arranged in space so as to form a *lattice*:

$$(1) \quad \psi(\mathbf{p}) = \sum_n c_n \varphi(|\mathbf{p} - \mathbf{r}_n|),$$

with \mathbf{r}_n fixed vectors ending at the lattice points.

The fundamental one-particle eigenfunction is characterized by $c_n = \text{const}$ and from this one we may construct the fundamental eigenfunction for a system of N (Bose) atoms:

$$(2) \quad \Psi(\mathbf{p}_1 \dots \mathbf{p}_N) = Q_N \prod_{\alpha=1}^N \sum_{n=1}^N \varphi(|\mathbf{p}_\alpha - \mathbf{r}_n|)$$

(which alone will be considered here).

One of the most simple checks of this formula is to see if one can find a lattice such that the radial distribution function $D(r)$ (*) deduced from (2) agrees with the experimental one, supposed not to differ markedly from that at 0°K (where (2) should be valid). Since however expression (2) involves the free overlapping of the one-particle eigenfunctions, it cannot be expected to give correct results in the region of small distances. A correction for this may be introduced by means of a factor [2, 3]

$$(3) \quad \prod_{(\alpha > \beta)} f(|\mathbf{p}_\alpha - \mathbf{p}_\beta|),$$

with $f(r)$ a suitable « continuized step-function » with asymptotic value unity.

Comparison between experimental $D(r)r^2$ and the distribution of distances in the collision between two He atoms at a suitable energy (about $15 \cdot 10^{-16}$ erg) [4]

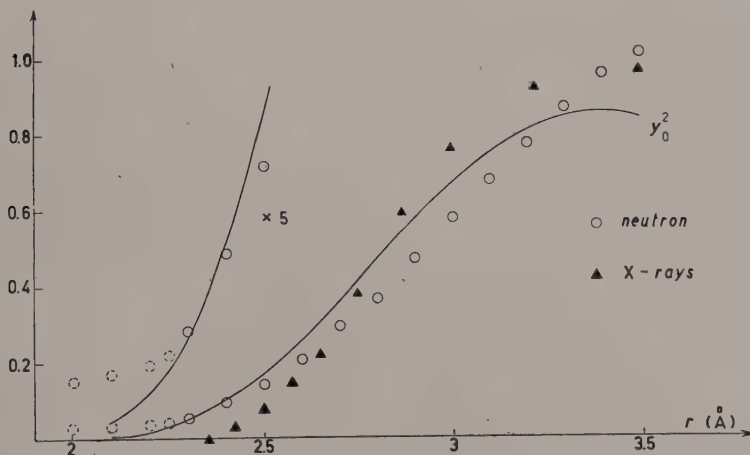


Fig. 1. — *Full curve*: The function $y_0^2 = r^2 R^2(r)$ (suitably normalized) with $R(r)$ the radial eigenfunction for the collision between two neutral helium atoms with $E = 15 \cdot 10^{-16}$ erg and $l=0$. ($l=2$ or $l=4$ would give practically the same result in the region of interest). *Circles*: Values of $D(r)r^2$ according to HURST and HENSHAW. (The dotted ones unreliable). Neutron diffraction, ref. [5]. *Triangles*: Values of $D(r)r^2$ from X-ray diffraction. (C. F. A. BEAUMONT and J. REEKIE: *Proc. Roy. Soc.*, **228**, 363 (1955)).

shows that $f(r)$ should be determined essentially by binary collisions, as was to be expected. It shows also that, at least for small distances ($2 \div 3 \text{ Å}$) neutron

(*) Defined so that $4\pi D(r)r^2 dr$ is the probability of finding an atom at a distance between r and $r+dr$ from a given one.

diffraction results are more reliable than those obtained with X-rays, so that the former ones have been preferred for the testing of the theory.

Combining (1), (2) and (3) one has the eigenfunction

$$(4) \quad \Psi = Q_N \prod_{\alpha=1}^N \sum_{n=1}^N \varphi(|\mathbf{p}_\alpha - \mathbf{r}_n|) \prod_{(\beta > \gamma)} \varphi(|\mathbf{p}_\beta - \mathbf{p}_\gamma|).$$

The procedure for deducing from this the radial distribution function $D(r)$ is a standard one. The basic formula turns out to be

$$D(r)r^2 dr = c \int_r^{r+dr} d^3\mathbf{p} \int_{-\infty}^{\infty} d^3\mathbf{p}_2 \sum_{n=1}^N \sum_{m=1}^N \varphi(|\mathbf{p} + \mathbf{p}_2 - \mathbf{r}_n|) \varphi(|\mathbf{p} + \mathbf{p}_2 - \mathbf{r}_m|) \cdot \\ \cdot \sum_{n=1}^N \sum_{m=1}^N \varphi(|\mathbf{p}_2 - \mathbf{r}_n|) \varphi(|\mathbf{p}_2 - \mathbf{r}_m|) f^2(\varrho).$$

In the double sums, the only terms that matter are those in which n, m are the same (main term in the final result) or else represent next-neighbouring lattice points (correction term of the order of $\sim 5\%$). The final formula (with some simplifications) is

$$D(r) = \text{const } f^2(r)r^{-1} \left[2\mathcal{G}(r) + \sum_n \frac{1}{r_n} \mathcal{F}(|r - r_n|) + \frac{2\sigma}{\pi} \sum_v \frac{1}{f_v} \mathcal{J}(r, f_v) \right].$$

Here \mathcal{G} , \mathcal{F} and \mathcal{J} are defined as follows. Put

$$\int_0^r \varphi^2(z)z dz = I(r),$$

then,

$$\mathcal{G}(r) = \int_0^\infty [I(r+z) - I(|r-z|)] \varphi^2(z)z dz,$$

$$\mathcal{F}(x) = \int_{-\infty}^\infty [I(\infty) - I|z|][I(\infty) - I|z-x|] dz,$$

$$\mathcal{J}(r, f_v) = I(r + f_v) - I(|r - f_v|).$$

As regards σ , this is an overlap integral between next-neighbouring local eigenfunctions (see [1] and [5]). The subscripts n and v number, respectively, the

lattice points and the points midway between next neighbouring lattice points, while r_n and f_n are the corresponding distances from a fixed lattice point. The structure of the lattice does not enter otherwise, so the testing of the various lattices is not too difficult.

The determination of $f(r)$ has not been settled in detail for the moment. Indeed, it affects the distribution only at distances $< 3 \text{ \AA}$, while the important region for deciding about the structure is that from, say, 3 to 10 \AA (where $f(r)$ would be practically unity).

The best result so far has been obtained with a face-centered cubic lattice. In the drawing, the full curve represents $D(r)r$ as given by HURST and HENSHAW [6] while the dotted (upper) curve represents the same quantity calculated as explained. The experimental curve would result from adding to the calculated

curve the lower (dotted) one and reducing by a factor 0.91. The overall density of the « correction distribution » amounts therefore to 9% of the total.

This result is not altogether unsatisfactory if one bears in mind that:

- a) deviations of the observed kind can be expected from the simplifications introduced (in particular the assumption of a *spherical* local eigenfunction $\varphi(r)$);
- b) the determination of $\varphi(r)$ itself is little more than a tentative one.

A fuller account will follow in due course.

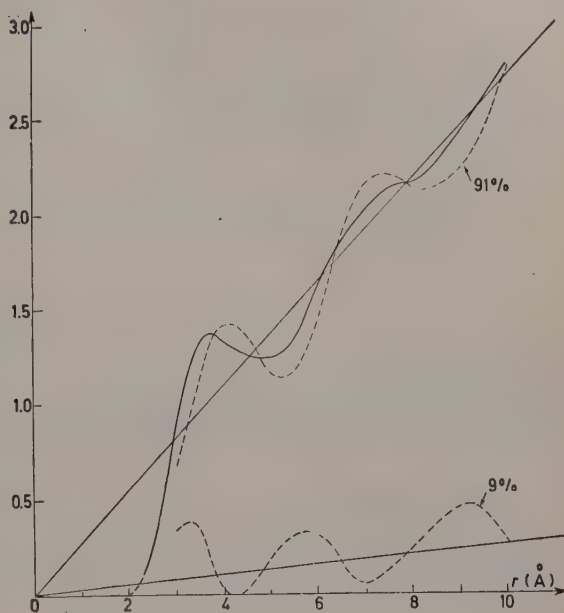


Fig. 2. — Full curve: $D(r)r$ as given by HURST and HENSHAW (ref. [7]). Upper dotted curve: The same, calculated as explained in the text. Lower dotted curve: « Correction distribution » (see text).

REFERENCES

- [1] S. FRANCHETTI: *Nuovo Cimento*, **12**, 743 (1954).
 - [2] N. F. MOTT: *Phil. Mag.*, **40**, 61 (1949).
 - [3] R. B. DINGLE: *Phil. Mag.*, **40**, 573 (1949).
 - [4] S. FRANCHETTI: *Nuovo Cimento*, **6**, 601 (1957).
 - [5] S. FRANCHETTI: *Nuovo Cimento*, **5**, 183 (1957).
 - [6] D. G. HURST and D. G. HENSHAW: *Phys. Rev.*, **100**, 994 (1955).
-

INTERVENTI E DISCUSSIONI

— O. K. RICE:

How do these results fit in with the considerations of F. LONDON, by means of which he estimated the potential energy and zero-point energy of liquid helium?

— S. FRANCHETTI:

I think the present treatment should be an improvement over the old London calculations, since it takes into account the large spreading of atoms around their equilibrium positions.

Velocity of Sound in Liquid Helium.

A. VAN ITTERBEEK

Instituut voor Lage Temperaturen en Technische Physica - Leuven

As is well known the velocity of sound in liquid helium has a very peculiar behaviour. In fig. 1 the change of the velocity of sound is graphically drawn as a function of temperature. Different investigators (e.g. FINDLAY [1], PEL-

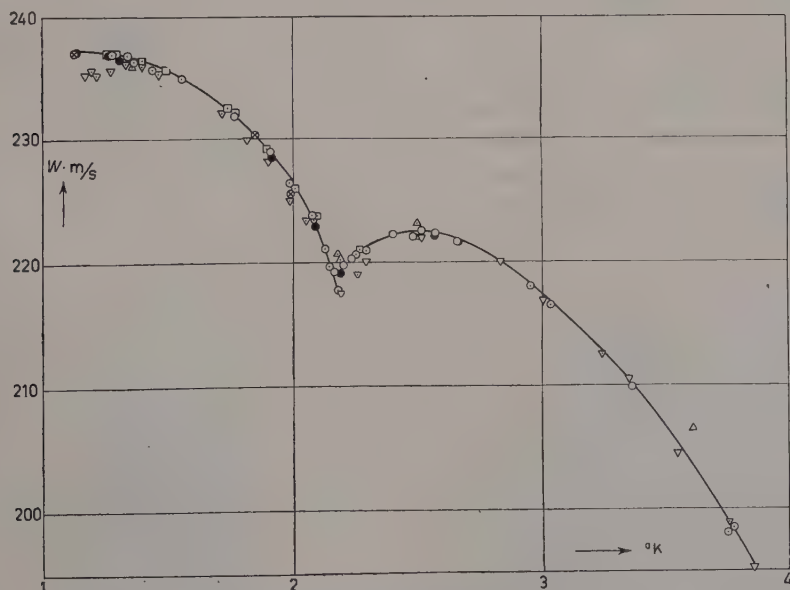


Fig. 1. — Velocity of sound as a function of temperature. FINDLAY 1.388 MHz; ATKINS and CHASE 14 MHz; VAN ITTERBEEK and FORREZ 520, 218, 423.91 and 800.95 kHz.

LAM and SQUIRE [2], ATKINS and CHASE [3], VAN ITTERBEEK and FORREZ [4], CHASE [5]) have contributed to establish this experimental curve.

We can firstly remark the special behaviour at the λ -point and further that no dispersion seems to appear. There are only the deviation of the measu-

rements of ATKINS and CHASE, but fit completely with our experiments. We examined specially the eventual appearance of a dispersion. Later on together with VAN DEN BERG, HERFKENS, and VAN AARDENNE [6] the same problem was examined with the optical method. But no dispersion could be detected. There is only a small doubt in the neighbourhood of the λ -point, where the measurements are very difficult. All these measurements were carried out only down to 1.93 °K.

In Fig. 2 is represented the peculiar behaviour of the sound absorption as a function of temperature in the neighbourhood of 1 °K.

We can again remark the specific behaviour of the absorption in the vicinity of the λ -point. Going down to lower temperature the absorption of sound increases

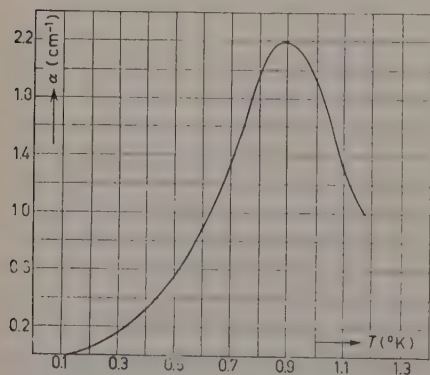


Fig. 2. — Absorption of sound as a function of temperature.

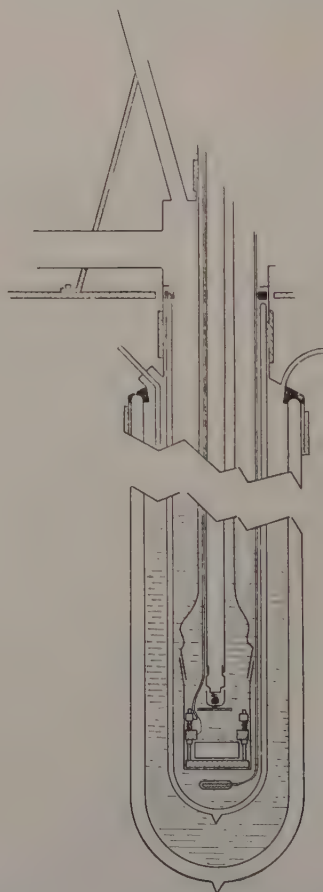


Fig. 3. — Acoustic interferometer with cryostat.

and there is a strong influence of the frequency. CHASE [7] and later on CHASE and HERLIN [8] succeeded in measuring the absorption of sound down to 0.1 °K using the pulse technique. They found the appear-

on between
present.
ted by
between

a dis-
in the

velocity
1 °K.

hod, which
accuracy was

herefore the,
n-pump. The

hood of 1 °K.

	umber i measu- rements	W average (m/s)	
	5	0.06	
	17	0.24	
	3	0.40	
5	3	0.02	
57	12	0.15	
1.48	10	0.16	
37.81h0	100	0.26	
237.68	7	0.63	
237.75	18	0.15	
238.05	11	0.24	
237.40	10	0.23	
237.22	16	0.37	
3	237.78	9	0.11
5	237.69	10	0.30
05	237.64	1	—

From these measurements we see again that there occurs no dispersion, within one part on 2400. Comparing also these results with those of Table I, we see that the velocity becomes constant as a function of temperature.

In Table II are indicated the values obtained by CHASE.

TABLE II.

T (°K)	Frequency (kHz)	W (m/s)	Remark
1.50	between 2.0 and 12.0	236.8	CHASE (private communication)
1.40		237.3	
1.2		237.7	
1.0		237.9	

From these measurements we see that no dispersion appears and that there is a good agreement with the measurements of CHASE (see Table II). Later on we connected the cryostat to a big « Edwards booster-pump » (see Fig. 4) and so we succeeded in reaching a temperature of 0.985 °K. The measurements were repeated with the same frequencies and the results are represented in Table III.

TABLE III. — Velocity of sound in liquid helium at 0.985 °K.

Date	p (mm Hg)	T (°K)	Frequency (kHz)	W (m/s)	Number of measurements	Remarks
20-11-1956	0.105	0.985	218.24	238.51	11	Large imped.
20-11-1956	—	0.985	218.012	239.35	9	Large imped.
—	—	—	214.257	238.27	8	Large imped.
—	—	—	226.385	237.81	6	Small imped.
—	—	—	226.241	237.65	8	Small imped.
—	—	—	226.242	237.63	9	Small imped.
9-11-1956	0.105	0.985	523.03	237.63	28	
12-10-1956	0.105	0.985	800.374	237.53	23	
21-9-1956	0.146	0.997	1455.78	237.73	19	

impedance or sound intensity seem however to have a small influence on the value of the velocity.

Recently we succeeded by using a method based on audible sound, to

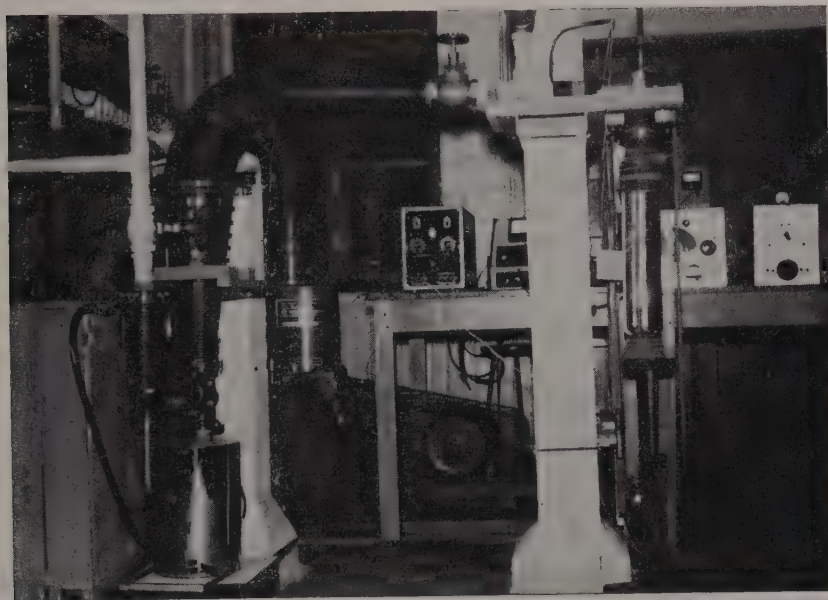


Fig. 4. — Photograph of the apparatus.

measure the velocity of sound in helium gas as a function of temperature at the corresponding vapour pressure.

The experimental results are graphically drawn in Fig. 5. From this figure we see that no discontinuity appears at the λ point in comparison with what happens for the sound velocity in the liquid.

We take the opportunity to express our truly thanks to Mr. G. FORREZ and M. TEIRLINCK for their help during the measurements.

Further I thank the Belgian Ministry of Education for its financial aid during these measurements.

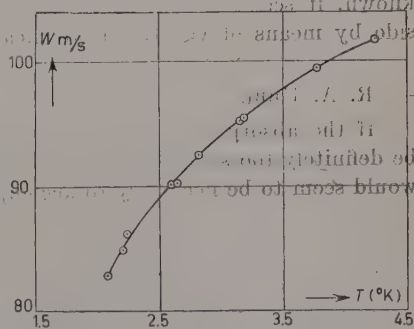


Fig. 5. — Velocity of sound in helium gas as a function of temperature at the corresponding vapour pressure.

REFERENCES

- [1] J. C. FINDLAY, A. PITT, U. GRAYSON SM²
54, 206 (1938).
- [2] J. P. PELLAM and CH. F. SQUIRE.
- [3] K. R. ATKINS and C. E. CHAS²
- [4] A. VAN ITTERBEEK and G
- [5] A. VAN ITTERBEEK, G. ²
- [6] G. J. VAN DEN BE²
KENS: *Phys²*
- [7] C. E. CHAS²
- [8] E. C. C²
- [9] L. ²

aligned at temperatures of the order of 5°K , the Fermi temperature for such a system, as the particles condense into the lowest energy levels. Since the particles thus aligned could not contribute to the magnetic susceptibility, this model would predict a nuclear magnetic susceptibility which deviates from the classical $1/T$ Curie law below 5°K becoming finally temperature independent as the absolute zero is approached.

Since nuclear magnetic moments are extremely small, conventional methods of susceptibility measurements are difficult [2], although HAMMEL *et al.* [3] have demonstrated the absence of ferromagnetism in liquid ^3He down to 1.2°K by this method. Nuclear resonance techniques [4-6], however, offer a convenient means of measuring very small susceptibilities. If the sample under investigation is immersed in a steady magnetic field H_0 and is excited at the Larmour frequency $\nu_0(H_0)$ of the nuclear spins by a weak radio frequency field at right angles to H_0 , then transitions will be induced among the energy levels of the spin system. For the ^3He nucleus there are two allowed orientations with respect to the field, separated in energy by $2\mu H_0$, where μ is the magnetic moment of the ^3He nucleus. Once thermal equilibrium is attained, there will be a surplus of spins in the lower state, and, during resonance, power will be absorbed by the sample from the radio frequency field. The power absorbed is directly proportional to the difference in population of the two spin states and therefore to the static nuclear susceptibility.

We have succeeded [7,8] in measuring the temperature dependence of the nuclear susceptibility of ^3He by observing the strength of the nuclear resonance absorption signal. Under the conditions of the experiment, the amplitude of the nuclear resonance signal, corrected for its small effect on the Q of the coil, is proportional to the nuclear volume susceptibility [4,5,7]. The experimental results for ^3He under its saturated vapor pressure are shown in Fig. 1. The molar susceptibility, χ , has been calculated from the volume susceptibility using the density measurements of KERR [9]. The signal in the gas at 4.2°K , where the susceptibility would be expected to be nearly classical, was used to normalize the data to the Curie curve. χT has been plotted vs T so that the Curie curve, 1, becomes a straight line parallel to the temperature axis. It is seen that the data fall between curve 1, and curve 3, the curve for an ideal Fermi-Dirac gas with a degeneracy temperature of 5°K , appropriate for an ideal gas of the same density and atomic mass as ^3He . For comparison, curve 2 is the curve for a Fermi-Dirac gas with a degeneracy temperature of 0.45°K , arbitrarily selected to give the best fit to the data. The normalization techniques mentioned above using the gas at 4.2°K are not sufficiently accurate to ascertain whether or not there is in reality a 5% departure from the Curie curve at 1.2°K as would be expected from Curie curve 2. We have drawn in the dashed curve as the data would appear if normalized to the Curie curve at 1.2°K . As will be discussed later, a com-

parison of susceptibility measurements as a function of pressure with the recent density data [10] gives some evidence that the degeneracy at 1.2 °K is less than 5%. The normalization indicated by the dashed curve will be used for comparing the data in Fig. 1 with the data taken under pressure.

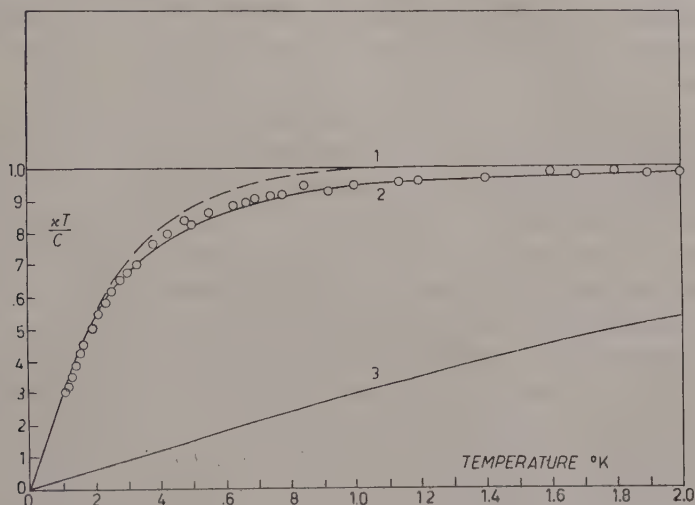


Fig. 1. — Plot of $\chi T/C$ vs. T . (χ = molar nuclear magnetic susceptibility of ^3He , T = absolute temperature, C = normalizing Curie constant). Curve 1 represents the Curie law expected from Boltzmann statistics, curve 3 represents an ideal Fermi-Dirac gas with the same density and atomic mass as liquid ^3He ($T_0 = 5^\circ$), curve 2 represents an ideal Fermi-Dirac gas with a degeneracy temperature $T_0 = 0.45^\circ\text{K}$. The circles represent the experimental points. The dashed curve represents the experimental data normalized to the Curie curve at 1.2° .

REMARK

on Fig. 1

It appears from this experiment that the nuclear spins of liquid ^3He line up antiparallel as would be expected of an ideal gas, but at temperatures an order of magnitude lower. At the lowest temperatures the susceptibility has become independent of temperature as expected of an ideal gas, but with a constant value about 10 times greater than the analogous gas model.

As will be pointed out by Dr. WEINSTOCK in the following talk, the specific heat data also seem to indicate spin ordering below 0.5°K , but does not bear the same type of relationship to an ideal gas shown by the susceptibility [11-13]. This difference has been stressed by BUCKINGHAM, who has pointed out that this implies the existence of strong spin dependent exchange forces tending toward parallel alignment of the spins which effect strongly the susceptibility, but not the specific heat. He has suggested [14] that under certain conditions, one might even expect the exchange forces tending toward parallel alignment to exceed the statistical forces tending toward antiparallel

...rie
..., which
... during de-
...riety of control-

...ved for solid ^3He in the
...nt fact does emerge. In each
...ve of spin alignment, occur at the
...re as in the liquid at melting pressure,
...stronger than the classical dipole interaction

... Fig. 2 that the spin ordering in the solid occurs at
...ature than in the liquid. Hence, at any given tempe-
...ut 0.4°K it would appear that the spin entropy is somewhat
...ne solid than in the liquid. An attempt was made to determine
... or not the total entropy of the solid was greater than the total entropy
...he liquid by allowing the solid to expand adiabatically into a liquid. It
...was found that heating occurred at the melting point for temperatures below
...about 0.4°K , and cooling occurred above this temperature. This would seem
...to indicate that the entropy in the solid is greater than the entropy in the

liquid below 0.4°K and that a minimum in the melting pressure curve should occur at this point, providing friction is not responsible for the heating.

When the experiment is performed on the solid which shows the anti-parallel alignment indicated in Fig. 2, the quantities of heat liberated below 0.4°K are measured to be approximately equal to the temperature times a reasonable estimate of the entropy differences between the solid and liquid as determined from the susceptibility data. This would be expected in the case of a reversible expansion. On the other hand, when the adiabatic expansion experiments were performed during the earlier runs in which the solid exhibited a tendency toward parallel alignment, it was found that approximately four times as much heat was released as would be expected. This is another important difference between the two results obtained in the solid. The large amount of heat liberated when the solid melted suggests an irreversible process in which some of the energy of compression was lost to heat. This suggests the presence of more strains or greater compression in the solid during the runs which showed a ferromagnetic tendency, and the possibility that the spin ordering in solid ^3He depends critically on the degree of compression or on the presence of strains. If friction were responsible for the heating, then there had to occur a large change in the amount of friction between the runs showing parallel alignment and the runs showing anti-parallel alignment.

GRILLY and MILLS [29] have reported a phase transition in solid ^3He . This solid-solid transition intersects the melting curve at 3.15°K and occurs at decreasing pressures as the temperature is reduced. It is interesting to speculate on whether the peculiar behavior of the spin system in the solid below 0.2°K is related to this phase change. In the experiment on melting mentioned above the expansion takes place suddenly when a pressure equal to the minimum in the melting pressure is reached and the capillary becomes unplugged. ONSAGER has pointed out that if the expansion in the parallel

alignment case is from a high pressure phase of the solid directly to the liquid without forming the intermediate lower pressure phase, the expansion would be irreversible.

Fig. 3 is a graph of the spin lattice relaxation time, T_1 , as

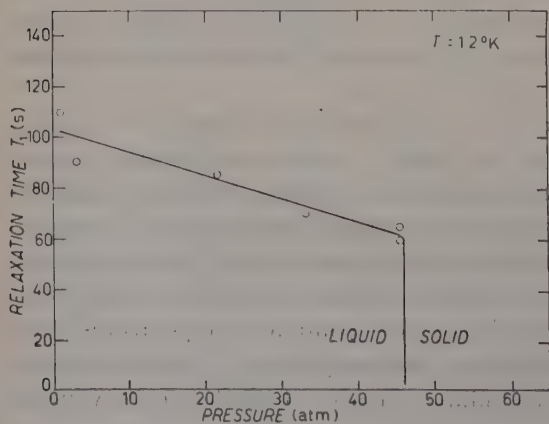


Fig. 3. — Plot of nuclear spin lattice relaxation time in liquid and solid ^3He vs. pressure in atmospheres.

the liquid-solid boundary is crossed. The very great drop in the value of T_1 from 60 s to less than 2 s enabled us to tell easily whether the sample was liquid or solid. If part of the sample were liquid and part solid it should have been possible to saturate the liquid part of the line. Such a mixture was not observed. By observing continually the spin-lattice relaxation time as the pressure was released from the solid ^3He , we were able to obtain a rough determination of the melting pressure curve. Our measurements are in agreement with those of ABRAHAM, OSBORNE and WEINSTOCK [30], showing a constant value of about 29 atm for the melting pressure below 0.4 °K. This does not preclude the slope of the curve becoming negative below 0.4 °K, since in our method just as in ABRAHAM, OSBORNE and WEINSTOCK's, the pressure of the minimum in the melting pressure curve would be observed for all lower temperatures.

The very short spin lattice relaxation time for the solid indicates that diffusion is still very great in the solid state. If we apply the theory of BLOOMBERGEN, POUND and PURCELL [5], we find that the relaxation time is close to its minimum value and that the coefficient of self-diffusion falls between the limits

$$10^{-8} < D < 10^{-6} \text{ (cm}^2 \text{ s}^{-1}\text{)}.$$

We have constructed spin-echo apparatus for determining both T_1 and T_2 accurately in the solid as a function of T and P .

In the process of investigating the susceptibility of ^3He - ^4He solutions, we have observed [31] a phase separation in which the ^3He - ^4He solution separates into two separate phases, one rich in ^3He and the other rich in ^4He . The ^3He rich portion, being the lighter, floats to the top. This phase separation had previously been predicted independently by SOMMERS [32], PRIGOGINE [33], and CHESTER [34]. Since the strength of the nuclear resonance signal is proportional to the number of ^3He nuclei in the vicinity of the resonance coil, it is possible to use the nuclear resonance techniques to observe the phase separation and measure the number of ^3He atoms in each phase. The sample container shown in Fig. 4 was designed for this purpose. It is divided

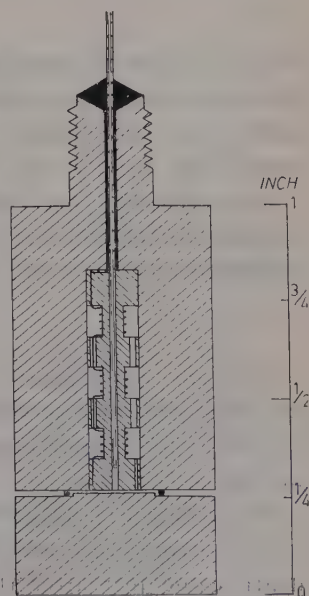


Fig. 4. — Sample container for liquid ^3He in nuclear resonance experiments designed to observe phase separation in liquid ^3He - ^4He solutions.

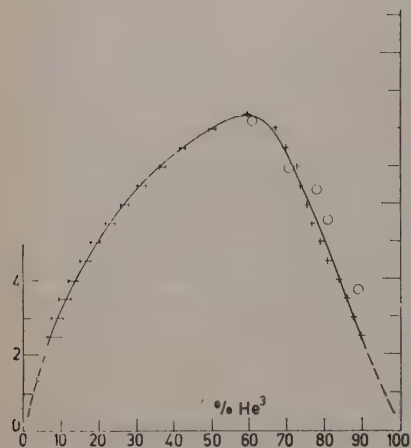


Fig. 5. — Phase diagram for ^3He - ^4He solutions. The crosses and the bars represent the experimental data. The open circles represent T_λ measurements of DAUNT and HEER.

phase diagram by vapor pressure measurements on ^3He - ^4He solutions. Professor MENDELSSOHN has reported that Professor PEŠKOV and Miss ZINOV'eva have made visual observations of the phase separation in ^3He - ^4He liquid mixtures below 1 °K, using a ^3He cryostat.

In conclusion we would like to state that WILLIAM B. ARD was largely responsible for the susceptibility measurements on liquid ^3He under its saturated vapor pressure, the work forming the subject of his doctors thesis.

* * *

We are also indebted to Professor WALTER GORDY and Dr. H. DEHMELT who were co-workers with us in the early stages of the experiment. We wish to thank the various members of the low temperature group at Duke for aid in taking the data.

We are especially indebted to Professor F. LONDON for his intense interest in this experiment and for his frequency theoretical advice. His untimely death came just after the initial results below 1 °K were obtained.

late (close hatch) three sections. Each placed in a magnetic field the magnetic field slowly modulated, resonance is observed at a slightly different time in each of the three cavities. Changes in the relative amplitudes of these peaks as a function of temperature give a measure of the concentration of ^3He in each section of the sample container, hence a measure of the ^3He concentration in each phase. Using this method on 40 %, 50 %, and 60 % solutions of ^3He in ^4He we have arrived at the phase diagram shown in Fig. 5. The open circles represent the lambda point measurements of DAUNT and HEER [35]. An interesting point, still to be determined, is whether these points represent the phase boundary or whether there is a lambda point in the upper phase.

K. W. TACONIS and H. A. FAIRBANK will present further evidence on the phase diagram in papers later this morning. T. R. ROBERTS and S. G. SYDORIAK [36] have also confirmed the existence of the

REFERENCES

- [1] I. POMERANČUK: *Žu. Eksper. Teor. Fiz., USSR*, **20**, 919 (1950).
- [2] B. G. LASAREW and L. W. SCHUBINIKOW: *Phys. Zeits. Sowjet*, **11**, 445 (1937).
- [3] E. F. HAMMEL, H. L. LAQUER, S. G. SYCORIAK and W. E. MCGEE: *Phys. Rev.*, **86**, 432 (1952).
- [4] F. BLOCH: *Phys. Rev.*, **70**, 460 (1946).
- [5] N. BLOEMBERGEN, E. M. PURCELL and R. V. POUND: *Phys. Rev.*, **73**, 679 (1948).
- [6] L. GOLDSTEIN and M. GOLDSTEIN: *Journ. Chem. Phys.*, **18**, 538 (1950).
- [7] W. M. FAIRBANK, W. B. ARD, H. G. DEHMELT, W. GORDY and S. R. WILLIAMS: *Phys. Rev.*, **92**, 208 (1953).
- [8] W. M. FAIRBANK, W. B. ARD and G. K. WALTERS: *Phys. Rev.*, **95**, 566 (1954).
- [9] E. C. KERR: *Phys. Rev.*, **96**, 551 (1954); W. F. KELLERS: *Phys. Rev.*, **98**, 1571 (1955).
- [10] R. H. SHERMAN and F. J. EDESKUTZ: *Proc. Symposium on Liquid and Solid ^3He* (Ohio State, 1957).
- [11] B. M. ABRAHAM, D. W. OSBORNE and B. WEINSTOCK: *Phys. Rev.*, **98**, 551 (1955).
- [12] T. R. ROBERTS and S. G. SYDORIAK: *Phys. Rev.*, **98**, 1672 (1955).
- [13] G. DE VRIES and J. G. DAUNT: *Phys. Rev.*, **93**, 631 (1954).
- [14] M. J. BUCKINGHAM: *Proc. Int. Conf. on Low Temp. Physics* (Paris, 1955).
- [15] K. A. BRUECKNER and J. L. GOMMEL: *Proc. Symposium on Liquid and Solid ^3He* (Ohio State, 1957).
- [16] P. J. PRICE: *Phys. Rev.*, **97**, 259 (1955).
- [17] O. K. RICE: *Phys. Rev.*, **97**, 263 (1955).
- [18] R. N. V. TEMPERLEY: *Proc. Phys. Soc.*, **68**, 1136 (1955).
- [19] L. GOLDSTEIN: *Phys. Rev.*, **102**, 1205 (1956).
- [20] W. V. HOUSTON and H. E. RORSCHACH: *Phys. Rev.*, **100**, 1003 (1955).
- [21] R. KIKUCHI: *Phys. Rev.*, **99**, 1684 (1955).
- [22] V. S. NANDA and S. K. TRIKHA: *Progr. Theor. Phys.*, **16**, 254 (1956).
- [23] Z. MIKURA: *Progr. Theor. Phys.*, **14**, 337 (1955).
- [24] S. M. BHAGAT: *Proc. Phys. Soc.*, B **69**, 1117 (1956).
- [25] S. YOMOSA: *Progr. Theor. Phys.*, **17**, 487 (1957).
- [26] G. K. WALTERS and W. M. FAIRBANK: *Phys. Rev.*, **103**, 263 (1956).
- [27] G. K. WALTERS and W. M. FAIRBANK: *Bull. Am. Phys. Soc.*, II, **2**, 183 (1957).
- [28] H. PRIMAKOFF: *Bull. Am. Phys. Soc.*, II, **2**, 63 (1957).
- [29] R. L. MILLS and E. R. GRILLY: *Proc. Symposium on Liquid and Solid ^3He* (Ohio State, 1957).
- [30] B. WEINSTOCK, B. M. ABRAHAM and D. W. OSBORNE: *Phys. Rev.*, **85**, 158 (1952).
- [31] G. K. WALTERS and W. M. FAIRBANK: *Phys. Rev.*, **103**, 262 (1956).
- [32] H. S. SOMMERS jr.: *Phys. Rev.*, **88**, 113 (1952).
- [33] I. PRIGOGINE, R. BINGEN and A. L. BELLEMANS: *Physica*, **20**, 633 (1954).
- [34] G. V. CHESTER: *Proc. Int. Conf. on Low Temp. Physics* (Paris, 1955), p. 385.
- [35] J. G. DAUNT and C. V. HEER: *Phys. Rev.*, **79**, 46 (1950).
- [36] T. R. ROBERTS and S. G. SYDORIAK: *Symposium on Liquid and Solid ^3He* (Ohio State, 1957).

Some Comments on the Theory of Liquid ^3He .

M. J. BUCKINGHAM

Physics Department, Duke University - Durham, N. C.

Helium is the lightest monotomic gas and is amongst those with the weakest interatomic forces. We might say that, at low temperatures, the stable isotopes of helium provide the condensed states of the *simplest* systems. We know however that they are far from providing us with the simplest condensed states. In fact they are unique in remaining liquid under their vapour pressure down to the lowest temperatures. The reason for this is understood and is due to this very smallness of mass and weakness of interaction. The zero point energy is too large to permit ordering in a crystal lattice and instead a kind of momentum order is achieved. This type of ordering at low temperature is analogous to that established in an ideal gas and it is by extending this analogy with the ideal gas that we obtain a qualitative understanding of the other properties.

How the properties of the ideal Bose gas provide a basis for the explanation of the λ -transition and the curious superfluid behaviour of the heavier isotope ^4He is well known. Although a complete statistical mechanics of this « simple system » is still non-existing, there appear to remain no fundamental mysteries.

In the case of the lighter isotope ^3He , we can take advantage of the analogy with the ideal Fermi gas of spin $\frac{1}{2}$ particles. Of course liquid ^3He is far from an ideal Fermi gas and the interactions play a very important part in determining the properties, but nevertheless some of the qualitative features of the ideal gas are preserved. In particular, provided the system does not establish a configuration ordering (such as a crystalline state, or bound pairs), we would still expect the existence of a large number of excited states of low energy. From a single particle point of view, there is a finite density of energy levels, n_0 say, at the surface of the Fermi sea. If n_0 is non-zero, the specific heat at lowest temperatures will be linear in the temperature, with a coef-

ficient determined only by n_0 . The actual value of the latter will, of course, be affected by the interaction between the atoms and in fact extrapolation to low temperatures of the existing specific heat measurements indicates that the value is about twice that of an ideal gas of the same particle mass and density as the liquid ^3He .

A more important effect of the interaction arises in connection with the magnetic properties of the liquid. If a system has magnetization due to an atomic magnetic moment μ , the magnetic susceptibility, χ , is determined by the free energy difference between the states of total spin S (magnetic moment M per unit volume) and those with $S = M = 0$; this difference is given for a volume V by $\frac{1}{2}M^2V/\chi$. If there were no spin dependent energy contribution, this would be the energy necessary for the redistribution amongst the energy levels, of density n_0 , required to produce the magnetization M and would equal $\frac{1}{2}M^2V^2/\mu^2n_0$. Then we would have the low temperature susceptibility given by $\chi^{-1} = N/\varrho\mu^2n_0$, where $\varrho = N/V$ is the particle density. (In the case of an ideal Fermi gas, $n_0 = 3\varrho V/2\zeta$, where ζ is the Fermi energy; this leads to the well known expression $\chi = 3\mu^2\varrho/2\zeta$ for the Pauli paramagnetism of the ideal gas.) Introducing the Curie-law susceptibility, $\chi_c = \varrho\mu^2/kT$, we find the ratio $\chi/\chi_c = kTn_0/N$.

As pointed out above the coefficient of the linear term in the specific heat at low temperatures is determined also by n_0 . Actually, $C_v/Nk = \frac{1}{3}\pi^2kTn_0/N$, so that the ratio, R , of the susceptibility ratio to the specific heat is given by, $R = (\chi/\chi_c)/(C_v/kN) = 3/\pi^2$, and is a pure number, independent of any further properties of the system, provided it is gas-like and has no spin dependent interaction.

The important effect of the interatomic interaction arises because it leads to an «exchange» interaction between particles with parallel spin, and which is thus spin dependent. In a state with $M \neq 0$, (total spin $S \neq 0$) there are more pairs of particles with parallel spins than in the state with $S = M = 0$. In fact there are $v_s = MV/\mu$ more spins in one direction than the other and $v_s^2/4$ more pairs of parallel spins. If we write $-\varepsilon_x/N$ for the exchange energy per parallel pair there is the additional term, $-\frac{1}{4}\varepsilon_xM^2V^2/\mu^2N$, to be added to what we found before for the energy difference between the state with magnetization M and that with $M = 0$. The expression for the susceptibility is now

$$\chi^{-1} = \left(\frac{N}{n_0} - \frac{1}{2}\varepsilon_x \right) / \varrho\mu^2;$$

thus the ratio R is not just $3/\pi^2$ as before but has the additional factor $(1 - \frac{1}{2}\varepsilon_x n_0/N)^{-1}$, since the spin dependent energy does not affect the low temperature specific heat, which, we repeat, depends only on the value of n_0 .

Now in general the exchange energy ε_x can be either positive or negative

depending on the interaction and the overlap of the particle wave functions and it is not easy to calculate. An empirical estimate for liquid ^3He can be obtained by comparing the observed susceptibility and specific heat extrapolated to low temperatures. Such an extrapolation yields for the ratio R about six times the value $3/\pi^2$. The sensitive dependence of R on the level density and exchange energy suggests that it will vary considerably with the liquid density. It may be noted that quite a small relative increase in the exchange energy would be sufficient to make the liquid a nuclear ferromagnet. This does not appear to occur at any accessible liquid density, although the susceptibility near the solidification pressure has been measured as about twice that under the vapour pressure. It will be interesting also to compare the specific heats when experimental results for the liquid under pressure become available.

The point of view here outlined provides an understanding of the qualitative properties of liquid ^3He but it is difficult to extend to quantitative calculations. Also this attitude cannot be applied to the solid state. One might expect that in the solid, not too far from the melting pressure, the exchange integral would be comparable in magnitude to that in the liquid and hence, that the susceptibility should depart from the Curie law value at temperatures not very much lower than in the liquid. The little experimental data available indicate that this is indeed the case, but a theory for the solid will require a very different approach than that discussed here.

Some encouraging progress towards a quantitative theory of the liquid has been made by BRÜCKNER, who has applied the methods developed for attacking the many body problem in nuclei to the case of liquid ^3He , which provides a kind of model of infinite «nuclear matter». The method requires a fast computer and, starting from first principles, leads to a self-consistent solution for a system of ^3He atoms interacting via their known interatomic forces. Results so far obtained are for the low temperature limit and give about the right value for the specific heat and also a large exchange energy, leading to semiquantitative agreement with the observed nuclear susceptibility. It is to be hoped that the method can be extended with equal success to the calculation of properties at higher temperatures.

INTERVENTI E DISCUSSIONI

— O. K. RICE:

It appears to me that the assumption that the energy levels are broadened into bands is not necessarily contrary to the spirit of the cell theory with pairs. Such a broadening of the levels enables one to change the specific heat at 0°K , but does not

essentially change the results at somewhat higher temperatures, say around 0.2°K . It is for explaining the results at such higher temperatures that the pair model is particularly adapted. Assuming the pairs to act like hindered plane rotators, one can achieve a good correlation between magnetic susceptibility and specific heat near and somewhat above 0.2°K . The hindering potential is due to interaction with neighboring atoms, and will be different for each cell; it indicates rather strong interaction between the cells. For this reason it is, indeed, to be expected that the energy levels will be broadened into bands.

— O. K. RICE, to the remark of Professor J. DE BOER:

I think that the rotations of more than two atoms at a time may contribute to the spreading of the energy levels, but that they cannot be of conclusive importance in the real case where interactions with the neighbours are taken into account. For one thing, such a cooperation of many atoms would increase the zero-point energy, and so would seem to be improbable.

— K. MENDELSSOHN:

Professor PESKOV and Miss ZINOV'EVA have made visual observations of the phase separation in ^3He - ^4He liquid mixtures below 1°K , using a ^3He cryostat. When I saw Professor PESKOV in Moscow two months ago, he gave me a photograph of this separation which he hoped to show at the presente conference. As he was unfortunately not able to attend, I like to draw attention to the recent paper (V. S. PEŠKOV and K. N. ZINOV'EVA: *Žu. Eksper. Teor. Fiz.*, 32, 1256 (1957)) which describes his work.

Some Properties of Liquid ^3He (*).

B. WEINSTOCK (+), B. M. ABRAHAM and D. W. OSBORNE

Argonne National Laboratory - Lemont, Ill.

The initial interest in liquid ^3He quite naturally arose from the suggestion of F. LONDON [1] that the lambda transition in liquid ^4He and the Bose-Einstein gas condensation were intimately related. Liquid ^3He offered the possibility of a simple and elegant test of this hypothesis, since ^3He , which follows Fermi-Dirac statistics, should show neither a lambda transition nor superfluidity if F. LONDON were correct. The interest in this question was sharpened by the polemic between LANDAU [2] and TISZA [3] concerning their different detailed theories for the hydrodynamics of liquid helium II; Tisza's theory made explicit use of Bose-Einstein statistics while Landau's theory appeared to be independent of statistics. The very first experiments relating to this question were done at Ohio State University by DAUNT, PROBST and JOHNSTON [4] and at Yale University by LANE and H. FAIRBANK [5], both groups collaborating with ALDRICH and NIER of the University of Minnesota. Even though the experimentalists were limited to an initial ^3He concentration of about 1 part per million, they were able to show respectively that ^3He did not participate in superfluid flow through slits and that ^3He could be swept away from a heated zone along with the normal particles—the « heat flush » technique. Although these experiments confirmed the predictions of ONSAGER [5] and FRANCK [6] that ^3He would not participate in the ^4He superflow because of its different statistics, LANDAU [2] pointed out that experiments with mixtures could not settle the question of the superfluidity of ^3He —pure ^3He being required to decide that question. This point has been investigated by GUTTMAN and ARNOLD [7], who showed that ^3He , which follows Bose-Einstein statistics, does not partake of superflow through slits when present in small concentration—the same result that was obtained with the dilute solutions of ^3He . The point is that even though ^4He obeys Bose-Einstein statistics it is distinguishable

(*) This work was performed under the auspices of the U.S. Atomic Energy Commission.

(+) John Simon Guggenheim Memorial Fellow; present address, The Clarendon Laboratory, Oxford.

from ^4He and cannot «condense» with the ^4He atoms—its own condensation (if F. London's hypothesis is correct) occurring at an unattainably low temperature because of its very small concentration in these experiments. Thus the relevance of statistics to superfluidity remained to be decided by experiments with pure ^3He .

The problem of obtaining pure ^3He was attacked with vigor at many laboratories and many ingenious low temperature techniques utilizing superfluidity were invented. However, the prospect of obtaining sufficient pure ^3He by isotope separation in order to study the properties of its condensed phase remained discouraging because of the small initial concentration provided by nature; ^3He is present in atmospheric helium in a concentration of 1 part per million and about one-tenth that concentration in gas well helium. The solution to the problem came about in a completely novel fashion; the ^3He was produced by the radioactive decay of tritium. In this process tritium is first created by an n, α reaction on ^6Li in a pile and then separated from the ^4He that is formed at the same time. The ^3He subsequently formed by the β -decay of this tritium (12.5 year half life) is isotopically pure provided that the simple purification of the tritium from the α -particles (^4He) was properly carried out. It is not surprising that the initial experiments with pure ^3He were then carried out at the Los Alamos and Argonne laboratories where this method of tritium preparation was also being investigated. As a matter of fact, the great majority of low temperature experiments that have been carried out with pure ^3He have used ^3He produced in this way by the United States Atomic Energy Commission. The current price of ^3He is rather nominal, one dollar and fifty cents per cubic centimeter of gas (*).

It is still perhaps of interest to recall that at one time a question was raised about the possibility of ^3He forming a stable liquid phase [8]. This suggestion followed from the considerations of SIMON [9] and F. LONDON [10], who had developed the concept that in liquid ^4He the zero point motion acts as a repulsive force and is mainly responsible for the absence of a triple point and for the exceptionally large molar volume of the liquid. In view of the delicate balance of forces in liquid ^4He , it was argued that ^3He might not liquefy at all since, owing to its lighter mass, it would have a larger zero point energy (at the same density) while the attractive forces for the two isotopes would be the same. Actually little difficulty was encountered in liquefying ^3He , this first being accomplished at Los Alamos by SYDORIAK, GRILLY and HAMMEL [11], who also reported preliminary measurements of the vapor pressure and critical constants. The vapor pressure measurements were repeated shortly thereafter at the Argonne [12] from 1 °K to the critical point, 3.35 °K, and

(*) Obtainable from Radioisotopes Sales Department, Operations Division, Oak Ridge National Laboratory, Oak Ridge, Tennessee.

more recently extended by ROBERTS and SYDORIAK [13] to 0.45 °K. The latter authors have incorporated the Argonne data with their own into an interpolation formula which covers the entire measured range. Although the liquefaction of ^3He offered no problems the effects arising from the zero point energy were nevertheless evident. The liquid volume became even greater than that of ^4He (about $\frac{4}{3}$ as large), the liquid range diminished to such an extent that the boiling point (3.2 °K) almost coincided with the critical point, and, most significantly, liquid ^3He like liquid ^4He does not have a triple point [14]. Also of interest is the fact that DE BOER, our chairman, and LUNBECK [15] predicted vapor pressures, density and critical point data for liquid ^3He quite successfully by means of a quantum theory of corresponding states. Surprisingly, these predictions were made before the first liquefaction and appeared to be of the same order of accuracy as the earliest preliminary vapor pressure measurements.

The question of immediate interest once ^3He had provided a liquid phase was whether it would have a superfluid transition. To answer this question my colleagues and I compared the relative rate of flow of liquid ^3He and liquid ^4He through a superleak [16]—a superleak being a channel so fine that only a superfluid can pass through readily. This experiment was similar to one that GIAUQUE, STOUT and BARIEAU [17] performed to measure the viscosity of liquid ^4He . The superleak was constructed by sealing a platinum wire into a pyrex capillary, the different coefficients of thermal expansion for platinum and pyrex providing an annulus on cooling of the order of a micron in width.

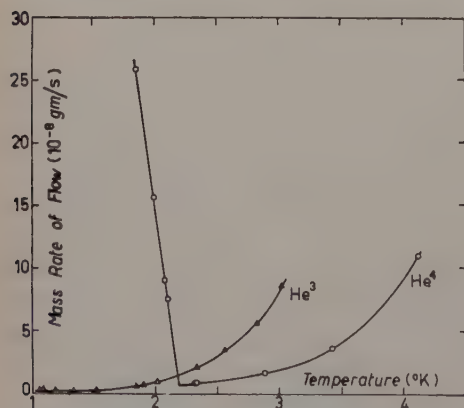


Fig. 1. — Mass rate of flow of liquid ^3He and of liquid ^4He through a $7 \cdot 10^{-6}$ cm annulus as a function of temperature.

Liquid ^4He and liquid ^3He were then separately condensed above the superleak, and their flow rates as a function of temperature were observed. As can be seen in Fig. 1, the rate of flow of liquid ^4He decreased with decreasing temperature until the lambda temperature was reached and then increased sharply. In contrast, liquid ^3He showed a continuously decreasing flow rate down to the lowest temperature observed, about 1 °K. This experiment clearly supported London's hypothesis that the lambda transition was related to Bose-Einstein statistics, but the question of whether 1 °K was sufficiently low to establish this point remained. However, if one tried to estimate the lambda point of ^3He from de Boer's theory by

whether 1 °K was sufficiently low to establish this point remained. However, if one tried to estimate the lambda point of ^3He from de Boer's theory by

substituting lambda points for triple points, then 1°K was well below any conceivable extrapolation of these other data.

By causing more and more liquid to condense above the superleak, different pressure heads could be applied to the liquid and the flow through the superleak was found to obey Poiseuille's law [18]. From these data the viscosity of liquid ^3He was derived and found to increase with decreasing temperature from 2.8 to 1.0°K . This is the expected fashion for a liquid and is contrary to the behavior of liquid ^4He which even above the lambda temperature has a constant or slightly decreasing viscosity with decreasing temperature. More recently, TAYLOR and DASH [19] have measured the viscosity of liquid ^3He in more detail by the oscillating disk method and have confirmed the preliminary measurements by this different technique. It is also reported that Miss ZINOV'EVA [20], in Russia, has found the viscosity to be still increasing at 0.35°K . This behavior of the viscosity further confirms the unlikelihood of ^3He becoming superfluid at any temperature.

The heat capacity measurements, which I shall discuss shortly in some detail, give a final negative answer to the question of whether ^3He can have a lambda transition similar to ^4He . These measurements [21] extend down to 0.23°K and no indication of a lambda anomaly has been observed. Further, there is insufficient entropy left in the liquid for it to have a lambda transition of similar magnitude to liquid ^4He . Thus, ^3He clearly established that F. London's hypothesis relating the lambda transition to Bose-Einstein statistics was a valid one. Regardless of this result, the differences between LANDAU and TISZA were largely resolved in favor of LANDAU but that is a more complicated matter and will not be discussed here.

Although liquid ^3He , in contrast to liquid ^4He , appears to be a fairly normal liquid, it does possess one distinction by virtue of its nuclear spin that is not possible for ^4He . The previous speaker has discussed the study of the partial orientation of these nuclear spins that was made by the technique of nuclear magnetic resonance [22]. In this discussion, this subject will be approached from a thermodynamic viewpoint and an attempt to correlate the susceptibility data and the thermodynamic data will be made.

The nuclear spin of ^3He is equal to $\frac{1}{2}$ and under conditions of random orientation contributes an amount equal to $R \ln 2$ ($1.38 \text{ cal deg}^{-1} \text{ mole}^{-1}$) to the entropy. Thus a sufficient but not entirely necessary criterion for partial orientation of the nuclear spins in liquid ^3He would be the fact that the entropy becomes less than $k \ln 2$. The determination of the entropy of liquid ^3He by the usual integration of the heat capacity from 0°K is not possible at the present time because at the lowest temperature of measurement, 0.23°K , the heat capacity is so high, $0.7 \text{ cal deg}^{-1} \text{ mole}^{-1}$, and the course of the curve still so uncertain that an extrapolation to absolute zero cannot be reliably made. However, the entropy of the liquid can alternately be obtained from the

entropy of the gas calculated by the Sakur-Tetrode equation and the entropy difference between gas and liquid derived from the heat of vaporization.

The heat of vaporization can be derived from vapor pressure data by the relation

$$(1) \quad \Delta H = T \frac{dP}{dT} (V_{\text{gas}} - V_{\text{liq}}),$$

but these values are uncertain by as much as 2 percent owing to uncertainties in the temperature scale and the second virial coefficients. By direct measurement the heat of vaporization is calculated from the relation

$$(2) \quad \Delta H = \frac{Q}{N_0} \left(1 - \frac{V_{\text{liq}}}{V_{\text{gas}}} \right),$$

which can be determined with much greater accuracy. The quantity of heat used, Q , and the apparent number of moles evaporated, N_0 , are readily measured to a few hundredths of a percent, and at 1.5 °K $V_{\text{liq}}/V_{\text{gas}}$ contributes an uncertainty of only 0.02 percent to ΔH for a 10 percent uncertainty in the second virial coefficient. Accordingly, we

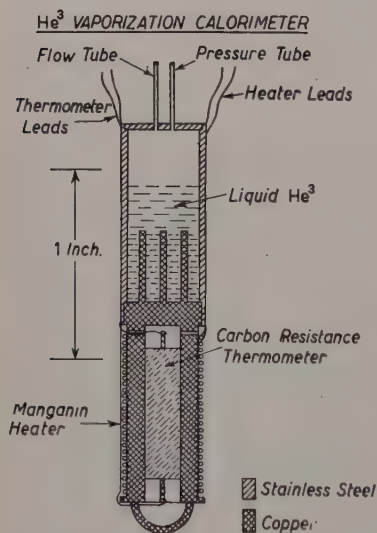


Fig. 2. - ^3He vaporization calorimeter.

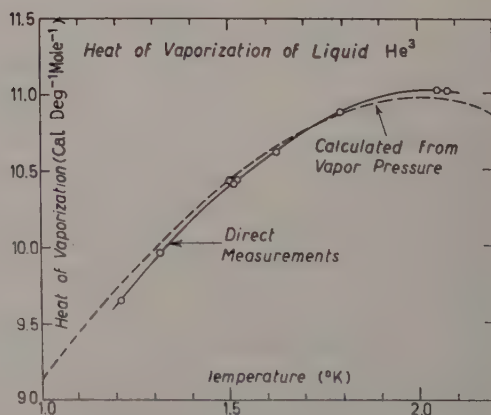


Fig. 3. - Heat of vaporization of liquid ^3He .

have made measurements of the heat of vaporization of liquid ^3He from 1.2 to 2.1 °K [23] in order to provide more accurate values of the entropy. In Fig. 2, a scale drawing of the tiny calorimeter used is shown. None of the details of design and technique that were devised in order to insure accurate measurements will be discussed here other than to state that, although at most only 0.009 moles of ^3He were evaporated in each experiment, the values obtained were accurate to 0.2 percent.

The experimental results are shown in Fig. 3 as well as the calculations from the vapor pressure equation. As expected, the two sets are not in exact agreement, the vapor pressure calculations being about 1% high at 1.2 °K and 0.5% low at 2.1 °K. The virial coefficients of KELLER [24] and the data of KERR [25] on the density of the liquid were used for the calculation of V_{gas} and V_{liq} respectively. The temperature of 1.5 °K was selected as the most reliable place to calculate the entropy of the vapor and to assign the entropy of the liquid. Two opposing tendencies are balanced in this choice, the uncertainty of the vapor pressure determination, which increases with decreasing temperature, and the gas imperfection correction, which is less certain at higher temperatures. Three determinations of the heat of vaporization were made at 1.5 °K, one at twice the heat input rate of the other two, and the results are seen to agree within the stated accuracy.

The calculation of the entropy of liquid ^3He is summarized in Table I and

TABLE I. — *Entropy of liquid ^3He at 1.5 °K.*

$S_{\text{ideal gas}}, P = 50.766 \text{ mm}$	9.746
$S_{\text{gas}} - S_{\text{ideal gas}}$	—0.204
S_{gas}	9.542
$S_{\text{gas}} - S_{\text{liquid}} = \Delta H/T$	—6.928
S_{liquid}	(2.614 \pm 0.03) cal deg $^{-1}$ mole $^{-1}$

the value of $(2.614 \pm 0.03) \text{ cal deg}^{-1} \text{ mole}^{-1}$ is found to differ significantly from the value of 2.52 ± 0.17 previously derived from the vapor pressure [21]. The entropy of the liquid can be accurately evaluated at other temperatures by means of heat capacity data and the relation

$$(3) \quad S = 2.614 + \int_{1.5}^T C_{\text{sat}} d \ln T.$$

The heat capacity data are shown in Fig. 4. The solid curve A, summarizes the Argonne measurements from 0.23 to 2 °K [21]; the data of ROBERTS and SYDORIAK [26], which extend down to 0.5 °K, are also plotted and found to be in good agreement. The calculation of C_v for a degenerate ideal Fermi-Dirac gas with degeneracy temperatures of 0.45 °K (curve B) and 4.98 °K (curve C) are also included in this plot for comparison and it appears that this model is unsatisfactory for liquid ^3He . The temperature of 4.98 °K is the degeneracy temperature of a gas composed of particles with the mass of ^3He and the liquid density; 0.45 °K is the degeneracy temperature used in the Fermi-Dirac functions by FAIRBANK, ARD and WALTERS [22] as an interpolation formula for their susceptibility measurements. Although very

good agreement was found between this Fermi-Dirac function and the susceptibility data, it nevertheless does not imply that ^3He is behaving as a degenerate Fermi-Dirac gas. In the Fermi-Dirac model the uncoupling of the nuclear spins is intimately related to the kinetic energy excitations so that the heat capacity corresponding to such a small degeneracy temperature as 0.45°K increases very rapidly with rising temperature contrary to the observed experimental data. The correction for the difference $C_{\text{sat}} - C_v$ has not been applied in Fig. 4 because of the lack of appropriate thermodynamic

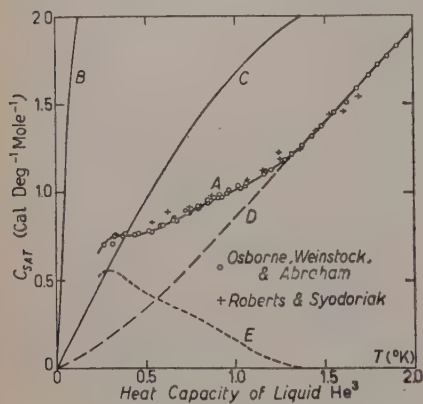


Fig. 4. — Heat capacity of liquid ^3He at its saturated vapor pressure. (A) experimental results; (B) and (C) C_v of ideal Fermi-Dirac gas with degeneracy temperatures of 0.45° and 4.98°K , respectively; (D) estimated non-spin heat capacity; (E) estimated spin heat capacity (curve A minus curve D).

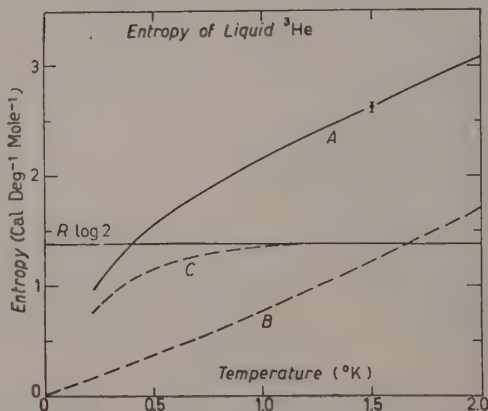


Fig. 5. — Entropy of liquid ^3He . (A) total entropy from the heat capacity data and the value $2.614 \text{ cal deg}^{-1} \text{ mole}^{-1}$ for the entropy at 1.5°K ; (B) estimated non-spin entropy [from integration of curve (D), Fig. 4]; (C) estimated spin entropy, S_{spin} [curve A minus curve B].

data. However, it can be evaluated at 1.2°K from the compressibility data of WALTERS and FAIRBANK [27] and the density data of KERR [25], and is found to be $+0.03 \text{ cal deg}^{-1} \text{ mole}^{-1}$, or only about 3 percent of the heat capacity. In all probability the correction will have an equally small effect at other temperatures within the range of the measurements.

The entropy of liquid ^3He calculated from equation (3) and the heat capacity data is shown as curve A in Fig. 5. The entropy is seen to become equal to $R \ln 2$ at 0.41°K and fall to the value of $0.96 \text{ cal deg}^{-1} \text{ mole}^{-1}$ at 0.23°K . These results confirm the fact that there has been a partial alignment of the nuclear spins in liquid ^3He although they cannot distinguish the sense of the alignment, parallel or antiparallel.

While this qualitative agreement between the susceptibility measurements and the thermodynamic data is satisfying, it would be of interest to attempt

a more quantitative comparison. In the absence of an adequate theory, a possible approach to this problem might be to resolve the heat capacity into two parts, the first part arising from the spin disordering and the second part from other thermal excitations.

Such a procedure has been successfully applied to heat capacity anomalies arising from magnetic transitions in solids [28, 29], the accuracy being limited by the reliability of the method used to evaluate the lattice heat capacity. A procedure for evaluating the «lattice» heat capacity of liquid ^3He was suggested by the similarity between the heat capacity of liquid ^4He above 2.5°K [30] with that of liquid ^3He above 1.4°K , both liquids appearing to have heat capacities that vary linearly with temperature and extrapolate nearly to zero. It seems reasonable to interpret this «high temperature» heat capacity as arising from thermal excitations in which statistics and spin do not make a sensible contribution. The deviation of the heat capacity curve of liquid ^3He from this linear course at about 1.4°K is then interpreted to be due to the onset of the antiferromagnetic ordering of the nuclear spins. The extrapolation of the linear part of the heat capacity below 1.4°K in order to estimate the «lattice» contribution to the heat capacity is perforce an arbitrary procedure since some curvature must be added at the lower end in order to have it pass through zero at 0°K . There is the useful restriction however, that when the «lattice» entropy calculated from this extrapolation is subtracted from the total entropy at 1.4°K , the difference must be precisely $R \ln 2$.

The result of such an extrapolation is also shown in Fig. 4, curve *D* being the «lattice» heat capacity and curve *E* the spin heat capacity (curve *A* - curve *D*). In Fig. 5 the entropy resolution derived from these heat capacities is shown, curve *B* being the lattice entropy and curve *C* the spin entropy. In Fig. 6 the values of the spin entropy (S_{spin}) from curve *C* (Fig. 5) divided by $R \ln 2$ are compared with the values of $\chi T/C$ obtained in the susceptibility experiments, and the agreement between the thermodynamic data and susceptibility data is seen to be fairly good. This correlation between $S_{\text{spin}}/R \ln 2$ and $\chi T/C$ would result from a model for liquid ^3He in which each unpaired spin contributed $k \ln 2$ to the total

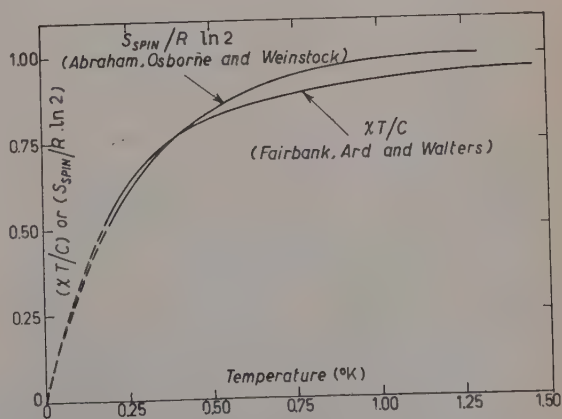


Fig. 6. - Comparison of $S_{\text{spin}}/R \ln 2$ with $\chi T/C$.

entropy and in which the susceptibility was also proportional to the number of unpaired spins [31]. Such a model is undoubtedly too simple for liquid ^3He but it is nevertheless interesting to see in a general way that the susceptibility data and thermodynamic data seem to be in accord.

At 0.33 °K, the melting pressure of ^3He obtained by the blocked capillary technique [14] becomes equal to 29.3 atmos, and appears to remain equal to that value at lower temperatures. In all probability the melting pressure actually passes through a minimum at this temperature, the failure of the blocked capillary technique to distinguish between a minimum or constant value being a limitation of that method. In either case, however, the slope of the melting curve becomes zero at that temperature so that the liquid and solid have the same entropy. Since nuclear alignment has not been observed in solid ^3He at 0.33 °K [32] its entropy and consequently that of the compressed liquid are equal to $R \ln 2$. From Fig. 4 the entropy of liquid ^3He in equilibrium with its saturated vapor is 1.22 cal deg $^{-1}$ mole $^{-1}$ at 0.33 °K, or 0.16 cal deg $^{-1}$ mole $^{-1}$ less than $R \ln 2$. This results shows that the liquid increases in entropy on compression in this temperature region, an unexpected result also indicated by the susceptibility measurements of WALTERS and FAIRBANK [27]. It follows from the relation

$$\left(\frac{\partial S}{\partial p}\right)_T = -\left(\frac{\partial V}{\partial T}\right)_p,$$

that the coefficient of isobaric thermal expansion of liquid ^3He near 0.33 °K is negative.

REFERENCES

- [1] F. LONDON: *Nature*, **141**, 643 (1938).
- [2] L. LANDAU: *Phys. Rev.*, **75**, 884 (1949).
- [3] L. TISZA: *Phys. Rev.*, **75**, 885 (1949).
- [4] J. G. DAUNT, R. E. PROBST, H. L. JOHNSTON, L. T. ALDRICH and A. O. NIER: *Phys. Rev.*, **72**, 502 (1947).
- [5] C. T. LANE, H. A. FAIRBANK, L. T. ALDRICH and A. O. NIER: *Phys. Rev.*, **73**, 256 (1948).
- [6] J. FRANCK: *Phys. Rev.*, **70**, 561 (1946).
- [7] L. GUTTMAN and J. R. ARNOLD: *Phys. Rev.*, **92**, 547 (1953).
- [8] F. LONDON and O. K. RICE: *Phys. Rev.*, **73**, 1188 (1948).
- [9] F. LONDON: *Proc. Roy. Soc., A* **153**, 576 (1936).
- [10] F. SIMON: *Nature*, **133**, 529 (1934).

- [11] S. G. SYDORIAK, E. R. GRILLY and E. F. HAMMEL: *Phys. Rev.*, **75**, 303 (1949).
- [12] B. M. ABRAHAM, D. W. OSBORNE and B. WEINSTOCK: *Phys. Rev.*, **80**, 366 (1950).
- [13] S. G. SYDORIAK and T. R. ROBERTS: *Phys. Rev.*, **106**, 175 (1957).
- [14] B. WEINSTOCK, B. M. ABRAHAM and D. W. OSBORNE: *Phys. Rev.*, **85**, 158 (1952).
- [15] J. DE BOER and R. J. LUNBECK: *Physica*, **14**, 510 (1948).
- [16] D. W. OSBORNE, B. WEINSTOCK and B. M. ABRAHAM: *Phys. Rev.*, **75**, 988 (1949).
- [17] W. F. GIAUQUE, J. W. STOUT and R. E. BARIEAU: *Journ. Am. Chem. Soc.*, **61**, 654 (1939).
- [18] B. WEINSTOCK, D. W. OSBORNE and B. M. ABRAHAM: *Proc. Conf. on Low Temp.* (Massachusetts Institute of Technology, 1949).
- [19] R. D. TAYLOR and J. G. DASH: *Phys. Rev.*, **106**, 398 (1957).
- [20] K. MENDELSSOHN: *Nature*, **180**, 460 (1957).
- [21] B. M. ABRAHAM, D. W. OSBORNE and B. WEINSTOCK: *Phys. Rev.*, **98**, 551 (1955).
- [22] W. K. FAIRBANK, W. B. ARD and G. K. WALTERS: *Phys. Rev.*, **95**, 566 (1954).
- [23] B. M. ABRAHAM, D. W. OSBORNE and B. WEINSTOCK: *Bull. Am. Phys. Soc.*, Series II, **1**, 349 (1956).
- [24] W. E. KELLER: *Phys. Rev.*, **98**, 1571 (1955).
- [25] E. C. KERR: *Phys. Rev.*, **96**, 551 (1954).
- [26] T. R. ROBERTS and S. G. SYDORIAK: *Phys. Rev.*, **93**, 1418 (1954); **98**, 1672 (1955).
- [27] G. K. WALTERS and W. M. FAIRBANK: *Phys. Rev.*, **103**, 263 (1956).
- [28] D. W. OSBORNE and E. F. WESTRUM jr.: *Journ. Chem. Phys.*, **21**, 1884 (1953).
- [29] J. W. STOUT and E. CATALANO: *Journ. Chem. Phys.*, **23**, 2013 (1955).
- [30] W. H. KEESOM: *Helium* (Amsterdam, 1942), p. 212.
- [31] L. GOLDSTEIN: *Phys. Rev.*, **96**, 1455 (1954).
- [32] G. K. WALTERS and W. M. FAIRBANK: *Bull. Am. Phys. Soc.*, Series II, **2**, 183 (1957).

INTERVENTI E DISCUSSIONI

— B. WEINSTOCK: to a question by K. MENDELSSOHN:

The heat capacity curve below the present measurements cannot be safely extrapolated to absolute zero at this time.

Some Experiments with ^3He - ^4He Mixtures (*).

K. W. TACONIS and D. H. N. WANSINK

Kamerlingh Onnes Laboratory - Leiden

Some time ago we built a special apparatus to study both the equilibrium between vapour and liquid of very dilute mixtures of ^3He in helium II [1] and the osmotic pressure of these mixtures of concentrations up to 4% ^3He [2].

1. - Phase equilibrium.

The apparatus (Fig. 1) consists of two vessels, *A* (volume 0.454 cm³) and *B*, which are connected by means of a superleak *S*. *B* is provided with a heating coil and a calibrated capillary *C* and is enclosed in a vacuum space. *A* is filled with approximately 15 mm³ of liquid mixture with a concentration of the order of 10⁻³ and in *B* pure ^4He is condensed. Heating of *B* creates a fountain pressure across the slit *S* which draws superfluid out of *A* when the fountain pressure is larger than the osmotic pressure exerted by the mixture in *A*. By increasing the temperature difference sufficiently *A* is drained completely with the exception of the He-film. In this state all ^3He is in the vapour phase, since it cannot leave *A* through the superleak and only a negligibly small amount is dissolved in the film. Assuming, that because of the low concentrations used, the partial pressure P_4 can be put equal to P_4^0 , the pure ^4He -vapour pressure, we can derive the total amount of ^3He in *A* from the vapour volume and from the excess pressure $\Delta P = P - P_4^0$, P being the

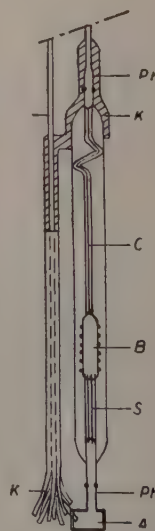


Fig. 1. - The apparatus.

(*) This paper has been submitted also to the *Proc. Int. Conf. on Low Temp. Physics* (Madison, 1957).

vapour pressure of the mixture. Then the heat input of B is switched off, the temperature difference decreases, and ^4He flows back into A because of the osmotic pressure. The amount of liquid entering A is calculated from the lowering of the liquid level in C . Some ^3He will dissolve in this amount of liquid and the vapour pressure in A will decrease accordingly. The new value of ΔP together with the vapour volume (i.e. the total volume of A , minus the liquid volume in A) yields the amount of ^3He remaining in the vapour. The difference from the total amount of ^3He gives the ^3He in the liquid. In this way all quantities needed to calculate both the liquid concentration C_L (*) and the vapour concentration C_V are known. The ratio of them, the distribution coefficient C_V/C_L , is given in Fig. 2: it fits well to Sommers' data [3] for concentrations of 2% and higher but differs from it at lower concentrations where our own values are considerably higher than his. Probably in Sommers' experiments a small heat flow has flushed some ^3He from the liquid surface to the wall of the equilibrium vessel.

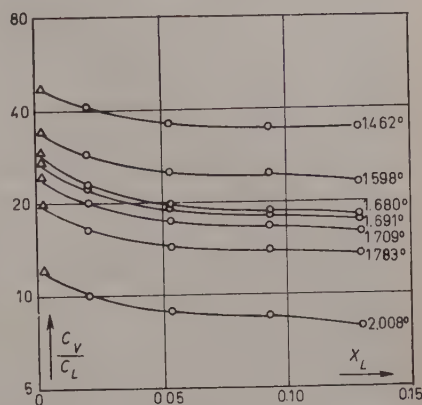


Fig. 2. — The distribution coefficient C_V/C_L as a function of the liquid concentration X_L at constant temperature. \circ : SOMMERS; Δ : the authors.

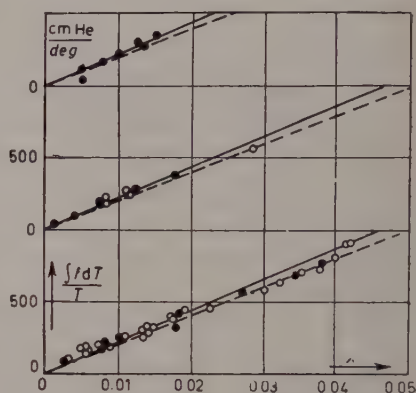
2. — Osmotic pressure.

The apparatus is filled in the same way as before, but now the heating current of B is kept so small that the resulting fountain pressure balances the osmotic pressure of the mixture in A . This equilibrium is obtained automatically, since e.g. a too large fountain pressure draws ^4He out of A , thus increasing the concentration in A and the osmotic pressure until equilibrium is reached. This is indicated by both the vapour pressure in A and the liquid level in C becoming steady. The vapour pressure in A gives the liquid concentration; the pressure in B the temperature difference ΔT across the slit which is transformed into the fountain pressure by using KRAMERS' entropy values [4]. A thermodynamic treatment of the quasi-equilibrium is given elsewhere [2]. In Fig. 3 the integrated fountain effect $\int f dT$ being cor-

(*) C denotes the number ratio N_3/N_4 of the two components whereas X denotes the number fraction $N_3/(N_3+N_4)$.

rected for vapour pressure differences etc., is plotted versus the concentration X . Van 't Hoff's law $P_{\text{osm}} = -\rho RT \ln(1 - X)/M$, where ρ denotes the density and M the molecular weight, valid for ideal solutions, represents the results fairly well. Taking into account the deviation of the mixture from the ideal solution, as it can be derived from the vapour pressure data [5], we obtain a small correction with respect to Van 't Hoff's law and complete agreement with the experimental data.

Fig. 3. — The fountain pressure $\int f dT$, divided by the bath temperature T , as a function of the concentration X . A: $T > 1.8^\circ\text{K}$; B: $1.4^\circ\text{K} < T < 1.7^\circ\text{K}$; C: $T < 1.3^\circ\text{K}$; —, ideal solution value; ---, non-ideal solution.



3. — The specific heat of ^3He - ^4He mixtures.

The specific heat of mixtures of low concentration (1, 2.5 and 7.13%) has been investigated by DOKOUPIL *et al.* [6, 7] in 1954 and 1955. The results, represented in Fig. 4 by the three curves lying closely to the pure ^4He -curve,

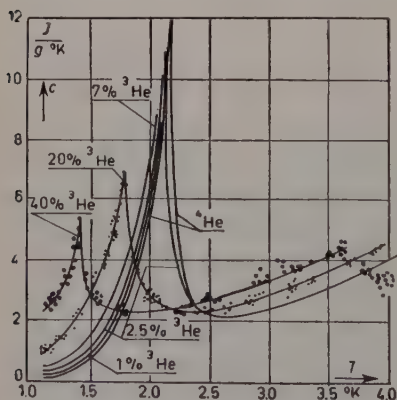


Fig. 4. — The specific heat of ^3He - ^4He mixtures.

have been compared by one of us (W) [5] with the vapour pressure data of SOMMERS [3], supplemented with our data for the lowest concentrations (see Sect. 1). From the vapour pressure the chemical potentials of mixing were derived; subsequently all other thermodynamic quantities of mixing were calculated from them. The results of these calculations were very satisfactory. The calculated specific heats agreed well with the experimental ones (see Fig. 5).

In the same way we tried to calculate the specific heat of mixtures of 20 and 40% ^3He , which have been measured by DOKOUPIL *et al.* [8]. However, the vapour pressure data for these concentrations determined by ESEL'SON and BEREZNIAC [9] especially in the neighbourhood of the λ -point of the mixture and 2.17°K are not accurate enough to yield any reasonable result.

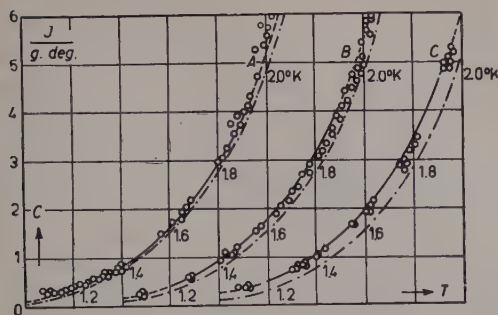


Fig. 5. — The specific heat of ^3He - ^4He mixtures as a function of the temperature at different concentrations. ---: specific heat of pure ^4He (KRAMERS *et al.* [5]); —: specific heat of mixtures, calculated curve; \circ : experimental values; A: $X = 0.010$; B: $X = 0.025$; C: $X = 0.0713$.

flow properties of ^3He - ^4He mixtures through narrow slits [11]. In Fig. 7 values for three concentrations are given. If we assume that a Tisza type of relation between the normal fluid fraction and the entropy of the ^4He is also valid in the case of a mixture, our values of Δx appear to agree reasonably well with the entropy as calculated from the vapour pressure data [5]. However, disagreement is found with the results of DASH and TAYLOR [12] and of PELLAM [13] who used the Andronikašvili type of experiment.

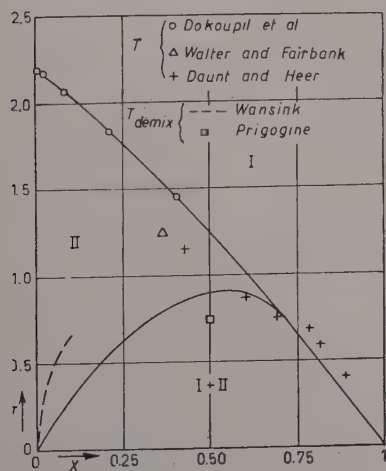


Fig. 6. — The T - X diagram of ^3He - ^4He mixtures. ---: WALTERS and FAIRBANK [10].

The λ -points for 20 and 40% concentration are shown in Fig. 6, which represents the complete T - X diagram for helium isotopes. The phase separation as found by WALTERS and FAIRBANK [10] followed also from the Gibbs-function of mixing which we derived from the vapour pressure as a function of the concentration. The dotted line gives the expected concentration for the helium II phase at very low temperature.

Finally the change of the normal fluid fraction in He II due to the presence of ^3He , Δx , has been estimated from experiments on the

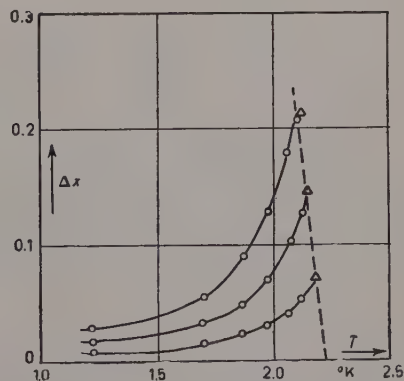


Fig. 7. — The increase Δx of the normal fluid fraction in He II due to the presence of ^3He , as a function of the temperature T . Upper curve: $X = 0.06$; middle curve: $X = 0.04$; lower curve: $X = 0.02$.

REFERENCES

- [1] D. H. N. WANSINK, K. W. TACONIS and F. A. STAAS: Commun. Kamerlingh Onnes Lab., Leiden, no. 304a; *Physica*, **22**, 449 (1956).
- [2] D. H. N. WANSINK and K. W. TACONIS: Commun. Kamerling Onnes Lab., Leiden, no. 305c; *Physica*, **23**, 125 (1957).
- [3] H. S. SOMMERS: *Phys. Rev.*, **88**, 113 (1952).
- [4] H. C. KRAMERS, J. D. WASSCHER and C. J. GORTER: Commun. Karmeling Onnes Lab., Leiden, no. 288c; *Physica*, **18**, 329 (1952).
- [5] D. H. N. WANSINK: Commun. Karmeling Onnes Lab., Leiden, Suppl. no. 112e; *Physica*, **23**, 140 (1957).
- [6] Z. DOKOUPIL, G. VAN SOEST, D. H. N. WANSINK and D. G. KAPADNIS: Commun. Kamerling Onnes Lab., Leiden, no. 298a; *Physica*, **20**, 1181 (1954).
- [7] D. G. KAPADNIS and Z. DOKOUPIL: Commun. Confér. de Phys. des basses Temp., **19** (1955); to be published in *Physica*.
- [8] Z. DOKOUPIL and K. SHREERAMAMURTY: to be published in *Physica*.
- [9] B. N. ESEL'SON and N. G. BEREZNIAK: *Žu. Ėksper. Teor. Fiz.*, **30**, 628 (1956); *Soviet Phys. JETP*, **3**, 568 (1956).
- [10] K. G. WALTERS and W. M. FAIRBANK: *Phys. Rev.*, **103**, 262 (1956).
- [11] D. H. N. WANSINK and K. W. TACONIS: Commun. Kamerling Onnes Lab., Leiden, no. 306b; *Physica*, **23**, 273 (1957).
- [12] J. G. DASH and R. D. TAYLOR: *Proc. Int. Conf. on Low Temp. Physics*, (Madison, 1957).
- [13] J. R. PELLAM: *Phys. Rev.*, **99**, 1327 (1955).

Second Sound in ^3He - ^4He Mixtures (*).

H. A. FAIRBANK

Sloane Physics Laboratory, Yale University - New Haven, Connecticut

1. - Introduction.

The addition of ^3He to liquid ^4He influences the properties of the liquid in several interesting ways. The lambda point is shifted to lower temperatures, the specific heat and entropy are increased, and characteristic superfluid properties of the liquid are affected. One such property that undergoes a drastic and significant change on the addition of even a small amount of ^3He is the velocity of second sound. Second sound is the name given to a phenomenon, unique to superfluid helium, in which a temperature variation propagated through the liquid obeys a wave equation. Its discovery by PESHKOV after the earlier predictions of TISZA [1] and LANDAU [2] was a triumph of the two-fluid model. Detailed measurements of the velocity of second sound in pure ^4He have played an important role in guiding and checking the theory. Likewise, second sound is a useful probe for studying the properties of superfluid ^3He - ^4He mixtures. A series of second sound experiments in these mixtures have been carried out at Yale by E. A. LYNTON, J. C. KING, and S. D. ELLIOTT in collaboration with the author. This work will be described briefly with particular reference to the information it gives on the normal component density of the liquid mixtures, the ^3He effective mass, the lambda transition temperature and the transition to two liquid phases that occurs in these mixtures at low temperatures.

2. - Method of measurements.

A variety of methods can and have been used to measure the velocity of second sound [3-5]. In measurements [6-9] on ^3He - ^4He mixtures a single pulse

(*) This work been supported in part by the Office of Ordnance Research and the National Science Foundation.

method was chosen for convenience and to minimize the possibility of « heat flush » causing isotopic inhomogeneities. Fig. 1 illustrates the method. The ap-

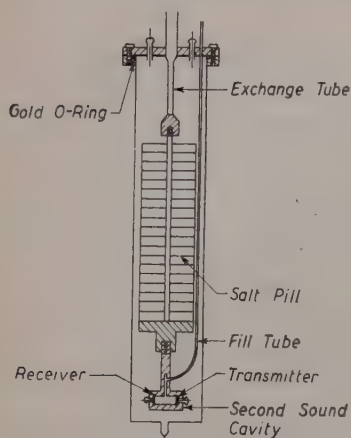


Fig. 1. — A simplified drawing of the apparatus used to measure the velocity of second sound at temperatures below 1°K.

paratus shown is immersed in a bath of liquid helium. Into the second sound cavity is condensed the appropriate mixture of ^3He - ^4He . The transmitter is a thin carbon film resistance across which a voltage pulse can be fed to produce the desired temperature pulse. The receiver for this temperature pulse is another carbon resistive film acting as a thermometer. The time of flight of the second sound pulse across the cavity is observed with the aid of a synchroscope. The cavity in Fig. 1 is thermally locked to a potassium chrome alum salt pill which serves as a refrigerant (by magnetic cooling) and as a thermometer for the measurements below 1°K. Full details of this method are given elsewhere [7].

3. — Pure ^4He .

Pure ^4He is necessarily the starting or reference point for the discussion of the properties of the mixtures. The second sound velocity u_2 as first given by LANDAU [1] is

$$(1) \quad u_2^2 = \frac{\varrho_s}{\varrho_n} \frac{T}{C} S^2,$$

where ϱ_s and ϱ_n are the superfluid and normal component densities; T , the absolute temperature; C and S the specific heat and entropy per unit mass. LANDAU assumes that the thermal motion is entirely associated with ϱ_n in the form of elementary excitations of two kinds, phonons and rotons, with energy spectra

$$(2) \quad E = cp \quad (\text{phonons}),$$

$$(3) \quad E = \Delta + \frac{(p - p_0)^2}{2\mu} \quad (\text{rotons}),$$

where E and p are the energy and momentum of the excitation, c is the velocity of sound, Δ is the energy gap between the lowest roton and phonon states, and p_0 is the momentum of the lowest roton state. The experimental depen-

dence of u_2 on the temperature is shown in curve A of Fig. 2. The general shape of the curve is in beautiful agreement with LANDAU's predictions. In the high temperature region where the roton excitations predominate, the velocity goes to zero as ϱ_n approaches zero at T_λ . The sharp rise of the velocity with decreasing temperature in the vicinity of 0.8°K is a consequence of the increased role of the phonons. At sufficiently low temperatures when only phonon excitations exist, the velocity should rise to $u_2 = u_1/\sqrt{3}$, where u_1 is the velocity of the phonons (or ordinary sound), provided the mean free

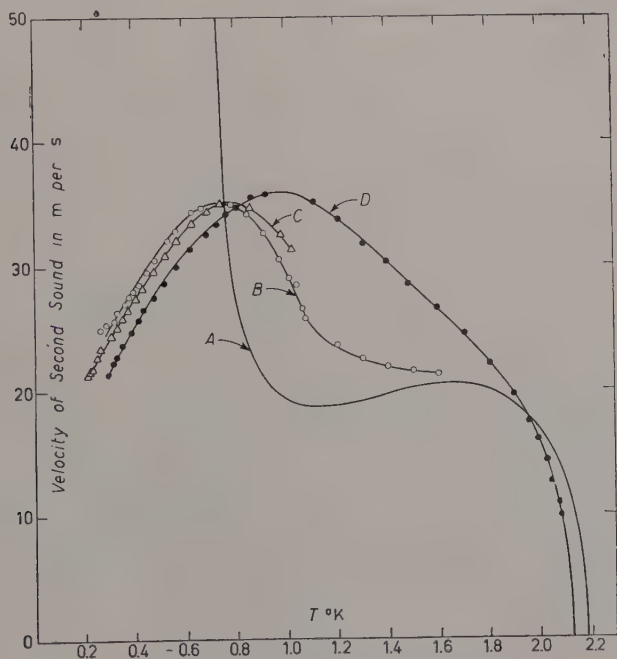


Fig. 2. — The velocity of second sound vs. temperature as measured by KING and FAIRBANK [7]. Curve A, pure ^4He . Curve B, 0.32% ^3He . Curve C, 0.62% ^3He . Curve D, 4.30% ^3He .

path for phonon-phonon interactions is sufficiently small (compared to the wave length of second sound and the cavity size) to propagate second sound in the ordinary sense. Below 0.6°K the heat pulses are observed to travel with a velocity approaching that of sound and they undergo a large spreading [10, 11, 7]. This behavior is consistent with the assumption that the excitations are exclusively phonons that have long mean free paths and are therefore scattered mainly by the walls of the container. The specific heat [12] and thermal conductivity data [13] support this picture.

4. - Dilute ^3He - ^4He solutions.

Second sound velocity measurements using the single pulse technique were first made at temperature above 1.2 °K in solutions up to 1% ^3He by LYNTON and FAIRBANK [6]. These measurements were extended down to 0.2 °K and to concentrations up to 4.3% ^3He by KING and FAIRBANK [7, 8]. Second sound measurements were also made by WEINSTOCK and PELLAM [14] on a 4% ^3He mixture using a thermal Rayleigh disc. Typical curves showing the dependence of velocity on temperature for 0.32% ^3He , 0.62% ^3He , and 4.30% ^3He are shown in Fig. 2 curves *B*, *C* and *D*. The influence of even a small amount of ^3He is pronounced. The lambda point is depressed to lower temperatures; in the intermediate temperature range the velocity is substantially increased; as the temperature is reduced below 1 °K the second sound velocity reaches a maximum value and falls towards zero instead of rising to high values as in the case of pure ^4He . Furthermore the spreading of the pulses observed in pure ^4He below about 0.6 °K does not occur in ^3He - ^4He mixtures. Indeed no significant change in the behavior in second sound occurs as the temperature is reduced to the lowest values other than the change in velocity.

A remarkably good description of this general behavior was given prior to the measurements by POMERANČUK [15]. In his theory which applies only to very dilute solutions, POMERANČUK starts with the two fluid hypothesis and further assumes that ^3He contributes only to the normal component density. He assumes that classical statistics can be applied to the ^3He atoms above about 0.2 °K. The expression for the velocity of second sound then is modified to the form

$$(4) \quad u_2^2 = \frac{\varrho_s}{\varrho_n} \frac{T}{C} \left[\left(S_0 + \frac{k\varepsilon}{m_4} \right)^2 + \frac{k\varepsilon C}{m_4} \right],$$

where S_0 is the entropy per gram of pure ^4He , m_4 is the mass of the ^4He atom, k is the Boltzmann constant, C is the heat capacity/gram of the solution and ε is the mole fraction N_3/N_4 . In this expression ϱ_s , ϱ_n and C depend upon ε . To evaluate these quantities POMERANČUK suggests that the elementary excitations connected with the foreign atoms, namely ^3He , will give rise to one of two possible energy spectra, either

$$(5) \quad E = E_0 + p^2/2\mu,$$

$$(6) \quad E = E_0 + (p - p_0)^2/2\mu,$$

He then obtains for ϱ_n and C on the two assumptions

$$(7) \quad C = C_0 + \frac{3}{2} \frac{k\varepsilon}{m_1} \quad [\text{for } p_0 = 0, \text{ assumption (5)}],$$

$$(8) \quad C = C_0 + \frac{1}{2} \frac{k\varepsilon}{m_4} \quad [\text{for } p_0 \neq 0, \text{ assumption (6)}],$$

$$(9) \quad \varrho_n = \varrho_{n0} + \frac{\varrho \mu \varepsilon}{m_4} \quad [\text{for } p_0 = 0, \text{ assumption (5)}],$$

$$(10) \quad \varrho_n = \varrho_{n0} + \frac{\varrho}{m_4} \frac{p_0^2}{3kT} \quad [\text{for } p_0 \neq 0, \text{ assumption (6)}],$$

where ϱ_{n0} and C_0 are the normal component density and heat capacity/gram for pure ^4He and μ is the effective mass of the ^3He atom in solution. ϱ_s is given by the expression

$$(11) \quad \varrho_s = \varrho - \varrho_n,$$

where ϱ is the total density of the mixture.

The experimental measurements of u_2 for solutions less than 1% ^3He are in good qualitative agreement with Pomerančuk's theory and in good quantitative agreement if the first energy spectrum for the impurity excitations is assumed (Eqn. (5) with $p_0 = 0$). However, the adjustable parameter μ turns out to be temperature dependent and larger than the ^3He mass as shown in Fig. 3. It should be pointed out that near the lambda point equation (9) cannot be correct as it makes no allowance for the depression of the lambda temperature in mixtures [16]. It is reasonable to attach more significance to the results well below 1°K where the ^3He excitations dominate the behavior and the approximations are consequently very much better. It is interesting to note that the effective mass μ near 0°K is close to the value 5.8 atomic mass units obtained theoretically by FEYNMAN [17].

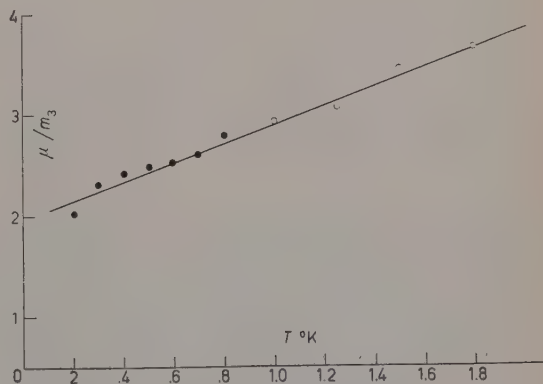


Fig. 3. — The ^3He effective mass relative to the atomic mass of ^3He as a function of temperature. Data of KING and FAIRBANK [7] and LYNTON and FAIRBANK [6].

atomic mass units obtained theoretically by

The lack of spreading of the pulses at the lowest temperature in contrast to the behavior in pure ^4He is a reasonable consequence of the fact that below 0.6°K the ^3He contribution to ρ_n , S and C is predominant. Second sound is propagated therefore by the ^3He excitations of short mean free path. It is interesting to note that on Pomerančuk's theory, equation (4) reduces to

$$u_2^2 = \frac{5}{3} \frac{kT}{\mu},$$

below about 0.5°K . This is just the velocity of sound in an ideal gas of particles of mass μ .

5. - Concentrated ^3He - ^4He solutions.

With the recent availability of larger amounts of ^3He , these measurements have been extended to higher ^3He concentrations in collaboration with S. D

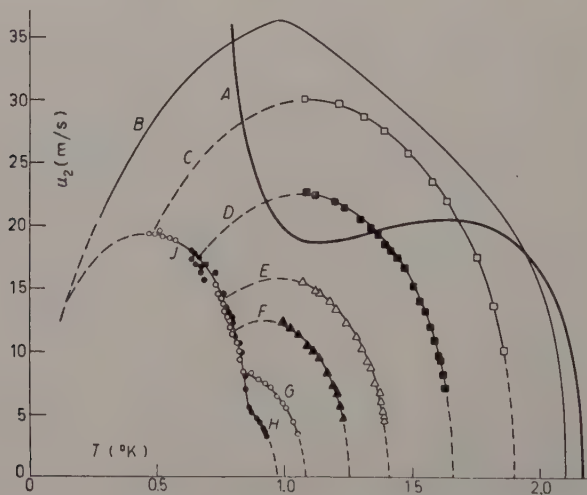


Fig. 4. - The velocity of second sound vs. temperature. Curve A, pure ^4He . Curve B, 4.30% ^3He . Curve C, 18.4% ^3He . Curve D, 31.4% ^3He . Curve E, 43.9% ^3He . Curve F, 50.5% ^3He . Curve G, 59.4% ^3He . Curve H, 63.9% ^3He .

ELLIOTT [9]. The temperature dependence of the velocity for concentrations up to 63.9% ^3He is shown in Fig. 4.

Extrapolation of these curves to zero velocity gives values of the lambda temperatures. These are plotted in Fig. 5 upper curve, along with some values obtained by other investigators using different methods [8, 16, 18-22]. The

lambda curve is clearly higher than indicated in the early pioneer work of ABRAHAM, WIENSTOCK and OSBORNE and DAUNT and HEER. Near zero concentration the slope of the $T_\lambda(x)$ curve is $-1.5^\circ\text{K}/\text{mole fraction}$ on the basis of the second sound results, T_λ measurements of ESEL'SON and LAZAREV[†][22] and of DASH and TAYLOR [16] are in excellent agreement. At higher concentrations the second sound values of T_λ and those obtained from vapor pressure measurements by ESEL'SON, BEREZNIJAK and KAGANOV [21] are in reasonable agreement.

Of particular interest is the behavior of the second sound velocity below 1°K where the liquid mixtures are known to separate into two liquid phases. The phase separation temperature $T_\phi(X)$ as first measured by WALTERS and W. FAIRBANK [20] using nuclear magnetic resonance techniques is shown in Fig. 5 (dotted curve).

In order to observe the second sound behavior in this two-phase region the second pulse was propagated horizontally as shown in Fig. 1 rather

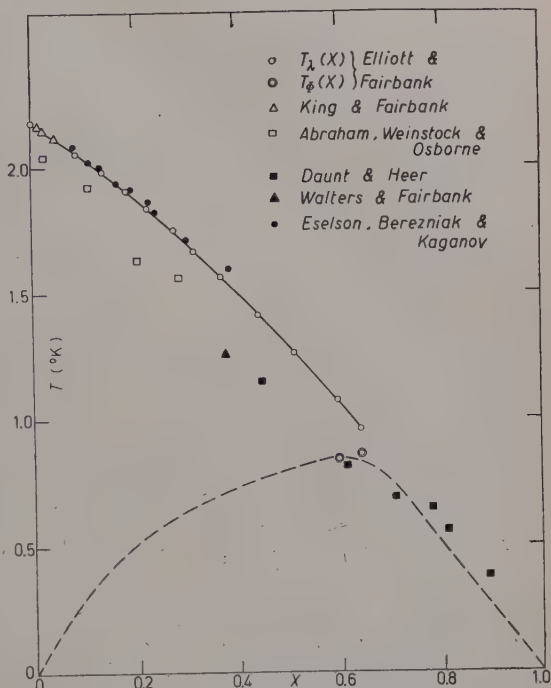


Fig. 5. — The λ temperature as a function of ^3He concentration is shown in the upper curve. The dotted curve is the phase equilibrium temperature as a function of ^3He concentration from the data of WALTERS and FAIRBANK [20].

than vertically as in previous arrangements. As the temperature is lowered through the phase transition region the liquid mixture separates into a ^3He rich phase and ^4He rich phase, the former occupying the upper part of the cavity. Thus a single temperature pulse at the transmitter would be split into two pulses traveling through the upper and lower phases, provided both phases are superfluid. The sharp break in curves *G* and *H* of Fig. 4 evidently occurs at the phase transition temperature. The high temperature part of these and the other curves gives the velocity in the single phase region. *J* is the velocity temperature curve for the ^4He rich phase in the two-phase region. Curves *B-F* have been extrapolated to join curve *J* at the phase transition temperatures given by WALTERS and FAIRBANK. The phase transition temperatures (0.84°K for 59.4% ^3He and 0.86°K for 63.9% ^3He) corresponding to the break in *G* and

H are plotted in Fig. 5 (as double circles). The agreement with the curve of Walters and Fairbank is reasonably good although there is a strong suggestion that the maximum of the curve should be shifted to a higher temperature and ^3He concentration.

An interesting question not yet answered is whether the ^3He rich phase is indeed superfluid. The lambda point measurements of DAUNT and HEER [19] would seem to indicate that this is so. However there is the possibility that the film flow they observed took place in the ^4He rich phase. The trend of the lambda curve in Fig. 5 indicates that it will either intercept the phase transition curve near its maximum or lie very close to the right hand side of this curve. In the first case the ^3He rich phase would not be superfluid. In the second case it would be superfluid but at a temperature very close to the lambda point. In the measurements so far no second sound pulse has been observed corresponding to transmission through the ^3He rich phase. It is dangerous to conclude from this, however, that this phase is not superfluid inasmuch as second sound is highly attenuated and hence difficult to observe very close to the lambda point. It is clear from the trend of data in Fig. 5 that the velocity will be very low (probably less than 1 m/s) if it does exist in this phase. Mr. S. D. ELLIOTT and I are continuing these measurements and a full account will be published in *Physical Review*.

REFERENCES

- [1] L. TISZA: *Compt. Rend. Acad. Sci.*, **207**, 1035, 1186 (1938).
- [2] L. D. LANDAU: *Journ. Phys. USSR*, **5**, 71 (1941).
- [3] V. P. PEŠKOV: *Journ. Phys. USSR*, **8**, 381 (1944).
- [4] C. T. LANE, H. A. FAIRBANK and W. M. FAIRBANK: *Phys. Rev.*, **71**, 600 (1947).
- [5] J. R. PELLAM: *Phys. Rev.*, **75**, 1183 (1949).
- [6] E. A. LYNTON and H. A. FAIRBANK: *Phys. Rev.*, **80**, 1043 (1950).
- [7] J. C. KING and H. A. FAIRBANK: *Phys. Rev.*, **93**, 21 (1954).
- [8] J. C. KING and H. A. FAIRBANK: *Phys. Rev.*, **91**, 489 (A) (1953).
- [9] S. D. ELLIOTT and H. A. FAIRBANK: *Proc. of the Fifth Int. Conf. on Low Temp. Physics* (Madison, 1957).
- [10] D. DE KLERK, R. P. HUDSON and J. R. PELLAM: *Phys. Rev.*, **93**, 28 (1954).
- [11] H. C. KRAMERS: *Proc. Kon. Ak. Wet. Amsterdam*, B **59**, 35, 48 (1956).
- [12] H. C. KRAMERS, J. D. WASSCHER and C. J. GORTER: *Physica*, **18**, 329 (1952).
- [13] H. A. FAIRBANK and J. WILKS: *Proc. Roy. Soc., A* **231**, 545 (1955).
- [14] B. WEINSTOCK and J. R. PELLAM: *Phys. Rev.*, **89**, 521 (1953).
- [15] I. POMERANČUK: *Žu. Ėksper. Teor. Fiz.*, **19**, 42 (1949).
- [16] J. G. DASH and R. D. TAYLOR: *Phys. Rev.*, **107**, 1228 (1957), suggest a modification of Pomerančuk's theory to avoid this difficulty. Values of μ have

also been obtained using the oscillating disk technique by J. G. DASH, R. D. TAYLOR *Phys. Rev.* **99**, 598 (1955) and J. R. PELLAM: *Phys. Rev.*, **99**, 1327 (1955) and H. G. BEREZNIAK and B. N. ESEL'SON: *Žu. Èksper. Teor. Fiz.*, **31**, 902 (1956).

- [17] R. P. FEYNMAN: *Phys. Rev.*, **94**, 262 (1954).
- [18] B. M. ABRAHAM, B. WEINSTOCK and D. W. OSBORNE: *Phys. Rev.*, **76**, 864 (1949).
- [19] J. G. DAUNT and C. V. HEER: *Phys. Rev.*, **79**, 46 (1950).
- [20] G. K. WALTERS and W. M. FAIRBANK: *Phys. Rev.*, **103**, 262 (1956).
- [21] B. N. ESEL'SON, H. G. BEREZNIJAK and M. I. KAGANOV: *Dokl. Akad. Nauk SSSR*, **111**, 568 (1956); *Soviet Physics JETP*, **1**, 683 (1956).
- [22] B. N. ESEL'SON and B. G. LAZAREV: *Dokl. Akad. Nauk SSSR*, **72**, 265 (1950).

INTERVENTI E DISCUSSIONI

— J. E. MAYER:

I would like to point out that there is, and should be, a correspondence between the temperature of the λ transition in ^4He and the effective temperature of the susceptibility curve in ^3He . Both are lower than those computed on a perfect gas model at the experimental density. Both decrease with increasing density.

The fact that the temperatures are lower than the perfect gas values is easily explained by the repulsive forces which prevent close approach of molecular pairs. However, the numerical application of our equation indicates that this alone is not a adequate to obtain the experimental value, but that also the Gaussian like decay of the off diagonal parts of the density matrix is steeper in the experimental liquids than in the perfect gas. This is reasonable and has already been predicted by FEYNMAN, namely that the reduced mass entering $\lambda = \hbar/\sqrt{2\pi mkT}$ should exceed the atomic mass. If, now, this mass increases with density the negative derivative of the two temperatures with increasing pressure is also to be expected.

Influence of ^3He on Some Flow Properties of He II (*).

J. G. DASH and R. D. TAYLOR

*University of California, Los Alamos Scientific Laboratory
Los Alamos, New Mexico*

In the nomenclature of the two-fluid model of He II, a complete description of the hydrodynamics of the liquid requires the specification of the normal fluid density ϱ_n , the normal fluid viscosity η , the critical velocity v_c of superfluid, and the resistance to flow of superfluid at velocities exceeding v_c . These properties are functions of the temperature and of ^3He isotope concentration: critical velocity phenomena appear to depend also upon the experimental liquid dimensions and surface conditions. Several of these properties may be studied by means of the torsion pendulum. Such a device, as used previously by ANDRONIKAŠVILI [1, 2] and HOLLIS-HALLET [3], has been applied to an investigation of the influence of ^3He on ϱ_n , η , and v_c .

A recent description of the method and theory of measurement of ϱ_n and η is given by DASH and TAYLOR [4] in connection with a study of pure ^4He below its λ -point. The details of the method will not be reported here; this communication will emphasize the recent experimental results and their implications.

1. - Normal fluid density of ^3He - ^4He solutions.

The torsion pendulum data on four liquid samples of ^3He molar concentration x_3 ranging between 0 and 11% and at temperatures from 1.3 °K and at temperatures from 1.3 °K to the λ -point, are shown in Fig. 1.

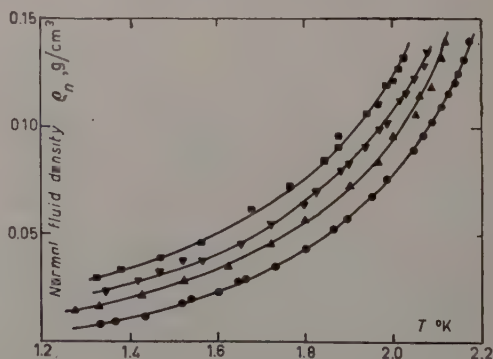


Fig. 1.

(*) Work performed under the auspices of the U.S. Atomic Energy Commission.

This family of curves show the influence of increasing ^3He concentration as three principal effects. These are the depressed λ temperatures T_λ , the lowered total densities ρ_λ at T_λ , and the increased asymptotic values of ρ_n at low temperatures.

The λ -point depressions appear to obey the semi-empirical rule given by GOLDSTEIN [5]:

$$(1) \quad T_\lambda = x_4^{\frac{3}{4}} T_\lambda^0,$$

where $T_\lambda^0 = 2.1735^\circ\text{K}$, the transition temperature of pure ^4He on the T_{55E} temperature scale.

The total density of liquid solutions at T_λ for ^3He concentrations up to 50% molar concentration have been measured by KERR [6] by the conventional volumetric method. These data are described to within 0.5% accuracy by the linear superposition formula

$$(2) \quad \rho_\lambda = \varphi_3 \rho_3 + \varphi_4 \rho_4; \quad \rho_3 = 0.08438 \text{ g/cm}^3, \quad \rho_4 = 0.14657 \text{ g/cm}^3,$$

where $\varphi_{3,4}$ are the volume concentrations of the isotopes.

The density of ^4He in Eq. (2) corresponds to the density of pure ^4He at T_λ^0 , but the density ρ_3 is approximately 8% higher than the density of pure ^3He at these temperatures, indicating a solution volume decrease proportional to the ^3He concentration. The torsion pendulum data appear to agree with the Eq. (2).

We wish to determine the influence of ^3He on the ρ_n of solutions at all temperatures $T \leq T_\lambda$, but the data indicate only the total ρ_n contributed by both ^3He and ^4He . In order to obtain the ^3He contribution, we are therefore forced to subtract from the measured ρ_n the ^4He contribution which we may deduce from auxiliary reasoning. The conditions under which we have analyzed the ρ_n data are:

- 1) $\rho_{3s} = 0$. The ^3He makes no contribution to the superfluid fraction [7].
- 2) $\rho_s(T_\lambda) = 0$. No superfluidity remains at the λ -point.
- 3) The addition of ^3He and ^4He contributions must be described in such a form that Eq. (2) is satisfied at T_λ .

A simple superposition formula satisfying all of these conditions is given by

$$(3) \quad \rho_n(\varphi_3, T^*) = \varphi_3 \rho_3^* + \varphi_4 \rho_n \quad (\varphi_3 = 0, T^*),$$

where $T^* = T/T_\lambda$ is the reduced temperature appropriate to the liquid of ^3He volume concentration φ_3 . Thus, the ^4He contribution to ρ_n of the solution

at a temperature T is taken to be proportional to the normal fluid density of pure ^4He at the temperature $T' = x_4^{\frac{2}{3}} T$. The « effective hydrodynamic density » ϱ_3^* of ^3He in solution can now be calculated from the measured quantities and the Eq. (3). The values of ϱ_3^* corresponding to all solutions and temperatures are given *versus* the superfluid density ϱ_s in Fig. 2. These data appear to give the linear relationship

$$(4) \quad \varrho_3^* = \varrho_s + 0.8 \varrho_s.$$

Eqs. (1)–(4) can be combined into a concise description of ϱ_n over the explored range of temperatures and concentrations. This description

can be easily extrapolated in both directions; we demonstrate that it is well-behaved over the entire range by giving the semi-analytic surface of ϱ_n *versus* x_3 and T , shown in perspective in Fig. 3.

The empirical behavior of ϱ_3^* appears to be qualitatively explained by classical hydrodynamic theory. If we may consider each ^3He atom as a sphere

moving through an ideal (super) fluid [8], then the effective ^3He atomic mass is increased proportionally to the density of fluid in relative motion:

$$m_3^* = m_3 + \frac{1}{2} v_3 \varrho_s,$$

where v_3 is the ^3He atomic volume. This yields, for the effective hydrodynamic density,

$$(5) \quad \varrho_3^* = \frac{m_3^*}{v_3} = \varrho_s + \frac{1}{2} \varrho_s,$$

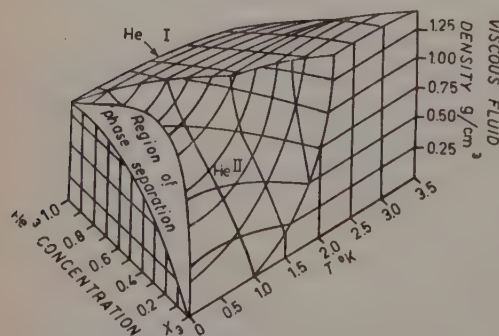


Fig. 3.

which is formally identical to the empirical Eq. (4) but has a coefficient considerably smaller than 0.8. This discrepancy is perhaps understandable in terms of the details of the classical problem, for we might expect that the motion of a ^3He atom should create a disturbance of greater relative extent among the surrounding atoms than if the velocity gradients could decrease in a microscopically smooth and continuous fashion.

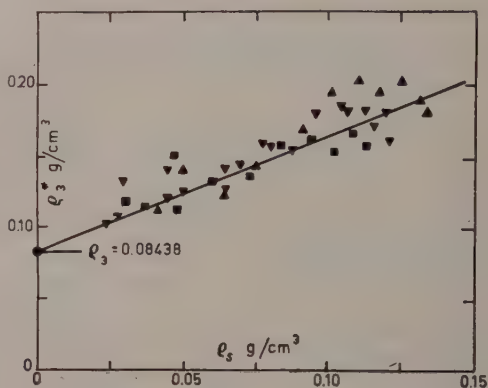


Fig. 2.

2. - Viscosity of normal fluid in ^3He - ^4He solutions.

The viscosity of normal fluid in He II appears to be, in its realm, as distinctive an attribute of superfluidity as is the normal fluid density. Little attention, however, has been paid to the theoretical problem of the influence of ^3He upon the viscosity. The complexity of the problem is suggested by the temperature dependence of the viscosity of pure ^4He , which decreases sharply with temperature below T_λ , displays a broad minimum at about 1.8°K , and then rises monotonically as the temperature is further decreased. When ^3He is added to the liquid, the anomalous behavior should be progressively weakened; such an effect is shown by the data given in Fig. 4. Curves shown are for liquids of $x_3 = 0.0$ (\bullet), 0.03 (\blacktriangle), 0.06 (\blacktriangledown), 0.1 (\blacksquare), and 1.0 ($+$). The family of curves show the following effects of increasing ^3He concentration:

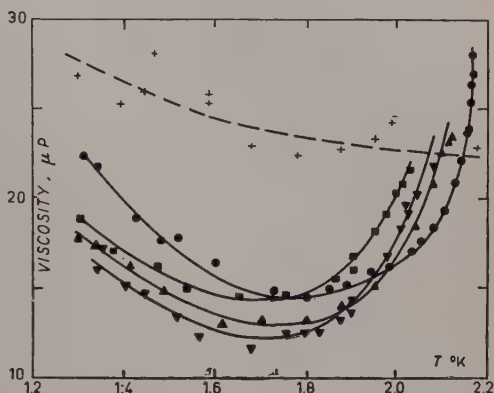


Fig. 4.

- 1) Depressed λ -point.
- 2) Depressed viscosity η_λ at T_λ .
- 3) An initial depression, then an increase of the viscosity η_{\min} of the minimum at $(1.7 \div 1.8)^\circ\text{K}$.
- 4) Lower temperature dependence of viscosity at low temperatures.

These features indicate that the viscosity of ^3He - ^4He solutions cannot be described by the superposition of separate isotopic contributions. The most remarkable feature is the depression of η_{\min} below the viscosities of either ^4He or ^3He liquids at any temperature; this phenomenon can apparently be explained in terms of the Landau-Halatsnikov model [9]. The viscosity at these temperatures is attributed in greatest part to the « roton gas » as the principal carrier of momentum. The individual rotons are quantized collective excitations of several (~ 7) ^4He atoms; they are imagined to be similar to microscopic vortices moving through the liquid. An encounter between such a ^4He vortex and a ^3He atom must evidently produce a strong deflection in the path of the roton, for it may not drift through the region of a ^3He atom without

a change in its quantized internal energy. The encounter is equivalent to a termination of the roton free path; this mechanism decreases the viscosity of the liquid. If there is any ^3He -induced change in the roton density, the effect on the viscosity should be an equal but opposite fractional change in the roton-roton collision mean free path. Finally, the ^3He atoms themselves, if sufficiently dilute, will not contribute a significant increase in momentum transport. The net effect of the ^3He is a decreased viscosity.

The empirical value $(d\eta/dx_3)_{x_3=0}$ affords a crude test of these ideas. This value, together with estimates of the roton density and effective mass indicate that the roton- ^3He cross-section is about 1.7 times that for roton-roton collisions. Using the semi-empirical value $5 \cdot 10^{-15} T^{\frac{1}{2}} \text{ cm}^2$ for the latter, we obtain about $6.3 \cdot 10^{-15} \text{ cm}^2$ for the collision cross-section of a ^3He atom with a roton. This value is approximately equal to the geometrical cross-section of a sphere of liquid containing 7 atoms of ^4He .

3. - Influence of ^3He on the critical velocity.

The problem of the critical velocity is one of great present interest and difficulty. Several theoretical attempts have had varied success; the experimental problem of measuring v_c appears to be equally difficult. The torsion pendulum provides one method for determining v_c in bulk fluid, but it is not

yet certain that this technique yields results equivalent to those obtained in other ways, for example, by steady flow through capillaries or by the conduction of heat. With these reservations, we may examine the present data.

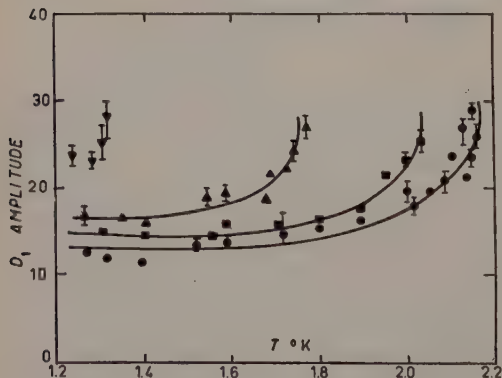


Fig. 5.

together with the cylinder radius and oscillation frequency, yields a velocity; we speak of it here as the critical velocity.

Critical velocities of several solutions are shown in Fig. 5. Concentrations are $x_3 = 0.0$ (\bullet), 0.1 (\blacksquare), 0.3 (\blacktriangle), and 0.5 (\blacktriangledown). The ordinates are given as the « critical amplitudes » of oscillation; cylinder radius and period are such that

the velocities range from 0.2 to 0.9 cm/s. These curves are similar to the behavior of pure ^4He as originally reported by HOLLIS-HALLETT [3]; the influence of ^3He in *raising* v_c is seen to be monotonic. Such behavior is in qualitative agreement with the phenomenological theory [10] which suggests that the origin of the critical velocity lies in the creation of phonons by the relative motion of superfluid along a surface. The semi-empirical formula for the critical velocity was given as

$$(6) \quad v_c = \text{const } c(a\rho_s/\rho)^{-\frac{1}{2}},$$

where c is the speed of first sound in the medium and a is a characteristic dimension of the liquid volume. The addition of ^3He , causing a decrease in ρ_s/ρ , is thus predicted to increase the value of v_c . Agreement, however, is found to be qualitative; the data shown appear to obey an equation in the form of Eq. (6), but with an exponent approximately equal to -0.3

REFERENCES

- [1] E. L. ANDRONIKAŠVILI: *Journ. Phys. USSR*, **10**, 201 (1946).
- [2] E. L. ANDRONIKAŠVILI: *Žu. Èksper. Teor. Fiz.*, **18**, 429 (1948).
- [3] A. C. HOLLIS-HALLETT: *Proc. Roy. Soc., A* **210**, 404 (1951).
- [4] J. G. DASH and R. D. TAYLOR: *Phys. Rev.*, **105**, 7 (1957).
- [5] L. GOLDSTEIN: *Phys. Rev.*, **95**, 869 (1954).
- [6] E. C. KERR: private communication (to be published).
- [7] L. LANDAU and I. POMERANČUK: *Dokl. Akad. Nauk SSSR*, **59**, 669 (1948).
- [8] R. P. FEYNMAN: *Phys. Rev.*, **94**, 262 (1954).
- [9] L. D. LANDAU and I. M. HALATNIKOV: *Žu. Èksper. Teor. Fiz.*, **19**, 637, 709 (1949).
- [10] J. G. DASH: *Phys. Rev.*, **94**, 1091 (1954).

INTERVENTI E DISCUSSIONI

— G. CARERI:

In the low concentration region, does the Pomerančuk theory describe your data? Can you express your data in terms of effective mass? The Feynman picture of the back flow applies only at absolute zero; is one allowed to apply it in your case?

— J. G. DASH:

The Pomerančuk description does not describe our data very well. There is, however, an indication that the Pomerančuk representation approaches the experimental results as $T, X_3 \rightarrow 0$.

The Feynman model of the ^3He effective mass does not apply in our case but it can be made to agree with the data if one applies the very simple extension of the model described in my talk.

— D. O. EDWARDS:

I would like to know how the new values for the viscosity of pure ^4He compare with those obtained previously with the oscillating disc and rotating cylinder viscometers. Results for η_1 calculated from heat conductivity measurements appear to agree well with the rotating cylinder viscometer and therefore indicate that the disc method may be unreliable, especially at low temperatures.

— J. G. DASH:

There appear to be satisfactory agreement between our recent results on pure ^4He and viscometer data of HEIKKILÄ and HALLETT in the range $1.5^\circ\text{K} \div T_\lambda$. An increasing divergence does appear at lower temperatures, however, the disk results lying approximately 60% higher than viscometer values at 1.3°K . This discrepancy is unresolved at present, and may be due to experimental difficulties associated with either, or both, techniques. The apparent agreement between the viscosity derived from heat conduction experiments and viscometer work may, however, be entirely accidental. Heat conduction in capillaries can be severely influenced by mean free path effects at low temperatures and this may cause a lowering of the deduced values of viscosity.

Velocity of Sound in a ^3He - ^4He Mixture.

E. W. GUPTILL

Dalhousie University - Halifax

A. C. HOLLIS HALLETT and C. C. LIM

University of Toronto - Toronto

Summary. — Cylindrical Barium Titanate transducers have been used to measure the velocity of sound in solid argon and in a 4% ^3He - ^4He mixture. In the case of solid argon, high attenuation resulted in rather poor accuracy (about 2%). The ^3He - ^4He measurements have an accuracy of 0.1% and show that the λ point for the mixture shifts towards lower temperature. Preliminary results indicate that the presence of ^3He lowers the attenuation in the region of the λ point and increases the attenuation above 2.3 °K.

PARTE NONA

Mixtures

Isotopic Mixtures.

I. PRIGOGINE and A. BELLEMANS

Faculté des Sciences, Université Libre de Bruxelles - Bruxelles

The present communication intends to summarize the theoretical results obtained in the field of isotopic mixtures by PRIGOGINE and his coworkers [1-4] and to compare them to the experimental data.

Let us consider a mixture of x_A mole of isotope A and x_B mole of isotope B at temperature T and pressure p , ($x_A + x_B = 1$). We assume that the intermolecular fields of A and B are the same. This is not strictly true [5] but the differences are so small that they cannot contribute significantly to the excess functions. Hence all deviations from ideality in isotopic mixtures are due to quantum effects.

The GIBBS free energy of mixing is

$$(1) \quad g^M = g_m(T, p, x_A, x_B) - x_A g_A(T, p) - x_B g_B(T, p)$$

and it can be rewritten using Helmholtz free energy « f » in the form

$$(2) \quad g^M = f_m(T, v_m, x_A, x_B) - x_A f_A(T, v_A) - x_B f_B(T, v_B) + p v^E$$

where v_m , v_A and v_B are respectively the volumes of one mole of the mixture, one mole of A and one mole of B at pressure p and temperature T ; v^E is the excess volume and as it is always very small the last term of (2) may safely be neglected.

Let us split (2) into two terms

$$(3) \quad g_I^M = x_A [f_A(T, v_m) - f_A(T, v_A)] + x_B [f_B(T, v_m) - f_B(T, v_B)],$$

$$(4) \quad g_{II}^M = f_m(T, v_m, x_A, x_B) - x_A f_A(T, v_m) - x_B f_B(T, v_m).$$

The first term g_I^M is equal to the work spent in changing the molar volumes

of pure A and B into v_m . This term can be evaluated directly from data on pure isotopes. It can be shown that this term is always positive [3]

$$(5) \quad g_I^M > 0.$$

The second term g_{II}^M corresponds to a process of mixing at constant volume. If no quantum effects were present g_{II}^M would be exactly equal to the ideal free energy of mixing. Actually on account of quantum effects one has

$$(6) \quad g_{II}^M = RT(x_A \ln x_A + x_B \ln x_B) + x_A x_B Q(T, v_m, x_A, x_B).$$

Now it has been shown by CHESTER [6] that at low temperature one has

$$(7) \quad Q > 0.$$

Hence from (5), (6) and (7) it is clear that the excess free energy is positive:

$$(8) \quad g^E > 0.$$

Now the quantum term Q has been evaluated for some simplified models [1, 2, 4]; for mixtures of H_2 - D_2 or 3He - 4He it is always very much smaller than g_I^M . Then to a reasonable approximation we may expect that

$$(9) \quad g^E \simeq g_I^M.$$

From this last expression all other excess functions can also be derived.

Table I shows some calculated and experimental data for g^E of isotopic mixtures. The agreement is satisfactory.

TABLE I. - *Theoretical and experimental excess free energies* [3].

	T (°K)	g^E calc. from (9); ($x = 0.5$)	g^E experim. ($x = 0.5$)
3He - 4He	1.5	0.8 cal	0.7 cal
H_2 - D_2	20	2.0 cal	~ 2 cal
H_2 -HD	20	0.6 cal	~ 1 cal

As the excess free energy is positive it is expected that an upper critical point will occur at low temperatures. A separation in two phases has indeed been observed recently for mixtures of 3He - 4He [7]. It should also be present in other mixtures such as H_2 - D_2 but it would be difficult to detect it because occurring in the solid state.

Equation (9) permits to calculate excess properties from the thermodynamic properties of pure isotopes but it may occur that these are not known with sufficient accuracy. In this case a graphical method has been developed in preceding papers [3] which gives the sign (and even the order of magnitude) of the excess functions. It may be interesting to mention that this graphical method predicts a positive excess volume for T_2 - D_2 mixtures and a negative excess volume for ^3He - ^4He mixtures in agreement with experimental data [8, 9].

Finally it is perhaps worth to point out that isotopic mixtures occupy a very special position in the field of mixtures. Their properties are determined by the masses M_A and M_B of the pure components. No new parameter is introduced by the mixing process and this is the reason why it is possible to calculate the properties of isotopic mixtures from those of the pure components.

REFERENCES

- [1] I. PRIGOGINE, R. BINGEN and J. JEENER: *Physica*, **20**, 303 (1954).
- [2] I. PRIGOGINE and J. JEENER: *Physica*, **20**, 516 (1954).
- [3] I. PRIGOGINE, R. BINGEN and A. BELLEMANS: *Physica*, **20**, 633 (1954).
- [4] J. HENRY: *Bull. Cl. Sci. Acad. Roy. Belg.*, **42**, 163 (1956).
- [5] A. BELLEMANS: in this issue, pag 181.
- [6] G. V. CHESTER: *Phys. Rev.*, **100**, 446 (1955).
- [7] K. G. WALTERS and W. M. FAIRBANKS: *Phys. Rev.*, **103**, 262 (1956).
- [8] E. KERR: *Journ. Amer. Chem. Soc.*, **74**, 824 (1952).
- [9] E. KERR: private communication.

INTERVENTI E DISCUSSIONI

— M. J. BUCKINGHAM:

Is it not true that your expression for the excess free energy should always be less than the observed one, since the neglected terms are essentially positive? I noticed from your figures that the calculated value for ^3He - ^4He is actually larger than the observed.

— A. BELLEMANS:

The calculation of g_I^M involves an accurate knowledge of the thermodynamic properties of the pure isotopes. Now for ^4He they are well known, but this is not the case for ^3He . Moreover, there could be also some effect related to the difference of statistics which were not considered by Chester and could eventually change the sign of Q in formula (7).

The Statistical Thermodynamics of a One-Dimensional Multicomponent Assembly.

H. C. LONGUET-HIGGINS

University Chemical Laboratory - Cambridge

Summary. — It is shown that a one-dimension multicomponent mixture with nearest neighbour interactions $u_{ij}(r)$ obeys the implicit equation of state

$$\Delta(\lambda_A, \lambda_B, \dots, T, P) \equiv |\lambda_i \eta_{ij} - \delta_{ij}| = 0,$$

where λ_i is the absolute activity of species i (divided by a kinetic factor) and

$$\eta_{ij}(T, P) = \int_0^\infty \exp[-\{u_{ij}(r) + P_r\}/kT] dr.$$

The concentration of species i is thence determined as

$$-\lambda_i \frac{\partial \Delta}{\partial \lambda_i} / kT \frac{\partial \Delta}{\partial P}.$$

A one-dimensional solution is ideal if, and only if, the matrix $[\eta_{ij}]$ is of rank unity. The excess free energy of a nearly ideal solution is found to be

$$(\Delta^*G)_{T,P} = \sum_{i < j} x_i x_j (G_{ij} + G_{ji} - G_{ii} - G_{jj}),$$

where $G_{ij}(T, P)$ is the (configurational) molar Gibbs free energy of a « hybrid » species with interaction potential $u_{ij}(r)$.

I should add that the work described was carried out in collaboration with Dr. J. A. POPE and with Mr. J. P. VALLEAU.

INTERVENTI E DISCUSSIONI

— A. MUNSTER:

The problem of the one-dimensional multi-component system has been treated recently by KIKUCHI, using the method of Laplace transforms introduced originally by Gürsey for all the one-dimensional one-component systems. Do you think that your method offers some advantages compared with Kikuchi's method?

— G. UHLENBECK:

Is the matrix of which you take the trace a symmetric matrix?

— H. C. LONGUET-HIGGINS:

Yes, the matrix can be transformed to $[(\lambda_i \lambda_j)^{\frac{1}{2}} \eta_{ij}]$ the eigenvalues of which are necessarily real.

— A. BELLEMANS:

I want to mention that we have used one-dimensional model in order to test the approximate tridimensional model for solutions. In the case of mixtures of molecules of the same size one gets interacting results, but for mixtures of molecules of different size, the one-dimensional model cannot lead to reliable results.

On the Statistical Theory of the Surface Tension of Binary Mixtures.

A. ENGLERT-CHWOLES (*) and I. PRIGOGINE

Faculty of Science, University of Brussels - Brussels

1. - Introduction.

The statistical mechanics of the surface tension of solutions is of fairly recent origin. The case of perfect solutions has been studied by SCHUCHOWITSKY [1], and by BELTON and EVANS [2]. The first consistent statistical calculation of the surface tension of an imperfect solution is due to GUGGENHEIM [3] and is based on his model of the regular solution.

The limitations of the model of the regular solution are well known [4]. It seemed therefore worth while to take up the problem again using the more elaborate theories of solutions developed recently, and in particular the theory based on the average potential model of PRIGOGINE, BELLEMANS and ENGLERT-CHWOLES [4, 5].

This theory is applicable to solutions the components of which satisfy the theorem of corresponding states. For such substances, the intermolecular interaction energy ε depends on two characteristic constants, an energetic constant ε^* and a dimensional constant r^* . It has the form

$$(1.1) \quad \varepsilon(r) = \varepsilon^* \varphi(r/r^*),$$

where r denotes the distance between the molecules and φ is a universal function.

It is convenient to introduce for a binary solution of components A and B the following parameters:

$$(1.2) \quad \left\{ \begin{array}{l} \theta = (\varepsilon_{AB}^* - \varepsilon_{AA}^*/2 - \varepsilon_{BB}^*/2)/\varepsilon_{AA}^*, \\ \delta = (\varepsilon_{BB}^*/\varepsilon_{AA}^*) - 1, \\ \varrho = (r_{BB}^*/r_{AA}^*) - 1. \end{array} \right.$$

(*) Present address: European Research Associates S.A., Brussels.

We shall assume that r_{AB}^* equals the arithmetic mean of r_{AA}^* and r_{BB}^* .

The average potential model is based on the following hypothesis: the exact interactions between the molecules can be replaced in the configurational partition function of the solution by average interactions which depend in the case of random mixing on the individual interactions and on the composition. By this hypothesis the theorem of corresponding states is extended to solutions.

The thermodynamic functions of the solution can be developed into a series of powers of θ , δ and ϱ , the coefficients of which are functions of the thermodynamic properties of a reference substance. To the first approximation this model gives identical results with those obtained in the theory of conformal solutions [6]. This latter does not allow the calculation of the second order terms; however, for the solutions considered the excess quantities are of second order of magnitude, the intermolecular forces being dispersion forces. The average potential model leads to a semi-quantitative evaluation of the terms of the second order. Comparison of calculated and experimental values of the excess functions shows satisfactory agreement [4].

2. - Surface tension in the average potential model.

Before passing to the calculation of the surface tension we shall recall some definitions which have to be introduced in the treatment of the average potential model [4].

Let us consider two molecules taken at random in the solution and let r be the distance between them. If one neglects order-disorder effects the mean interaction $\langle \varepsilon(r) \rangle$ of these molecules will be given by

$$(2.1) \quad \langle \varepsilon(r) \rangle = x_A^2 \varepsilon_{AA}^* \varphi(r/r_{AA}^*) + 2x_A x_B \varepsilon_{AB}^* \varphi(r/r_{AB}^*) + x_B^2 \varepsilon_{BB}^* \varphi(r/r_{BB}^*),$$

where x_A and x_B denote the mole fractions of A and B . One can write (2.1) in a form analogous to (1.1)

$$(2.2) \quad \langle \varepsilon(r) \rangle = \langle \varepsilon^* \rangle \varphi(r/\langle r^* \rangle),$$

where $\langle \varepsilon^* \rangle$ and $\langle r^* \rangle$ are the mean interaction parameters. They are functions of the mole fractions and of the parameters ε^* and r^* of all the different types of pairs which are present in the solution. The values of these parameters depend on the analytical form of the function $\varphi(r/r^*)$. When this latter is given by Lennard-Jones' 6-12 law, one has:

$$(2.3) \quad \langle \varepsilon^* \rangle / \varepsilon_{AA}^* = 1 + \delta x_B + 2\theta x_A x_B - 18\varrho^2 x_A x_B,$$

$$(2.4) \quad \langle r^* \rangle / r_{AA}^* = 1 + \varrho x_B + \frac{17}{4} \varrho^2 x_A x_B + \frac{1}{2} \varrho \delta x_A x_B.$$

One can then define reduced mean variables for the solution from (2.3) and (2.4)

$$(2.3) \quad \langle \tilde{T} \rangle = kT / \langle \varepsilon^* \rangle, \quad \tilde{V} = V / N \langle v^* \rangle^3, \quad \tilde{P} = p \langle v^* \rangle^3 / \langle \varepsilon^* \rangle.$$

In terms of these variables all configurational thermodynamic functions of the solution have the same form as in the case of the pure liquid.

For example, one has for the configurational free energy

$$(2.6) \quad G^{\text{conf}} / RT = \xi(\langle \tilde{T} \rangle, \langle \tilde{P} \rangle) + x_A \ln x_A + x_B \ln x_B,$$

where ξ is the same function as for the pure liquid. However, the situation is not the same as regards surface properties. In the neighbourhood of the surface which separates the solution from the vapour phase, there exists a gradient of concentration; one can no longer define a unique set of parameters $\langle \varepsilon^* \rangle$ and $\langle v^* \rangle$ for the solution.

However, the formalism of the model can be preserved in the following way.

Let us regard the surface phase as a monomolecular layer [7] and let σ be the surface tension.

We denote by the suffix C the properties of the surface phase and by the suffix L those of the bulk solution. We introduce further a quantity Δx_A defined by

$$(2.7) \quad \Delta x_A = x_A^C - x_A^L.$$

We develop the surface tension into a series of powers of Δx_A in the neighbourhood of $\Delta x_A = 0$ and neglect the terms of higher than second order

$$(2.8) \quad \sigma = \sigma_0 + \Delta x_A \left(\frac{\partial \sigma}{\partial \Delta x_A} \right)_0 + \frac{1}{2} (\Delta x_A)^2 \left(\frac{\partial^2 \sigma}{\partial \Delta x_A^2} \right)_0.$$

It is reasonable to anticipate that Δx_A is of the same order of magnitude as θ , δ and ϱ defined by (1.2).

The term σ_0 can be calculated easily from the average potential model. Obviously one has

$$(2.9) \quad \tilde{\sigma}_0 = \tilde{\sigma}(\langle \tilde{T} \rangle),$$

where σ is the reduced surface tension, $\tilde{\sigma}(\tilde{T})$ denotes the same function as for the pure liquid and $\langle \tilde{T} \rangle$ is the reduced mean temperature corresponding to the composition of the bulk solution.

It is worth pointing out that the quantity σ_0 can be identified with the dynamic surface tension [8]. We now express all quantities in (2.8) in terms of σ_0 . To do this we have to consider how the surface tension can be ex-

pressed in terms of activity coefficients. This can be done by equating the chemical potential of the bulk phase μ_A^L and of the surface phase μ_A^c . The chemical potential μ_A^c is related to the molecular free energy of the surface phase λ_A^c by the equation [7]

$$(2.10) \quad \mu_A^c = \lambda_A^c - \sigma \omega_A,$$

where ω_A is the molecular surface area. One has

$$(2.11) \quad \omega_A = \left(\frac{\partial \Omega}{\partial N_A^c} \right)_{T, P, \sigma, N_B^c},$$

where Ω is the area separating the vapour phase from the liquid phase and N_A^c , N_B^c are the numbers of particles of the components A and B respectively in the surface phase.

In equilibrium the following relations hold

$$(2.12) \quad \mu_A^L = \mu_A^c = \lambda_A^c - \sigma \omega_A, \quad \mu_B^L = \mu_B^c = \lambda_B^c - \sigma \omega_B.$$

One has in terms of activity coefficients [7, 9]

$$(2.13) \quad \mu_A^L = \mu_{AA}^L + kT \ln x_A^L + kT \ln \gamma_A^L, \quad \lambda_A^c = \lambda_{AA}^c + kT \ln x_A^c + kT \ln \gamma_A^c.$$

The double index AA denotes quantities referring to the pure component and the γ are the activity coefficients.

From (2.12) and (2.13) one obtains the following expression for the surface tension

$$(2.14) \quad \begin{aligned} \sigma \bar{\omega} = & x_A^c [\sigma_{AA} \omega_{AA} + kT \ln (x_A^c/x_A^L) + kT \ln (\gamma_A^c/\gamma_A^L)] + \\ & + x_B^c [\sigma_{BB} \omega_{BB} + kT \ln (x_B^c/x_B^L) + kT \ln (\gamma_B^c/\gamma_B^L)], \end{aligned}$$

with

$$(2.15) \quad \bar{\omega} = x_A^c \omega_A + x_B^c \omega_B.$$

From (2.14) one deduces easily σ_0

$$(2.16) \quad \sigma \omega_0 = x_A \sigma_{AA} \omega_{AA} + x_B \sigma_{BB} \omega_{BB} + x_A kT \ln \gamma_A^c(x_A) + x_B kT \ln \gamma_B^c(x_A),$$

where

$$(2.17) \quad \omega = x_A \omega_A + x_B \omega_B$$

and $\gamma_A^c(x_A)$ and $\gamma_B^c(x_A)$ are the surface activity coefficients corresponding to the macroscopic composition x_A .

One obtains from equations (2.12) to (2.16), (the details of the calculation can be found in reference [8])

$$(2.18) \quad \sigma = \sigma_0 - \left(\frac{1}{2} \frac{x_A x_B \omega}{kT} \right) \left(\frac{\partial \sigma_0}{\partial x_A} \right)^2$$

Utilizing equation (2.9) one has also

$$(2.19) \quad \tilde{\sigma} = \tilde{\sigma}(\langle \tilde{T} \rangle) - \left(\frac{1}{2} \frac{x_A x_B \tilde{\omega}}{\tilde{T}} \right) \left(\frac{\partial \tilde{\sigma}(\langle \tilde{T} \rangle)}{\partial x_A} \right)^2.$$

This equation allows one to deduce the surface tension of the solution if one knows how the surface tension of one of the components, taken as reference substance, depends on temperature.

This equation is based on two hypotheses: first that the use of mean interactions is justifiable even in the surface phase and secondly that the surface phase is monomolecular.

3. - Surface tension and intermolecular forces.

Let us express (2.19) in terms of the parameters θ , δ and ϱ . To do this we develop $\tilde{\sigma}(\langle \tilde{T} \rangle)$ in the neighbourhood of the reduced temperature of one of the components, e.g. \tilde{T}_{AA} , in terms of $1/\langle \tilde{T} \rangle - 1/\tilde{T}_{AA}$. Neglecting terms of higher than second order and returning to thermodynamical variables one obtains

$$(3.1) \quad \frac{\sigma_e}{x_A x_B} = \left(\frac{\sigma - x_A \sigma_{AA} - x_B \sigma_{BB}}{x_A x_B} \right) = \sigma_{AA} \left(\frac{23}{2} \varrho^2 - \varrho \delta \right) + \\ + (\sigma'_{AA} - T \sigma_{AA}) (2\theta - 18\varrho^2 - 4\theta \varrho x_B + 2\varrho \delta) + \frac{1}{2} T^2 \sigma''_{AA} (-\delta^2 + 4\theta \delta x_B + 4\theta^2 x_A x_B) - \\ - \frac{1}{2} [(\sigma_{AA} - T \sigma'_{AA})(-\delta + 2\theta x_B - 2\theta x_A) + 2\varrho \sigma_{AA}]^2 \omega / kT,$$

σ'_{AA} , σ''_{AA} are the first and second derivatives of σ with respect to temperature and σ_e is the excess surface tension.

Using the thermodynamical surface functions of nitrogen at its boiling point [10] taken as reference substance, one can examine the influence of the intermolecular forces on σ_e [8].

For the case of the solutions considered, ε_{AB}^* is close to the geometric mean of ε_{AA}^* and ε_{BB}^* (dispersion forces); θ is then given by

$$\theta = -\delta^2/8.$$

We have then

$$\sigma_e < 0.$$

The difference in the sizes of the molecules of the two components has a considerable influence on σ_e .

Examination of (3.1) shows also that the excess surface tension is of opposite sign to the excess free energy and that one increases in absolute magnitude with the other.

4. - Comparison with experimental data.

The surface tensions of four mixtures of comparatively simple components have been measured recently by MATHOT, BOTTELIER and ROMEROWSKI [11]:

They are cyclohexane and carbon tetrachloride, cyclohexane and neopentane, carbon tetrachloride and neopentane, and benzene and neopentane.

The presence of benzene in the fourth system makes it less suitable for quantitative comparison with theory.

Experimental and calculated values are compared in Table I.

TABLE I. - Comparison of the experiment and calculated values of the excess surface tension ($T = 20^\circ\text{C}$, $x = 0.5$).

Substance	ϱ	δ	σ_e^{exp}	$\sigma_e^{\text{calc.}}$
			dyn/cm	
Cyclohexane + CMe_4	0.00 ± 0.01	-0.23 ± 0.01	-1.50	-1.8
CCl_4 + CMe_4	0.042 ± 0.01	-0.23 ± 0.01	-2.55	-2.9
Benzene + CMe_4	0.087 ± 0.02	-0.24 ± 0.01	-4.33	-3.6
CCl_4 + cyclohexane	0.033 ± 0.01	0.00 ± 0.01	-0.54	-0.42

CMe_4 = neopentane. The reference substance is always given first.

The parameters δ and ϱ have been calculated from the critical properties, the heats of vaporization and from the densities [4].

The uncertainty of these values arises chiefly from the deviations from the theorem of corresponding states for the substances under consideration.

For the three systems comprising neopentane the calculated value of the excess surface tension can depend on the choice of the reference substance since for these systems δ is rather large [4, 5]. In the absence of data for pure neopentane, we have calculated the excess surface tension always by taking the other component as reference substance.

In spite of these limitations the agreement between the experimental and calculated values of σ_e for these four systems is satisfactory.

5. - Solutions of light isotopes at low temperatures.

A generalization of the cell model applied to quantum liquids such as helium, hydrogen and their isotopes has led PRIGOGINE, BINGEN and BELLEMANS [12] to express the properties of solutions of isotopes in a form analogous to that of the average potential model. Here again one can express the surface tension of the solution in terms of the surface tensions of the pure isotopic components by the use of (2.19).

Quantum effects at low temperatures are due to the zero point energy. When the molecular volume is large, as in the case of the quantum liquids considered, the motion of the molecules about their equilibrium positions is very unharmonic.

The zero point energy is then proportional to the square of the reduced de Broglie wavelength, $\tilde{\lambda}$ defined by the equation (cf. e.g. [4])

$$(5.1) \quad \tilde{\lambda} = \frac{h}{d^* \sqrt{m \varepsilon^*}}.$$

Here h is Plank's constant, d^* the collision diameter of the two particles, proportional to r^* , and m is the mass.

The zero point energy can be written

$$(5.2) \quad E(0) = \tilde{\lambda}^2 (\tilde{V}),$$

where \tilde{V} is the reduced volume defined by (2.5).

One can show that the free energy of the quantum liquid at a given reduced temperature and pressure is in first approximation a universal function of $\tilde{\lambda}^2$.

The zero point energy of a mixture of two isotopes is a linear function of the zero point energies of the two isotopes and is, therefore, proportional to $x_A \tilde{\lambda}_{AA}^2 + x_B \tilde{\lambda}_{BB}^2$.

Let us introduce the average square wavelength $\langle \tilde{\lambda}^2 \rangle$ defined by

$$(5.3) \quad \langle \tilde{\lambda}^2 \rangle = x_A \tilde{\lambda}_{AA}^2 + x_B \tilde{\lambda}_{BB}^2.$$

All thermodynamical properties of a mixture of isotopes are then, within the approximation which we consider, the same universal functions of $\langle \tilde{\lambda}^2 \rangle$ as in case of a pure substance at the same reduced temperature and pressure.

In particular one has

$$(5.4) \quad \tilde{\sigma}_0 = \tilde{\sigma}(\langle \tilde{\Lambda}^2 \rangle),$$

where $\tilde{\sigma}(\langle \tilde{\Lambda}^2 \rangle)$ denotes the universal function.

This function can be obtained from the experimental values of the surface tension of the different pure isotopes measured at the same reduced temperature.

Equation (2.19) gives us then the surface tension of the mixture,

$$(5.5) \quad \sigma = \tilde{\sigma}(\langle \tilde{\Lambda}^2 \rangle) \varepsilon^* / d^{*2} - \left(\frac{1}{2} x_A x_B \omega \varepsilon^* / k T d^{*2} \right) \left[\frac{\partial \tilde{\sigma}(\langle \tilde{\Lambda}^2 \rangle)}{\partial x_A} \right]^2.$$

By developing $\sigma(\langle \tilde{\Lambda}^2 \rangle)$ in the neighbourhood of $\tilde{\Lambda}_{AA}^2$ in terms of $\tilde{\Lambda}_{AA}^2 - \tilde{\Lambda}_{BB}^2$, one obtains

$$(5.6) \quad \sigma_e = \sigma - x_A \sigma_{AA} - x_B \sigma_{BB} = -\frac{1}{2} x_A x_B \left[\frac{\partial^2 \sigma}{\partial (\tilde{\Lambda}^2)^2} \right]_{AA} (\tilde{\Lambda}_{AA}^2 - \tilde{\Lambda}_{BB}^2)^2 - \left(\frac{\frac{1}{2} x_A x_B \omega}{k T} \right) (\sigma_{AA} - \sigma_{BB})^2.$$

The last term in (5.6) is due to the preferential adsorption at the surface of the component with lower surface tension. The sign of the excess surface tension depends on the sign of $\partial^2 \sigma / \partial (\tilde{\Lambda}^2)^2$, that is to say on the curvature of the surface tension as a function of $\tilde{\Lambda}^2$. The experimental data show that this latter is positive. We can conclude that quantum effects lower the surface tension.

The only system for which experimental values exist is a very dilute solution of ^3He in ^4He , which has been studied between 1.35 °K and 2.1 °K by ESELSOHN and BEREZNIJAK [13] in U.S.S.R. At a mole fraction 0.05 of ^3He the observed excess surface tension is -0.03 dyn/cm, the calculated excess surface tension is -0.02 dyn/cm; one half of the last value is due to preferential adsorption at the surface.

In this example, the calculated and observed values are not very exact. However, the agreement between them is in favour of the proposed model.

* * *

Our thanks are due to Dr. A. BELLEMANS and Prof. R. DEFAY for interesting suggestions which we have used in the course of this work. One of us (A. E.-C.) expresses her gratitude to European Research Associates, Brussels, who have permitted her to finish this work.

REFERENCES

- [1] A. SCHUCHOWITSKY: *Acta Physicochim U.R.S.S.*, **19**, 176, 508 (1944).
- [2] J. W. BELTON and M. G. EVANS: *Trans. Faraday Soc.*, **41**, 1 (1945).
- [3] E. A. GUGGENHEIM: *Trans. Faraday Soc.*, **41**, 150 (1945).
- [4] I. PRIGOGINE: *The Molecular Theory of Solutions* (Amsterdam, 1957).
- [5] I. PRIGOGINE, A. BELLEMANS and A. ENGLERT-CHWOLES: *Journ. Chem. Phys.*, **25**, 518 (1956).
- [6] H. C. LONGUET-HIGGINS: *Proc. Roy. Soc.*, A **205**, 247 (1951).
- [7] R. DEFAY and I. PRIGOGINE: *Tension superficielle et adsorption* (Liège, 1951), Chap. XII; E. A. GUGGENHEIM: *Mixtures*, (Oxford, 1952), Chap. IX.
- [8] A. ENGLERT-CHWOLES and I. PRIGOGINE: *Journ. de Chim. Phys.*, **55**, 16 (1958).
- [9] J. A. V. BUTLER: *Proc. Roy. Soc.*, A **135**, 348 (1932).
- [10] E. A. GUGGENHEIM: *Journ. Chem. Phys.*, **13**, 253 (1945).
- [11] V. MATHOT: *Journ. Phys. Chem.*, in the press; P. BOTTELIER: *Mémoire de Licence*, Bruxelles (1955); M. ROMEROWSKI: *Mémoire de Licence*, Bruxelles (1956).
- [12] I. PRIGOGINE, R. BINGEN and A. BELLEMANS: *Physica*, **20**, 383 (1954).
- [13] B. N. ESEL'SON and N. G. BEREZNAK: *Dokl. Akad. Nauk SSSR*, **98**, 569 (1954).

INTERVENTI E DISCUSSIONI

— A. PRINS:

Quand on étend la surface d'une solution il faut un certain temps afin que l'équilibre se constitue par diffusion de certaines molécules de l'intérieur à la surface. Est-ce que vos calculations donnent ce temps?

— A. ENGLERT-CHWOLES:

Nous calculons seulement la tension superficielle immédiatement après formation de la surface ou après un temps infini. Le temps n'entre pas dans nos considérations.

— A. PRINS:

Peut-on déduire de vos calculs le temps nécessaire pour arriver à l'équilibre d'adsorption?

— A. ENGLERT-CHWOLES:

Non, puisque dans nos expressions n'interviennent pas les considérations cinétiques.

Thermodynamic Properties of the System Argon-Methane Liquid.

V. MATHOT

Université Libre de Bruxelles - Bruxelles

Summary. — Vapor pressure and volume changes on mixing of the system argon-methane have been measured at 86.74 °K (triple point of trifluoro-chloromethane) by a technique essentially similar to that used for the carbon monoxide-methane system (*Trans. Far. Soc.*, **52**, 1488 (1956)). Heats of mixing and volume changes on mixing have been directly measured at slightly above 90.7 °K by the technique described by JEENER (*Rev. Sci. Instr.*, **28**, 263 (1957)). Excess properties have been worked out taking account for non-ideality of both liquid and vapor phases and compared to the prediction of the average potential theory developed by PRIGOGINE and coworkers (see *The Molecular Theory of Solutions*, (Amsterdam 1957)) Table I gives

TABLE I.

Excess property φ^E/x_1x_2 1 = argon	Unit	$\varphi^E/x_1x_2 = A + B(x_1 - x_2)$				Equation
		Experimental		Theoretical		
		A	B	A	B	
g^E/x_1x_2	cal/mole	72.7	6.5	195.5	0.0	(10.7.4)
h^E/x_1x_2	»	94.3	2.2	282.7	0.0	(10.7.5)
Ts^E/x_1x_2	»	21.6	— 4.3	87.2	0.0	(10.7.6)
v^E/x_1x_2	cm ³ /mole	0.6 ₃	0.0	1.8 ₂	0.0	(10.7.8)

The column of the theoretical values of A , B , has been worked out from the expression between brackets appearing in *The Molecular Theory of Solutions*; using the data of table 9.5.1 and 11.4.1; taking for ϵ^*/k and for σ the values 119.8 and 148.2 °K, 3.405 and 3.817 angstrom resp. for argon and methane; using argon as reference substance. and assuming $\theta = -\delta^2/8$

the main results. There is qualitative agreement between column 3 and 4 (right sign of the excess functions) though the theoretical expressions appear 2 to 3 times larger than the experimental ones. This is presumably to be ascribed to the relatively large value of $\rho = (r_{22}^* - r_{11}^*)/r_{11}$ (about 12%) whose influence appears to be overestimated in the average potential theory.

INTERVENTI E DISCUSSIONI

— VAN DER WAALS:

1) The comparison between theoretical and experimental values of the excess functions for $A + CH_4$ based on one adjustable parameter θ . It is true that you have taken the values of θ corresponding to the «geometrical mean law» for the form constants, and is not the result very sensitive to this choice of θ ?

2) From the cell theory of solutions it follows that *e.g.* the excess entropy consists of three terms:

a) configurational entropy;

b) change of entropy due to the altered frequency of oscillation of the molecules in the field of their neighbours;

c) the entropy of expanding the lattice.

Since c) is probably considerable it would be useful to compare the excess functions at constant volume, when c) is absent.

— V. MATHOT:

1) The results are indeed very sensitive to the choice of the θ . We have used in our calculation the «geometrical mean law» for there is no apparent reason to depart from this «law» for such simple molecules.

2) Yes.

— E. A. GUGGENHEIM:

Since Mathot's treatment assumes the principle of corresponding states, his predictions cannot be more accurate than this principle. Consequently he could obtain accurate values of his parameters θ and ϱ from the critical constants instead of using the many times less accurate values from second virial coefficients.

— V. MATHOT:

I agree that it would be more logical to use critical data throughout in order to calculate the parameters δ and ϱ .

— J. C. KIRKWOOD:

The principle of corresponding states for mixtures used by V. MATHOT is based upon the first moment approximation to the order-disorder problem, leading to random mixing. This approximation becomes poor for molecules of appreciably different size.

An Experiment on the Interaction of Dissimilar Molecules (*).

A. MICHELS

Van der Waals Laboratorium, Gemeente Universiteit, Amsterdam

It is hardly surprising that the interest in molecular interaction has not been restricted to the case of identical molecules. However, the treatment of the interaction between dissimilar molecules provides by its very nature additional difficulties, so that the fundamental approach to a mixture lags behind the treatment of the one-component system. Nevertheless, after each step taken forward in the case of a single system, application of the results to a mixture is considered. So, *e.g.*, VAN DER WAALS developed his theory of binary mixtures after his equation for a one-component system had found experimental confirmation. He found that, by replacing the attraction constant a and volume correction b by quadratic functions of the molar fractions (x and $1 - x$), he could describe qualitatively all phenomena which occur in practice. The quadratic functions are:

$$(1) \quad a = a_1(1 - x)^2 + 2a_{12}x(1 - x) + a_2x^2,$$

and

$$(2) \quad b = b_1(1 - x)^2 + 2b_{12}x(1 - x) + b_2x^2,$$

where a_1 , a_2 , b_1 and b_2 are the Van der Waals constants for the pure substances and a_{12} and b_{12} are the corresponding quantities referring to two different molecules.

While the fundamental physicist struggled to understand better the interaction of two simple identical molecules and its influence on the structure of the gas and liquid phase (a struggle which has not yet ended), experimentalists concerned with the solution of technical problems collected a considerable amount of information on the binary and more complicated systems. The results proved to be of highest importance, *e.g.*, in distillation techniques.

(*) 159th publication of the Van der Waals Fund.

After the introduction of the Lennard-Jones conception for the interaction potential of identical spherical molecules, the interest for understanding the interaction between different molecules flared up again. In a way not unlike Van der Waals' approach, the interaction was described with the parameters ϵ_{12} and σ_{12} , where, on semi-experimental grounds, for spherical non-polar molecules it was assumed that

$$(3) \quad \epsilon_{12}^2 = \epsilon_1 \epsilon_2,$$

and

$$(4) \quad \sigma_{12} = (\sigma_1 + \sigma_2)/2.$$

If the equation of state for dilute gas mixtures is expressed in the normal way as

$$(5) \quad pV/RT = 1 + B,$$

B can again be expressed by an equation quadratic in the molar fractions

$$(6) \quad B = B_1x^2 + 2B_{12}x(1-x) + B_2(1-x)^2,$$

where B_{12} is related to the interaction potential of two different molecules in the normal way as given for identical molecules. From (3) and (4) B_{12} can be calculated. The results agree reasonably well with the results of experiments in which the volume change is determined when two quantities of gas are mixed at one atm. Some results are shown in Table I.

TABLE I. — *Experimental and calculated values of B_{12} for some mixtures at 25 °C.*

Mixture	B_{12} at 25 °C in cm ³ /mole	
	theory	measured
H ₂ -N ₂	11.5	12.9
H ₂ -CO ₂	3.03	— 1.1
N ₂ -CO ₂	— 41.1	— 41.71
N ₂ -CH ₃ F	— 40.6	— 39.04
CO ₂ -CH ₃ F	— 105	— 149
NH ₃ -Kr	— 50.3	— 49.05

For higher densities no simple relation has as yet been derived. Some experiments carried out a few years ago in the Van der Waals Laboratory as a result of a suggestion made by an industrial laboratory gave results which required further clarification.

The equilibrium of a two-phase system consisting of a mixture of NH_3 , H_2 and N_2 (the molar ratio of H_2 and N_2 is 3:1) was studied. This system behaves as a two-component system. The concentrations of both gas and

liquid phase were analysed as a function of temperature and pressure up to 800 atm. Results are shown in Fig. 1.

A more detailed study of the results disclosed that, as a result of the few percent solution of H_2 and N_2 in the liquid phase, the apparent partial vapour pressure of ammonia increases in an unexpected way. This partial pressure is here defined as the product of the mole fraction of NH_3 in the gas phase and the total pressure.

Table II shows the results for 50 °C together

Fig. 1. — Pressure-composition diagram for a mixture of ammonia, hydrogen and nitrogen.

with the partial vapour pressure expected if Raoult's law would hold and the gas could be considered ideal under the conditions of the experiment.

TABLE II. — The partial vapour pressure of ammonia as measured and calculated according to Raoult's law in the ammonia-hydrogen-nitrogen system for 50 °C. p_0 is the vapour pressure of pure ammonia. The concentrations of ammonia in the gas and liquid phase are x_1 and x_2 , respectively.

$\text{NH}_3\text{--N}_2\text{--H}_2$ 50 °C		
p (atm)	measured px_1	calculated p_0x_2
49.1	22.88	19.87
102.—	26.42	19.73
196.6	32.34	19.51
292.7	38.78	19.33
782.5	70.58	18.54
$p_0 = 19.93$ atm		

Although the latter assumption is certainly not right, the order of magnitude of the discrepancy was considered too high to be accounted for by deviation from the ideal gas law.

It was considered appropriate to repeat the experiments with a simpler mixture, for which $\text{NH}_3\text{-A}$ was chosen.

First information was obtained about the interaction in the dilute gas state. Measurement of the volume expansion by mixing at one atm resulted in a B_{12}

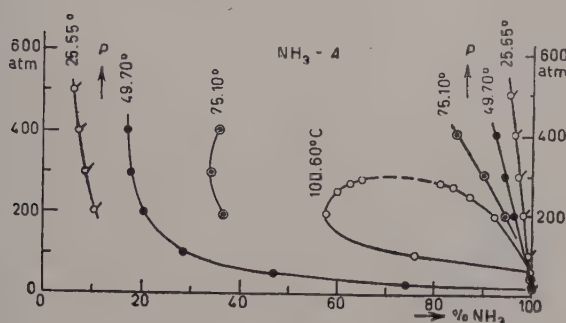


Fig. 2. — Pressure-composition diagram for a mixture of ammonia and argon.

of $-40.7 \text{ cm}^3/\text{mole}$ while HIRSCHFELDER's result, based on the values of the molecular constants of the pure component gases, predicted $-29.4 \text{ cm}^3/\text{mole}$. The experiments of the two phase equilibrium were then carried out up to pressures of 800 atm at 25, 50, 75 and 100 °C. Results are given in Fig. 2. As an example the data for 50 °C are given in Table III.

TABLE III. — The partial vapour pressure of ammonia as measured and calculated according to Raoult's law in the ammonia-argon system for 50 °C. p_0 is the vapour pressure of pure ammonia. The concentrations of ammonia in the gas and liquid phase are x_1 and x_2 , respectively.

NH ₃ -A 50 °C		
p (atm)	measured px_1	calculated p_0x_2
50.08	23.30	19.79
100.09	27.86	19.53
199.53	39.49	19.08
300.81	54.12	18.68
801.78	131.33	17.68
$p_0 = 19.93 \text{ atm}$		

It is obvious that in this system the partial vapour pressure of ammonia rises even more than in the mixture first studied. A higher temperature (Table IV) shows that the partial vapour pressure of ammonia can even remarkably exceed its critical pressure although liquid is still present.

The results at 25 °C for the two mixtures are compared in Table V.

This table shows that the higher increase of the partial vapour pressure goes together with a higher solubility of the gas in the liquid. For theoretical considerations it is desirable to know the respective densities of both phases. Measurements to obtain this information are presently carried out. However,

TABLE IV. — The partial vapour pressure of ammonia as measured and calculated according to Raoult's law in the ammonia-argon system for 75 °C. p_0 is the vapour pressure of pure ammonia. p_c is the critical vapour pressure of pure ammonia. The concentrations of ammonia in the gas and liquid phase are x_1 and x_2 , respectively.

NH ₃ -A 75 °C		
p (atm)	measured px_1	calculated p_0x_2
100	50.17	35.86
300	102.1	33.02
500	188.0	30.02
$p_0 = 36.7$ atm		
$p_c = 111.3$ atm		

TABLE V. — Comparison of the solubility of the gas in the liquid phase and the partial vapour pressure of NH₃ for the systems NH₃-N₂-H₂ and NH₃-A at 25 °C. In both mixtures the concentration of the gas component in the liquid phase is $1 - x_2$. The concentration of NH₃ in the gas phase is x_1 .

25 °C	NH ₃ -N ₂ -H ₂		NH ₃ -A	
p (atm)	$1 - x_2$	px_1	$1 - x_2$	px_1
100	0.0043	13.33	0.0161	14.67
200	0.0122	15.92	0.0275	21.12
400	0.0261	22.28	0.0474	33.32
600	0.0376	28.67	0.0569	49.43
800	0.0454	35.53	0.0624	59.81

$$p_0 = 10.0 \text{ atm}$$

TABLE VI. — The number density of ammonia in the gas phase as a function of the argon concentration in the liquid phase at 25 °C. The concentration of ammonia in the gas phase is x_1 . The concentration of argon in the liquid phase is $1 - x_2$. The density of ammonia in the gas phase is denoted by d in amagat units.

25 °C	x_1	d	d/d_{pure}	$1 - x_2$
p (atm)				
200	0.1059	20.5	2.05	0.0275
300	0.0915	25.2	2.52	0.0391
400	0.0834	28.5	2.85	0.0474
500	0.0823	32.5	3.25	0.0534
600	0.0795	34.6	3.46	0.0569
700	0.0784	36.8	3.68	0.0597
800	0.0747	37.2	3.72	0.0624

$$d_{\text{pure}} = 10.0 \text{ amagat}$$

some indication can already be deduced from the data available, under the simplifying assumption that the density of the gas phase is not highly influenced by the presence of a few per cent of ammonia. From the p - V - T -data published for argon and the saturated vapour density of NH_3 the increase of the number of NH_3 molecules per unit volume of the gas mixture can be calculated. The results are given in Table VI.

They show that there is a remarkable increase of the density of ammonia in the gas phase. The data suggest that this increase is proportional to the concentration of argon dissolved in the liquid phase.

Some justification of the assumption made can be found in a so-called *barotropic* phenomenon (Fig. 3).

If pure argon is compressed gradually a point is reached at a pressure of about 400 atm where gaseous argon obtains a density higher than the density of liquid NH_3 and liquid starts floating on top of the gas. This situation was observed and its position coincides within the experimental accuracy with the point calculated for a pure NH_3 liquid and pure argon gas phase.

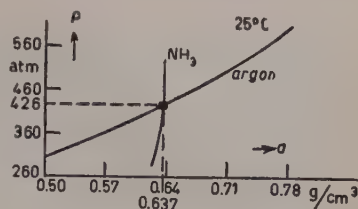


Fig. 3. — Density *vs.* pressure diagram of both the pure components argon and ammonia.

BIBLIOGRAPHY

- A. MICHELS, G. F. SKELTON and E. DUMOULIN: *Physica*, **16**, 831 (1950).
 A. MICHELS and A. J. H. BOERBOOM: *Bulletin des Sociétés Chimiques Belges*, n. 62 (1953).

INTERVENTI E DISCUSSIONI

— K. BEENAKKER:

You found a rather big increase in the NH_3 vapour pressure. Why compare rather approximate calculations based on a Lennard-Jones potential and neglect the solubility with these results?

— A. MICHELS:

Certainly the phenomenon is not known, and is also reported at low temperatures with the vapour pressure of water in the presence of CO_2 .

On thermodynamical grounds it has also been predicted by Van der Waals in his theory of linear mixtures. However this does not give enough information on a molecular basis. Neither can the difference between the observed B_{12} and the calculated one account for the high increase of the vapour pressure.

— J. REUSS:

I agree with Prof. MICHELS with regard to the mentioned difficulties in calculating the increase of partial vapour pressure of NH_3 under high A-pressures. When the gas density is comparable with the liquid density, you have to consider 1) in the liquid solved A-atoms and 2) Virial-coefficient higher than second order, for which combination does not exist.

— V. MATHOT:

I did not quite understand the nature of the disagreement between calculated and measured partial vapour pressure.

I think that the following approximate expression might throw some light on the question

$$p_1 = p_1^0 x_1 f_1 \exp \left[\frac{v_1 - B_{11}}{RT} \right] (p - p_1^0)$$

p_1 = partial pressure of 1 in liquid solution;

p_1^0 = vapour pressure of pure 1;

x_1 = liquid mole fraction of 1;

v_1 = specific volume of liquid 1;

B_{11} = virial coefficient of pure gaseous 1;

p = total pressure;

f_1 = activity coefficient of 1 in liquid solution.

Solid Solutions of Argon and Krypton.

R. HEASTIE and G. O. JONES

Department of Physics, Queen Mary College, University of London - London.

The measurements described in this contribution have been made because of the suitability of argon and krypton mixtures as models for comparison with solution theories. The molecules have spherically symmetrical force fields and their molecular radii differ by about 7%. The vapour pressure of solid and liquid solutions has been determined over the whole composition range and the phase equilibrium diagram has been derived.

The solid-liquid phase equilibrium diagram (Fig. 1) shows large deviations from ideality for small proportions of krypton with a tendency to ideality for krypton-rich mixtures. The vapour pressure measurements indicate that the solid solutions deviate positively from ideality.

These latter measurements may be compared with a) the strictly regular, b) the cell, c) the conformal solution theories. All three theories predict a dependence of the excess free energy (G^e) on composition of the form:

$$(1) \quad G^e = \sigma x_1 x_2,$$

where x_1 and x_2 are the mole fractions of the components and σ is independent of x_1 and x_2 .

It follows from equation (1) that the vapour pressure (P) of the solution

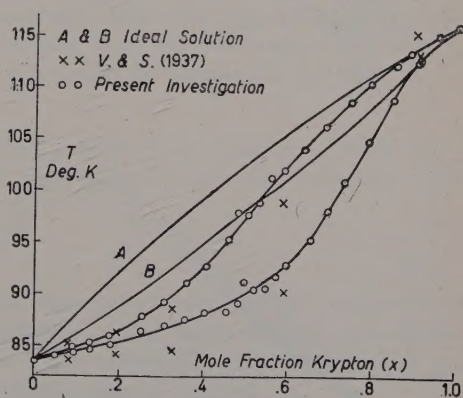


Fig. 1. — The solid-liquid phase equilibrium diagram of argon and krypton. A and B ideal liquidus and solidus. 1) to experimental VEITH and SCHRÖDER [4]; 2) to experimental HEASTIE [5].

is given by:

$$(2) \quad P = x_1 p_1^0 \exp [\sigma x_2^2 / RT] + x_2 p_2^0 \exp [\sigma x_1^2 / RT],$$

where p_1^0 and p_2^0 are the vapour pressures of the two components at the temperature T . The values of σ at $T = 82.9^\circ \text{K}$ have been calculated from equation (2) and the results are shown in Fig. 2. It may be seen from the figure that σ is not independent of x_2 .

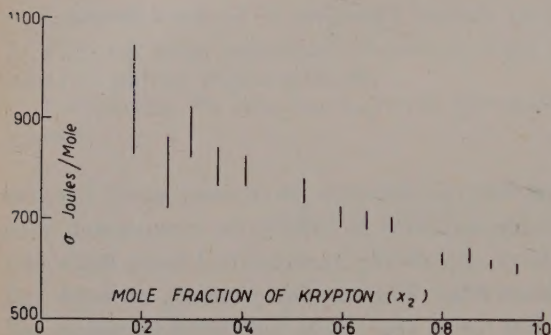


Fig. 2. — The variation of the parameter σ with the composition of the solid solutions. The lengths of the lines show the experimental uncertainty in the calculated values of σ .

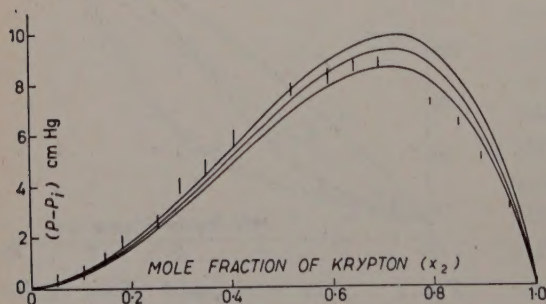


Fig. 3. — The variation of $(P - P^i)$ with the composition of the solid solutions. | experiment;
1) $\sigma = 675 \text{ J/mole}$; 2) $\sigma = 716 \text{ J/mole}$;
3) $\sigma = 750 \text{ J/mole}$.

The cell theory of solutions permits a value of σ to be calculated. Using an expression (1) for G^e , which takes account of the difference in the molecular radii of argon and krypton, σ has been determined to be 716 joule/mole at $T = 82.9^\circ \text{K}$. The quantity $(P - P^i)$ (where P^i is the vapour pressure of the ideal solution at the temperature T) has been calculated at $T = 82.9^\circ \text{K}$ for three different values of σ and its variation with the mole fraction of krypton (x_2) is shown in Fig. 3. This figure shows that the experimental results are inconsistent with equation (2) but that the value of σ predicted by the cell theory fits the experimental results closely.

Since solid solutions of argon and krypton exhibit positive deviations, a separation of the solution into two phases would be expected at low tem-

peratures. No sign of such a phase change has been observed in either the specific heat or vapour pressure measurements. The excess entropy (S^e) of the solid solution has been calculated from the measured values of the

specific heat [2] of an equimolar mixture and the published values [3] of the specific heat of argon and krypton. The value of S^e , thus calculated, is negligible compared with $R \ln 2$.

REFERENCES

- [1] I. PRIGOGINE *The molecular Theory of Solutions* (Amsterdam, 1957), eq. (10.4.17).
- [2] B. F. FIGGINS: in course of publication.
- [3] K. CLUSIUS: *Zeits. Phys. Chem.*, B **31**, 459 (1936).
- [4] H. VEITH and E. SCHRÖDER: *Zeits. Phys. Chem.*, A **179**, 16 (1937).
- [5] R. HEASTIE: *Nature*, **176**, 747 (1955).

INTERVENTI E DISCUSSIONI

— J. BEENAKKER:

Can you tell me how long you kept your specimen at low temperature as for a spatial phase separation the small mobility in the crystal will give a very large relaxation time.

— G. O. JONES:

Experiments have normally extended over periods of the order of $8 \div 12$ h, and we have observed no differences of behaviour according to the rate of heating within this range.

— V. MATHOT:

In calculating the vapour pressure of the solution from the average potential theory did you take into account gas-phase non-ideality? This might actually introduce up to $(10 \div 20)\%$ corrections on the calculated vapour pressures and would be very much felt on the excess vapour pressure, as I understand you plotted.

— G. O. JONES:

The results presented do not take these corrections into account; they are being evaluated with the use of extrapolated virial coefficients.

— R. A. UBBELOHDE:

Order-disorder transformations in solids seem likely to involve rapidly increasing relaxation times as the critical transformation temperature falls; falling transformation temperatures imply smaller energy differences ΔE between the ordered and disordered states. On the other hand the activation energy for diffusion in the crystals which usually controls the relaxation time will not fall in general as ΔE decreases, since such

activation energies are mainly determined by repulsion potentials between the atoms. This seems to be the reason why ordered solid solutions are not much more commonly found at low temperature even when thermodynamically they should appear.

— G. O. JONES:

We are hoping to measure the self-diffusion coefficient in solid krypton directly, using a tracer method.

— B. ALDER:

I believe that a phase separation has been observed in the system of rare gases by Halsey and coworkers in thin, solid layers of these mixtures however the mechanism by which this was achieved is possibly not by diffusion in the solid.

— E. A. GUGGENHEIM:

In mixed crystals of atoms as similar as argon and krypton the thermodynamic energy, determining the tendency to separate, is so small while the energy of activation, required for separation to take place, is so large that it seems safe to predict that separation definitely cannot take place at any temperature in the solid. This metastability in the translational degree of freedom is frozen in just as is the metastability in the rotational degree of freedom in crystals of CO or NNO. The behaviour of liquids is of course entirely different.

PROPRIETÀ LETTERARIA RISERVATA

Direttore responsabile: G. POLVANI

Tipografia Compositori - Bologna

Questo fascicolo del *Supplemento* è stato licenziato dai torchi il 23-X-1958